Synthesis, purification, and characterization of tetraphosphine ligands

Deniz Cevik

▶ **To cite this version:**

Deniz Cevik. Synthesis, purification, and characterization of tetraphosphine ligands. Other. Université Paris Saclay (COmUE), 2017. English. NNT : 2017SACLX026 . tel-01631221

HAL Id: tel-01631221
https://pastel.hal.science/tel-01631221

Submitted on 8 Nov 2017

HAL is a multi-disciplinary open access archive for the deposit and dissemination of scientific research documents, whether they are published or not. The documents may come from teaching and research institutions in France or abroad, or from public or private research centers.

L'archive ouverte pluridisciplinaire **HAL**, est destinée au dépôt et à la diffusion de documents scientifiques de niveau recherche, publiés ou non, émanant des établissements d'enseignement et de recherche français ou étrangers, des laboratoires publics ou privés.

NNT : 2017SACLX026

THESE DE DOCTORAT
DE
L'UNIVERSITE PARIS-SACLAY
PREPAREE A
ÉCOLE POLYTECHNIQUE

ECOLE DOCTORALE N° 517
2MIB | Sciences chimiques :
Molécules, matériaux, instrumentation et biosystèmes

Spécialité de doctorat : Chimie

Par

Mme. Deniz Çevik

Synthesis, Purification, and Characterization of Tetraphosphine Ligands

Thèse présentée et soutenue à Palaiseau, le 17. Juillet 2017 :

Composition du Jury :

Mme. Hii, King Kuok (Mimi)	Professeur Imperial College London	Rapporteure
M. Manoury, Eric	DR - CNRS au LCC (Toulouse)	Rapporteur
M. Voituriez, Arnaud	DR - CNRS á l'ICSN	Président
M. van Leeuwen, Piet	Chaire d'Attractivité au LPCNO, INSA-Toulouse	Co-directeur de thèse
M. Carmichael, Duncan	CR - CNRS á LCM (École Polytechnique)	Directeur de thèse

Index

I want to dedicate this work to my family

and to Friedrich & Ingrid von Rosen.

"Our true mentor in life is science."

Mustafa Kemal Atatürk

Acknowledgment

Firstly, I would like to express my sincere gratitude to my advisors Prof. Dr. Piet W.N.M. van Leeuwen and Dr. Duncan Carmichael for the continuous support of my Ph.D study and related research, for their patience, motivation, and immense knowledge. Their guidance helped me in all the time of research and writing. I thank as well Prof. Dr. Paul Kamer for the collaboration on hydroformylation, his support and knowledge were very inspiring.

Besides my advisors, I would like to thank the rest of my thesis committee: Prof. Hii (Mimi), Dr. Manoury, and Dr. Voituriez, for their insightful comments and encouragement, but also for the hard questions which allowed me to broaden my research from various perspectives.

I want to thank the European commission for the financial support in form of the Marie-Curie-ITN7 SusPhos network.

My sincere thanks also goes to Dr. Andrew Chapman, Dr. Prasad Ganji, Dr. Mathieu Tschan, and Dr. Estefanía Arroni and all of the other labmates, who provided me with many ideas and support in the team at the ICIQ under Prof. Dr. Piet van Leeuwen. Especially I thank Marta Serrano for her help at the beginning of this rough road. Moreover I would like to thank both of the secretaries Maria-José and Marta for all the administrative support and private help provided in this new environment. I valued all dinners and lunches and field trip to the Pyrenees, which gave us the opportunity to know each other better and enjoy leisure time together.

I want to thank Prof. Dr. Pau Ballester and his group for the joint sessions and all the suggestions and questions, as well as for the opportunity to discuss and listen regularly to supramolecular chemistry.

I want to thank the ICIQ research supporting units for all their professional help and the nice talks during our coffee and lunch breaks. I want to thank as well the employees of the administration of the ICIQ who provided me with enormous support during the organization of a SusPhos workshop in Tarragona. Thanks to them it was a great success! I want to thank María at the reception, who always was a great help and welcomed us every day with a smile on her face.

Moreover I want to thank Asraa, Cayetana, Bazzo, Sofía, Idoia, María, Jenny, Olga, Gael, Nestor, Riccardo, Noel, Fany and many more for the nice moments we spent together!

My sincere thanks also goes to Dr. Aike Nijland, Dr. Thibault Cheisson, Dr. Éléonore de la Garanderie, and Dr. Gregory Danoun for their open ears and suggestions towards my research and all of the other labmates, in the team at the École Polytechnique under Dr. Duncan Carmichael. I thank Anne-Flo for her help and support in all administrative questions, which was quite stressful and tough due to many reasons, she always showed patience and did her best. I thank the director of the LCM lab Prof. Dr. Corinne Gosmini

for welcoming me in her group and helping me out quite a few time, especially during the end of my thesis.

Marie Cordier for all the X-ray analyses, Sophie Bourcier for the HPLC-Ms, Stéphane Bouchonnet for the GC-Ms, Elodie for the synthetic help and the organization of all the practical things in the lab, and Louis for all the computer problems I had.

I thank my mates Irene, Arnaud, Matthieu, Alice, Greg, Bibi, Yingxiao, Louis, Violaine, and Yann for all the nice chats and after work gatherings we spent together, especially Alice for organizing the first trip to Milano for us students!

I thank so much Aike for being in my office and enduring all my stupid talks and problems, for his special way of sarcasm and irony and for always correcting my English. I enjoyed my office time a lot and my off time as well thanks to him.

I thank a lot Ikbal, without her constant help and support I probably would have never finished, she was always there for me for any kind of problem and kicked me if necessary! Thanks!

I thank all my fellow labmates in for the stimulating discussions, and for all the fun we have had in the last four years.

I want thank Baron Friedrich von Rosen (God bless him) and Ingrid von Rosen for everything they have done for me, without them I wouldn't have had the opportunity to do even a PhD. Kind hearted people who supported in very difficult times and guided me throughout those times with knowledge, and continuous support. I thank you a lot!

Last but not the least, I would like to thank my family for supporting me emotionally throughout this thesis and my life in general. Without they valuable support it would not be possible to conduct this research.

Annotations

Abbreviations:

Ph	phenyl
Ar	aryl
t-Bu	*tert*-butyl
i-Pr	*iso*-propyl
COD	cyclooctadienyl
Cy	cyclohexyl
dba	trans, trans - dibenzylideneacetone
Et	ethyl
Ms	mesyl
TBAB	tetra-*n*-butylammonium bromide
n-BuLi	*n*-Butyllithium
acac	acetylacetate
NBS	*N*-bromosuccinimide
r.t.	room temperature
et al.	*et alii*
e.g.	exempli gratia
g	gram
mL	milliliter
d	density
L	ligand ; liter
p	*para*
R	unspecified organic group
Rac	Racemic
SPS	switchable polarity solvents
NMR	nuclear magnetic field
GC- MS	gas chromatography- mass spectrometry
TOF	time of flight / turnover frequency
bp	boiling point
calcd	calculated
THF	tetrahydrofurane
DCM	dicholormethane
ETOAc	ethylacetate
DMF	dimethylformamide
DMSO	dimethylsulfoxide
δ	chemical shift
J	coupling constant

s	singlet
d	doublet
t	triplet
q	quadruplet
m	multiplet
dd	double doublet
b	broad
ppm	parts per million

Chapter 1 Introduction

1.1 Phosphine Ligands in Homogeneous Catalysis

In homogenous catalysis the catalyst and the reactants are in the same phase, most often the liquid phase. Ligand effects play a major role in the efficiency of catalysts based on organometallic complexes. If the coordinating ligand to one specific metal is modified, the reaction can lead to different products. Phosphine based ligands have proven to be very useful in organometallic chemistry and industrial applications of homogeneous catalysis.[1]

1.1.1 Ligand Effects of Phosphines

The reactivity of transition-metal catalyzed reactions can be influenced greatly by the steric and electronic effect of ligands, hence the activity and selectivity of homogeneous catalytic processes. A study of the catalytic system, especially the influence of the ligand properties in the key step of the catalytic cycle, promotes the determination of a ligand design for specific catalytic reactions, avoiding the expensive and time consuming trial and error method.[1]

1.1.1.1 Electronic and Steric Parameters of Monophosphines

The electronic parameters of phosphorus(III) ligands have been investigated by various methods. One approach determines by IR and NMR spectroscopy phosphorus and non-phosphorus mixed ligand complexes and evaluates the reaction of the non-phosphorus ligands to electronic changes at the metal center effected by the phosphine ligand. This method is especially suitable when carbonyls are employed as co-ligands.[1,2] The IR frequencies are useful when comparing the electronic parameters of a series of phosphorus ligands towards a specific metal. The characteristics of phosphorus ligands can also be determined by assessing the CO stretching vibrations in $CrL(CO)_5$ (L= PR_3).[3,4] Tolman has described an electronic parameter based on the vibrational spectra[a] of $NiL(CO)_3$ using L = P(*t*-Bu)$_3$ as reference ligand. The electronic parameter χ for the other ligands is simply characterized through differences in the IR frequencies of the symmetric stretches; individual contributions of the substituents are additive.[5]

[a] IR spectra

Phosphine ligands can furthermore be divided into two types: σ – donors and π – back-donors (Figure 1). The lone pair of the phosphorus is responsible for the σ – donation towards empty orbitals. The π-back-donation occurs from filled metal orbitals to empty orbitals of the ligands; the literature suggests that back-donation occurs from the metal d-orbitals into the σ*- orbitals of the phosphorus ligand.[6,7]

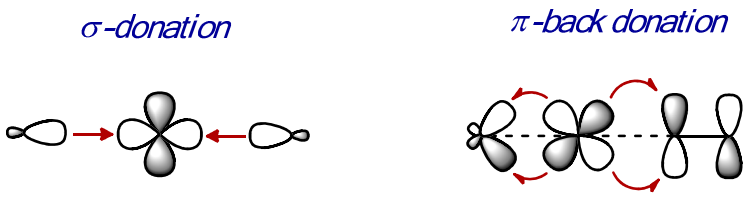

Figure 1: σ- donor and π- back donation interactions in phosphine ligands. On the left side, strong σ – donation occurs, and on the right side a weak π –back-donation to the M–L bond occurs with an increase in CO stretching band frequency.[2]

Studies of the stretching frequencies of the coordinated carbon monoxide ligands in complexes like $NiL(CO)_3$ or $CrL(CO)_5$ (L = phosphorus ligand) can explain the overall σ – basicity and π – acidity of the phosphorus ligands. If the employed phosphine is a strong σ – donor ligand the electron density on the metal is increased and hence a substantial back donation to the CO ligands occurs, resulting in lowered IR frequencies (M (t_{2g} orbital)- π* (CO)). On the contrary a poor σ – donor but a strong π –acceptor ligand competes with CO for the electron back donation and the CO stretch frequencies remain high.[1]

Similar to studies of electronic parameters, several steric parameters have been proposed. The most often used Tolman's parameter θ measures the steric bulk of a phosphine ligand from CPK[a] models. From the metal center, located at a distance of 2.28 Å[b] from the phosphorus atom in the appropriate direction, a cone is constructed which just embraces all the atoms of the substituents on the phosphorus atom (Figure 2).[5] The cone angle θ is a measure for the steric bulk of ligands; however ligands hardly ever form a perfect cone. An analysis of crystal structures has shown that the angles realized in the structure are smaller than the θ – values would

[a] Space-filling model by **C**orey-**P**auling-**K**oltun.[329,330]

[b] A typical P–Ni distance, as a result the cone angle of a ligand is essentially to a certain degree dependent upon the transition metal.

suggest. An intermeshing of the R-substituents of complexes can lead to smaller effective cone angles.[1,8–11]

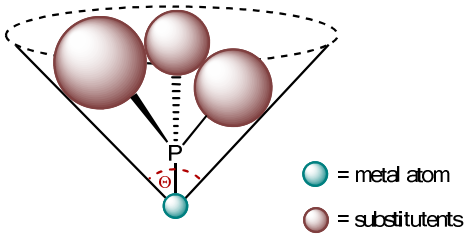

Figure 2: Tolman's cone angle.[5]

White et al. suggested the model of solid angles[12,13], in which the Van der Waals radii of the ligand atoms, either obtained from crystal or calculated structures, are projected onto the Van der Waals surface of the metal center. The extent of coverage, given by the solid angle, is a measure of the steric bulk around the metal.[12–14] Although the assessment of steric bulk is mostly geometric in nature, it can be as well described as a repulsive energy (E_R) promoted by the ligand in the complex. *Brown et al.* illustrated a steric repulsive energy parameter, that is established on a molecular mechanics computational model of $CrL(CO)_5$. The van der Waals repulsive force is calculated between the metal complex and the ligand (F_{vdw}), the repulsive energy is hence the product of this van der Waals repulsive force and the M–L bond distance. [15,16] Sophisticated computer models that simultaneously evaluate bulk and electronics are now providing ligand "maps"[17] that allow for predictive replacement of one phosphine by another for the optimization of catalytic processes.[18]

1.1.2 Describing Diphosphines

Diphosphines often offer a better command over regio- and stereoselectivity in catalytic reactions compared to monodentate ligands. An advantage of bidentate ligands is the chelating effect; it reduces the inclination for phosphine dissociation during the catalytic cycle. As a result the number of species present under catalytic conditions is decreased, which improves transfer of regio- and stereoselectivity from the ligand to the substrate. Tolman's cone angle is widely accepted for monodentate ligands; however it delivers poor descriptions for bidentate ligands.[19] The crucial difference between mono- and bidentate ligands is the ligand backbone, which can preserve two phosphorus donor atoms at a specific distance (Figure 3). This distance is ligand

specific and an important parameter, together with the scaffold flexibility. As a consequence a bite angle with designated M–P bond lengths and a metal atom, that does not favor a specific P–M–P angle would be an appropriate method to compare bidentate ligands methodically.[20,21]

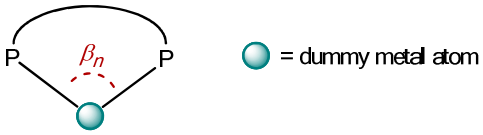

Figure 3: Bidentate phosphine ligand.[1,20–22]

In an attempt to compare diphosphines, the concept of natural bite angles, based on molecular mechanics, was established by *Casey et. al*.[22] A dummy metal atom is introduced coordinating to both P-donor atoms at a distance of 2.315 Å; as a result only ligand geometries are included coordinating to the transition metal (Figure 4). By setting the P–M–P force constant to zero during the geometry optimization a purely ligand induced P–M–P angle can be determined to make different bidentate angles comparable.

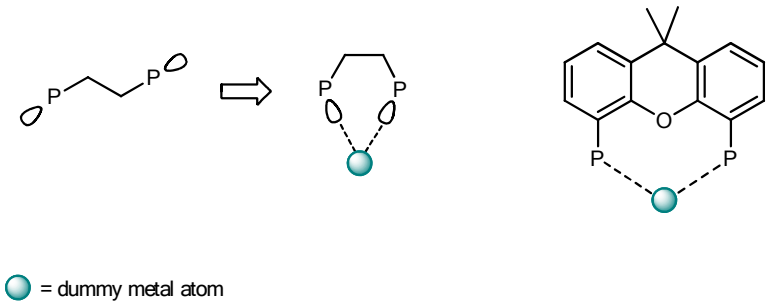

Figure 4: Definition of the bite angle with a fixed P–M distance using a dummy metal atom.[1,22]

The bite angle effect is reflected in the modifications in steric interactions occurring when the bidentate ligand is modified, while retaining the substituents at the donor atoms (Figure 5). Ligand-ligand and ligand-substrate interactions influence the relative energies of stable intermediates and transition states of the catalytic cycle, as a result the modification of the bite angle affects directly the activity and regioselectivity of the catalyst system. The group of *Barron et al.* introduced the concept of the "pocket angle", which is a semiquantitative ligand parameter portraying the steric bulk of bidentate ligands.[23]

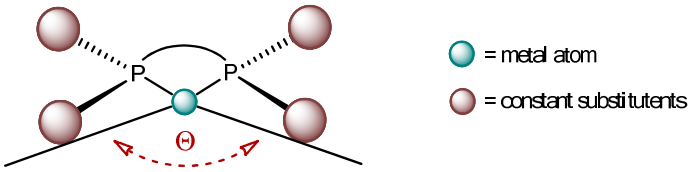

Figure 5: The steric bite angle effect is here represented by the pocket angle Θ by *Barron et. al*.[23]

Purely steric bite angle effects are rare in catalysis, however there are few examples representing this type of influence. For instance on the regioselectivity the Rh-diphosphine catalyzed hydroformylation of alkenes or the product selectivity in the CO/ethylene copolymerization is mainly the result of steric interactions.[24]

1.2 Bimetallic Catalysts

Bimetallic catalysis is a common phenomenon in many reactions occurring in nature; especially enzymes are frequently involved in multimetallic catalyzed reaction processes. In last decades scientific society tried to mimic these multimetallic systems for "man-made" catalytic reactions. Cooperativity in a multimetallic system is mainly useful and beneficial if the activity demonstrated by the multimetallic core surpasses the results obtained from the corresponding mononuclear center, or it induces a reactivity that would not be possible under other conditions.[25,26] As a result mono- and binuclear complexes have become the subject of extensive investigation. Numerous systems were reported, both homobimetallic and heterobimetallic, while herein the focus will be on homobimetallic catalyzed reactions in homogeneous catalysis, with special focus on bimetallic carbonylation reactions and cross coupling reactions.

1.2.1 Enzyme catalysis

The catalytic power of enzymes lies in their ability to bring substrates together in favorable orientations when they interact with the active site. This capability has made enzymes the fastest and most selective catalysts known. There are also enzymes known with active sites that contain two metal centers working cooperatively. The reactions that are catalyzed by these enzymes show a broad variety, including redox type reactions, such as oxygen atom transfer, reduction of ribonucleotides to deoxyribonucleotides, or thiosulfate oxidation to sulfate.[27] The best known bimetallic enzymes have active sites containing mostly dinuclear copper or iron

compounds designed for reversible binding or activation of oxygen. For instance the dinuclear copper active site of hemocyanin binds oxygen and the dinuclear iron containing hemerythrin is also an oxygen carrying enzyme. However little is known about these enzymes and the mechanisms of the reactions they catalyze.[27] Enzymes like superoxidase dismutase (Figure 6) that is capable of eliminating the highly reactive and toxic superoxide radical, $O_2^{\cdot-}$ to H_2O_2 and O_2 contains two different metals in its active site, i.e. copper and zinc.[27,28]

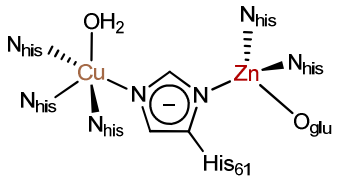

Figure 6: The bimetallic enzyme superoxidase dismutase.[27,28]

1.2.2 Synthetic bimetallic catalysts

Bimetallic systems emerge in many forms, the metals in binuclear complexes can be the same (homo bimetallic) or different (hetero bimetallic). Hetero bimetallic systems try to combine different properties of two metals and thus create two active sites with different reactivities. For these systems d_0-d_8 early-late transition metals are often used. In the field of polymer catalysis bimetallic cooperativity is well established, with a milestone by *Coates et al.* on the CO_2-propylene oxide copolymerization systems outperforming their mononuclear equivalents.[29,30] Well known is the Sharpless epoxidation, in which a binuclear titanium catalyst enables a high regio- and stereoselective epoxidation of double bonds.[31,32] The work of Jacobsen induces selective ring opening of epoxides using a dicobalt species.[1,33]

The activity of catalytic reactions depends on the structure of the complex, in consequence the rational design of binucleating ligands becomes of utmost importance when attempting to elicit metal cooperativity by complexing to metal centers. The scaffold determines the nature of the metal ions, and the metal-metal distance in the binuclear complex (often less than 5 Å[25,34]), hence for the synthesis of well-defined bimetallic complexes the choice of the ligand system is of great importance.[24,27,35,36] Variable parameters within the ligand are for instance the backbone flexibility, the donor-atoms coordinating to the metal center (N, P, O, S, C, etc.), electronic and steric parameters, as well as the bite-angle. Rational combination of these parameters might be able to deliver a tailored ligand for a specific catalysis.[2] Binucleating ligands

have to fulfill a number of requirements; most importantly the ligand has to be apt to contain two metals. Furthermore, the choice of the coordination environment[a] is essential, since it defines the nature of the metal ions[b]. Ultimately the metal-metal distance has a key role in the activity of the designed complexes. Binucleating ligands can be divided into three types.[27]

- Ligands forming complexes in which at least one donor-atom is shared with the metal ions. The ligands contain neighboring sites in which the central donor moiety provides a bridge between the metals (compartmental ligands).[27]
- Ligands in which no donor atom is shared in-between the metal ions, the donor-sets are separated.[27]
- Ligands in which the metal centers are connected to one another (side-by-side).[34]

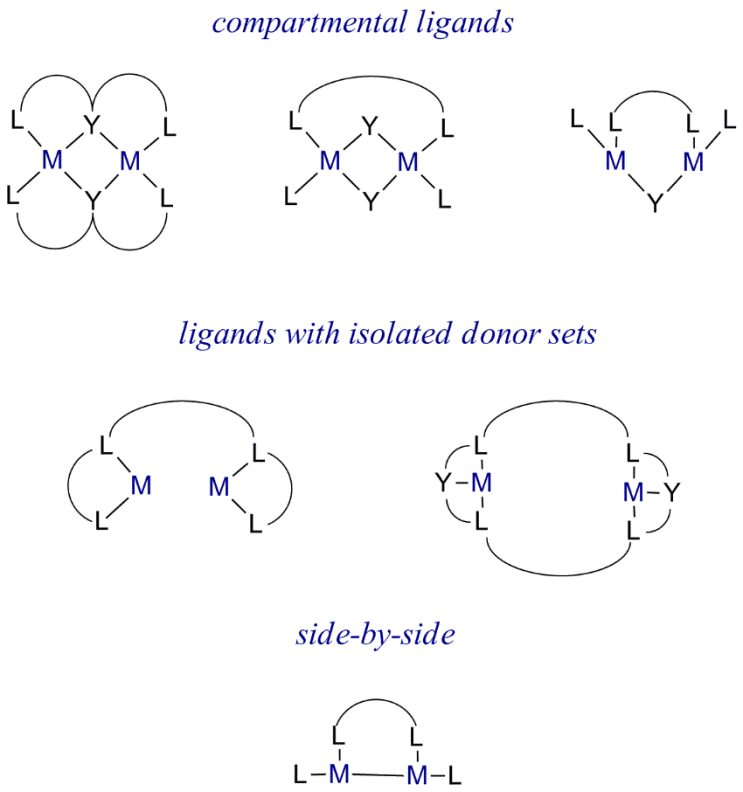

Figure 7: A schematic representation of binucleating ligands and their potential coordination complexes.[27,34]

[a] For instance ligand effects like flexibility, steric, electronic, bridging ligand moieties, etc.

[b] For instance type of metals, oxidation states, homo- or heterobimetallic.

There are three different coordination modes in which two metals in bimetallic complexes can act cooperatively (Figure 8). A substrate can be coordinated to both metal ions concurrently (**I**), the substrate can be activated and reaction with another molecule either bound to a metal or unbound can occur. In another form the substrate is bound to one metal and the reactant to another metal (**II**), activation of the substrate and reactant can lead to a reaction between these two molecules. In the third case (**III**) the second metal does not contribute to the catalytic reaction, but stabilizes the reaction center, for instance by donating or withdrawing electron density, or by stabilizing a specific geometry at the binuclear site.[25,27,37,38]

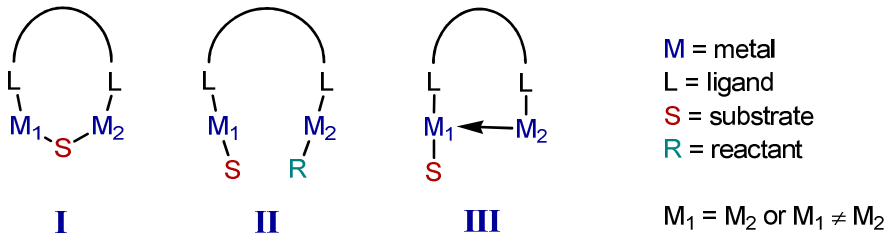

Figure 8: The three mechanisms in which two metals can be used cooperatively.[27,37,38]

An example of substrate and reactant activation (**II**) by cooperation between two metal centers is the ruthenium catalyzed formation of butadiene from ethylene using a bis-ruthenium complex developed by *Knox et al.* (**Scheme 1**The complex brings two ethylene molecules in close proximity and activates them. Under normal conditions two ethylene molecules would not react with one another.[37,39,40]

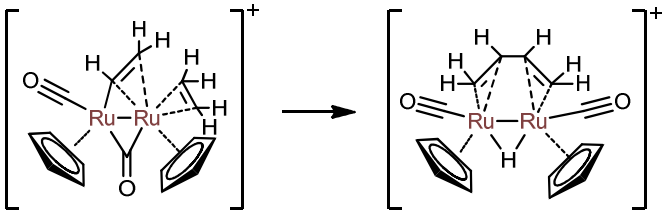

Scheme 1: The proposed bimetallic ruthenium system for the formation of butadiene from two ethane molecules developed by *Knox et. al.*[37,40]

Bimetallic systems can also be used to facilitate multi electron transfer processes. This can be used for instance in the reduction of N_2 to NH_3, an important industrial process. The Haber-Bosch process uses N_2 as nitrogen source and requires extremely harsh conditions in

order to activate the N_2; hence the process is very energy consuming. In consequence the development of a process that enables direct transformation of N_2 into compounds like NH_3 under mild conditions is an important goal. A bimetallic system which could convert N_2 to NH_3 is the ruthenium-tungsten system developed by *Hidai et. al*., the obtained yields were moderate, however it is still a good model of the potential of bimetallic systems.[39,41,42]

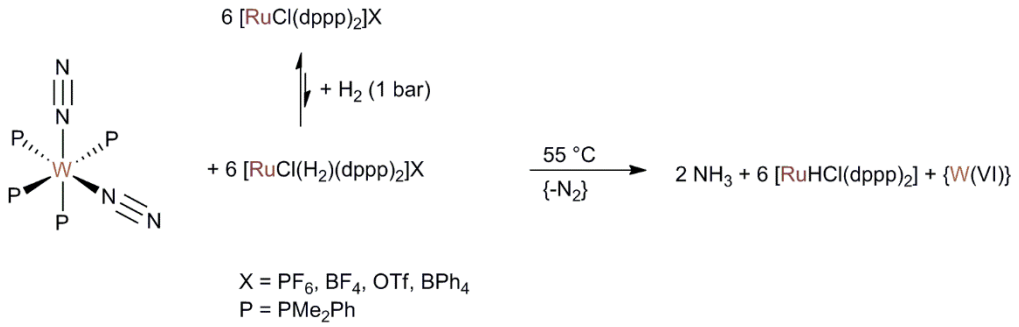

Scheme 2: The bimetallic reduction of N_2 to NH_3 at 55 °C and 1 atm developed by *Morris* and *Hidai et. al*.[39,41–44]

M−M bonds (**III**) bear "disguised" sites for coordination of substrates; therefore no ligand dissociation is required to open coordination sites. Such bonds could enhance the rate of the reaction, but only if the ligand dissociation is the slowest step in the catalytic cycle. Weak M−M bonds can eliminate the necessity for ligand dissociation, and can stabilize the complex sufficiently to ensure that no decomposition occurs under non-catalytic conditions. A bimetallic mixed-metal system, consisting of metals with different properties, increases the possibility for selective activation of two or more different substrates.[27]

As described previously, various possibilities can be distinguished in which two metals might cooperate in catalytic reactions. However the classification of two center catalysis is still incomplete, although the number of bimetallic systems increased tremendously in the last decade. There are various borderline examples like the copper-catalyzed 1,4-addition of Grignard reagents to *α,β*-unsaturated carbonyl compounds (Scheme 3).[45] The Mg^{2+} is coordinated to the carbonyl oxygen and the Cu^{+} center to the double bound of the enone, subsequently the nucleophile is transferred from the Cu^{+} center to the enone. If the bonding and activation is considered from the Mg^{2+} center, then this example would represent two-center catalysis. However, if the Mg^{2+} center is regarded as only a spatial component, it would not participate in the acti-

vation, the reaction would not be two-centered, because both reactants are principally coordinated to the Cu^{+} center.[46] This example shows clearly the difficulty in assessing a general classification, because real interactions in catalysis can often not be measured accurately.[45]

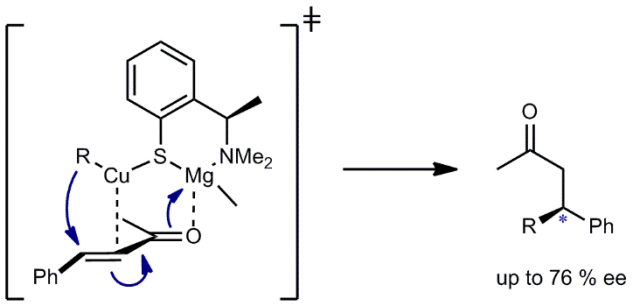

Scheme 3: Enantioselective 1.4-addition of RMgX to enones.[46,a]

Nevertheless, in strict terms,[b] bimetallic catalysis refers to cases where the substrate and reactant are connected and activated at the binuclear center. The control of the reactant and substrate is often a key aspect of these systems (**II**, Figure 8).[27] An example for this kind of binuclear catalysis is present in the phosphohydrolases, which are known to have a binuclear active site containing iron, zinc, manganese or magnesium, and are able to hydrolyze phosphate.[47] For example a binuclear iron site is found in *mammalian purple acid phosphatases* (PAP); *kidney bean purple acid phosphatase* on the other hand contains a heterobimetallic Fe(II)Zn(II) site. The PAP mediated hydrolysis occurs with inversion of configuration at the phosphorus through a pentacoordinated intermediate, which seems to be stabilized by the metal ions and two histidines. In the postulated mechanism, the phosphate ester is coordinated to M(II) [Fe (II) or Zn(II)] and the hydroxide connected to the Fe (III) attacks the phosphate ester to generate the intermediate (Scheme 4).[47]

[a] The alkali metals might control the geometry and/or act as Lewis acid.[46]

[b] There are other bimetallic systems which will be neglected here, since they would not be applicable to our ligand design.

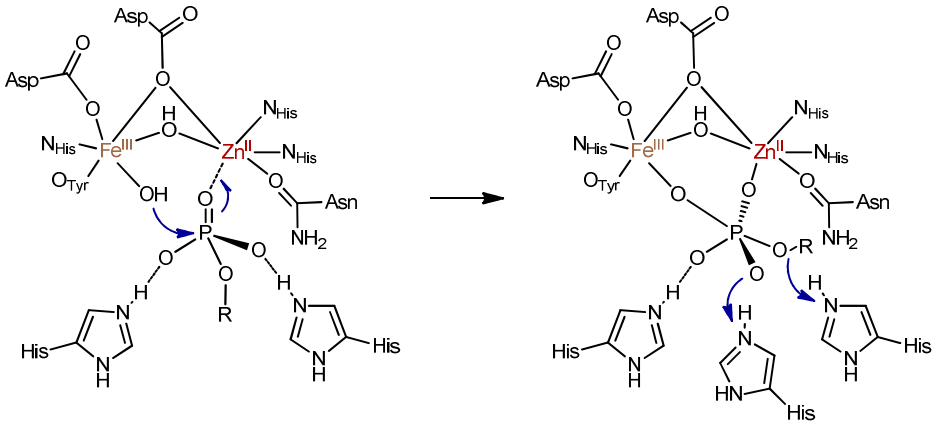

Scheme 4: Postulated mechanism for the phosphate ester hydrolysis at the kidney purple acid phosphate Fe(III)Zn(II) binuclear site.[47]

Bimetallic catalysis might appear even if the two metal centers are not connected by one ligand and still cooperatively catalyze the reaction. There exist many examples in the literature regarding these types of binuclear cooperativity. A general description distinguishes three different possibilities displayed in Figure 9.

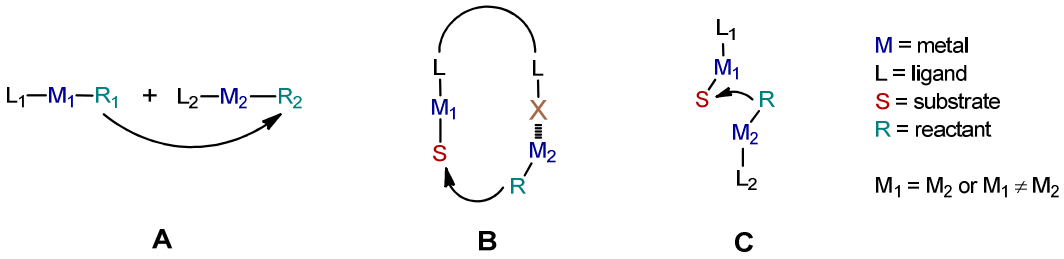

Figure 9: Types of two component metal cooperativity.[27]

Type **A**, a two component catalysis involves two different transition metal complexes, in which simply a double activation from M_1 and M_2 takes place for the reaction to progress. For instance Hidai and co-workers developed various bimetallic catalysts containing a $Co_2(CO)_8$-$Ru_3(CO)_{12}$ system for hydroformylation of olefins and the $PdCl_2(PPh_3)_2$-$Ru_3(CO)_{12}$ system for formylation of aryl iodides and vinyl iodides, which are twice as active as the corresponding mononuclear complex.[48] Type **B** applies to one metal component containing a basic site (X), even though two metals are cooperating during the key catalytic step M_2 is supplied by the stoichiometric reagent and displaced after the catalytic cycle. An example therefore is the binuclear zinc intermediate elaborated in the enantioselective 1.2-addition of organozinc

reagents to aldehydes using a chiral aminoalcohol ligand.[49,a] Type **C** is a combination of a bimetallic system connected by one ligand and type **A** described above, two metal complexes activate their respective substrates and mobilize the formation of a bimetallic site in which both ligands contribute to direct selectivity. Many supramolecular catalysts are grounded on this type of metal cooperativity.[50,51] A very appealing catalysis of type C is the kinetic resolution of epoxides by *Jacobsen et. al*.[1,33] The work of Jacobsen induces enantioselective ring opening of epoxides using a chiral dicobalt species,[1,33] the high enantioselectivity might be credited to a bimetallic catalysis in which the two molecules cooperate to activate both epoxide and water as demonstrated in Figure 10. Currently this concept was elaborated using supramolecular bowl-shaped structures.[52]

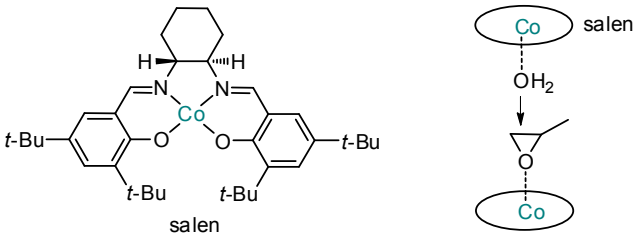

Figure 10: Enantioselective sandwich-type two center catalysis by *Jacobsen et. al*.[33]

1.2.2.1 Synthesis and Characterization

The preparation of bimetallic or cluster complexes is often challenging. There are two main problems:

- The preparation of these complexes in high yields.
- The stability under catalytic reaction conditions.

Novel synthetic routes have been designed (e.g. the use of suitable ligand-systems that can act as a template for the assembly of polymetallic complexes) to synthesize multinuclear complexes in acceptable yields. Due to improved spectroscopic techniques it is now possible to characterize catalytic systems during the reaction.[1] This has proven that many of early bimetallic systems were not stable under catalytic conditions and fragmented to mono nuclear complexes that were responsible for the catalysis. The inhibition of fragmentation of dimer and

[a] In this case even the resting state of the catalyst is binuclear.[27]

cluster systems generally centers on the employment of strong M−M bonds; this eliminates the advantage of M−M bonds as reaction sites, or the employment of multi-dentate ligand systems that supports the metal centers. Various systems in recent years were developed, however without proper characterization during the reaction it might be presumptuous to assume bimetallic cooperativity.[25,27]

1.2.3 Homobimetallic Catalysts

The majority of cases of cooperation between two soft metal centers exist for homobimetallic[a] complexes containing palladium[25,27,48,53–68], which has proven to be a versatile metal in numerous catalytic reactions.[69] Ligands of binuclear complexes mimicking enzyme active sites are mostly compartmental containing bridges between the two metal centers and as a result ensuring a fixed distance between them. Robson type compartmental ligands contain a sulfur atom, forming a bridge in-between the metal centers in its binuclear palladium complex, which catalyzes the hydration of acetonitrile to acetamide through a bimetallic pathway. They postulated a mechanism in which both acetonitrile and the nucleophilic hydroxide were concurrently coordinated to different Pd(II) centers of the homobimetallic complex, bringing both activated reactants in close proximity.[27,70] This bonding mode is very similar to the bonding in ureases with nickel centers, one Ni activates the carbonyl group of urea as an electrophile, and the other center generates the nucleophilic hydroxide attacking the activated electrophile intramolecular (Scheme 5).[68,70]

[a] As well heterobimetallic palladium complexes, especially in the field of transmetallation reactions.

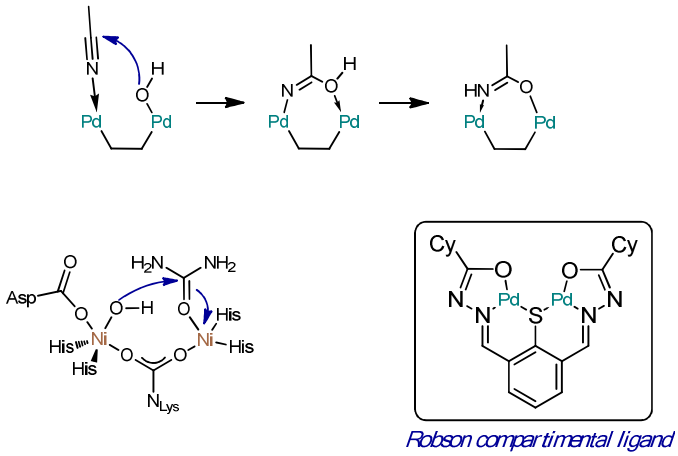

Scheme 5: Postulated mechanism for the hydrolysis of acetonitrile catalyzed by Robsons bimetallic Pd(II) complex (top). For comparison, the activation via ureases is also shown (left).[68,70]

Ozerov et al. reported a Pd(I)PNP[a] dimer, its formation proceeds through photolytic homolysis of Pd–C bonds[71] generating monomeric (PNP)-Pd fragments dimerizing to the binuclear species (Scheme 6). This Pd–Pd single bond is unsupported and can consequently be considered as a prospective two-electron reductant. This is suitable for the bimetallic, homolytic activation of H-E[b] bonds, added to the Pd–Pd bond it results in the (PNP)PdH and (PNP)PdE complexes, respectively, which would be considered a binuclear oxidative addition.[25,72] The PNP ligand would be considered a ligand of type **III** in Figure 8, containing a direct M–M bond.

[a] PNP = bis[2-(diisopropyl-phosphanyl)-4-methylphenyl]amido, a pincer ligand.

[b] i.e.: NH_3 and H_2O.[25]

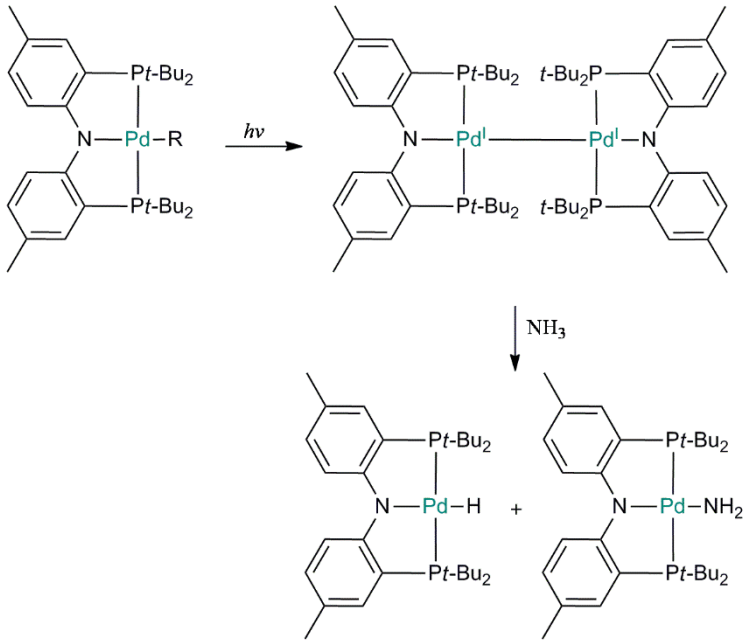

Scheme 6: Binuclear activitation of ammonia at a Pd^{I}–Pd^{I} dimer.[72]

The chemistry of Pd(0), Pd(I), Pd(II) and Pd(IV) is well investigated[63,67,73–78], however only few Pd(III) complexes in catalysis have been established yet. A recent example for bimetallic Pd(III)[a] complexes catalyzing carbon-heteroatom bond formation was developed by Powers and Ritter (Scheme 7). They formed a Pd(II) (d^8) complex, through cyclopalladation, in which the Pd–Pd distance is fixed in a close proximity to each other (Pd–Pd distance of 2.8419(8) Å) due to bridging acetate ligands. This bimetallic complex can be oxidized by two-electrons with an oxidant X_2 (X = Cl, Br), each Pd is oxidized by one electron forming d^7-complexes. A d^7 electronic configuration is anticipated to form a Pd–Pd single bond. The C–X bond of the d^7 dipalladium complex can be eliminated reductively by redox chemistry; each Pd has to contribute and is reduced by one electron. During this process the lowest unoccupied orbital (LUMO) of the d^7 dipalladium complex, which is antibonding in respect to the Pd–Pd bond, is occupied with two electrons, and hence Pd–Pd bond cleavage and reduction of both Pd(III) atoms by one electron occurs ($d^7 \rightarrow d^8$).[53–55]

[a] A mechanistic alternative to catalytic Pd(II)/Pd(IV) redox cycles in the acetoxylation of 2-phenylpyridine.[53–55]

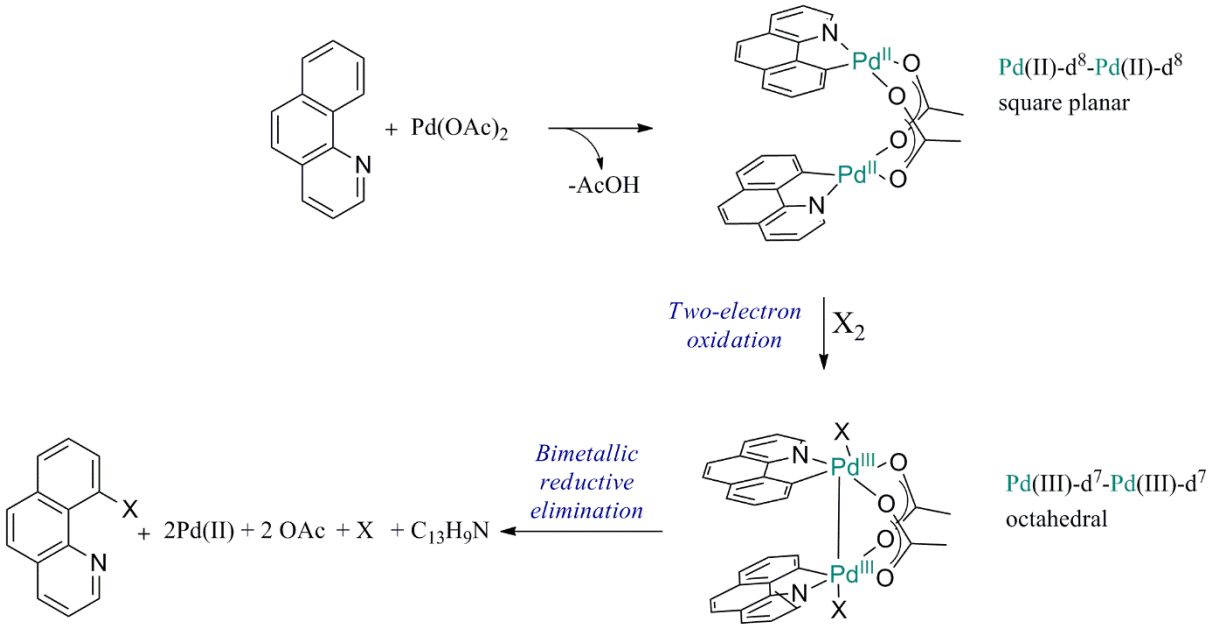

Scheme 7: Two-electron oxidation and bimetallic reductive elimination by Powers and Ritter.[53–55]

An electrochemical application of dipalladium complexes was developed by *Dubois et. al.*; in the literature, it is well known that bimetallic cooperativity might improve CO_2 binding[79], and his bimetallic catalyst reduces CO_2 to CO[80,81] with better activity than the mononuclear corresponding species[82]. They proposed that both Pd centers interact cooperatively: with a low acid concentration the reaction rate shows a first order dependence on the acid concentration, whereas for the mononuclear analogues a second-order dependence has been detected. This observation suggests a cooperative mechanism for the bimetallic catalyst as displayed in Scheme 8. They presume that both CO_2 and one catalyst molecule are involved, since at high acid concentration first-order dependence of the rate-determining step is consistent with two palladium atoms and one CO_2 molecule in the transition state, which could indicate cooperative binding.[80,83]

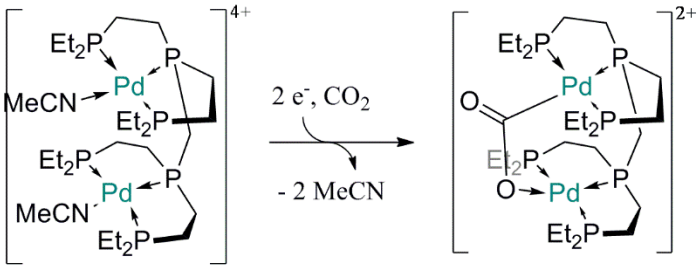

Scheme 8: First steps of the electrochemical reduction of CO_2 to CO catalyzed by a dipalladium complex developed by Dubois.[80]

A highlight[a] in bimetallic catalysis was achieved by *Stanley et al.* with a binuclear rhodium catalyst for hydroformylation of α-olefins with a chelating and bridging tetraphosphine ligand.[84,85] Hydroformylation, also known as the oxo-process, is the transition-metal catalyzed conversion from olefins to aldehydes using carbon monoxide and hydrogen (Scheme 9). Important factors in this process are the catalytic activity, chemoselectivity and regioselectivity.

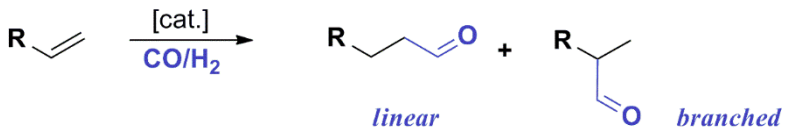

Scheme 9: Hydroformylation of 1-octene, showing the possible formation of linear and/or branched aldehydes. R = *n*-C_6H_{13}.

Their objective was to obtain bimetallic cooperativity through the synthesis of a bridging moiety in their tetraphosphine ligand, the *rac*-$[Rh_2(nbd)_2(et,ph\text{-}\mathbf{P4})]^{2+}(BF_4)_2$ (nbd = norbornadiene) catalyst (Figure 11, left) showed high conversion and good product selectivity towards linear aldehydes in the hydroformylation of 1-hexene, minimizing undesired side reactions like isomerization and hydrogenation. The *meso* form also shows better catalytic activity than the isolated monomer, the performance of which is admittedly poor (Table 1),[84] and is 40% faster than the commercially established Rh/PPh_3 catalyst.[27] They justified the catalyst structure by FT-IR and NMR spectroscopic analyses and proposed a mechanism.[85,86]

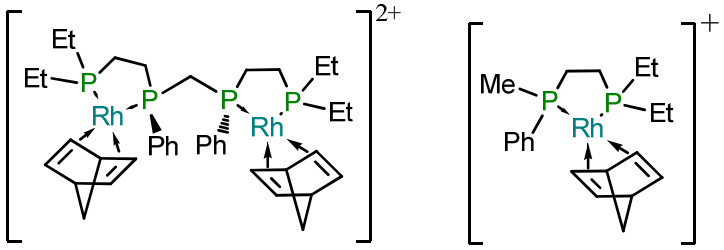

Figure 11: The *rac*-form of the bimetallic rhodium catalyst by *Stanley et al.* showed better catalytic activity and selectivity in comparison to the mono-nuclear equivalent in the hydroformylation of 1-hexene.[84,85,87]

catalyst	TOF/min^{-1}	Conv. %	Lin:br	Isom %	Hydrog. %

[a] Not concentrating on biomimetic systems.[27]

Mono	0.02 (2)	1.1 (3)	3.1 (2)	42 (3)	14 (4)
Rac-	10.6 (5)	85 (1)	27 (1)	8 (1)	3.4 (3)
Meso-	0.9 (1)	16 (3)	14 (2)	4(1)	2.3 (3)

Table 1: Catalyst activity of the mono-nuclear complex in comparison to the dinuclear strongly suggests metal cooperativity in Stanley's system.[84,85]

Reek et al. reported a similar mechanism in the cooperative Rh-catalyzed asymmetric hydrogenation of olefins.[88] The developed catalyst is a binuclear neutral Rh–P–N–Rh-bridged complex; it outperformed other catalysts in hydrogenation of sterically hindered substrates Table 1). Kinetic studies of the catalytic reaction suggest that the dimeric structure is stable during the catalysis, and NMR studies disclosed that the dimer shown in Figure 11 is the resting state of the catalytic cycle. Further computational studies indicate a short Rh–Rh distance, implies a cooperative effect during the substrate activation.[83,88]

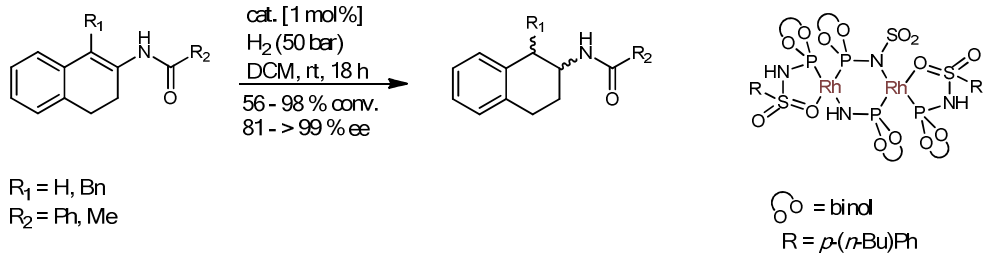

Scheme 10: Cooperative Rh-catalyzed asymmetric hydrogenation of olefins effected by *Reek et al.* [85]

1.2.4 Heterobimetallic Catalyst

As previously mentioned heterobimetallic complexes augment the variability for the coordination of two metal centers by employing different metals with complementary properties. Often hard and soft metals are combined in one complex; the incorporation of a hard metal center (i.e. a Lewis acid site) close to a soft mononuclear center might significantly modify the reactivity and selectivity.[27,83,89] Rh–Ti and Rh–Zr complexes delivered good results for the hydroformylation of olefins.[90] Assuming that the reaction proceeds through the Rh center, the second metal regulates the electron density at the Rh center during the catalysis.[91–93] In hydrogenation another heterobimetallic complex type $[H(CO)(PPh_3)_2Ru(\mu\text{-bim})M(cod)]$ (bim = 2,2'-bisimidazolate, cod = 1,5-cyclooctadiene, M = Rh, Ir) displayed related cooperativity; these catalysts show

roughly 30 times higher activity in the hydrogenation of cyclohexene than the corresponding mononuclear model complexes.[94]

1.2.5 Bimetallic Catalysts developed by van Leeuwen and Co-Workers

For many decades van Leeuwen and co-workers have been interested in the optimization of homogeneous catalysts with special focus on the bite angle.[20,21,24,95–99] In recent years they developed various wide bite-angle ligands forming bimetallic catalysts based on the scaffolds of SPANphos,[100,101] DBDOCphos[34] and BFBFphos.[34] The dirhodium complexes of SPANphos type ligands and DBDOCphos (Figure 12) were tested in the carbonylation of methanol and showed better activity than comparable monometallic species (**Table 2**). It was discovered that SPANphos could not only trans-chelate as a monometallic compound: a derivative SPAN-POP for instance showed approximately four times higher activity upon changing the ligand-to-metal ratio from one to two, indicating a bimetallic species.[100,101] The backbone flexibility due to the spiro-moiety enabled the ligand to adopt different coordination modes. If this structural flexibility is not desired the scaffold needs to be changed to provide a more rigid backbone or the bite angle had to be changed. As a result the group designed rationally a new family of diphosphines to produce exclusively bimetallic complexes retaining a P···P connectivity that is similar to that found in SPANphos type.

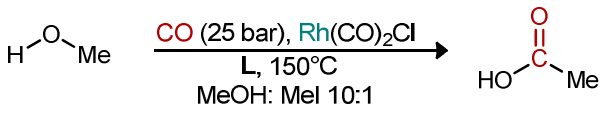

Scheme 11: Reaction conditions for the carbonylation of methanol with different ligands.[34,100,101]

L	L:M	TOF ($h^{-1}L^{-1}$)	TON (on L)	t (h)	Conv %	MeOH:Rh
SPANphos	1	728	1093	1.5	11.3	9670
SPAN-POP	1	483	725	1.5	7.5	9670
SPAN-POP	2	1842	2764	1.5	14.3	9670
DBDOCphos	1	979	1468	1.5	13.8	4835

Table 2: Activity of different diphosphine ligands on the Rh- catalyzed carbonylation of methanol.[34,100,101]

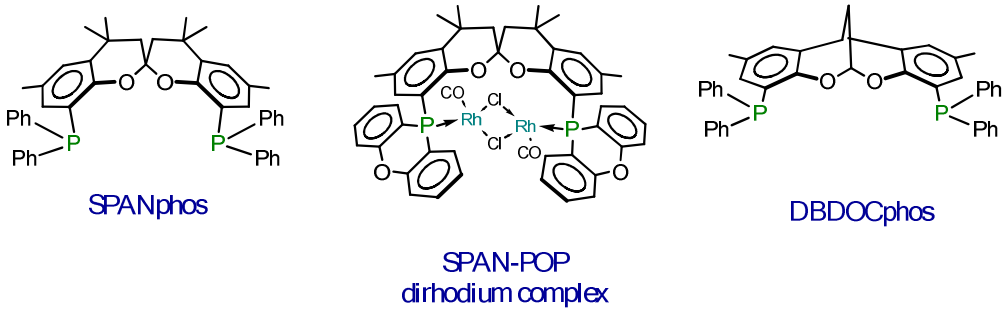

Figure 12: Structures of SPANphos, the proposed dirhodium complex of SPAN-POP and DBDOCphos.

The use of the 2,10-dimethyl-12H-6,12-methanodibenzo[d,g][1,3]dioxocin (DBDOC) and 5a,10b-dihydrobenzofuro[2,3-b]benzofuran (BFBF) scaffolds enabled bimetallic coordination, however these scaffolds proved to be able to coordinate in two different bimetallic modes, as a bimetallic dimer and as a mono-ligand bimetallic halogen bridged species.[34,102–104] Hence it is difficult to control which complex is the active species during the catalytic process. To reduce complexity, a ligand had to be designed which favors one specific coordination mode. A possibility to promote the formation of well identified single complexes would be to add two chelating moieties, as will be described in the following chapter.

Chapter 2 Design and Synthesis of Tetraphosphine Ligands

2.1 Introduction

An important method to improve the catalytic efficiency in homogeneous catalysis concerns the design of new phosphine-based catalysts facilitating the required steps of the mechanism through optimization of electronic and steric effects. In recent years the use of bimetallic transition metal complexes and metal-clusters for homogeneous catalysis has received great interest because it is recognized that the possibility of multi-electron transfer or the ability to form multicenter metal-to-ligand bonds may significantly aid in the activation of the substituents.[105] As discussed in the introduction, bimetallic catalysis provides interesting options,[1,25,28,48,50,53,55–57,65,84–87,95,97,105–130] such as *Stanley et al's.* bimetallic rhodium catalyst for hydroformylation (Figure 13), where the idea was to obtain bimetallic cooperativity through the synthesis of a bridging tetraphosphine ligand. The *rac*-catalyst showed high conversion and good product selectivity towards linear aldehydes, and minimized undesired side reactions like isomerization and hydrogenation. The *meso* form also shows better catalytic activity than the isolated monomer, the performance of which is poor.[84]

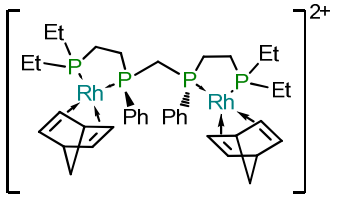

Figure 13: The *rac*-form of the bimetallic rhodium catalyst by *Stanley et al.* showed improved catalytic activity in hydroformylation relative to a mononuclear analogue.[87]

Our ligand design has superficial similarities to the tetraphosphine of Stanley and in the next section its composition will be discussed in detail. The ligands that we have developed may clearly have quite widespread application, but were envisaged primarily for the palladium catalyzed hydroformylation of 1-alkenes. Certain aspects of their structure reflect this: for instance, palladium catalysts tend to operate better with very basic ligands, in combination with moderately coordinating anions that confer a moderate electrophilicity at the metal center (see in detail chapter Chapter 1).[131] There are three essential features of the molecular architecture of our ligands (Figure 14). We use a spacer, which is a rigid organic backbone ensuring exclusively

the formation of bimetallic coordinated species. This is based either on benzofurobenzofuran (BFBF) or methanodibenzodioxocin (DBDOC) frameworks, which have been previously used as ligand scaffolds by the group of *van Leeuwen et al*. (Figure 15). This binucleogenesis arises from the seven quite rigidly linked backbone atoms that separate the two phosphines (Figure 16).[34] The innovation in the work here is a further alkyl-chain of potentially variable length that creates a chelating diphosphine on each half of the backbone. The number of carbon atoms in this chelating functionality can, at least in principle, be varied as a function of the catalytic system envisaged. The third important consequence of our design is that the phosphines connected to the backbone have chirality centered at the phosphorus atoms, which increases the number of isomers. Whilst increasing the possibility of finding the most efficient catalyst through generating multiple diastereomeric formulations, and providing obvious capacity for enantioselection, this feature complicates the synthetic protocol and has clear disadvantages in terms of atom economy. We will return to this below.

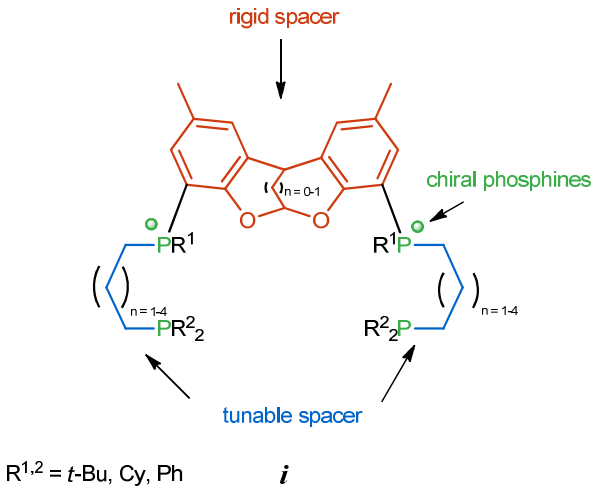

Figure 14: The ligand has a rigid backbone spacer and tunable chelating diphosphines. The phosphines connected to the backbone have chirality centered on the phosphorus atom.

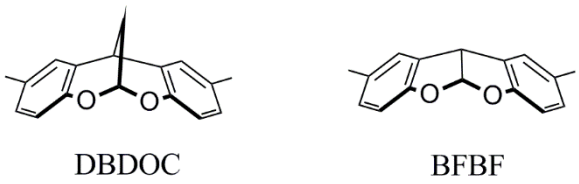

Figure 15: The two rigid organic spacers employed to ensure the formation of exclusively bimetallic species.[34,132]

The proposed ligands could theoretically form two broad classes of complexes (Figure 17). In one case, the metals could coordinate independently to the chelating arms (**2**); in the other, they could be linked through halogen- or carbonyl-bridges (**3**). In an ideal (intermediate) case that we target, both forms might feature; here cooperative catalysis between the two centers might occur, through the formation of transient bridged species, without the formation of very stable bridged dimers that would be likely to provide thermodynamic sinks and prevent catalytic turn-over. Thus, it can be hoped that a well-designed system might allow these metal complexes to undergo cooperativity, improving the catalytic activity in homogenous catalysis.[86]

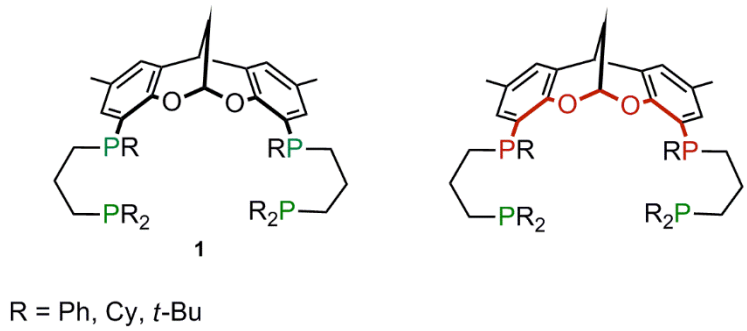

Figure 16: Schematic structure of the tetraphosphine ligands targeted in this work. The chelating phosphines are separated by seven atoms, as exemplified here for the DBDOC backbone.[34]

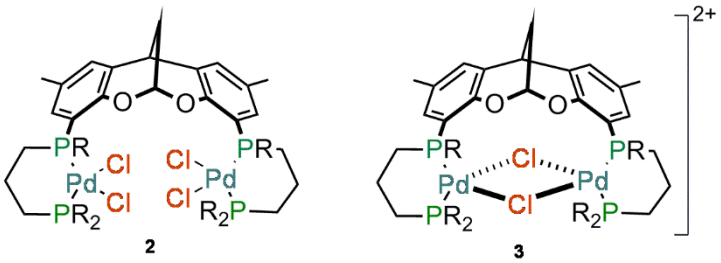

Figure 17: Bimetallic species that might be generated by a tetraphosphine. The case illustrated has a three- carbon linker between the chelating phosphorus atoms with Pd(II) centers. Complex 2 has non-cooperative metal centers whilst complex 3 is a dicationic chloride-bridged Pd(II) complex.

2.2 Symmetry of the Target Ligands

The symmetry and stereochemistry of our targeted molecules is a little complex, as a result of the combination of the organic framework with two chiral phosphines.

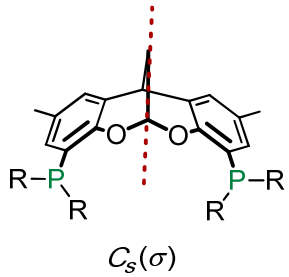

Figure 18: The DBDOCphos class of ligands, in which all phosphine R-substitutuents are identical, have a mirror plane in the plane of the C3 bridge, which gives rise to C_s symmetry.

In the DBDOCphos class of ligands, given in Figure 18, the mirror plane gives rise to C_s symmetry. However, when we introduce chiral phosphines, the symmetry is lowered significantly. In all of our target molecules, both phosphines connected to the backbone carry the same R- and R'-groups, and summing two equally composed non-resolved chiral centers obviously generates a *rac*- and *meso*-combination of phosphines (Scheme 12). Once these are recognized, it is necessary to introduce the backbone component, which has C_s (*meso*-) symmetry.

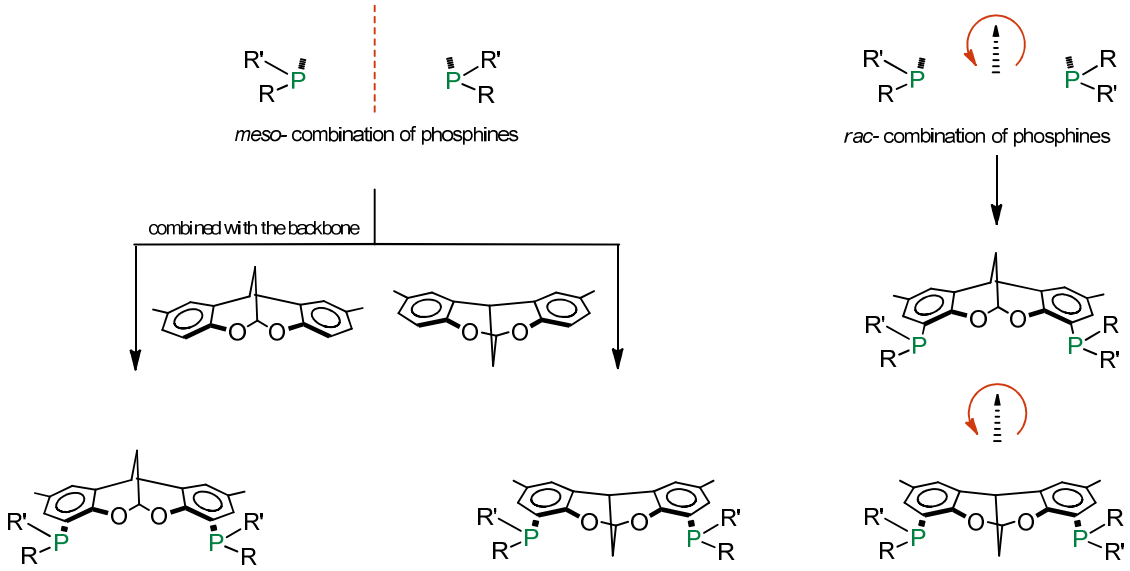

Scheme 12: The symmetry of DBDOC backbones bearing chiral phosphines shows in the case of a *meso*-phosphine combination, C_s symmetry (left), for the *rac*-phosphine combination, the target ligand has C_1 symmetry (right).

The *meso*-phosphine combination has the same symmetry properties as the non-elaborated backbone: a σ-mirror plane between the phosphines of opposing chirality, and this combination

of an σ- (mirror) backbone and σ- (mirror) phosphine symmetry obviously leads to overall σ-mirror (C_s) symmetry. It should be noted that the backbone does not have a horizontal mirror plane, so that it can take up two different orientations relative to the *meso*-phosphine pair. This gives rise to two different "meso-"forms, since the "up" or "down" orientation of the bridgehead generates diastereomers. The chiral phosphine substituents thus generate a *pseudo*-chiral center at the acetal carbon.[a] According to the Cahn-Ingold-Prelog (CIP) rules[133] this results in **A**, described as (*r*) and **B**, described as (*s*).

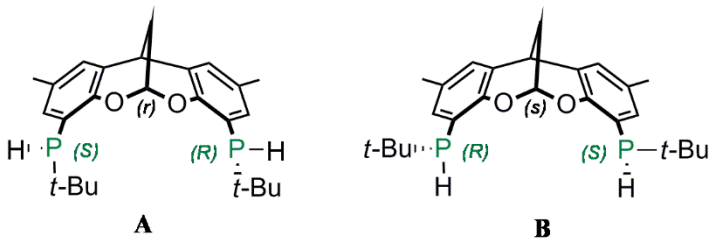

Figure 19: Symmetry of *meso*-di(*sec*-phosphines) of the type targeted in this work displays two different orientations. The different orientations of the *t*-Bu groups relative to the bridgehead carbon clearly show that two *meso*-compounds are non-superimposable. Following the Cahn-Ingold-Prelog rules, A is defined (*r*) at the bridgehead, B is (*s*).

When the backbone is substituted by the *rac*-phosphine combination, which has a C_2 rotational symmetry axis, one single diastereomer is observed. This may not be intuitive, but the 180° turn about the C_2 rotation axis that relates the phosphines also has the effect of 'inverting' the backbone, so that the 'up' and 'down' positions of the backbone in the molecule are chemically indistinguishable within a C_2 frame of reference (Scheme 12). This is an expression of the fact that the C_2 axis does not define distinct sides to the horizontal plane that bisects the phosphorus atoms in the way that the *meso* phosphine combination does. Unlike the case of the "*meso*-" diastereomers observed above, this "*rac*-" form does not have a mirror in the plane of the three-carbon bridge (this, of course, is a prerequisite for a *rac*- phosphine pair), so that the two halves of the molecule are non-equivalent. One obvious consequence of this reduced degree of symmetry is that, for example, the ^{31}P–NMR of the "*rac*" diastereomer will take the form of two lines, whilst each "*meso*" diastereomer gives rise to one line only.

[a] Of course, it simultaneously generates pseudochirality at the other terminal carbon atom of the 3-carbon bridge of the dibenzodioxocin, but either of the two descriptors alone is enough to fully describe the structure. In the case shown in Figure 19, the stereodescriptor of the second pseudochiral centre is the same as that of the first, making further descriptors redundant.

In total we obtain three diastereomers, two C_S-symmetric *meso*-diphosphines, and a C_1-symmetric *rac*-diphosphine: *R*,*S*,*r*; *R*,*S*,*s*; (±)*R**,*R** respectively.[134] A consequence of the statistics of the synthesis of the *rac*-diphosphine from either of the (entirely formal) "up" and "down" backbone configurations is that, were the relative product ratios of the three diastereomers to be governed entirely by statistics, the *rac*- compound would appear in double the amount of each *meso*-compound.

2.3 Retrosynthetic Analyses of the Designed Ligand system

To find suitable synthetic methods, a retrosynthetic analysis of the target is necessary. The potential synthetic approaches, which were intended to be compatible with eventual scale-up, were conditioned by three self-imposed guidelines:

- Where possible, costly or toxic reagents were to be avoided.
- Individual steps were to be as high – yielding as possible, so as to ensure reproducibility and facilitate purification (even where this means adding more steps).
- Avoidance of chromatographic separations wherever possible, including in the separation step of the diastereomers.

Furthermore, a flexible synthetic route to the ligands (***i***, Figure 14) was desirable to allow access to a variety of structural analogues. Clearly, in an idealized case, it would also be desirable to find a synthesis avoiding any complex separation of diastereomers.

To obtain the tetraphosphine ligands, there are two main disconnection points (Figure 20). The discussion here will mainly concern the DBDOC backbone but it is reasonable to assume that the retrosynthetic principles derived for DBDOC can equally be applied to BFBF.

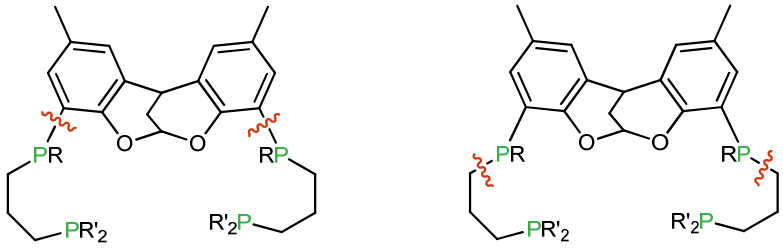

Figure 20: Two main retrosynthetic methods have to be regarded. In molecule 4, preformed diphosphine chains can be introduced, whilst in molecule 5 the two side-arm phosphine pairs are introduced one by one (initially the backbone proximal-, then the end chain-phosphines) to the backbone. For clarity, the DBDOC backbone is demonstrated here, though the BFBF system could equally be elaborated in a similar manner.

Molecule **4** shows the disconnection point between the diphosphine chains and the backbone; there are various methods applicable to synthesize the target molecule following this disconnection method depending on the synthons of the corresponding molecules. Molecule **5** has a second disconnection point in-between the two chelating phosphines, implying that the two different ends of each chelating phosphines are introduced stepwise into the backbone. We will discuss in detail the retrosynthetic possibilities for these two main disconnection methods below.

2.3.1 Retrosyntheses of the Introduction of Two Diphosphine Chains

The retrosynthetic analysis using the designated disconnection points in molecule **4** is outlined in Scheme 13. The disconnection point is between the backbone and the diphosphine-chains. It can give rise to two methods using opposing polarities. Method **A** employs electrophilic diphosphine chains (**7**) and a nucleophilic backbone (**6**) and can be considered to be a 'natural' disconnection; it allows nucleophilic displacement from phosphorus of a suitable leaving group (LG), for instance chloride (**9**), upon reaction with an organometallic reagent such as a lithiated backbone (**8**). In method **B,** the backbone is electrophilic (**10**) and the diphosphine chains nucleophilic (**11**). This gives rise to a formally 'unnatural' (S_N2) reaction at the aryl group, which is normally disfavored. The disconnection therefore requires metal-mediated catalytic coupling reactions of an aryl-bromide (**12**) or its equivalent with a secondary phosphine on the diphosphine chains (**13**). Typical transition metals for these catalytic methods are palladium, copper or nickel.[135–142]

An analysis presented in the terms above would normally imply that method **A** would be preferred over **B**, but this is not likely to be the case here; a side-arm synthon having a sec-phosphine functionality (as required by methods **B**) is likely to be vastly easier to prepare- and,

especially, to purify- than one having a leaving group at the phosphorus (needed in **A**). In this context, it should be noted that the catalytic nature of method **B** is likely to make it quite highly dependent on the substrate purity, to limit catalyst poisoning.

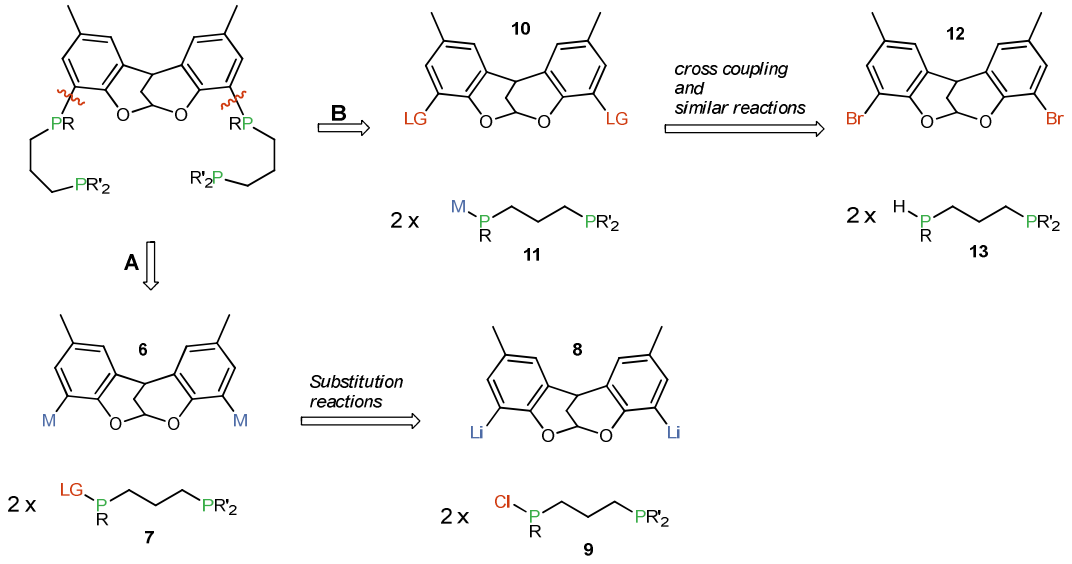

Scheme 13: Retrosyntheses for connecting preformed diphosphine-chains to the DBDOC backbone. Two complementary retrosyntheses are given. Method A employs a nucleophilic backbone and electrophilic diphosphines, exemplified by a lithiated backbone and chloro-diphosphines undergoing a simple substitution reaction. Method B, on the contrary, involves an electrophilic backbone and "nucleophilic" diphosphines, for instance a backbone-bromide could react with a secondary diphosphine chain in a cross-coupling reaction.

2.3.2 Retrosyntheses of the Introduction of the Phosphines 2-by-2 (stepwise)

A different generalized retrosynthetic pathway in molecule **5** involves the stepwise introduction of the different pairs of phosphines that form the chelate rings. In Scheme 14 the first retrosynthetic step is a substitution involving a nucleophilic backbone (**6**) and electrophilic phosphines (**17**). Methods for achieving this, such as the use of bulky R-groups or phosphorus electrophiles having the general formulation PRXY where X and Y are leaving groups of different basicity, will be described in the section that treats experimental detail. Chiral phosphines are generated in this step.

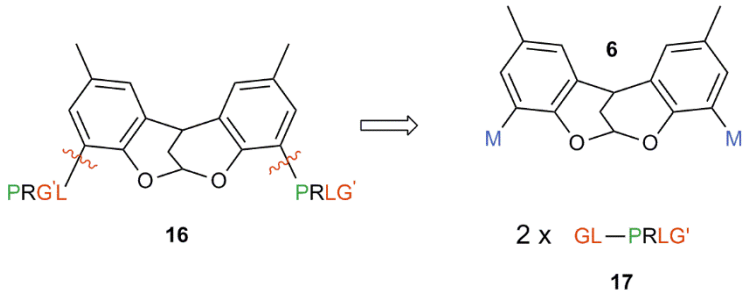

Scheme 14: In the first step of the retrosynthetic analysis electrophilic phosphines with nucleophilic backbones undergo nucleophilic substitution.

If we take a closer look into the possible disconnection points of molecule **5** and its retrosynthetic approaches, we will see that there are different possibilities (Scheme 15). Method **C** constitutes a simple nucleophilic substitution between nucleophilic phosphides (**21**) on the backbone and electrophiles having the desired carbon chain length and bearing terminal phosphines (**20**). The corresponding synthetic routes can be expected to be very efficient under well-chosen conditions.[143]

Retrosynthetic approach **D** involves the attachment of preelaborated phosphines (**20**), with the desired carbon chain length and bearing a leaving group. These electrophiles undergo with the nucleophilic backbone-*bis*-(*sec*-phosphine) (**21**) a simple S_N2 substitution reaction. A related approach employs cyclic sulfates in the first step: an initial ring opening with the metallated backbone-*bis*-(*sec*-phosphine) gives the corresponding sulfate-anion (**24**), whose sulfate group can act as a leaving group and gives rise to the target molecule upon reaction with lithiated phosphines (**25**). Cyclic sulfates have the great advantage of being available in a variety of different ring-sizes[144–146]; consequently a number of different ligands could be obtained in a short time using simple readily available starting material.

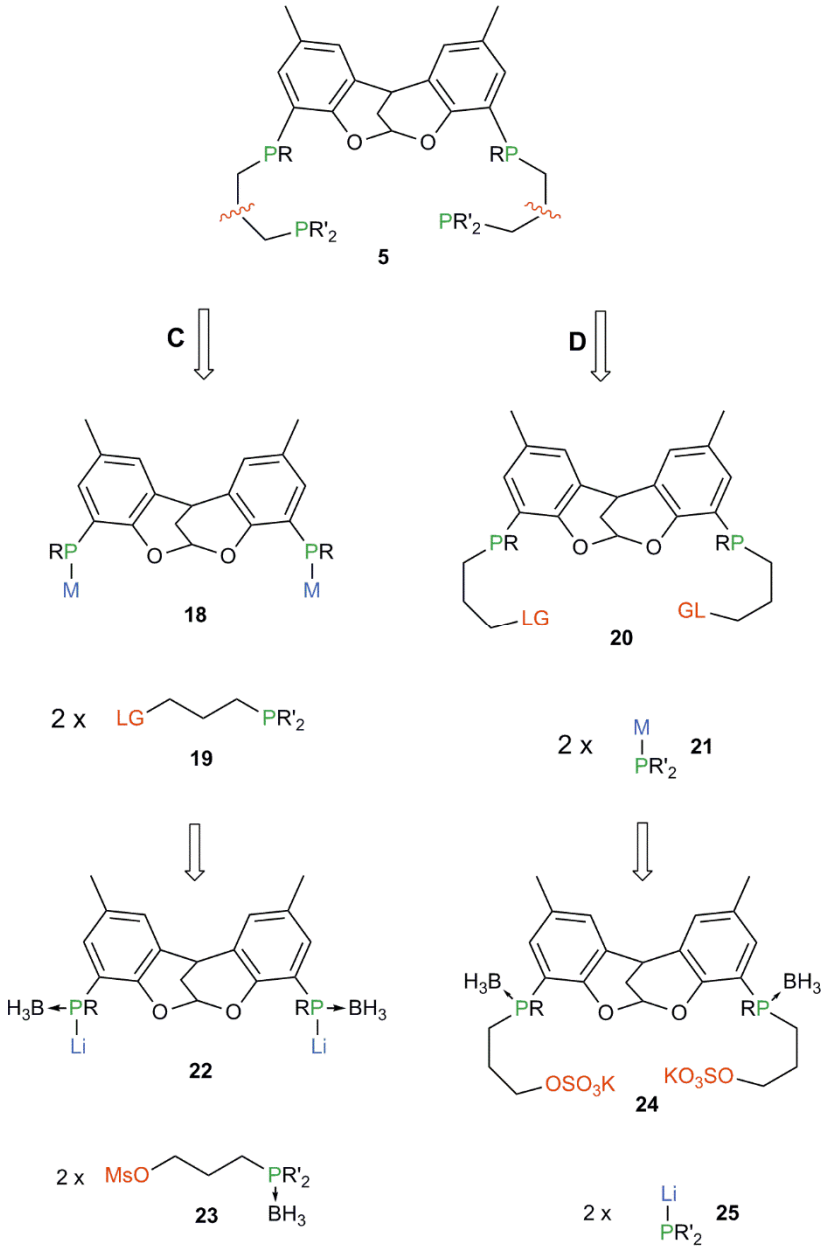

Scheme 15: Retrosyntheses for tetraphosphines through the stepwise introducion of phosphines to the DBDOC backbone. The examples here are shown for a C-3 chelating chain.

This retrosynthetic analysis of the tetraphosphine compounds shows that there are a number of versatile approaches to obtain the desired molecule family. These have been explored in detail. The best synthetic results have been obtained using method **C.** This approach leads to tunable side-arm length, which could be quite interesting for different catalytic reactions. Method **D** is very versatile in providing a concise route to different tetraphosphines due to the commercial availability of various cyclic sulfates. The retrosynthetic approaches **A** and **B** have been found

to be difficult because of the inaccessibility of the requisite diphosphine synthons. Various methods were applied while none showed good results. Subsequently the synthetic routes will be discussed in detail, explaining the advantages, challenges and problems of several methods.

2.3.3 Protection of Phosphines

In many of the retrosyntheses described above, there are inherent incompatibilities between nucleophilic $\sigma^3\lambda^3$-phosphorus centers and a variety of electrophilic functionalities, which often need to be present on the same molecular fragment. These incompatibilities obviously mean that some sort of reversible protection will have to be brought to the system. Because many $\sigma^3\lambda^3$-phosphorus centers are inherently difficult and unpleasant to handle, (malodorousness, oxidation sensitivity, potential pyrophoricity, toxicity) it is usually the phosphorus lone pair that receives the protection. The most common "protecting groups" are oxides, sulfides and boranes (Figure 21). Their individual advantages and disadvantages are treated briefly here.

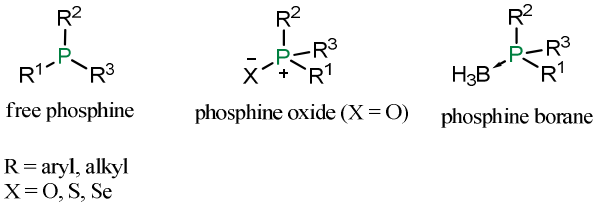

Figure 21: Free and protected phosphines. P-X (X = O, S, Se) and P-BH_3 are displayed.

Phosphine boranes: in these compounds, boron is connected to phosphorus through a dative bond. $R_3B{\bullet}PR_3$ complexes generally exhibit high thermal stability[70] and, due to the low polarity of the P–B and B–H bonds, they are normally stable and rather unreactive. Their stability towards hydrolysis and oxidation, for instance, reflects the basicity of the phosphine, and falls as a function of R in the order R= alkyl > aryl >> H and this stability enormously simplifies the purification of key tertiary phosphine intermediates. Another useful feature in synthetic terms is that hydrogen atoms or methyl groups adjacent to the phosphorus atom are activated; the first of these is especially useful for the functionalization of our backbone secondary phosphines, as well as in our diphosphine chain synthesis.

One problem with phosphine boranes in synthetic terms relates to their observation by ^{31}P–NMR. The ^{31}P isotope has a natural abundance of 100 %, a spin of ½, and very high sensitivity, 377 times that of ^{13}C[147], all of which facilitate the interpretation of ongoing reactions by *in situ*

NMR studies.[148] Phosphine boranes negate many of these advantages, because ^{10}B and ^{11}B have both quadrupolar relaxation that broadens the NMR signal.[59] This may cause a problems in detecting individual resonances which lie close to each other in the PNMR spectrum (such as diastereomers; Figure 22, **39c** vs **38c**) and the very broad signals that they generate obviously reduce the sensitivity of any measurement. The cleavage of the P–B bond is uncomplicated and can be achieved using amines (classically $NHEt_2$, DABCO, etc.) in straightforward S_N2 reactions at boron which require moderate to high temperatures (40- >100°C as a function of the substituents). These temperatures may become high enough to cause racemization of enantiopure phosphines during the deboronation step when all substituents are alkyl.[77] In such cases, acids ($HBF_4 \cdot Et_2O$), group[76] can be used to provide fast deboronation at low temperatures. Both methods proceed under retention of configuration at phosphorus.[56,69,71–77] Another advantage of acid- induced deboronation is the short reaction time of 1-2 h, whereas deprotection using amines can take more than 12 h.

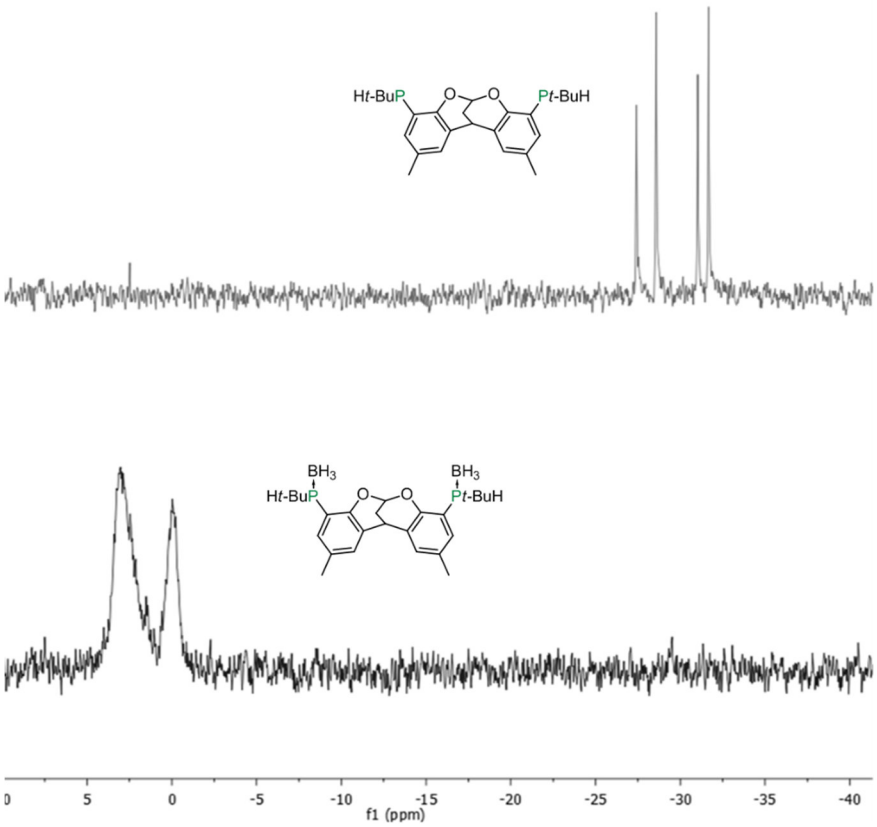

Figure 22: Illustration of line- broadening effects in the $^{31}P\{^1H\}$–NMR spectra of phosphine borane complexes. Above **38c**: The diastereomers result in four singlets (free phosphines demonstrated), which comprise one signal each for the two *meso*-compounds, and two signals for the *rac*-compound whose structure has C_1 symmetry and in which the two phosphines are non-equivalent. Below, **39c**: after protection of the phosphines with borane-

groups, the four signals shift downfield and appear as two broad overlapping sets of signals, which are difficult to distinguish.

Phosphine chalcogenides[148]: Phosphine oxides are polar, air-stable compounds and this second property facilitates their synthetic handling. They are more similar to phosphine boranes than is generally recognized because, rather than being a true double bond, all data indicate that the PO interaction is a comprised of a P-O single bond with a very significant negative hyperconjugation between the electron- rich oxygen and the formally positively charged phosphorus. As a consequence, the P-O bond has an order of about 1.3 and a cylindrical electron distribution around the PO bond means that the P and O atoms can rotate freely.[148–150] As with the phosphine boranes, the resulting high positive charge at phosphorus makes any associated PH and PCH groups rather acid, which aids in their functionalization. It is synthetically important to note that secondary phosphine oxides can be deprotonated and then reacted with electrophiles with complete retention of stereochemistry at phosphorus.[151–153]

Phosphine oxides present potential difficulties associated with their reduction through pseudorotation[a,b] process of intermediate pentacoordinated phosphoranes.[152–155] Few reagents allow the reduction of phosphine oxides without racemization.[156] Common reducing agents such as $HSiCl_3/Et_3N$ or SmI_2/THF require long reaction times[157], the stereoinformation obtained is highly dependant upon on the compound and the reducing conditions.[156] Another more recent method by *Imamoto et al.* reduces P–O compounds using methylation reagents like MeOTf and lithium aluminium hydride.[158]

As regards spectroscopy, P=X (X = O, S, Se) signals show similar sharpness to the free phosphines, so closely spaced signals arising from diastereomers can usually be distinguished by ^{31}P NMR spectroscopy.[148] In conclusion, where chirality criteria are not overwhelming, P=X (X = O, S, Se) compounds are ideal, in providing conditions where ^{31}P–NMR spectroscopy can be used as a fast tool of analysis and generating air stable compounds.

Synthetic methods based both on phosphine boranes and oxides will be used in this work. The importance of scale-up for our work requires a method generating stable diphosphine backbones

[a] Pseudorotation is a low-energy process; the axial and equatorial substituents are exchanged pairwise, from a trigonal bipyramidal structure. The presence of a pentacoordinate intermediate does not ensure racemization, although multiple successive pseudorotations will cause inversion of an organophosphorus compound.[154,331]

[b] There are different opinions about pseudorotation in the chemical community, *Kyba et al.* provides evidence for the absence of any pseudorotation in the potential intermediate and suggests that substitution might be considered to be a typical S_N2-type reaction.[332] For a recent discussion, see: E. V. Jennings, K. Nikitin, Y. Ortin, and D. G. Gilheany *J. Am. Chem. Soc*. 2014, 136, 16217−16226

for storage; hence air stable compounds are desirable. Perhaps predictably, phosphine boranes have produced the best result.

2.4 Synthetic Methods

In the following sections the synthetic routes applied to our target systems will be described in detail. The synthesis of the activated aromatic backbones (DBDOC, BFBF) for functionalization is the starting point for all approaches; hence it will be explained separately.

2.4.1 Synthesis of the DBDOC-H_2 Ligand Precursor

Banihashemi and *Rahmatpour* reported the synthesis of 2,10-dimethyl-12H-6,12-methanodibenzo[d,g][1,3]dioxocine (DBDOC) skeleton obtaining a yield of 91 %, from an acid catalyzed condensation reaction between two moles of *p*-cresol (**26**) and malonaldehyde tetramethyl acetal (**27**). Various acids were tested, and their optimal procedure employs trifluoroacetic acid (TFA) acting as solvent and catalyst. Their proposed mechanism has a proton-induced Friedel-Crafts reaction to give **28** as the first step, followed by entropically favored intramolecular acetalization (Scheme 16).[132,159]

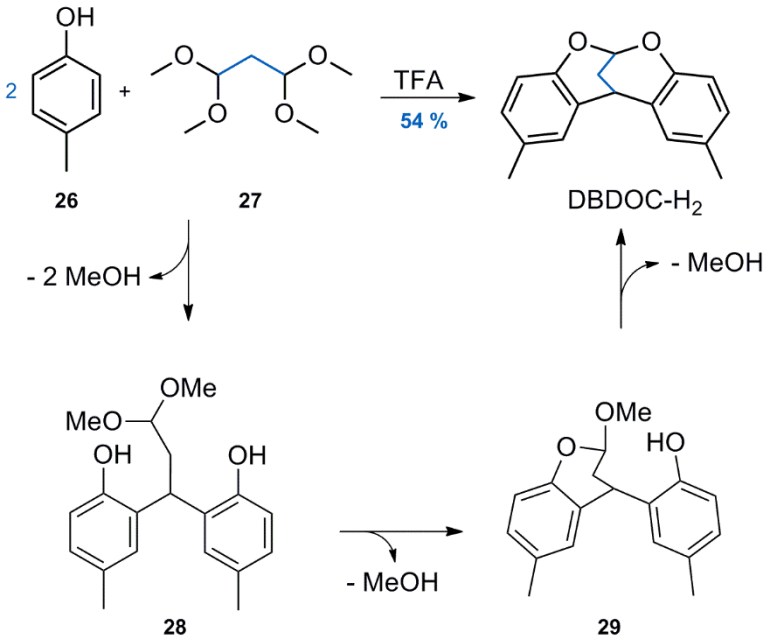

Scheme 16: According to *Banihashemi* and *Rahmatpour* DBDOC-H_2 is obtained through an acid catalyzed condensation reaction; in the first step a Friedels-Crafts condensation precedes, followed by an intramolecular ring closure.[132,159]

We were interested to increase the reaction scale without changing the literature reaction conditions significantly; *Banihashemi* and *Rahmatpour* successfully obtained very good yields of product form relatively small amounts of solvent on modest reaction scales. However, due to the vigorous exothermic reaction starting 30 seconds after adding *p*-cresol (0.6 M) and tetramethoxypropane[a] (0.3 M), the scale up of the described procedure was difficult and could only be taken to 40 g for safety reasons. The current best practice involves cooling conical flasks containing TFA (150mL) in an ice bath, and simultaneously adding the two reactants over one minute whilst stirring powerfully to continue mixing for as long as possible before the reaction mixture solidifies. This gave approximately 40 g product per flask. After the very exothermic reaction slowed down, the reaction mixture was allowed to stir in a well-ventilated fume hood for two more days. Subsequently the reaction was treated as described in the literature with acetic acid, followed by methanol.[132,159,160] Finally, trituration of the mixture in boiling acetone gave acceptably pure product. If required, further recrystallization from acetone gave pure white needles that were suitable for an Xray diffraction study (Figure 23). No attempt was made to

[a] It has to be noted that during the reaction methyl trifluoroacetate with a boiling point of 43 °C could be formed and that during the exothermic reaction its bp is exceeded, which could be dangerous due to its toxicity.

reproduce the yield stated in the literature; the synthesis in its present form, matching very closely the procedures of *Banihashemi*, seems to maintain a good compromise between scalability and safety requirements for a potentially dangerous reaction.

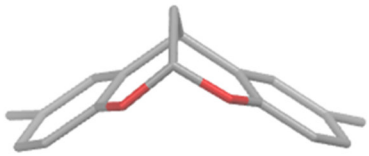

Figure 23: X-ray structure of DBDOC-H_2. Non-relevant hydrogen atoms have been hidden for the sake of clarity.

2.4.2 Synthesis of the BFBF-H_2 Ligand Precursor

Rosenthal and *Zaionchkovsky* reported in 1960 a synthesis of 5a,10b-dihydrobenzofuro[2,3-b]benzofuran skeletons based on an acid-catalyzed condensation reaction between two moles of *p*-substituted phenols and glyoxal. Their best experimental procedure for BFBF-H_2 was the condensation of glyoxal (**30**) with 2 equivalents of *p*-cresol (**26**) in acetic acid, subsequently adding to the preheated reaction mixture dropwise concentrated sulphuric acid acting as the catalyst; a crystalline material of 70 % yield could be obtained.[132,160,161]

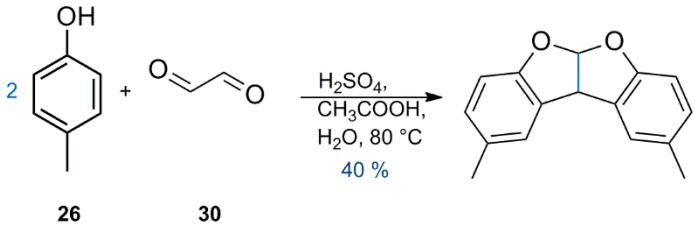

Scheme 17: The synthesis of BFBF-H_2 involves an acid-catalyzed condensation reaction between two moles of *p*-cresol and glyoxal.[160]

In the same manner as in DBDOC-H_2, we were interested in scaling up the procedure. However, in contrast to the DBDOC-H_2 case, we did not change the reaction conditions. The largest prac-

ticable scale was in a 4 L flask with a total volume of 3.5 L, requiring 0.5 L concentrated sulphuric acid leading to a yield about 80 g (Figure 24). If necessary the product can be recrystallized from acetone.

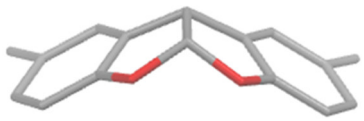

Figure 24: The X-Ray structure of BFBF-H_2 obtained from $CDCl_3$.

In conclusion, the synthesis of BFBF-H_2 is essentially as straightforward as that of DBDOC-H_2; but DBDOC-H_2 gives a higher E factor[162,a] . It is reasonable to assume that, in essence, the chemistry developed for one backbone could be transferred to the other. After multiple experiments DBDOC-H_2 has proven to be a good choice of backbonein combination with bulky substitutents (*vide infra*) because it facilitated the separation of the diastereomers of the corresponding *bis*(*sec*-phosphine borane) intermediate **38c** *(vide infra)*.

2.4.3 Bromination of the DBDOC Backbone

Unpublished results within the group of *van Leeuwen* suggest that direct metalation at the *o*-position of DBDOC-H_2, as is used in the xanthene (**31**) case for the synthesis of Xantphos (**32**Scheme 18)[163], leads to ring opening of the backbone. It is probable that a nucleophilic ring opening of the acetal bicycle takes place; the *n*-Bu-anion is then probably directed to the acetal group rather than the aromatic.[b] Consequently, functionalization of the arene positions *ortho* to the acetal oxygen atoms requires prior substitution by suitable groups, such as bromide. Our organic frameworks are anisole-type aromatics, which facilitates the functionalization of the desired *o*-position to the acetal, since both other activated positions in the aromatic are blocked

[a] The E factor reflects the yield kg product/yield kg reactants including solvents and purification process.

[b] Note that acetal groups (and particularly chiral acetals) are often used in DoM (directed *ortho* metallation) and related reactions.[333] It is noteworthy that they can sometimes undergo reaction at the acetal rather than at an associated aromatic (or homologue).[334]

by either the non-aromatic cycle on the second *o*-position or another alkyl group (Me/*t*-Bu) on the *p*-position. This implies a straightforward electrophilic functionalization of the free *o*-position (Figure 25).

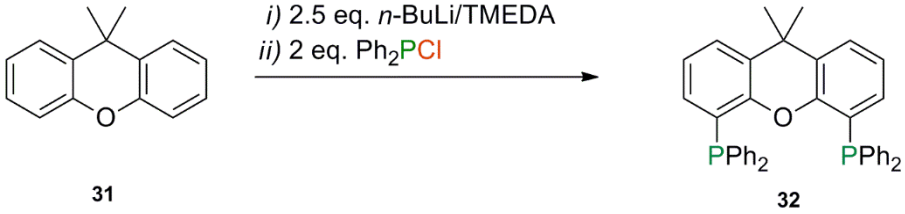

31 32

Scheme 18: Xantphos synthesis is available through direct metalation of the *o*-position.[163]

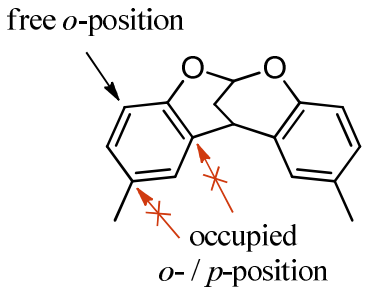

Figure 25: Functionalization of the organic backbones of DBDOC-H_2 and BFBF-H_2. Only one *o*-position is free in the aromatic rings with the other *o*- and *p*-positions being blocked by substituents. , and exemplary demonstrated with DBDOC-H_2.

Initially the protocol used to obtain the dibromide was the previously reported *van Leeuwen* method of NBS in DMF; in this case, the reaction was monitored by GC chromatography, resulting after 12 h in a yield of 69 %, with a mono-bromination by-product.[159] Many bromination methods using elemental bromine are known in the literature, but local safety regulations in Palaiseau led to retention of NBS as the source of the electrophilic bromonium ion that substitutes the activated aromatic.[164] The protocol of *Freixa* and *van Leeuwen* was amended to use conditions, using acetone as the solvent in the presence of traces (0.2 % v/v) of concentrated hydrochloric acid (36 % aq.) as catalyst,[165] which tremendously accelerated the reaction and proved to be useful to scale-up, 100 g scales were attempted without any significant problem. In a typical experiment, 80 g (0.317 mol) DBDOC-H_2 was added 2.3 eq. NBS (130 g, 0.73 mol) and dissolved in bulk acetone (ca. 700 mL) at just below boiling temperature until a saturated

solution was obtained; subsequently the mixture was treated with 1.5 mL conc. HCl (36 % aq.). The reaction refluxed briefly and, after a few seconds the solution turned dark orange and then lightened, indicating the formation of the dibromide. The solution was allowed to cool to room temperature and was stirred for further 45 minutes, and the product was collected in a frit. The crude product was washed with hot water, and after drying a pure, white solid of $DBDOCBr_2$ dibromide in a yield of ca. 60 % could be obtained in roughly two hours of work. The yield could be optimized through evaporating the filtrate and washing it with hot water (90 °C) on a frit, yielding another 20 % of product. However, the by-product of this procedure is bromoacetone[166], a lachrymator, which complicates the removal of the solvent from the filtrate significantly. The optimized protocol has proven to be useful for scale-up, so that adequate quantities of backbone precursor could be obtained for the subsequent functionalization.

2.5 Introduction of the Phosphines 2-by-2

In the retrosynthetic analysis, the introduction of the phosphines 2-by-2 was described briefly; in the next section the possible synthetic approaches will be reviewed in detail. As mentioned previously this requires in the first step the phosphination of the backbones and in the second step a substitution reaction with an electrophile. Our main objective is to use a modular approach facilitating the synthesis of various ligands with the same skeleton.

2.5.1 Phosphination of the Backbone

The halogen-lithium exchange, used for the synthesis of a series of new wide bite angle diphosphines by *van Leeuwen et al.,*[159] is a reasonable starting point for preparing our target phosphines. They employed lithium-halogen exchange, followed by phosphination with chlorodiphenylphosphine to give an overall yield of 62 % of the triarylphosphine DBDOCphos on 1 g scale.[132,159]

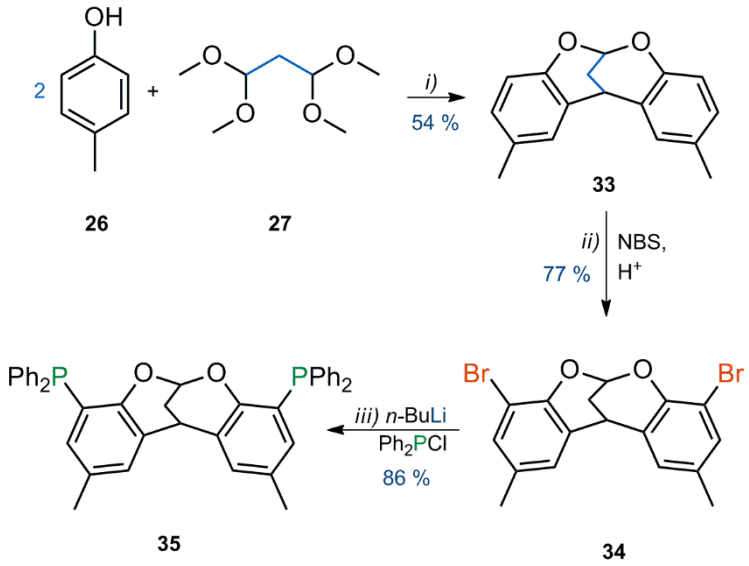

Scheme 19: Synthesis of DBDOCphos. BFBFphos is obtained analogously.[159]

This synthesis is straightforward and does not produce many by-products, whilst the advantage of the easy purification methods and the cheap starting materials make it an attractive system for industrial use.

As previously described the halogen-lithium exchange, used for the synthesis of a series of new wide bite angle diphosphines by *van Leeuwen et. al.*[159], justifies the same approach for our target phosphines. In our case a second, different, group has to be linked to the backbone phosphines in a later step, so two asymmetric phosphine centers appear at the backbone. In principle, the required *bis*-(chlorophosphine) intermediates **36** can be prepared easily, for instance by a straightforward substitution reaction using dichlorophosphines. However, in practice, it is well-known that monosubstitutions of $RPCl_2$ compounds can be difficult to effect. Once formed, their reduction with lithium aluminium hydride should allow access to the secondary phosphines, and subsequent functionalization (Scheme 20). Preparing enantiopure phosphines from simple secondary phosphines is extremely difficult because of the inherent ease of inversion of P- chiral secondary phosphines, and the lack of difference between the formal "charge" and the "lone pair" in the phosphide anion, so when scalemic phosphines are required, different synthons are used. The *bis*(*sec*-phosphines) **37** that we wish to prepare are not enantiopure but, as discussed in section 2.2, the combination of *(R-)* and *(S-)* chiralities at the backbone- connected phosphorus centers in our target phosphines gives rise to diastereomers, so that the ability to generate single diastereomers of our desired product tetraphosphines cleanly requires the

use of approaches that allow chirality to be controlled. The most commonly used approach employs enantiopure *sec* phosphine boranes, which are quite configurationally stable.[143,167–171,a] For the reasons described in section 2.3.3, it was decided to focus on the use of such phosphine boranes.

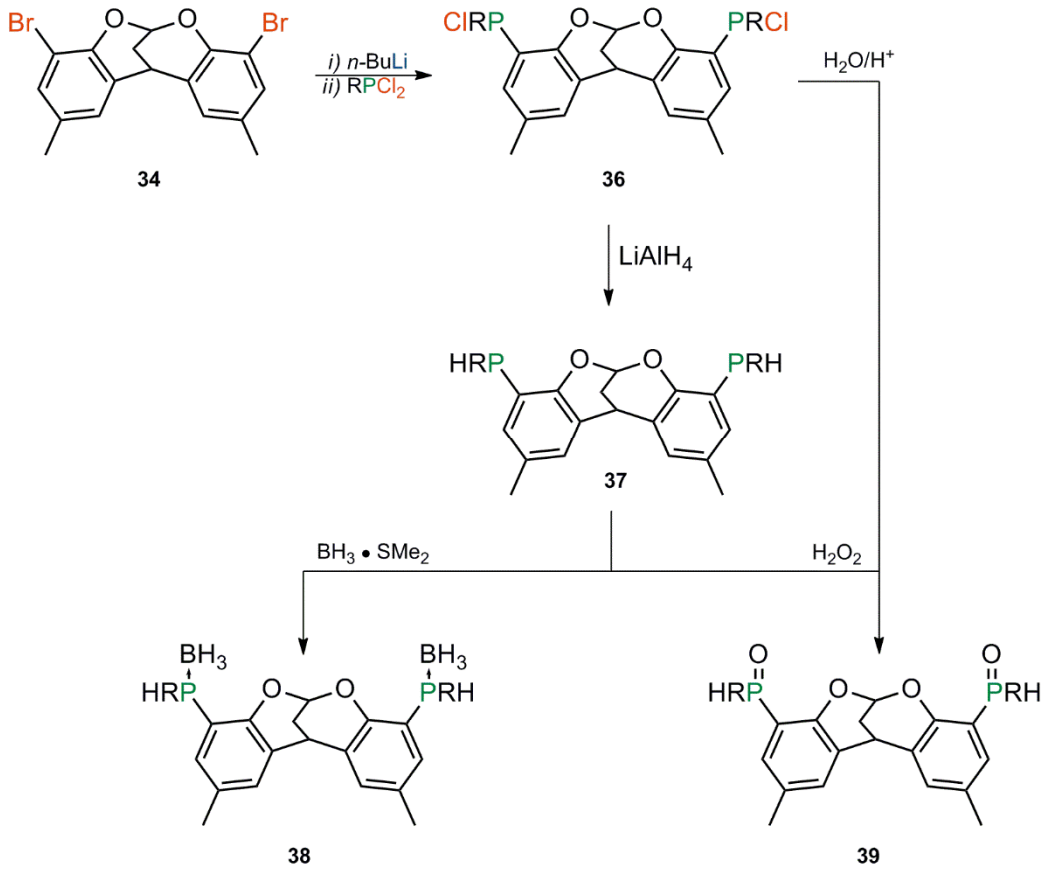

Scheme 20: General method for generating secondary phosphines on the DBDOC backbone, and the methods to protect the free phosphines as phosphine boranes or phosphine oxides; R = *t*-Bu, Ph, Cy.

2.5.2 Generating Secondary Phosphines on the Backbones

DBDOCphos type ligands were obtained by a simple substitution reaction of the lithiated backbone and appropiate chloro-di-R-phosphines.[159] The first obstacle to overcome in our case was the poor solubility of **34** in THF at low temperatures. The metalation was performed with 2.2 eq. *n*-BuLi on the heterogeneous THF suspension of **34** and starting the reaction at – 78 °C

[a] It should be noted in the context of section 2.3.3 that *sec*- phosphine oxides can also be alkylated with complete control of stereochemistry, so the widespread preference for the boranes seems to reflect their far more robust retention of stereochemistry during deprotection.

stirring for 1.5 h prior to letting it warm up slowly (45 min) and subsequently stirring 20 min more. Recooling to – 78 °C delivered quantitative conversion to the desired lithiated backbone species according to quenching experiments with H_2O.

Because of the potential for double substitution at phosphorus, our initial optimizations were conducted with *t*-$BuPCl_2$ as the electrophile. This was expected to inhibit double substitution for steric reasons[172] and, as expected, clean mono-substitution could be deduced from inspection of the crude $^{31}P\{^1H\}$–NMR spectra after the initial substitution reaction. In theory, it might be assumed that adding the solution of $DBDOCLi_2$ dropwise to *t*-$BuPCl_2$ would more efficiently ensure mono-substitution than the addition of *t*-$BuPCl_2$ to $DBDOCLi_2$; however in practice both paths showed similar results. Equally, the use of commercial (pure) *t*-$BuPCl_2$ gave the same outcome as a solution of *t*-$BuPCl_2$ that had been prepared *in situ* from *t*-BuMgCl and PCl_3. The reagent in this second case obviously contains large quantities of magnesium salts, which might be expected to provide a more smooth and controlled substitution reaction. In the event, the two approaches were essentially indistinguishable, which serves as an indication of the capacity of two relatively bulky groups, (backbone and *t*-Bu) to limit tri-substitution at phosphorus.

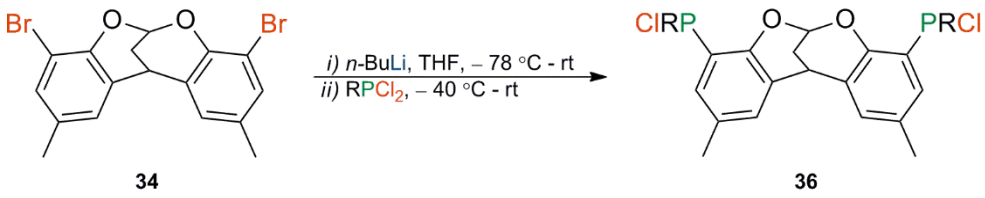

34 **36**

Scheme 21: Procedure of the synthesis of backbone-chlorophosphines involves lithiation of the backbone, followed by phosphination by a substitution reaction.

As discussed in section 2.2, the target **36** has three diastereomers, which theoretically give rise to four signals in the $^{31}P\{^1H\}$–NMR spectrum (because of the non-equivalence of the phosphines in the *rac*-diastereomer). These four signals are not clearly delineated after the phosphination step with *t*-$BuPCl_2$; instead, two distinct broad signals of differing intensity were observed in the region for *sec*-chlorophosphines at around 104 ppm, which suggests an overlap of the diastereomic resonances (Figure 26). The frequency for ^{31}P measurements of 120 MHz is relatively low and might not produce sufficient line separation to analyze the multiplet. The only apparent by-product was excess *t*-$BuCl_2$; this is non-constraining, in that it can be easily removed after the reduction step, which converts it into the very volatile *t*-$BuPH_2$.

The reduction of **36c** to **37c** was effected by excess lithium aluminum hydride (3 eq.); lithium aluminium hydride pellets were carefully, freshly, crushed and added slowly to dry THF under stirring, subsequently the solution was cooled to 0 °C and the crude solution of **36** was added slowly through a dropping funnel or a cannula over 1 h, depending on the volume to be added. After all of the chlorophosphine was added, the reaction was allowed to warm up slowly to rt and the excess lithium aluminium hydride was quenched[173] with great care because of the reaction scale; the reaction mixture was recooled to 0 °C, and degassed water was added slowly and stirred for 10 min, followed by the same amount of degassed 15 % aqueous sodium hydroxide solution and stirred 10 min, and repeatedly 3x of the same amount degassed water was added, each time stirred for 10 min in-between, until the hydrogen gas production stopped. Finally the reaction mixture was allowed to warm up to rt and stirred for further 30 min, so as to give microcrystalline aluminium salts. The heterogeneous reaction mixture was then filtered through celite to give a clear solution of the desired secondary phosphines **37c**. These air-sensitive products were not isolated, but were instead protected *in situ*. The product mixture after the reduction to the secondary phosphines displayed four distinct signals.

The method of choice for the protection of these *sec*-phosphines was to use borane protecting groups because their installation and removal are facile and straightforward, and the reactions of phosphine boranes are easy to operate and normally go with complete retention of configuration. Pure borane dimethyl sulfide was employed as the boronation agent and, in general, 3-5 eq. of the BH_3•SMe_2 complex were sufficient to form compound **38**. If the reaction mixture was not initially filtered free from lithium aluminium hydride, the required amount increased up to 10 eq. The BH_3•SMe_2 complex was added dropwise at 0 °C and stirred 1 h to ensure completion of the reaction. The removal of the SMe_2 by-product is easily (and potentially malodorously) achieved due to its low boiling point, and the crude mixed sec-phosphine borane diastereomers could easily be obtained cleanly.

Ultimately all three steps described, the phosphination using dichlorophosphines, followed by reduction with lithium aluminum hydride and borane protection could be carried out without isolation of any intermediates (*in situ*), which facilitates the synthetic procedure tremendously. The desired stable secondary phosphines could be synthesized in a day from $DBDOCBr_2$ (Scheme 22). The theoretical yields of each step were between 80-100 %, as estimated by ^{31}P NMR.

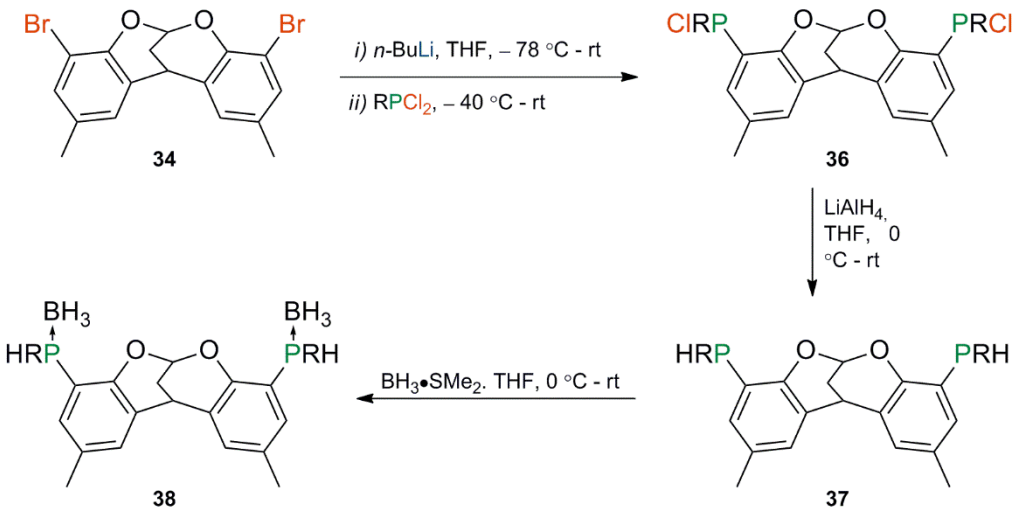

Scheme 22: The synthesis of the stable key intermediate **38** is performed without isolation of intermediates and involves phosphination, reduction and boronation.

After the boronation step an overall yield of 86 % of mixed diastereomers of (**38c**) was obtained according to Scheme 22. Upon trituration under ethyl acetate, a solid was obtained wherein the four signals simplified into two equally intense broad boron-coupled resonances (Figure 26). These unhelpfully broad spectra are typical of the phosphine boranes studied, and ^{1}H–NMR and ^{13}C{^{31}P}–NMR were often required to reveal how many diastereomers were present. The acetal proton at ca. 6 ppm in the ^{1}H-NMR is particularly revealing of the number of species present, being a resonance in a region largely devoid of other resonances, but recourse to ^{13}C{^{1}H}–NMR was often necessary for a more thorough investigation of the number of diastereomers present.

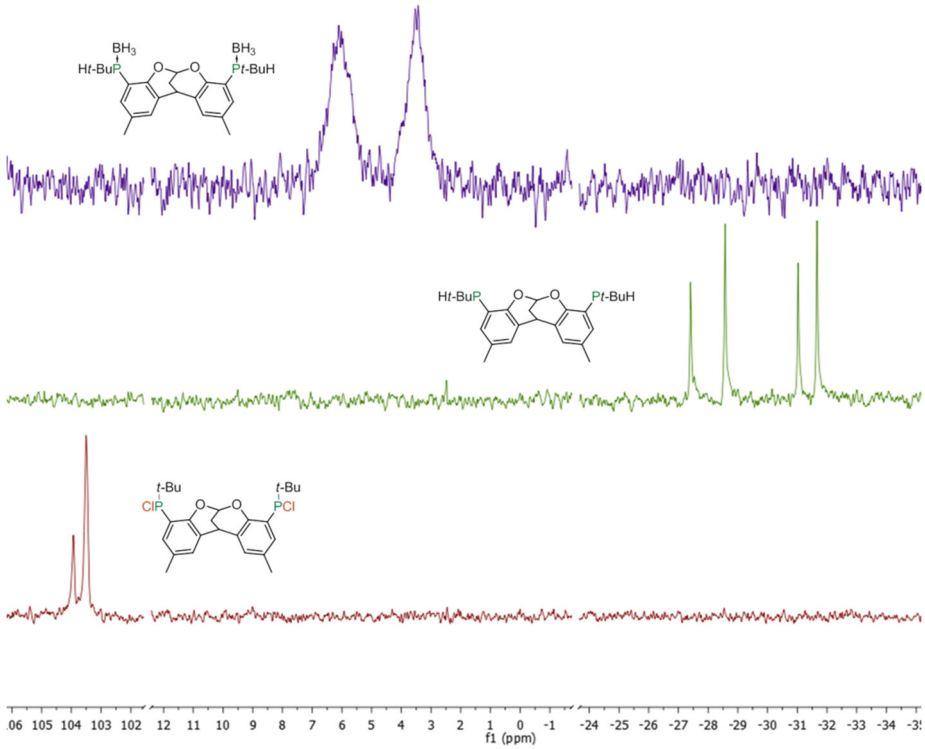

Figure 26: Progression of the $^{31}P\{^{1}H\}$–NMR spectra during the transformation of **36** into **38c**. Phosphination (bottom), followed by the reduction (middle) and boronation (top) using R = *t*-Bu. The spectra were cut in-between to amplify the signals.

In the ^{1}H-NMR, resonances of equal intensity at 5.62 and 5.49 ppm are attributable to P–H groups, and P–H couplings of $^{1}J_{(P,\,H)}$ = 381.51 Hz at 5.62 ppm and $^{1}J_{(P,\,H)}$ = 382.18 Hz at 5.49 ppm were observed. Corresponding resonances attributable to the *t*-Bu groups at 1.2 ppm with a $^{3}J_{(P,\,H(t\text{-Bu}))}$ = 15 Hz at 1.1 ppm, and the aromatic protons at were observed at 7.2 ppm $^{3}J_{(P,\,H(Ar))}$ = 13 Hz (Figure 27). These data are promising, but do not differentiate between two *meso* isomers in a ratio of 1/1, or the presence of pure *rac* compound **38c**. The ^{13}C–NMR, which shows sharp lines and is split out over a wide range of chemical shifts could be expected to display one resonance for the acetal carbon (C10) of each diastereomer (Figure 28), and therefore indicate directly if multiple diastereomers are present. In the case of the product **38c**, C10 shows only one resonance, as do the lines attributable to the bridgehead carbon (C11) and the ternary carbon that links the two aromatics (C13). The vast majority of the other carbons, especially the aromatic carbons, resonate anisochronously. This NMR spectrum can only rise from the *rac* form, since in the *rac* form all of the aromatic carbon nuclei are chemically inequivalent, and hence anisochronous, whilst there is only one bridge.

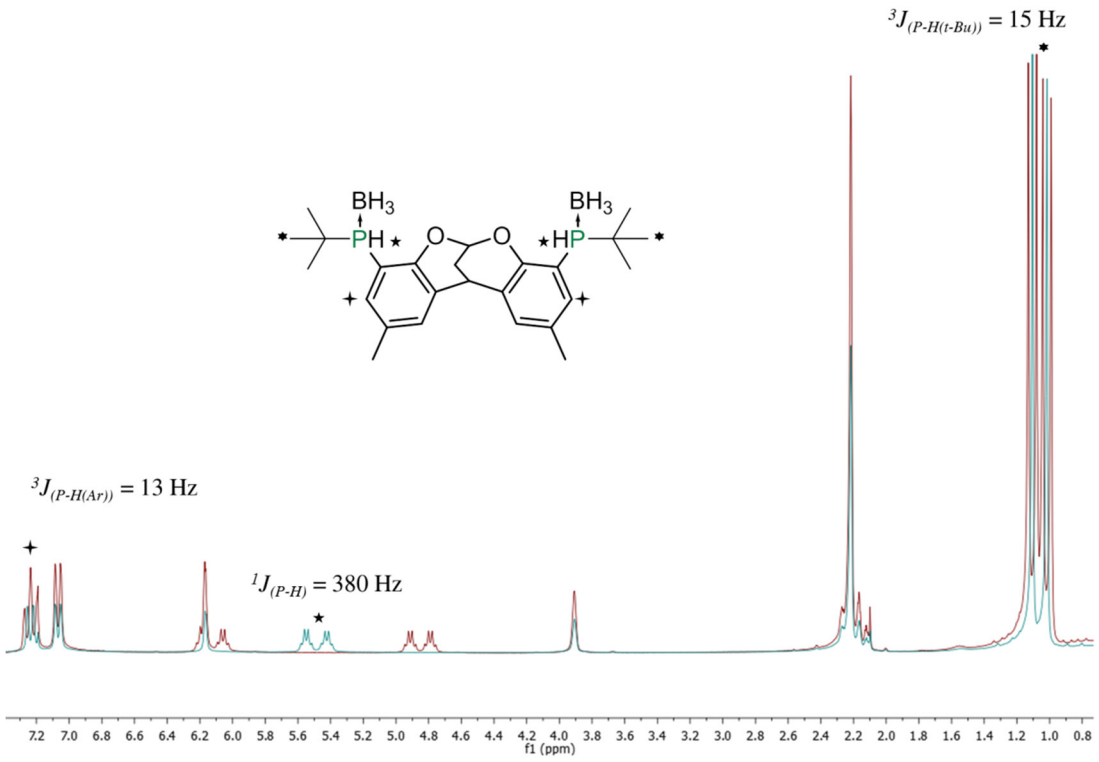

Figure 27: Overlaid ^{1}H-NMR spectra (^{31}P coupled in red and $\{^{31}P\}$ decoupled in green) of *rac*-**38c**. The spectra show the $^1J_{(P\text{-}H)}$ and $^3J_{(P\text{-}H)}$ couplings of the secondary *t*-Bu phosphine boranes on the DBDOC backbone.

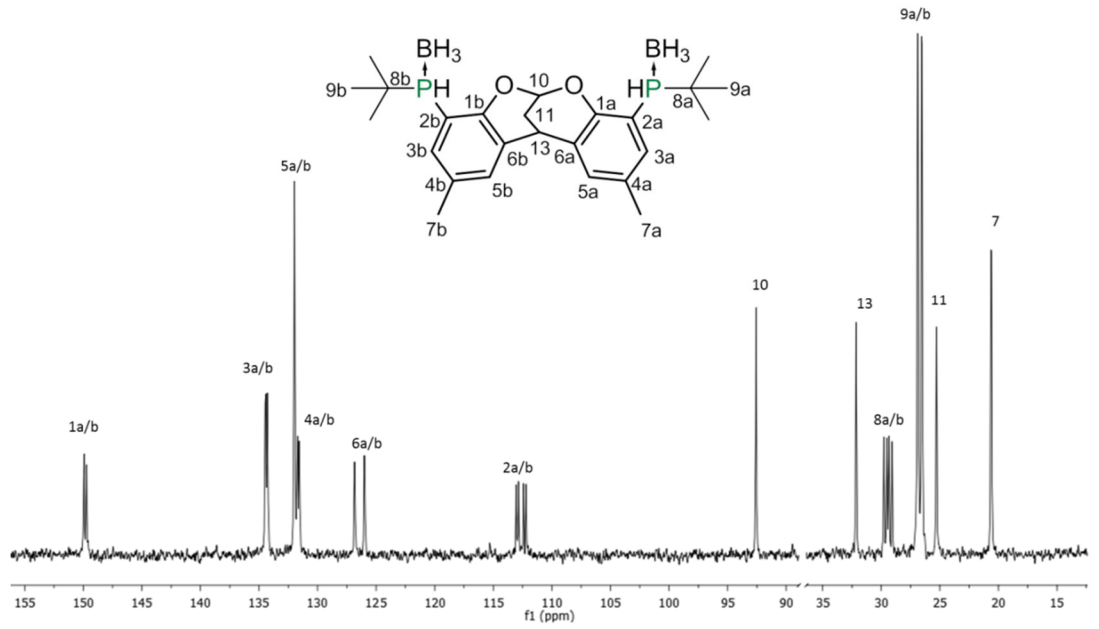

Figure 28: The $^{13}C\{^1H\}$ -NMR spectrum of *rac*-**38c**. The spectrum shows clearly that there is only one acetal carbon (10), while all aromatic carbons and the t-Bu-groups are anisochronous, noted with a/b suffixes. The spectrum is cut between carbon 10 and 13.

After purification by simple trituration in EtOAc, *rac* secondary diphosphine **38c** was obtained in an isolated yield of ~80 % and was pure according to NMR. The NMR analysis was consistent with a crystal structure of **38c**, which also showed the *rac* form (Figure 29). The method described therefore constitutes a facile, short and diastereoselective synthesis of wide bite angle di(*sec.* phosphine)s, which should be apt for transformation into the desired tetraphosphines without the use of complicated or time consuming purification methods.

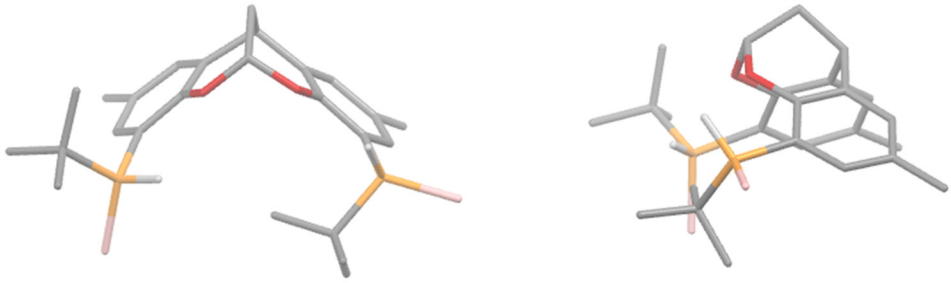

Figure 29: X-Ray structure of *rac* **38c**. Non-relevant hydrogen atoms have been hidden for the sake of clarity.

The ethyl acetate mother liquors from the trituration process leading to *rac*- **38c** contained diastereomerically enriched *meso*-forms; D. Carmichael recrystallized the mixture in DCM and obtained one pure *meso*-form, in the $^{31}P\{^{1}H\}$–NMR only one resonance at 2.4 ppm appeared, and the ^{1}H–NMR shows besides the solvent signals one pure *meso*-compound with a $^{1}J_{(P,\,H)}$ = 377 Hz at 5.60 ppm and a $^{3}J_{(P,\,H(t\text{-}Bu))}$ = 15 Hz at 1.31 ppm (Figure 30). The comparison of the *rac*- and *meso*-^{1}H–spectra shows the expected simplification in the case of the *meso*-compound, whose P-atoms are chemically equivalent. It could not be determined which *meso*-compound we obtained. The absence of scalar coupling between the stereocenters, and the absence of the second *meso* diastereomer- which clearly prevents comparative nOe analysis- means that the relative configuration could not be determined from the NMR spectrum.

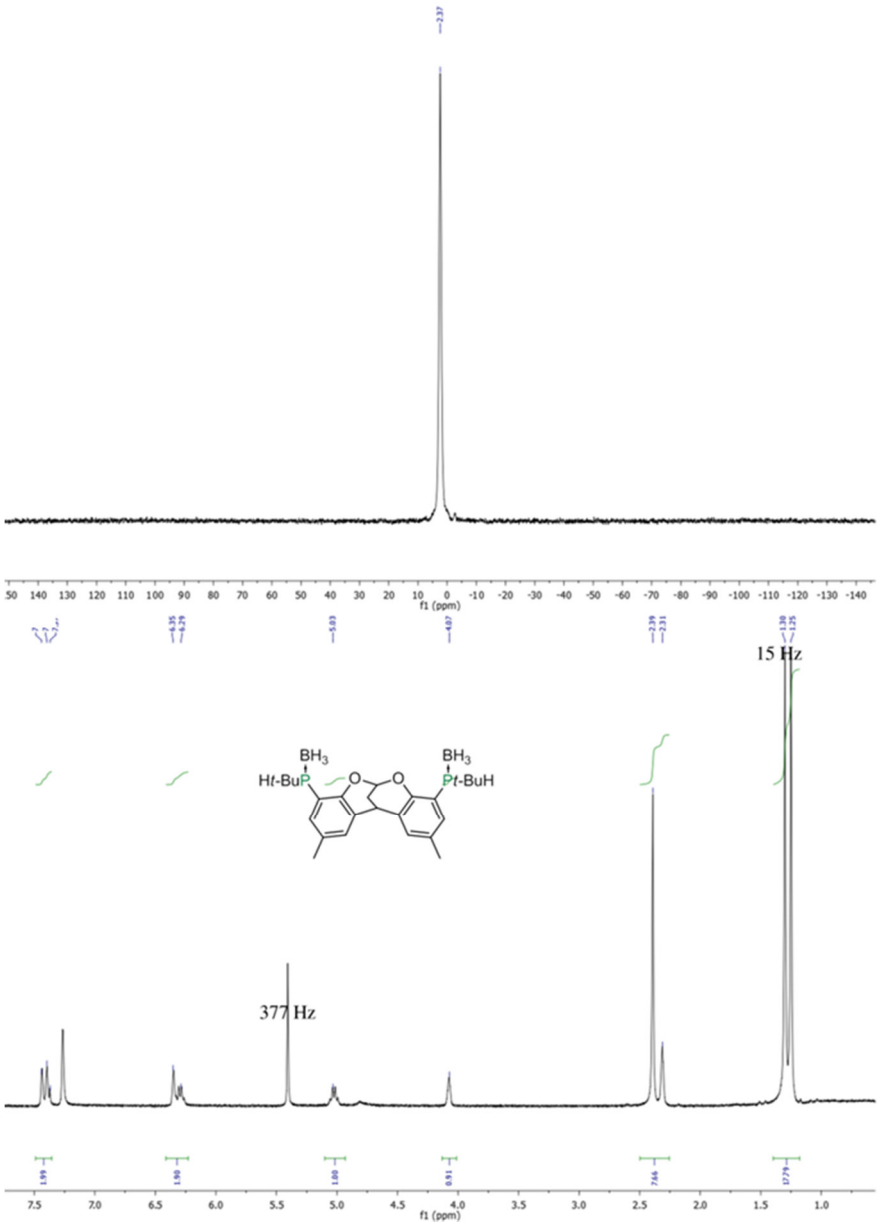

Figure 30: The $^{31}P\{^{1}H\}$–NMR (above) and ^{1}H–NMR (below) spectra of the isolated form of *meso*-**38c**. A dichloromethane impurity is present.

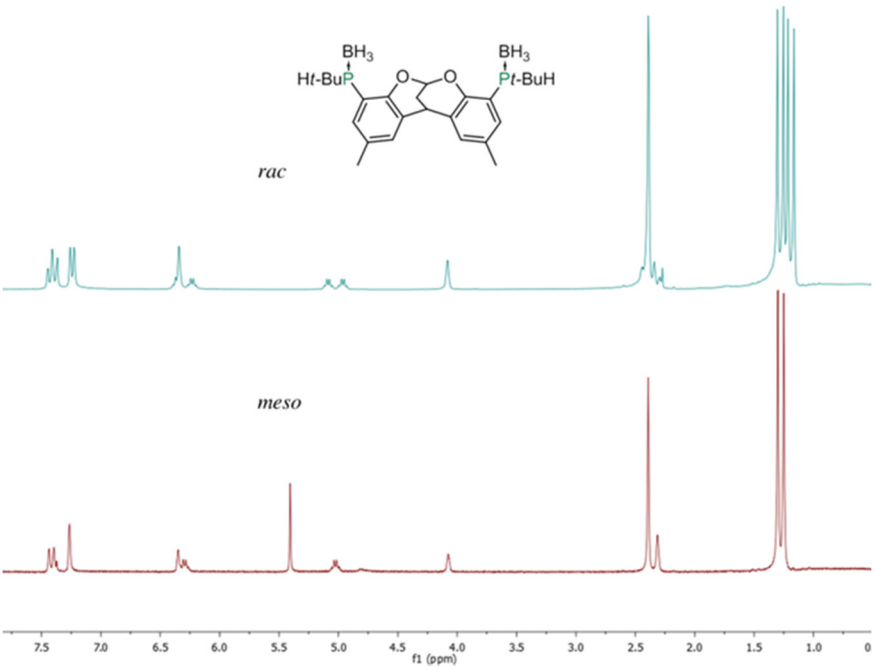

Figure 31: The ^{1}H–NMR spectra of the isolated *rac*-(above) and *meso*- (below) forms of **38c**. The spectra show clearly only one P–H coupling in the *meso* form, indicating equivalent P-atoms.

The tert butyl substituents used above can be considered to provide something close to an 'ideal case' for study. Upon lowering the steric bulk of the R group, different results were obtained. For instance changing the *t*-Bu group to the sterically less hindered Cy appeared to be unproblematic at the phosphination step; four resonances around 100 ppm appeared (Figure 32). As with R = *t*-Bu, commercial and *in situ* prepared $CyPCl_2$ containing magnesium salts gave broadly equivalent performance. As with R = *t*-Bu, the reduction, followed by protection with the borane group were easily achieved. However in contrast to the bulky *t*-Bu group, no diastereoselectivity occurred during the boronation step; consequently molecule **38b** shows four broad resonances, which is in accord with the presence of the three anticipated product diastereomers. One *meso*-form appears to be less favored, but which of the two diastereomers this might be could not be determined.

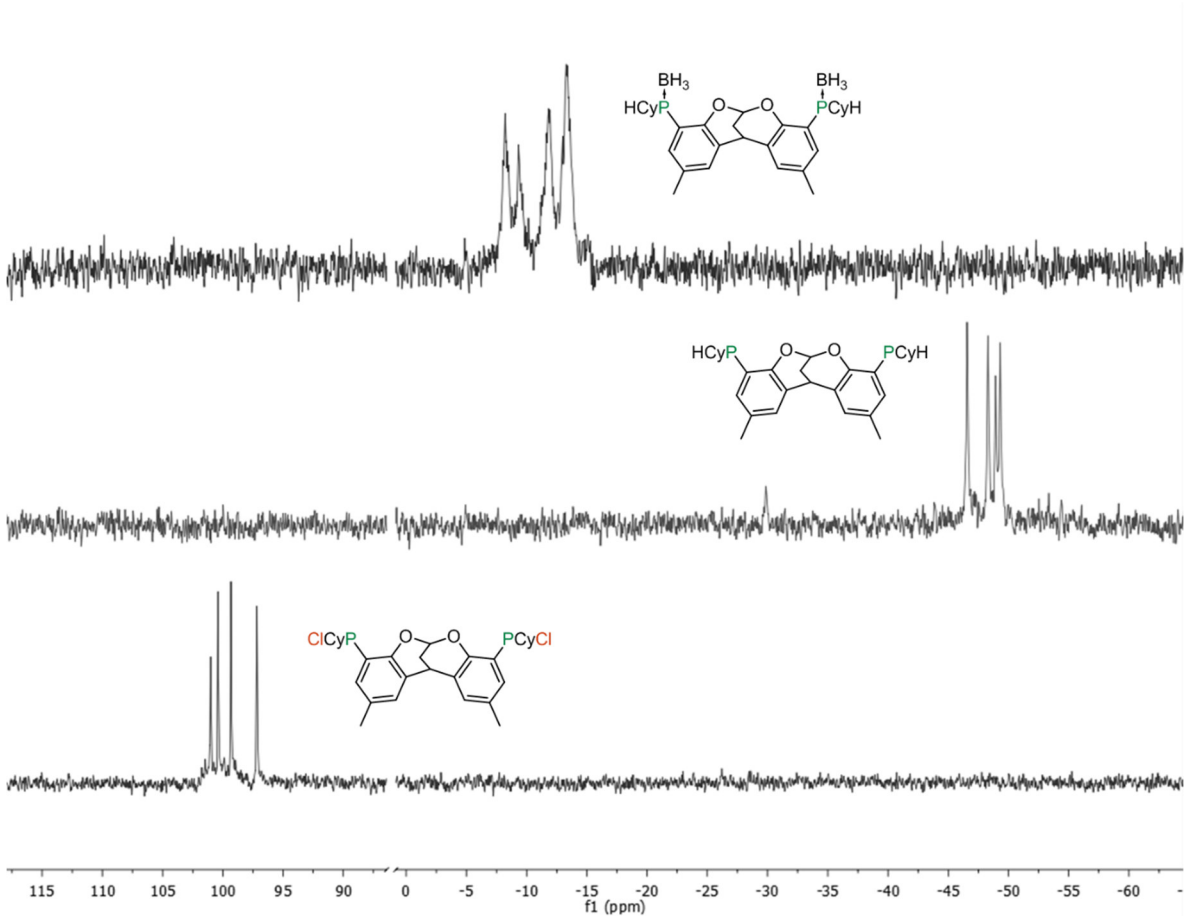

Figure 32: The $^{31}P\{^{1}H\}$–NMR spectra demonstrate that using R = Cy the synthesis of pure secondary phosphine is applicable, in contrast to the *t*-Bu group the boronation step is not diastereoselective. The spectrum was cut between 90 and 0 ppm to amplify the resonances.

In contrast, the case of R = Ph suggests imperfect phosphination. In reactions using precisely stoichiometric amounts of reagents, large (*ca* 30%) quantities of $PhPCl_2$ remained unreacted, as estimated by $^{31}P\{^{1}H\}$–NMR (Figure 33). Instead of sharp lines in the region expected for *sec.* chlorophosphines (ca 77 ppm), there was evidence of broad complex multiplets. Additionally, some resonances appeared in regions around – 25 ppm that are normally associated with tertiary phosphines. These were taken to be signs of partial double substitution at P. The oligomeric by-products were detected in the $^{31}P\{^{1}H\}$–NMR spectrum due to as multiple resonances around – 20 - 25 ppm.

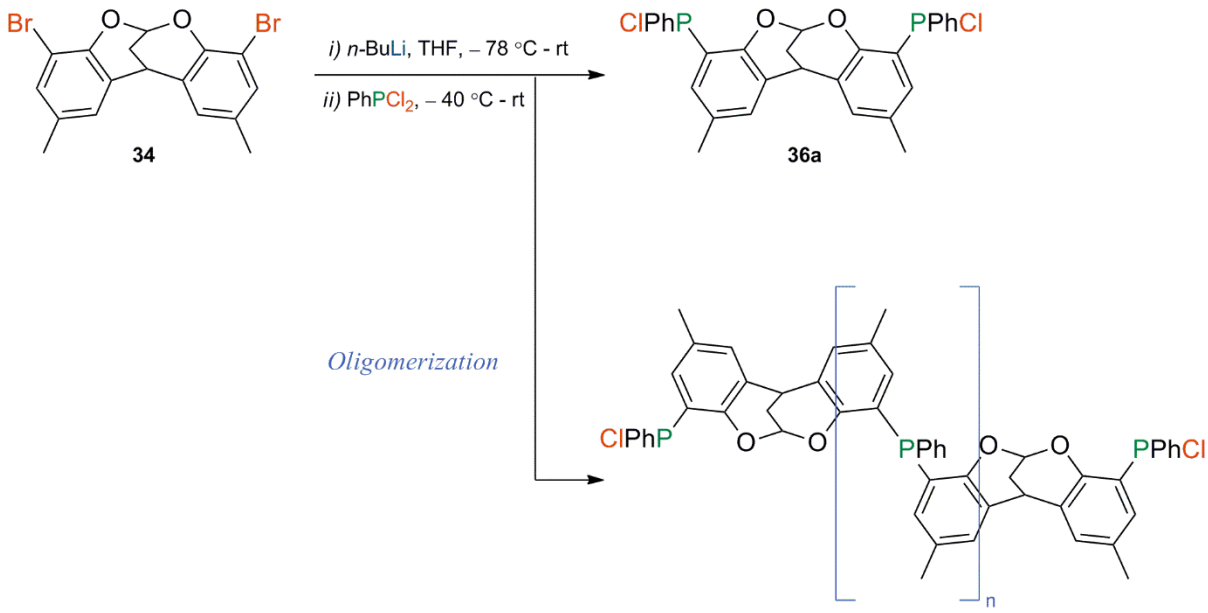

Scheme 23: Oligomeric by-products observed during the phosphination of $DBDOCLi_2$ with $PhPCl_2$.

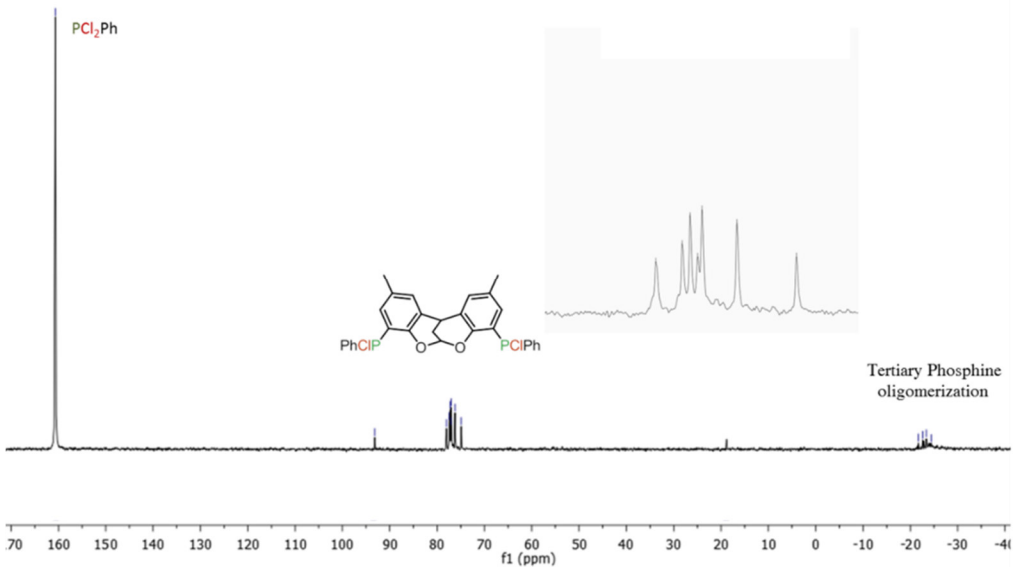

Figure 33: The $^{31}P\{^{1}H\}$–NMR spectra for the phosphination of $DBDOCLi_2$ with $PhPCl_2$. The low conversion and oligomeric (~ – 25 ppm) by-products indicate some disubstitution of the incoming electrophile.

To conclude, it seems clear that steric interactions are of importance for obtaining clean secondary phosphine boranes **38a-c**. Physically small groups like phenyls increase the possibility of a second nucleophilic substitution at the dichlorophenylphosphine leading to oligomeric by-products, while a bulkier group like cyclohexyl appears to preclude this second substitution. The even bulkier R = *t*-Bu case additionally gave a strong preference for one of the diastereomers: *rac* **38c**.

2.5.3 Backbone flexibility and Steric Interactions in DBDOC derivatives

We were interested to see how the substituents influence the structure of the backbone, and also why the molecule appears to disfavour the *meso*-configuration in **38**c. To get a better understanding of the reaction which has occurred leading to the *rac* phosphines, it might be useful to understand the problems associated with the resolution of free phosphines.

Typical methods to resolve free secondary methods known in the literature are based on the protection of the phosphine from protons by coordination to metal ions[174], chalcogens[175], or boranes[176], but the corresponding optically active secondary phosphines could not be recovered from their adducts.[134,177] The first resolution of free chiral secondary phosphines (diastereomers of (-)-menthylmesityl-phosphine) could be accomplished by fractionized crystallization in a solvent like acetonitrile and a proton scavenger like [Na]acac by Wild and co-workers[177], they could recover 48 % of highly pure diastereomers (94 % enriched spectra were obtained) after seven recrystallization steps from purified acetonitrile.[177] This example demonstrates clearly the difficulty of obtaining diastereomeric pure product from free *sec*-phosphines; as a consequence we decided to protect our secondary phosphines with borane to resolve the diastereomers.

Our free secondary phosphines **37c** show a statistical distribution of the ^{31}P resonances in the NMR spectrum. However, after the boronation to give **38c** we obtained principally the *rac*-phosphine ***rac*-38c**, which is easily collected after trituration with ethylacetate. This statistical distribution of the resonances of the free phosphines needs to be considered in the light of their low inversion energies; chiral secondary phosphines can show a significant barrier to inversion of >97.5 ± 0.5 kJ for (±)-PHPh*i*Pr, but traces of protons or bases allow facile inversion.[134,177] This easy inversion was confirmed in our case by deboronation of the pure *rac*-form **38c** to the free phosphine **37c** using HBF_4•Et_2O, which again generated a statistical distribution of the diastereomers in the ^{31}P–NMR.

The yields of up to ~80 % of the *rac*-diastereomer after purification were not expected and, since they were not observed with less hindered groups, it can be assumed that this occurred due to the steric stress associated with the bulky *t*-Bu groups. It seems reasonable to assume that *meso* structures would normally be privileged with symmetrical backbones such as DBDOC, in that a same favored arrangement of the phosphine substituent with respect to the backbone could then be achieved on both sides of the molecule. Thus, the product would most

likely be *meso* in the absence of an interaction between the two 'hemispheres' of the backbone. Evaluation of the crystal structure shows two different (*t*-Bu) conformations that are, clearly, energetically accessible, the *t*-Bu group on the left of Figure 34 is located *exo* to the space occupied by the backbone, whilst on the right hemisphere the *t*-Bu group is close to the backbone median axis defined by the three carbon atoms of the bridge. There appears to be no reason why a *meso*-configured molecule adopting the *exo*-configuration for both hemispheres could not form, so one is led to conclude that the site close to the median axis is probably strongly favored for one of the *t*-Bu groups. Steric interactions then presumably eliminate the possibility of the second phosphine adopting a similar configuration, since the two *t*-Bu groups would then be in very close proximity to one another. This second group therefore adopts the *exo* position (Figure 34).

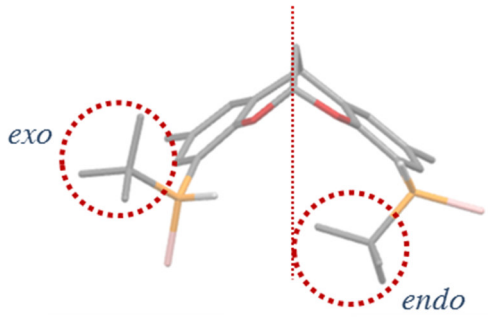

Figure 34: X-Ray structure of *rac*-**38c**. Note the very different positions in space of the two BH_3 functionalities. Non-relevant hydrogen atoms have been hidden for the sake of clarity.

With the assumption of a late transition state, which would be consistent with a kinetic resolution of a fast-equilibrating mixture of diastereomers, and a further assumption that the phosphine whose *t*-Bu group lies *endo* to the backbone will be boronated first (because of the very unhindered trajectories indicated for access of the borane to this phosphorus in the structure of the product), it is then necessary to imagine that the boronation of the group whose *t*-Bu lies *exo*- to the backbone is the step at which the diastereomeric selection occurs. Given the position of the *t*-Bu group in unhindered space *exo*- to the backbone, and assuming that rotation is relatively high in energy (*vide infra*), the possible product diastereomers are the H/lone pair invertomers at this phosphorus. These are the observed *rac* form ±-(*S***S**), or the *meso*-isomer RsS. Given that the trajectory leading to the *rac*-diastereomer provides far greater space for the borane to enter (under kinetic control[178]), and for locating the BH_3 group comfortably in the

product (thermodynamic), it seems reasonable that this *rac* product should be strongly favored and this is observed.[a]

An analysis of the DBDOC scaffold itself in different substituted molecules might be expected to provide more information regarding the steric interactions of the substituents as a function of backbone distortion. The flexibility of the molecule due to the non-aromatic bicycle element might cause the P–P distance to be influenced strongly by steric interactions. It can be seen that the molecule not only bends, but also twists, depending on steric stress. Bending, as defined by comparison of the angle in-between the acetal of different substituted backbones (Table 3) might indicate how strong steric interactions effect the bending and the measurement of the torsion angles ($C_{ipso} - O - C_{acetal} - C_{bridgehead}$) of the two non-aromatic cycles described in the Figure of Table 3 shows the twisting of the scaffold. DBDOC-H_2, its dibromide (**34**), *rac*-**38c** and the later discussed racemic tertiary *t*-Bu-ester diphosphine borane (**40**) were compared. The intersection of the planes made by the two phenyl-rings were used to calculate the angle at the dioxocin carbon as shown in Figure 35.

[a] Unfortunately, this analysis provides few clear clues as to the nature of the unknown *meso* isomer. Should the energetically dominant structural motif be the presence of a *t*-Bu group *endo* form might be expected to become the *(R,s,S)* form if the *t*-Bu group of the second phosphine remains located in unencumbered space (as is the case in the analysis above) and the lone pair lies *endo* to the cavity below the three- carbon bridge. This scenario would seem to be ideal, save for the fact that this diastereomer requires the delivery of the second borane protecting group through very hindered space. Another access would involve rotation of the *t*-Bu group of the first boronated phosphine out from under the C_3 bridge into the *exo*- position, a corresponding rotation of the second non-complexed phosphine into the *endo*- space below the backbone and subsequent boronation of the lone pair oriented into the highly exposed face *exo*- to the backbone. If, on the contrary, the *(R,r,S)* diastereomer is to be favored, then one option is that neither of the phosphine groups has the *t*-Bu group adopting the apparently favored position *endo*- to the backbone and close to the plane defined by the three carbon bridge, but they instead both take up the position of the *exo*- oriented phosphorus in the case above, and are both then boronated in relatively unhindered space *exo* to the cavity; a second access to this compound involves a reaction scheme similar to that of the *rac* product, except that in this case the initial boronation occurs at the lone pair in a more hindered inverted configuration close to the bridge of the backbone; this structure is available through interchanging the H and the lone pairs in the first step of the scheme described above for generating the *rac* structure. The second boronation, if realized as described in the *rac* case, then again provides *(R,r,S)*. Given that there are no common intermediate structures on the pathways leading to these two different *meso*-diastereomers, and the energetic factors affecting the different intermediates are difficult to quantify, the stereochemistry of the *meso*-form that is obtained remains unclear. Intuitively, one might feel inclined to prefer *(R,r,S)*.

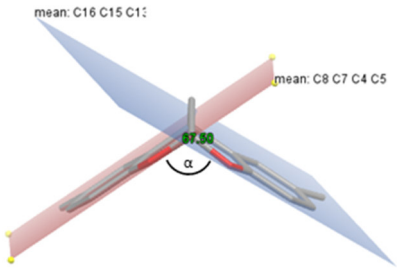

Figure 35: The angle representing the 'opening' of the DBDOC skeleton, calculated from the intersection of the Ph group best planes. Example given: DBDOC.

The measured angles of the different compounds are indicating that not only "folding" appears; the backbone can also twist depending on the steric interactions. The DBDOC scaffold has an angle of 67.5° and nearly no twisting appears. The free backbone does not bear steric hindered groups and it can assumed that this is the most relaxed conformation, however the measured torsion angles of A vs. B demonstrate already that the molecule itself is not 100 % symmetric (Table 3). The substitution to more spacious bromides (**34**) increases the angle 4° to 71.78°, the torsion angles are changing as well slightly. This implies that the primary interaction here is between the bromides and the scaffold.

The replacement of the bromide by the secondary *tert*-butyl phosphine forming **38c** reveals a tremendous change in the torsion-/angles compared to DBDOC-H_2**;** its angle is 12° wider (79.06° in **38c**) and the torsion angles imply a stronger twisting. This might be because of the steric interaction between not only the scaffold and the two secondary phosphine boranes, but as well the steric interaction between the two bulky *t*-Bu groups with one another, as a result the scaffold is forced to unfold to provide sufficient space for the bulky groups, but due to the steric interaction between these bulky groups the non-aromatic bicycle is as well forced to twist to a certain degree more than the non-hindered compounds (Figure 36, Table 3).

The X-ray structure of **38c** displays as well that the trajectory for attacks is less hindered on the right phosphine borane. Transformation to tertiary phosphine boranes, here an ester containing alkyl chain (**40**), diminishes the angle of the scaffold to 62.84°, the scaffold is now stronger bend than in DBDOC, at the same time the compound is stronger twisted, because the bulky groups require more space. The displacement of the proton of the secondary phosphine borane undergoes retention of configuration, but the conformation of **38c** is not sustainable with the longer alkyl-chain containing an ester group, the increased steric environment has strong inter-

actions with the scaffold and furthermore the R-groups on the phosphine boranes with one another, leading to a substantial twisting of the of the scaffold. The esters groups are remaining in the *rac* form, and only the phosphine borane on the right side of the molecule seems to have rotated slightly. This might be an indication that the substitution on the phosphine borane of the right side occurred first, and during the second substitution, because of the steric stress, the phosphine on the right side was forced to rotate slightly.

The P–P distance is increased in **40** due to the bulky alkyl ester groups, interacting with the *t*-Bu groups as well as with the scaffold, pushing the phosphine boranes more apart to avoid stress as much as possible. Therefore the molecule **38c** might bend more because the R^2 = H is a small group, so the rotation is inhibited due to the steric hindrance of the *t*-Bu groups towards one another, however, displacing the proton with a bulkier group requires more space, consequently the molecule has to open up to create space and less steric stress, but the change of the angle alone appears to be insufficient, hence the molecule twists more increasing the P–P distance.

Compounds	**P-P distance / Å**	**Angle / °**	**Torsion Angle / °**	
			A	**B**
DBDOC-H_2	--	67.5	35.59	25.96
34	--	71.78	36.48	28.12
38c	6.52	79.06	27.06	41.36
40	7.913	62.84	36.96	16.32

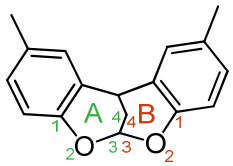

Table 3: Selected X-ray data from the DBDOC backbones of **33** and **34**, ***rac* 38c** and ***rac* 40**. Measured angles in-between the acetal of the four different compounds indicates a strong dependency on the steric interaction in the molecule and the torsion angles indicating the twist depending of the steric interaction. A and B are defining the torsion angles according to the figure in this table.

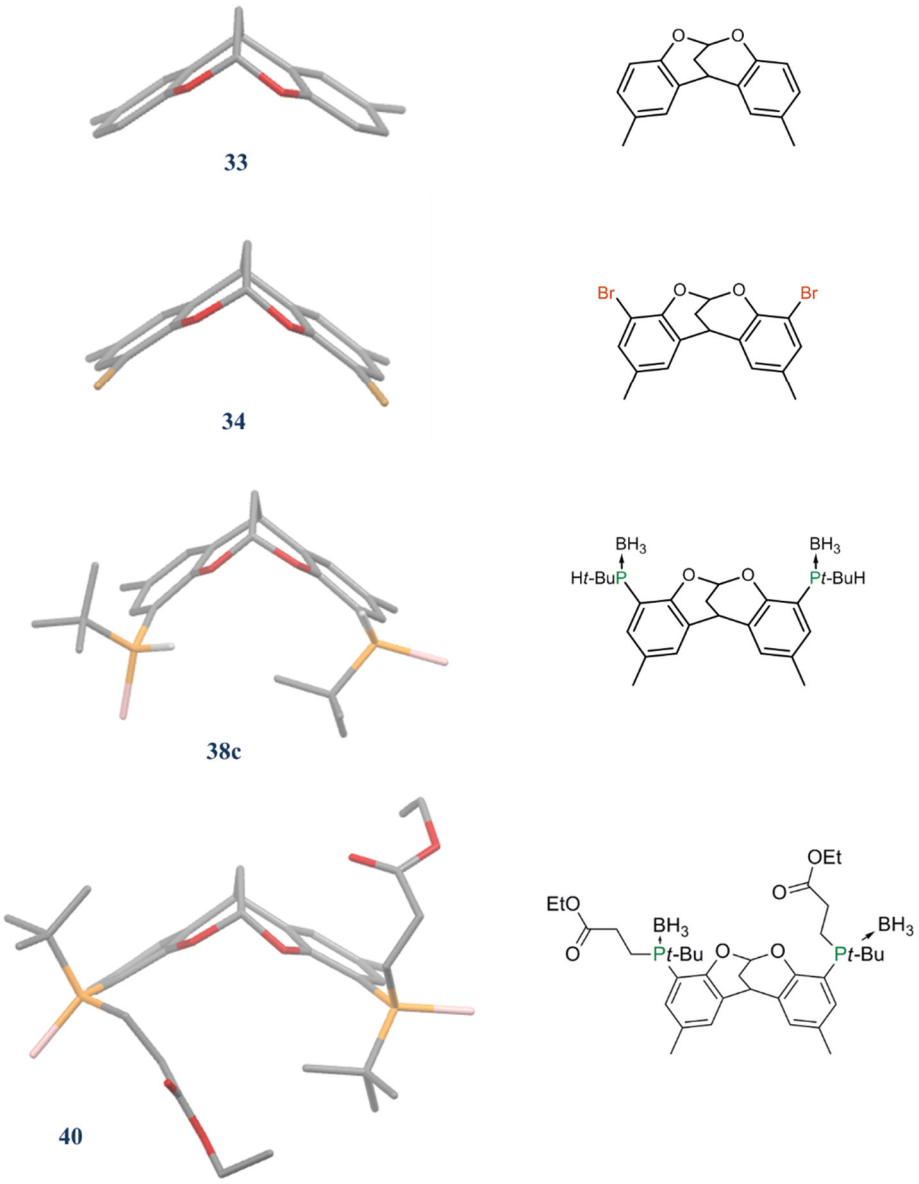

Figure 36: Crystal structures of DBDOC (**33**), its **34**, ***rac*** **38c** and ***rac*** **40**. Non-relevant hydrogen atoms have been omitted for the sake of clarity. Relevent numerical data are given in Table 4.

2.5.4 Alternative Routes to Generate Secondary Phosphines on the Backbone

The work above provides the essential starting materials that we required for the retrosyntheses C and D described in section 2.3.2. Nonetheless, we were interested to explore complementary paths to these kinds of precursors, which might have advantages in terms of different function-alitites, cost, ease of scaleup, etc. These approaches are outlined here.

One alternative path to generate secondary phosphines is the use of phosphinates, which are good sources of the corresponding P–H compounds,[179,180] and hence we attempted to connect *H*-phosphinates to the DBDOC backbone. Phosphinates have been investigated in recent years as an alternative to the industrial widely applied PCl_3, because they are versatile, have few problems regarding solubility, air-sensitivity, and toxicity[a], and are therefore well suited alternatives[b]. Three kinds of phosphinates exist depending on the atoms attached to the P(O)(OR) moiety: phosphinates **a** (derivatives of the hypophosphorus acid, hypophosphites, R^1 = H), *H*-phosphinates **a** (R^1 = C), and disubstituted phosphinates. With at least one hydrogen atom attached the phosphinylidene group can tautomerize to the corresponding P-OH (**b)** form:

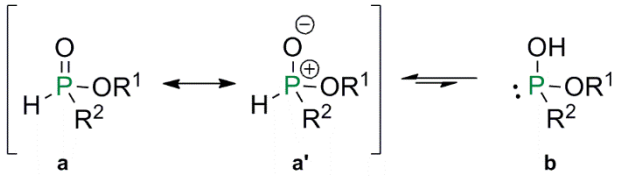

Scheme 24: The phosphinates a have a more accurate ionic resonance form a' and can tautomerize to b.

Multiple methods for a P–C bond formation using phosphinates are known, typical methods being[181]:

1. Cross-Coupling
2. Phosphorylation (Addition reaction)
    a. Transition metal-catalyzed reactions
    b. Free radical reactions
3. Alkylation

In cross-coupling the phosphorus species acts as the nucleophile; a major side-reaction with hypophosphites, which are strong reducing agents, is transfer hydrogenation.[179,182,183] *Montchamp* and coworkers developed general conditions for palladium-catalyzed cross coupling of hypophosphites[184] and *H*-phosphinates[185,186] employing $\geq 2\ mol\%$ of palladium and common ligands like PPh_3, dppp, dppf, or Xantphos, with or without solvent additives like ethylene glycol (EG) or 1,2-dimethoxyethane (Scheme 25).[179,186]

[a] Little is known about the toxicity of phosphinates yet, though they have been used as food additives.

[b] A green chemical alternative.

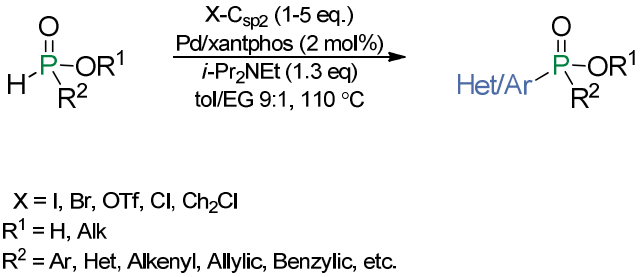

Scheme 25: A general palladium-catalyzed procedure for *H*-phosphinates using Xantphos. Work by by *Montchamp et al*. is shown.[179,186]

Phosphorylation, the addition of phosphinates to unsaturated hydrocarbons, is probably the most important and atom-efficient reaction for the preparation of organophosphorus intermediates.[181] There are two different methods used: transition-metal catalyzed reactions and free radical reactions.[179] In transition-metal catalyzed reactions the formation of a metal hydride complex to phosphinidene oxide should be slowed down by the applied ligand[a], which could be achieved using metal hydrides with alkenes or alkynes[b]. The phosphorylation of *H*-phosphinates is more difficult than hypophosphites (except R^1 = Ph), however it can be achieved using an ethylene glycol (EG) additive.[179,187] Pd catalysis is quite versatile for the synthesis of phosphinates, using low catalyst loading or a reusable catalyst.[179] A cheaper method focuses on the use of nickel, *Han et al.* and *Montchamp et al.* independently obtained promising results using $NiCl_2$, an external ligand and additionally a base like potassium phosphate.[c,142,188,189] In addition to transition metal catalyzed reactions, radical reactions could be used to phosphorylate compounds,[190–195] but the reaction of *H*-phosphinates is more challenging and requires special initiators except in the case of aryl-*H*-phosphinate esters (Scheme 26, R^2 = aryl).[195,196] A very common method is the alkylation of phosphinates akin to the sila-Arbuzov[197] or Michaelis-Becker phosphonate synthesis. *H*-phosphinates are easily alkylated.[198–202] Direct alkylation under equimolar conditions can be achieved using unreactive electrophiles like chloride or tosylate (Scheme 26).[198]

[a] It should slow down the *β*-hydrogen elimination in the case of hypophosphites.[179]

[b] The reaction fails when 1,2-disubstituted alkenes are used, because the reverse *β*-hydrogen elimination is favored.

[c] Though not only the metal is to consider in a cheaper process, ligands, turnover numbers, etc. have to be considered as well. For instance $PdCl_2$ is 2 times more expensive than $NiCl_2$, however $Ni(COD)_2$ costs the same and requires additionally inert atmosphere.

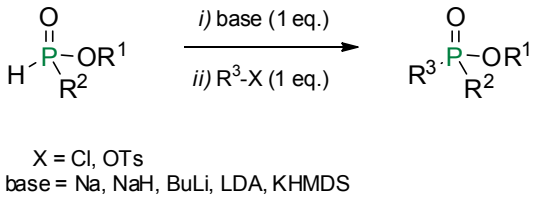

Scheme 26: Direct alkylation of *H*-phosphinate esters using strong bases at low temperature. [198]

To obtain secondary phosphines, *H*-phosphinates are required. We attempted cross-coupling reactions delivering satisfactory result.

2.5.4.1 Palladium-Catalyzed Cross-Coupling of H-Phosphinates

An obvious way of generating aryl- functionalized secondary phosphines and their derivatives is by cross coupling reactions. Palladium catalyzed C_{sp2}–P bond formation reactions have been extensively used for the functionalization of organic aromatic skeletons. These reactions can be performed in both the P(III) and P(V) levels, with the P(V) level generally being preferred for reasons of air stability in the products and a lesser chance of the product phosphine coordinating to and deactivating the catalyst. Excellent protocols for the general case of phosphine oxide formation through catalytic processes, generally based upon conditions developed by Hayashi[203] and Morgens[204], are available, and asymmetric methodologies[205] have been developed. Generating precursors for secondary rather than tertiary phosphines, which use *H*-phosphinates as the phosphorus source, according to *Montchamp et al.*, is slightly more complex in that tautomerization reactions of the *H*-phosphinates can intervene to diminish the effective concentration of reagent **a** (Scheme 24).

Montchamp and coworkers have recently developed an efficient methodology: palladium acetate using Xantphos as a ligand and ethylene glycol as a promoter, or dppf as the ligand and DME as the promoter, both in the presence of DIPEA as base (Scheme 25). The precise mode of action of the promoters is not clear, but the wide bite angle ligands are necessary to prevent the quite reducing phosphinate substrate from acting as a source of H in a competing transfer hydrogenation system (presumably of the DMAc solvent).[109] The additives can cause transesterification reactions at phosphorus, although this is not likely to a difficulty in a case such as ours where the phosphination is followed by exhaustive reduction.

This potentially straightforward access to secondary phosphine oxides is an interesting complement to the more classical non-catalytic routes employed above, in that it is likely to function well when the phosphorus R- substituent is small, which is not the case in the successful approach described above. Hence we decided to apply *H*-phosphinate esters[109] in the phosphorylation step, to target both secondary phosphines (**37a**) through reduction[66] and the corresponding stereochemically stable SPOs[126] (**39**) which can be expected to be easily separated by chiral HPLC (Scheme 27).

Our coupling system of the dibromo aryl compound (**34**) with two equivalents ethyl phenylphosphinate did not seem to cause transesterification, so we decided not to include solvent additives.[185,186]

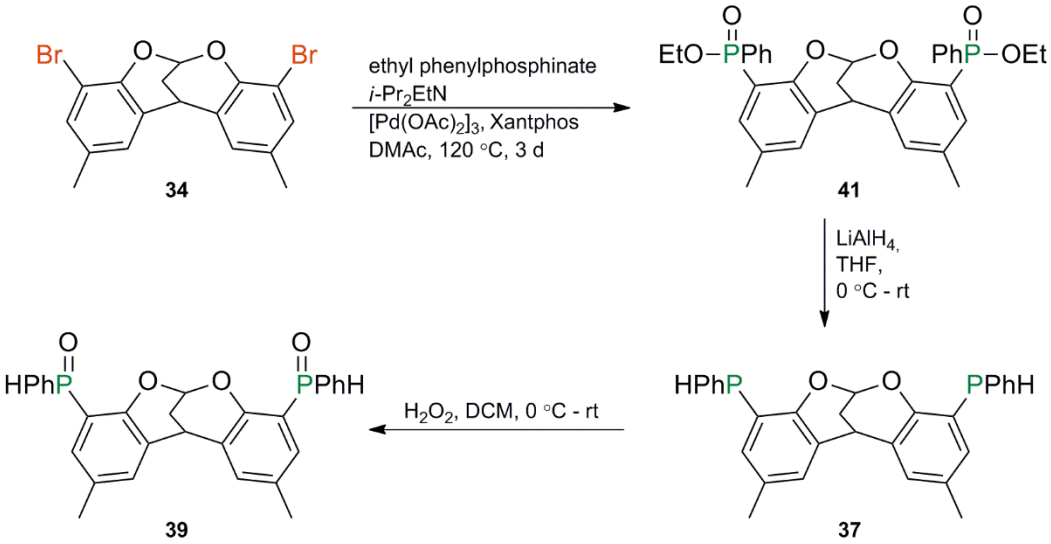

Scheme 27: Phosphorylation with ethyl phenylphosphinate. After palladium-catalyzed cross-coupling using $Pd(OAc)_2$ as precursor and Xantphos as ligand in combination with the Hünig base in DMAc under reflux 3d, the backbone phosphinate products were subsequently reduced (**37**) and oxidized to give the stable *secondary* phosphine oxides (**39**).[158,186,206]

The coupling conditions[a] involve palladium acetate (10 mol%) as precursor. We chose Xantphos as the phosphine (20 mol%), and the Hünig base (4 eq., pK_a = 10.75) as the final proton acceptor to deprotonate ethyl phenylphosphinate (2.2 eq.) which is the chosen nucleophile. 1 eq. of **36** was used as the formal electrophile. A slight excess of ethyl phenylphosphinate (5.12 mmol) and the Hünig base (9.75 mmol) were dissolved in 10 mL DMAc and stirred for

[a] The protocol was commonly used in the *van Leeuwen* group.

30 min to ensure deprotonation (formation of the phosphinite anion nucleophile); simultaneously, the metal precursor (0.24 mmol) and Xantphos (0.48 mmol) were stirred and dissolved in 5 mL DMAc (forming the catalyst). Subsequently the nucleophile was added to the compound **34** (2.44 mmol) dissolved in 10 mL DMAc, and afterwards added to the catalyst. The reaction mixture was heated to 120 °C, and stirred for three days. Upon removal of the solvent a brown solid was obtained, which was washed in hot hexane or toluene and flash crystallized in the freezer. This resulted in a 70 % isolated yield of a light brown solid.

The mixture from this phosphorylation showed four distinct resonances around 33 ppm in the $^{31}P\{^{1}H\}$–NMR, suggesting the formation of the three expected diastereomers (Section2.2). Smaller quantities of by-products were also observed (Figure 37) The phosphinate **41** was reduced using freshly crushed lithium aluminium hydride pellets (6 eq.) in a solvent mixture of Et_2O/THF[71]. To form a stable key intermediate **39** we attempted to oxidize the secondary phosphines using excess hydrogen peroxide resulting in compound **39**.[126] This reaction was not as straightforward as anticipated, and competitive overoxidation with insertion of oxygen into the P–H bond generated a mixture of products.

Whilst four distinct resonances in the $^{31}P\{^{1}H\}$–NMR appeared, one *meso*-compound appears to be less favored; it is interesting to note in the case of phosphine boranes only one *meso* compound could be isolated for **41**.

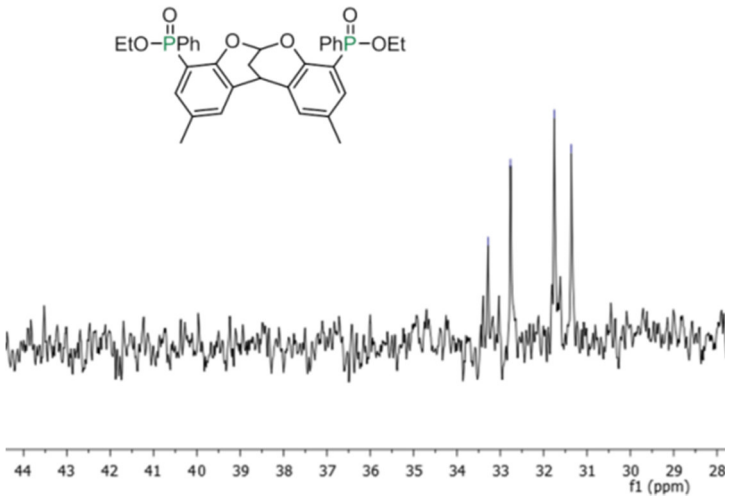

Figure 37: Phosphinylation of DBDOCBr$_2$. The $^{31}P\{^{1}H\}$–NMR spectrum of **41** after work-up shows four resonances, which do not couple to protons, indicating the completion of the phosphorylation and suggesting the formation of the three diastereomers.[158,206]

This approach was not carried further, for a number of reasons including a transfer to the Paris laboratory, where the phosphine borane work was effected. Scalability was not as straightforward as in the phosphine borane approach, the system TON is currently rather low, some reproducibility issues were encountered, the precursor phosphinite requires synthesis, and finding satisfactory separation procedures for the SPO products proved complicated. But, nonetheless, it is clear that the underlying chemistry is promising, and that this approach provides an interesting alternative to the non-catalytic methods described above.

2.5.5 Conclusion

The generation of secondary phosphines derived from dibenzodioxocins can be achieved by various methods. The phosphine borane approach has the disadvantage of broad $^{31}P\{^{1}H\}$–NMR resonances which complicates analysis during the developmental stages but this is not an impediment once good systems are found. It has the great advantage of straightforwardly producing compounds that are facile in their synthetic handling and easy in their complexation and decomplexation. The protocol using four *in-situ* steps can furthermore be scaled-up easily; it is therefore the best choice for producing the key-intermediate**s,** which have protected secondary phosphines on the backbone, in a fast, cheap and easy scalable manner. We focused our research upon R = *t*-Bu, for ease of synthesis and because the *rac* secondary phosphines (***rac* 38c**), could be isolated at scale with great simplicity after boronation. This is important because, in principle, the functionalization of all of the subsequent phosphine boranes should occur with complete retention of stereochemical information at phosphorus.

Secondary phosphine-boranes react well with electrophiles in the presence of a base (e.g. BuLi, NaH) under mild conditions to afford other kinds of functionalized phosphine boranes in good to high yields, without racemization under normal conditions.[167–169,176,207–209] The ability of this deprotonation / electrophile process to produce substituted phosphine derivatives without any loss in optical purity may depend on the deprotonation agents employed. The use of butyllithium usually affords the products with high enantiomeric excess in good to high yields.[167] The lithiated phosphine borane products can be used in reactions with numerous electrophiles, with reactive alkyl halides and epoxides (or their surrogates, cyclic sulfates) being the most frequently used reagents.[167,176,209] The Michael-type addition of deprotonated secondary phosphines to Michael acceptors can proceed with almost perfect retention of *ee*.[167,176,209] Secondary phosphine-boranes also efficiently undergo substitution reactions with aryl iodides, palladium-

catalyzed ($Pd(PPh_3)_4$).[167] In all cases the borane group remains unchanged.[171] These *sec*-phosphine borane precursors are therefore excellent sources of nucleophilic synthons for the synthesis of the desired tetraphosphines.

H-phosphinates are promising alternatives that are very versatile in terms of R- group variation. *H*-phosphinate (RPH(O)OR) precursors having smaller R groups are likely to be good reagents for this system, which is not the case for the phosphine borane- based approach which currently requires bulky R- groups. The two methods are therefore complementary. Furthermore, the *H*-phosphinate based method is a "green" chemical procedure, avoiding the use of chlorophosphines. However, some optimization will be required to produce a truly viable synthesis based upon this methodology and some reproducibility problems remain to be resolved. The protocol could probably be optimized.

2.6 Electrophiles suitable for the introduction of chelating sidearms

With a good source of nucleophilic backbone equivalents available, we can turn attention to the synthesis of electrophiles that would be appropriate for completing the preparation of the tetraphosphines.

Modular approaches allow systematic variation of the ligand structure. Modularity is essential in optimizing catalyst substrate interactions and, therefore, in helping to understand the structure-selectivity relationship. Driven by a desire to provide a modular ligand family, we therefore explored three different approaches for the sequential ('two by two') introduction of phosphines onto the backbone, two of these being modular. The idealized intention was to develop a good approach that would be accessible on a multigram scale in good yields starting from commercially available reagents and preferably involve only a few steps. A further requirement was that the resulting ligand families should include tetraphosphine donors forming bimetallic complexes with varying donor strength and different bite angles provided by the chelate arms. The synthetic approach was also intended to facilitate the change of the carbon number in-between the diphosphine chains (for instance changeable chain length could provide five- vs. six-membered chelate rings as demonstrated in Figure 14).

2.6.1 Preparation of the Electrophilic Phosphine Precursors

In Scheme 28 the two main methods are described which are suitable for elaboration of *rac*-**38c**. The upper method involves phosphine boranes with a leaving group at the end of the chain which, after lithiation of **38c**, undergoes a nucleophilic substitution reaction with retention of configuration at phosphorus.[170,210] The method below involves cyclic sulfates, generating through ring opening the electrophilic compound (leaving group = sulfate) either on the backbone (such as displayed in Scheme 28) or generating a side-arm equivalent leading, which will be explained later, to the desired tetraphosphines. Cyclic sulfates provide two major advantages, they undergo very fast reactions and many of them are commercially available.[144,211] The stepwise character of their functionalization allows systematic and modular variation of the ligand structure, which has been utilized to investigate the relationship between the ligand structure and their control of enantioselectivity.[20,212,213]

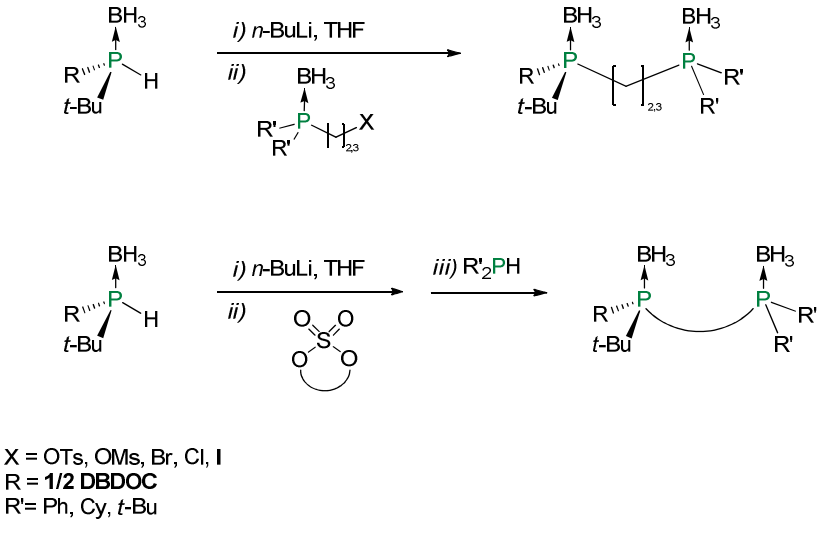

Scheme 28: The potentially modular methods for generating the target tetraphosphines from *sec*-phosphine boranes such as **38c**. The reaction above involves a typical alkylation, the lower reaction involves cyclic sulfates.

2.6.2 Synthesis of a 'Side-Arm' Electrophile bearing Phosphine Borane groups

The synthesis of an electrophile that acts as a provider of a phosphinylated side-arm is a multistep process that is likely to be delicate to operate *in situ*. Hence it is desirable to have stable, storable intermediates, and steps that are reliable and applicable to scale-up that are based upon commercially available starting materials. *Imamoto et al.* synthesized BisP* borane precursors using phosphine borane alkylesters, reducing them to the corresponding alcohols, followed by

the transformation into a tosylate/mesylate, and finally undergoing a substitution with another phosphide borane.[143]

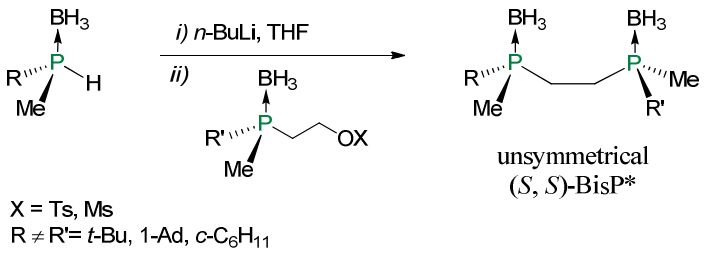

Scheme 29: Synthesis of unsymmetrical BisP* diphosphine by *Imamoto et. al.*[170]

Since we desire tunable chain length we used to generate the phosphine borane esters through a nucleophilic substitution of a phosphide borane with compounds like ethyl 3-bromopropionate (producing a C_3-chain).[a] This is a multistep process; however due to the facile reaction conditions and the possibility to isolate and scale-up each intermediate it is a very favorable approach.

A possibility to avoid side reactions like quartenization would be to protect the phosphines with borane-groups, the corresponding nucleophiles are then mildly basic anions and unlikely to abstract a proton of the alkyl chain.[214] *Livinghouse et al.* showed that this method is applicable in the synthesis of diphosphines that alkylates phosphine-borane anions with homochiral ditosylates without side reactions[214]; we observed equally positive results using mesylate as leaving group.

The synthetic method employed is a well-known organic reaction sequence that comprises four relatively simple steps (Scheme 30). It starts with the purified (*sec*-) phosphineborane, conversion into the corresponding nucleophile by deprotonation using *n*-BuLi and reaction with the desired ω-bromo-alkylester. This yields the P-borane complexed 1-di(R)phosphinoalkyl-ω-ester. Subsequent reduction of the ester function with lithium aluminium hydride gave the alcohol and this was then transformed into the mesylate, a suitable and well known[143] leaving group. In the case where R= Cy, this mesylate can be transformed further into the corresponding iodide[167] (Scheme 30) but this transformation works poorly when R= Ph because of deboronation and

[a] A related method introduced by *Issleib et al.* in the '60s using free phosphines gave very poor results and rather intractable products[216]

subsequent side reactions.[143,215,216] All reaction steps could be easily handled on a 20 g scale, and the starting material is commercially available and relatively cheap.

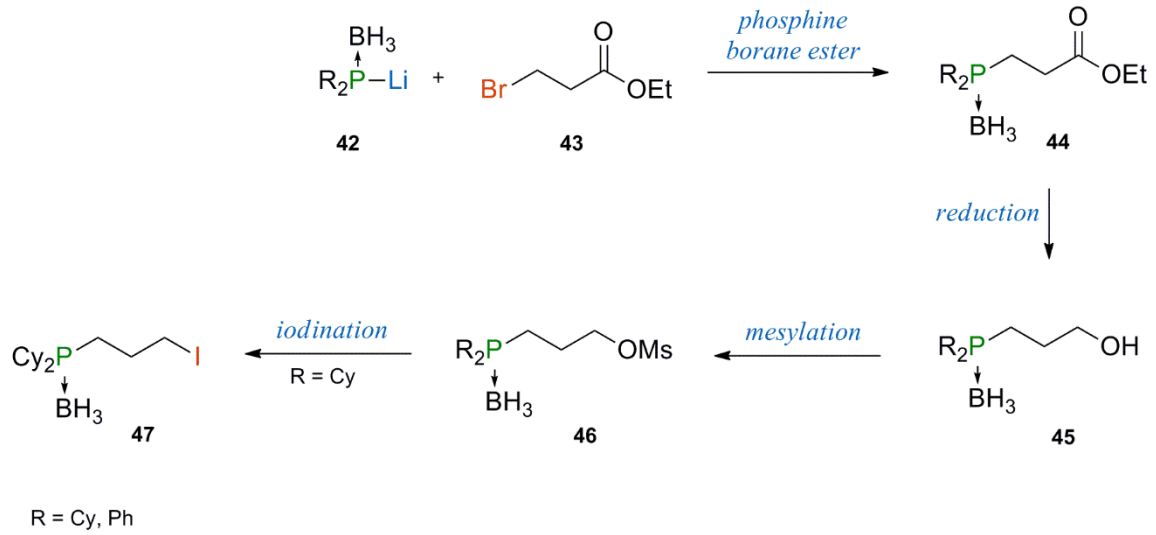

Scheme 30: Synthesis of the side-arm phosphine boranes. In the first step the phosphine borane ester is obtained, the ester is then reduced with $LiAlH_4$ and the resulting alcohol converted into a mesylate leaving group.[170,176,215,217] With R = Cy, iodination was successfully accomplished.

The secondary phosphine borane $R_2PH(BH_3)$ (22.35 mmol, R = Ph, Cy) was dissolved in dry, degassed THF cooled to –78 °C and deprotonated with *n*-BuLi (14 mL, 1.6 M solution in hexane, 22.35 mmol). The reaction was followed by $^{31}P\{^1H\}$–NMR, completion was observed in a upfield shift to –40 ppm, subsequently the phosphide borane was added to the bromo-propionate at –78 °C. Curiously some quenching occurred during this reaction step, since the ^{31}P–NMR spectra shows a mixture of the starting diphosphine borane and **44** (Figure 38). It can only be assumed that there were traces of water in the reaction mixture. The two compounds could be separated easily by a short column chromatography (9:1, pentane:EtOAc) and 3.2 g (10.28 mmol, 46 %) of a white powder could be acquired.[a]

[a] For large scale (50g) preparations, this purification can be advantageously be deferred until after the reduction step, when the very large R_f differences between the *sec*- phosphine borane and the phosphine- functionalized alcohol **47** make the separation extremely simple.

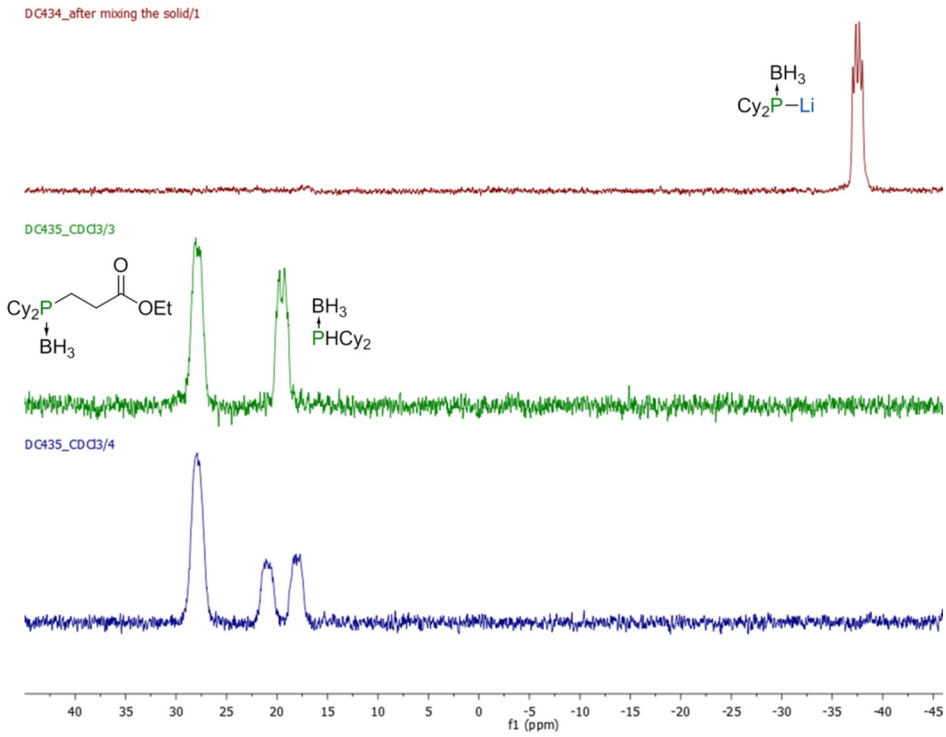

Figure 38: Quenching occurring during the reaction of ethyl bromopropionate with dilithiated **38c**. The $^{31}P\{^{1}H\}$–NMR spectra indicate that quenching occurred during the phosphine borane addition to the ethyl bromo-propionate and a 1:1 mixture of the starting phosphine and product was obtained.

Subsequently the ethyl 3-(dicyclohexylphosphinyl)propionate borane (**44**, R=Cy) (or ethyl 3-(diphenylphosphinyl)propionate borane) was reduced with freshly crushed lithium aluminium hydride pellets (4 eq., 3.4 g, 89.67 mmol) at 0 °C in THF and quenched as described previously.[173] Whilst the reaction is generally perfectly clean, any starting material was either further reduced or simply separated with a short column chromatography (7:3, pentane: EtOAc, $R_{f(46)}$ = 0.73). The product **45**, R=Cy was determined by ^{1}H–NMR (Figure 39), the protons next to the hydroxyl-group are downfield shifted to 3.7 ppm indicating the formation of the alcohol, although the Cy-groups are very broad and overlaying the resonances of C2 and C3. Integration of the compounds were as expected, the expected product **45**, R=Cy was formed successfully in a yield of 2.7 g (97%).

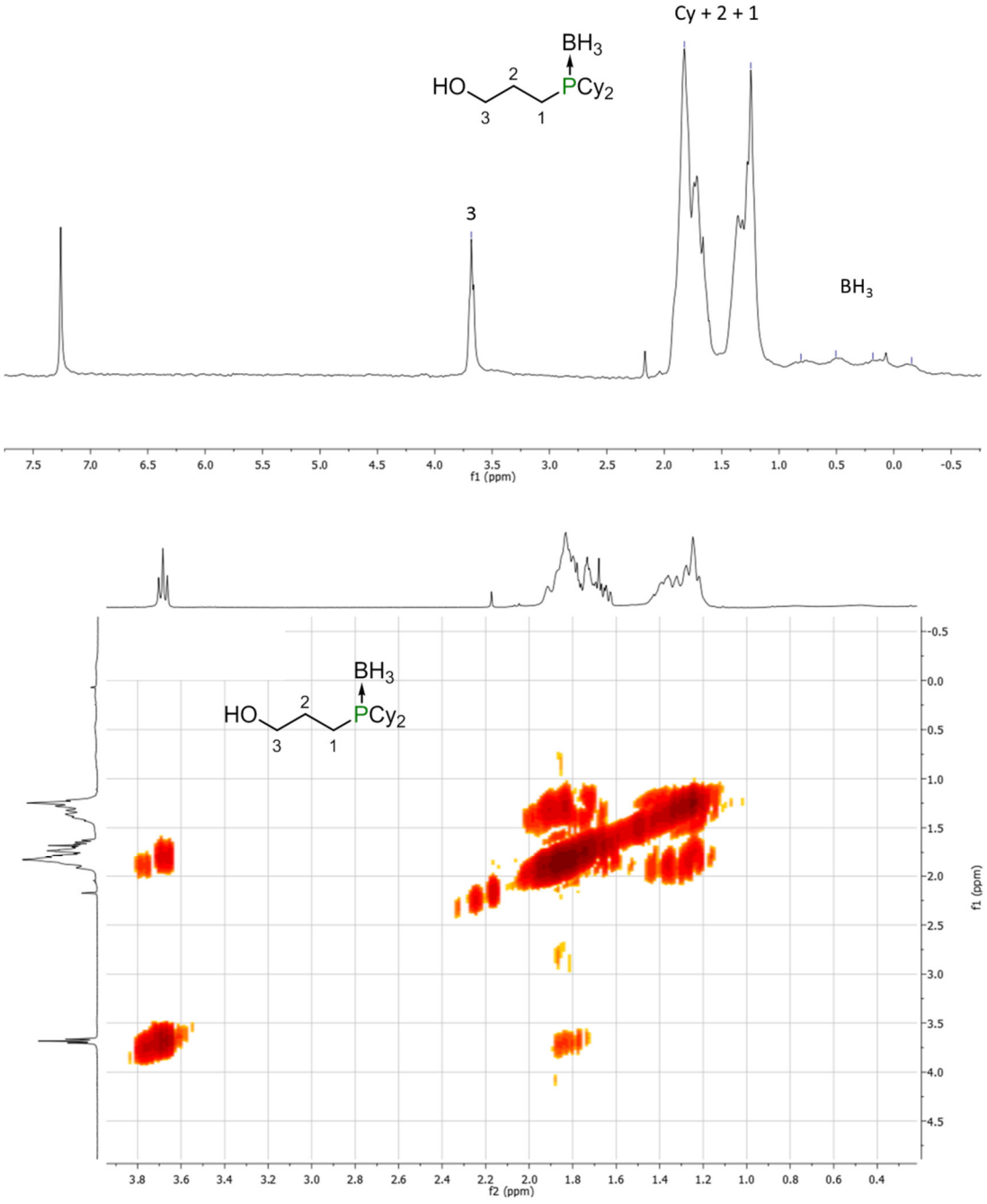

Figure 39: ^{1}H–NMR (in $CDCl_3$) on the top and the corresponding COSY ((in $CDCl_3$)) the of the alcohol **45** with R = Cy.

Finally a typical mesylation protocol[218] was used to obtain the desired product, determined by ^{1}H–NMR. The alcohol **45**, R=Cy (18.83 mmol. 5.09 g) was dissolved in 30 mL dry DCM and 2.3 eq. triethylamine (3.2 mL), subsequently the reaction mixture was cooled to 0 °C and during 1h mesyl chloride was added dropwise maintaining the temperature. The excess mesyl chloride was quenched with 2 M ammonium chloride solution (5 mL, aq), the reaction mixture was

washed with brine (2 x 10 mL) to remove the excess MsCl from the reaction mixture and the product **46**, R=Cy extracted with DCM (2 x 30 mL). Whilst the reaction is clean, any starting material was simply separated with a short column chromatography (9:1, pentane:EtOAc). The mesylation step led generally to a yield between 80-95%. The ^{1}H–NMR shows clearly the downfield shift of the C3 protons to 4.26 ppm and appearance of the S-methyl-group at 3.0 ppm (Figure 40). The phosphine borane resonance did not change, since its chemical environment did not change. For cases where the mesylate group might not be ideal, we transformed mesylates into iodides; here, a downfield shift of the C3 protons to 4.7 could be observed.

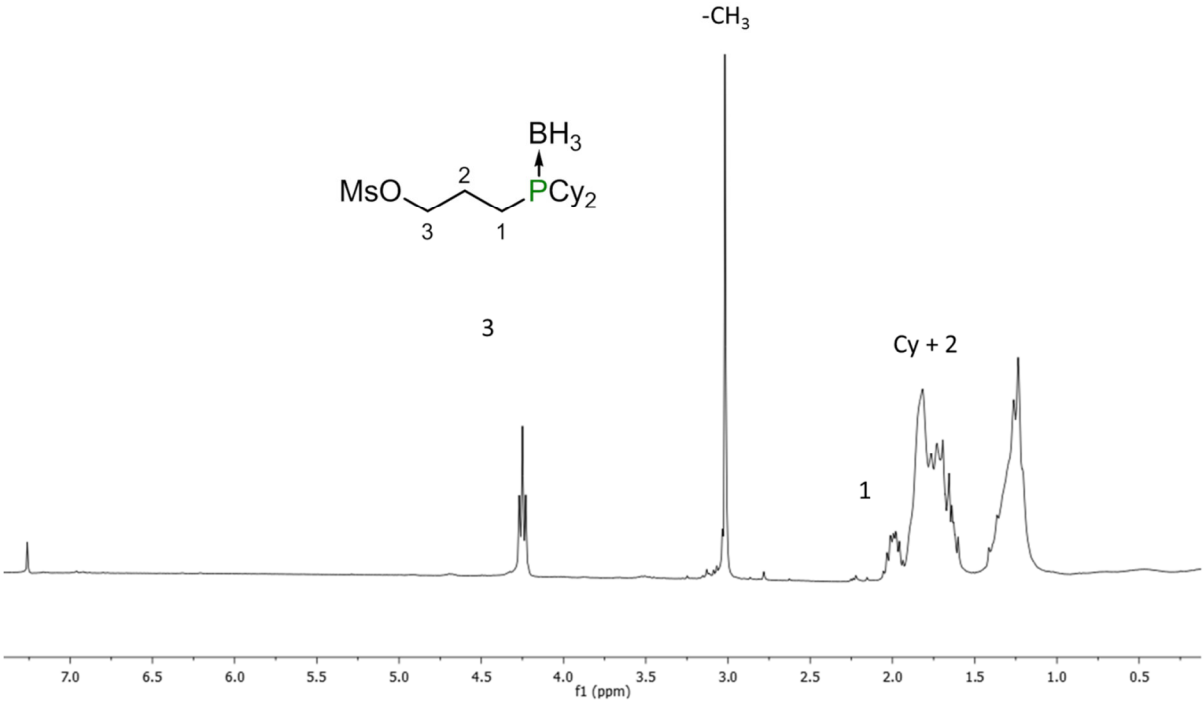

Figure 40: ^{1}H–NMR (in $CDCl_3$) of **46**, here with R = Cy.

As aforementioned during the formation of **44** (R=Cy) approximately 50 % conversion was observed, so we opted to try another electrophile for introducing the C3 chain: a Michael-acceptor (Scheme 31).[167,219,220] A secondary phosphine borane was reacted with ethyl acrylate using sodium ethanoate in THF/EtOH as the base. This reaction proceeds at rt, the desired diphosphine borane (10 g, 47.128 mmol) is dissolved in dry THF (700 mL) and dry EtOH (10 mL), the reactions mixture was cooled down to – 40 °C and subsequently sodium (0.5 eq, 0.5 g, 23 mmol) was added form the base sodium ethanoate (NaOEt) that abstracts the proton of

the phosphine borane. The reaction mixture was stirred for 15-30 min, and then the ethyl acrylate (1.1 eq., 5.5 mL, 51.85 mmol, filtered through alumina to remove aqueous residues and polymers) was added to the solution. 70 % of the phosphine boranes were converted to the desired product **44** R=Cy. Excess sodium was removed from the reactions mixture, which was concentrated and then washed with water (2 x 200 mL) to remove excess base from the mixture. The product **44** R=Cy was extracted with DCM (2 x 200 mL). The main by-product is 3-ethoxypropionic acid ethyl ester, which is well known in the literature to form by an oxa-Michael addition promoted under basic conditions.[221,222] The separation from the product **44** R=Cy was completed after the reduction with lithium aluminium hydride to the 3-ethoxypropan-1-ol, which could be removed easily by washing with sodium bicarbonate. The reduction to **45** R=Cy and mesylation to **46** R=Cy were accomplished corresponding to the protocols described previously.

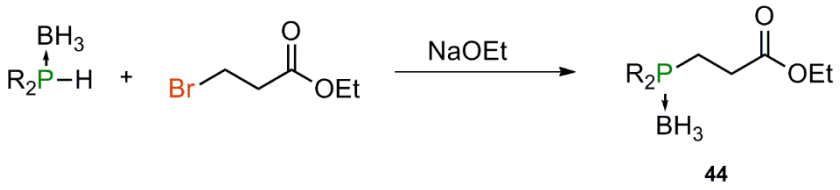

Scheme 31: A Michael acceptor may be used to generate the C3-esters on the backbone.[167,219,223]

2.6.2.1 Syntheses of Alternative 'Side-Arm' Electrophiles

In section 2.5.1 the advantages and disadvantages of free phosphines, phosphine oxides and phosphine boranes were discussed. The method for generating electrophiles containing phosphine borane functionalitites given above is reliable and versatile, but requires multiple steps, and a number of other approaches to preoparing electrophiles suitable for the interoduction of sidearms have been evaluated. These are addressed here.

Syntheses employing free phosphine or phosphine oxide containing electrophiles are likely to be nicely compatible with backbone SPOs; phosphine borane end groups and backbone phosphine oxide functionalities make an unattractive combination within a single molecule due to the increasing complexity of the removal of two different protective groups. Of the multiple methods that could be used to generate an electrophilic side-arm, attempts were principally made to use secondary phosphines and secondary phosphine oxides as nucleophiles and to react them with electrophiles containing either a symmetric (dibromopropane) or unsymmetric (bromochloropropane) or an allylchloride.

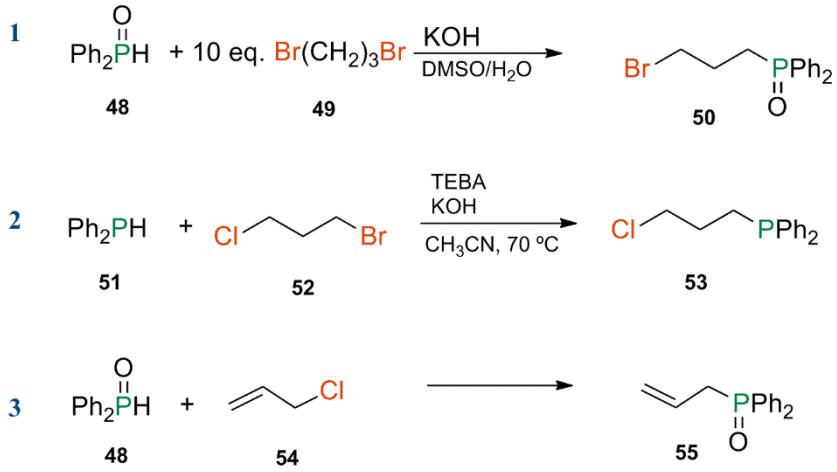

Scheme 32: The attempted electrophilic side-arm syntheses include radical addition and alkylation requiring a leaving group.[171,224–226]

In Scheme 32 are described the attempts for the synthesis of electrophiles; route **1** and **2** generate electrophiles containing a leaving group.[171,224–226] Method 2[225,226] is literature known and results in a 70 % yield of the 3-chloropropyl diphenylphosphine (**53**), a transparent oil, at −14.08 ppm in the $^{31}P\{^{1}H\}$–NMR. Method **1** (Scheme 33) reflects a desire to use the readily available 1,3-dibromopropane (**49**); this starting material is also known for the synthesis of bis(phosphine)s under stoichiometric conditions.[224] Monophosphination of the 1,3-dibromopropane was attempted through changing the stoichiometry, where it was assumed that an excess of 10 eq.[a] of **49** would shift the reaction towards mono-phosphination. Various bases to deprotonate the diphenylphosphine and solvents were screened. The best results were obtained using KOH/NaOH in a DMSO/water (9/1) mixture (Table 5), the $^{31}P\{^{1}H\}$–NMR of the crude reaction indicated only the product resonance at 34.29 ppm, with a conversion of up to 90 %. The crude ^{1}H– and ^{13}C–NMR($CDCl_3$) also showed the formation of the desired product. Unfortunately the obtained results were not reproducible. In case of Cs_2CO_3 as the base, disubstitution was the major by-product and its separation was not achieved.The purification proved difficult[b] and these methods were finally rejected mainly because of poor results or difficulties in the purifi-

[a] *Katti et al*. functionalized selectively from dibromopropane using 0.2 eq. $P(OEt)_3$ 3-bromopropylphosphonate.[335]

[b] The phosphine oxides showed a tendency to stick on columns, hence chromatographic separation was difficult; and the nature of the products, as oils, made purification complicated.

cation as mentioned above. Clearly, had these syntheses been successful, the subsequent tetraphosphine synthesis would then have been analogous to the borane alternative through a nucleophilic substitution (Scheme 34).

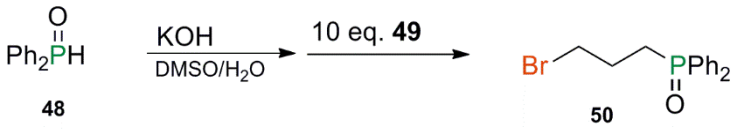

Scheme 33: Synthesis of 3-bromopropyl diphenylphosphine oxide was achieved using an excess of the dibromopropane to ensure mono-substitution.

Exp.	Base	Solvent	T/°C	t/h	yield/%
1	Cs_2CO_3	anhydrous acetone	20	88	89
2	NaH	DMSO/H_2O (9:1)	25	60	73
3	KOH	DMSO/H_2O (9:1)	25	60	80

Table 5: The best results of the screening of various bases in combination with solvents to synthesize 3-bromopropyl diphenylphosphine oxide.

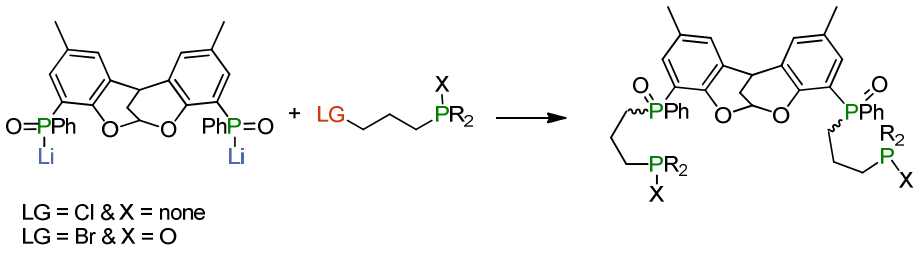

Scheme 34: Potential nucleophilic substitution to synthesize the tetraphosphine target.

Method **3**[167] (Scheme 32) involves an allyl-component bearing a leaving group (**54**), the Cl leaving group was substituted first to form the desired allyl-phosphine oxides **55** ($^{31}P\{^1H\}$–NMR: 33.14 ppm, estimated yield 50 %[a]). **55** was anticipated to undergo with the backbone SPOs **39** a radical addition with radical starters like AIBN as described in Scheme 35, producing tetraphosphines bearing a C3 chain analogous to the phosphine borane method with Michael acceptors[b].

[a] The yield estimated by $^{31}P\{^1H\}$–NMR shows only two resonances, the starting secondary diphenylphosphine oxide and the product.

[b] Not radical in this case.

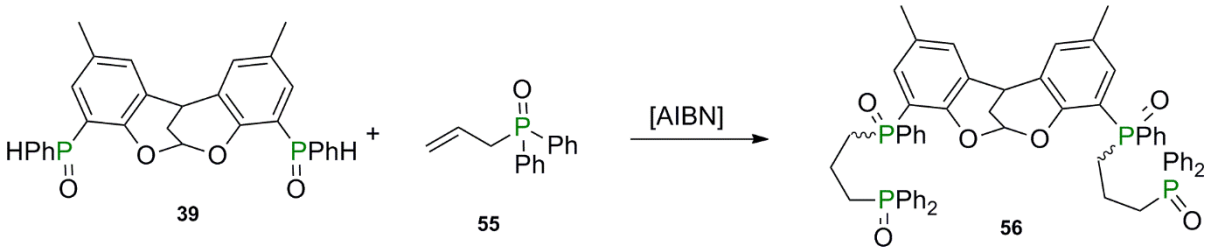

Scheme 35: Potential synthesis of tetraphosphines using allyl phosphine oxides. The reaction would occur under radical addition conditions with a suitable radical starter like AIBN.[167]

Finally we rejected these phosphine oxide-based methods, because the systems were more complicated than anticipated, the synthesis often led to by-products which were difficult to remove, and any tetraphosphines that might be obtained would be mixed diastereomers. Furthermore phosphine oxides are laborious in their reduction. A major problem was the reproducibility of the reactions and scalability, especially of the backbone phosphorylation mentioned previously, which ultimately led to rejection of this method.

2.7 Synthesis of Tetraphosphines

The preparation of a useful nucleophile precursor **38c** and several suitable electrophiles allows the synthesis of tetraphosphines to be attempted. The first procedure employed for the synthesis of the target tetraphosphines involves the deprotonation of the backbone phosphines using KO*t*-Bu at 0 °C – 25°C, followed by the addition of the mesylate side-arm phosphines of interest (Scheme 36).

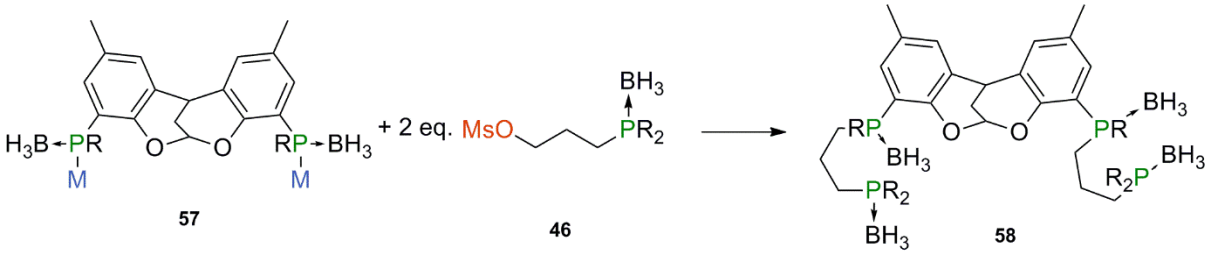

Scheme 36: Synthesis of a tetraphosphine borane through nucleophilic substitution.

The deprotonation of the **38c** followed by the nucleophilic substitution did not occur as smoothly as expected. It is probable that compound **38c** partially inverts at phosphorus during the deprotonation. If the borane groups are positioned in close proximity to the acetal-oxygens they might be coordinated by the oxygen atoms, this forces the phosphorus to change its tetrahedral geometry to flatten (planarization) and hence it loses its stereoinformation. Two theories regarding similar molecular systems are proposed by *Imamoto et. al*.[167,176] He suggested that the deprotonated species, especially with an anisole-like structure in combination with R = *t*-Bu or Cy are very stable due to the coordination of the cation (Li/K) to the oxygen[176], but he observed racemization in tertiary phosphine boranes with less bulky groups (Ph, Me); upon heating the compound shown in Scheme 37 racemises.[167,176] They suggest that this occurs due to the proximity effect of the *o*-methoxy group[167]. The dioxocin-group of **38c** might act similarly to the *o*-methoxy group in *Imamoto's* example. In conclusion it might be that slight inversion is observed due to the *o*-methoxy proximity effect, but, in accordance to *Imamoto's* results regarding bulkier groups on the secondary phosphine borane, our product indicated only maximal 10 % inversion.

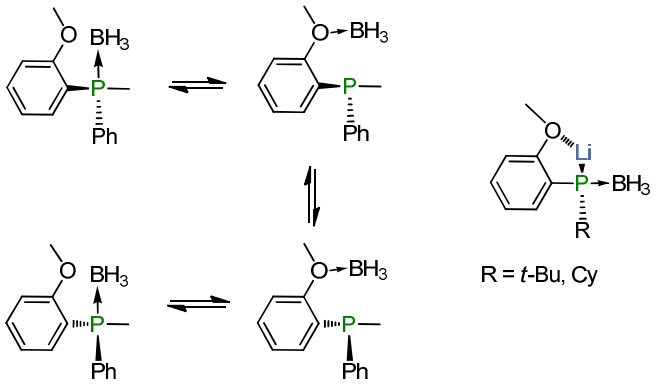

Scheme 37: Iversion of tertiary phosphine boranes bearing anisole substituents. This phenomenon, observed by Imamoto and co-workers,[167] occurs upon warming when with non-bulky groups are present. However bulky groups like *t*-Bu and Cy stabilize the alkali cation, minimizing or avoiding racemization.[176]

Whilst this method successfully produced borane- protected tetraphosphines in good yields (56 %), chromatography to separate the product diastereomers proved extremely difficult, so another approach was sought.

An alternative method to obtain the tetraphosphines, in an attempt to avoid inversion, involves the direct functionalization of the backbone phosphine boranes *rac* **38c**, transformation into

chains containing terminal electrophiles and subsequent phosphination. The metallated backbone **57** (1.17 g, 2.26 mmol) was dissolved in 80 mL dry THF, cooled to – 78 °C and subsequently ethyl 3-bromopropionate (2.1 eq., 0.6 mL, 4.75 mmol, Scheme 38, or if desired other ω-bromoalkyl esters) was added slowly. However, the reaction displayed low conversion and mixed products *vide infra*.

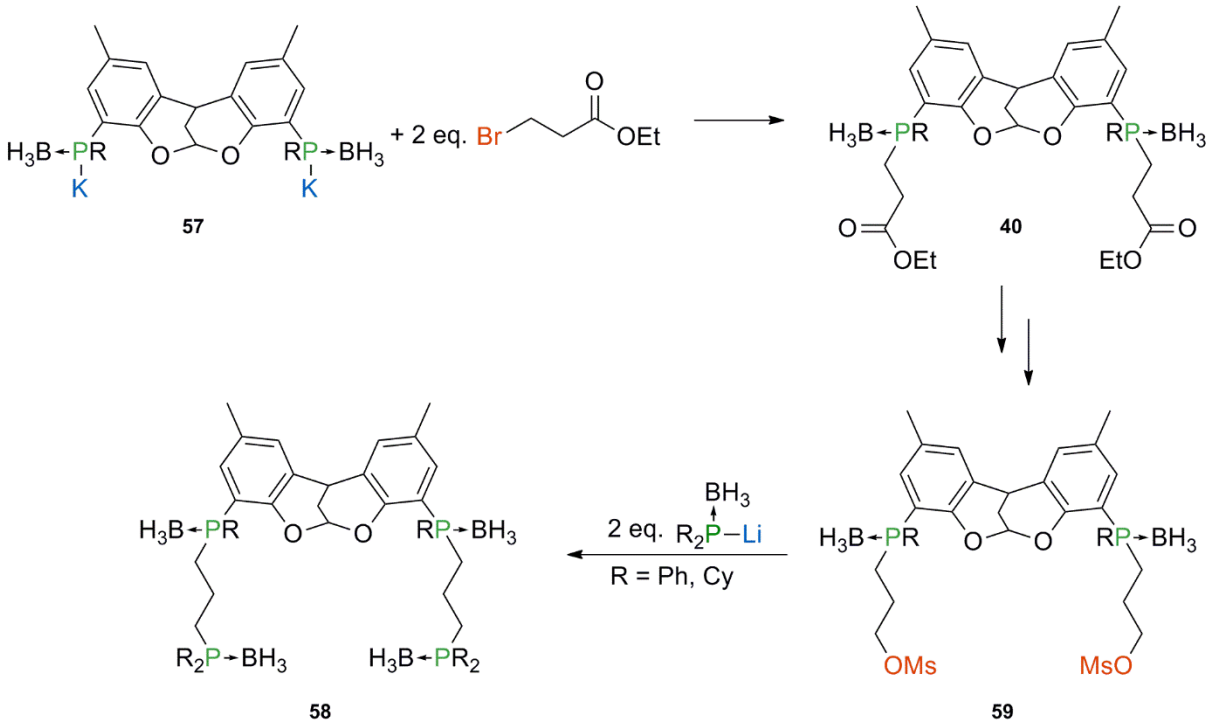

Scheme 38: Synthesis of compound 43 was not as straightforward as expected. The synthesis of the tetraphosphines follows a similar approach as described in Scheme 30 and Scheme 36.

This reaction is very easy to interpret, because it allows direct observation of any occurrence of phosphorus inversion during the transformation into the tertiary phosphine borane compounds **40** (Scheme 38). Another advantage is if diastereopure starting material were obtained, the reduction and mesylation maintained the stereoinformation and a nucleophilic substitution with simple diphosphine boranes should allow a facile synthesis of various tetraphosphines.

However the formation of the phosphine boranes elaborated with terminal ester groups **40** resulted in a low conversion (50 % of the lithiated compound was quenched), analogous to the side-arm synthesis (Figure 41), and a mixture of mono- and di-functionalization was obtained. The crude reaction mixture displays in the $^{31}P\{^{1}H\}$–NMR the formation of tertiary phosphines

at 34.26 ppm. However as well the starting material *rac* **38c** at 3.46 ppm and – 0.08 ppm, however the ratio of the two resonances from compound *rac* **38c** changed slightly, which indicates partial mono-substitution. The crude ^{1}H–NMR ($CDCl_3$) shows the appearance of multiple backbone molecules, (as evidenced by multiple lines in the acetal region) which supports the assumption of mono-substitution[a], but the products were not separated, hence no clarification was acquired. Due to the low conversion of only 50 % yield[b] and the appearance of multiple products this method was rejected.

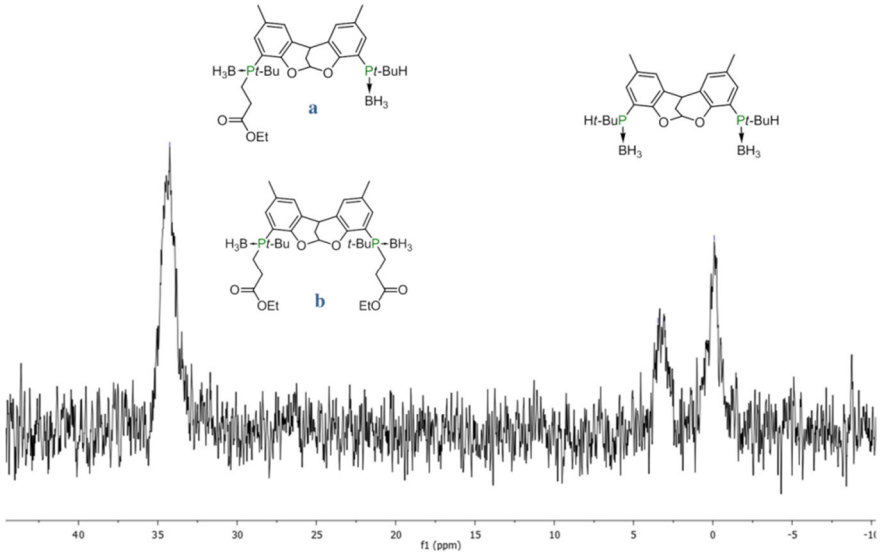

Figure 41: The crude ^{31}P{^{1}H}–NMR ($CDCl_3$) of **40** prepared through metallation of **38c** with *n*-BuLi and reaction with ethyl 3-bromopropionate. It is apparent that some addition occurred, however it seems that predominantly one phosphine borane of the backbone is functionalized, since the ratio in the backbone phosphine boranes changed. It is conceivable that, during the process, racemization occurs leading to one resonance at 34.26 ppm.

Nonetheless this method seemed promising, since it allowed the direct observation of change in the stereoinformation after the transformation from *rac* **38c** to **40**, and its optimization. In conclusion we focused on this method, but changed the reactant 3-bromopropionate, due to its poor results, to ethyl acrylate, a Michael acceptor. A preliminary reaction of the metallated compound *rac* **38c** with the Michael acceptor ethyl acrylate (Scheme 39), generating an electrophilic backbone, occurred with undetectable loss of stereochemistry at phosphorus. In this procedure all steps (Michael addition, reduction and mesylation) were the same as those for the synthesis of a side-arm **46** (Scheme 30).

[a] Partially inversion may have also occurred, but this could not be proven.

[b] Estimated by ^{31}P{^{1}H}–NMR.

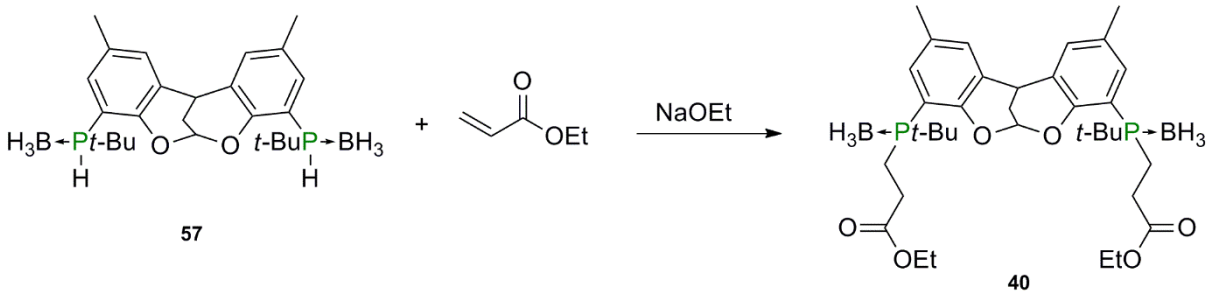

Scheme 39: Michael addition of metallated compound *rac* **38c** with ethyl acrylate and sodium ethanolate (base) leading to the backbone ester **40** with retention of configuration.

This approach worked smoothly without the occurrence of inversion. The secondary phosphine boranes *rac* **38c** (5 g, 10.97 mmol) underwent Michael addition with ethyl acrylate (2.2 eq., 2.6 mL, 24.11 mmol) using as base sodium ethoxide, formed *in situ* from EtOH and elemental sodium (~ 1 eq, 300 mg, 13,05 mmol), in a mixture of THF/EtOH (95/5, 400 mL/20 mL) with undetectable loss of stereochemistry at phosphorus (Scheme 39, Figure 13). The reaction probably occurred around 0 - 10 °C because, if the temperature is raised to quickly to room temperature, slight inversion was observed. As in the synthesis of the side-arm, oxa-Michael addition occurred, but now the by-product could be removed more easily by washing, because the desired product *rac* **40** is a solid, whilst the oxa-Michael by-product is an oil. A white powder of 95 % yield was isolated. The $^{31}P\{^{1}H\}$–NMR indicates a shift of the two phosphine borane resonances to 37 and 41 ppm maintaining the same ratio as displayed by the secondary phosphines *rac* **38c** (Figure 42). Evidence of diastereomeric purity could be determined by ^{1}H–NMR (Figure 43) and ^{13}C–NMR (Figure 28), and a crystal structure displaying the *rac* form of compound **40** was obtained (Figure 45).

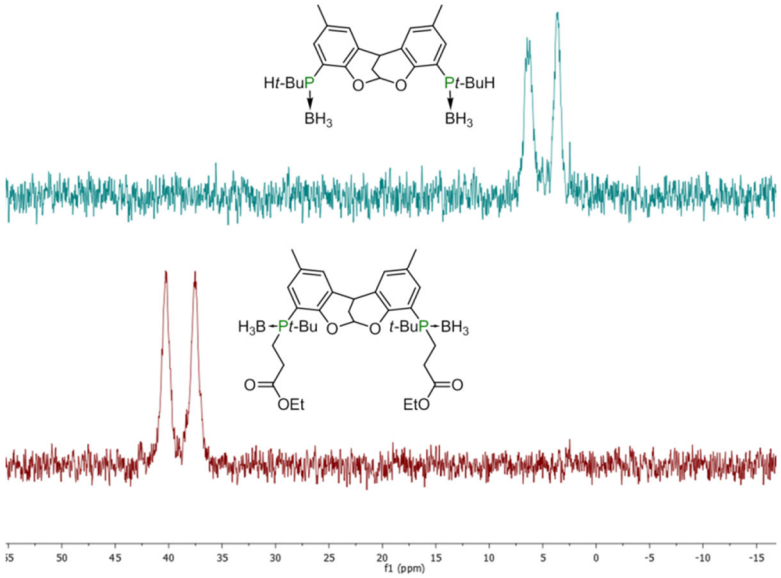

Figure 42: In the $^{31}P\{^{1}H\}$–NMR the shift of the two *rac*-**40** resonance after the Michael addition indicates clearly that the ratio of the resonances did not change and the reaction underwent retention of configuration.

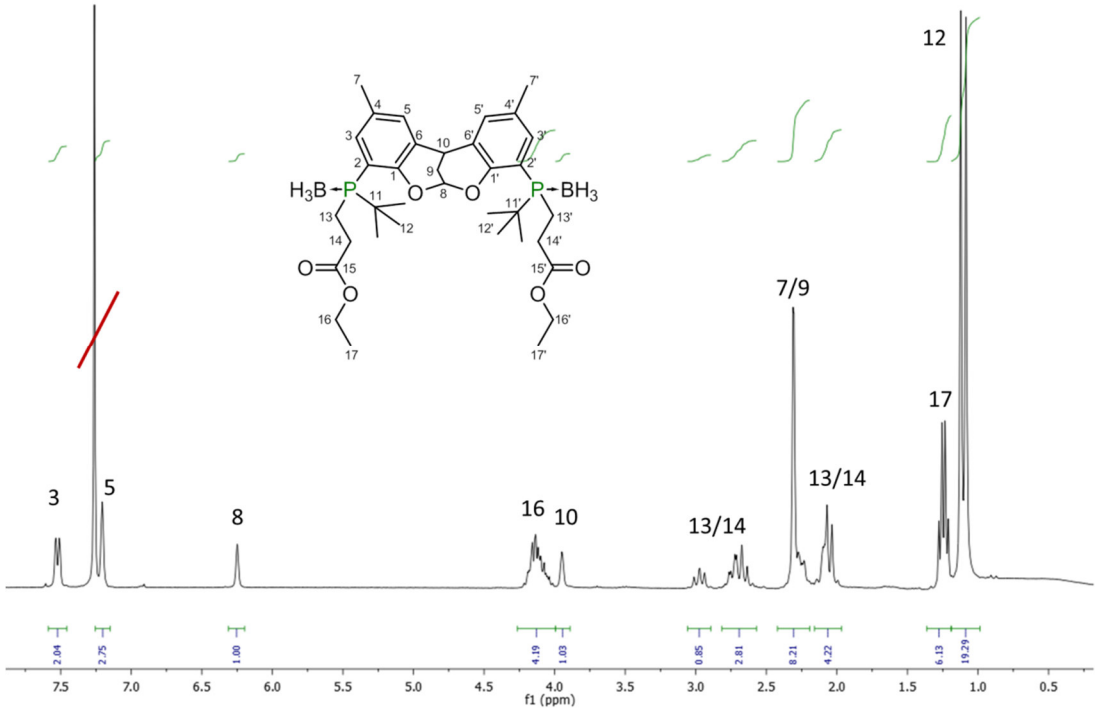

Figure 43: The ^{1}H–NMR ($CDCl_3$) of pure *rac* 40

The ^{1}H–NMR($CDCl_3$) of **40** shows a clean spectrum. The resonances, as well as the integration of the resonances, fit the assumption that we obtained one clean compound. A close look at the ^{13}C–NMR($CDCl_3$) was therefore required. As with the analysis of the secondary phosphines

rac **38c**, the aromatic region of molecule **40** is decisive in the analysis. A comparison of the aromatic resonances of *rac* **38c** and **40** shows clearly that the pattern is similar, and that the C8 carbon displays only one resonance. In conclusion this is a feasible method to generate tertiary phosphines maintaining the same configuration as displayed in the starting material *rac* **38c**.

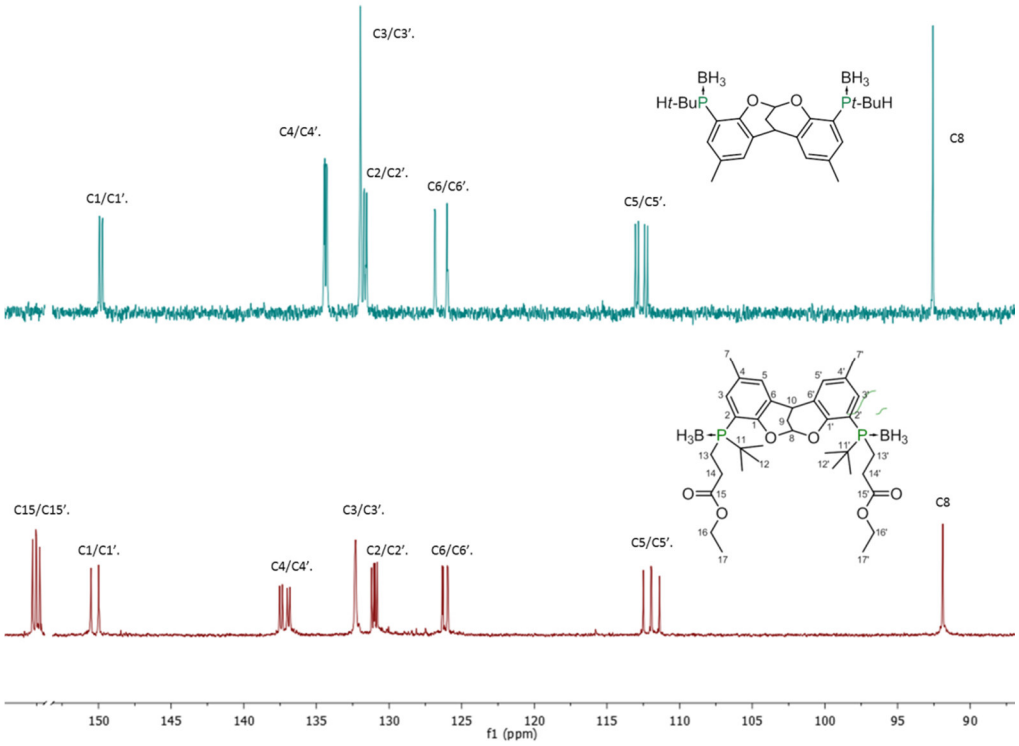

Figure 44: $^{13}C\{^{1}H\}$–NMR spectra of the aromatic region of compound **38c** and its derivative **40**. The spectra clearly show the same patterns, and only one resonance for C8. In conclusion the reaction proceeds with retention of a *rac* configuration. Spectrum cut between C15 and C1.

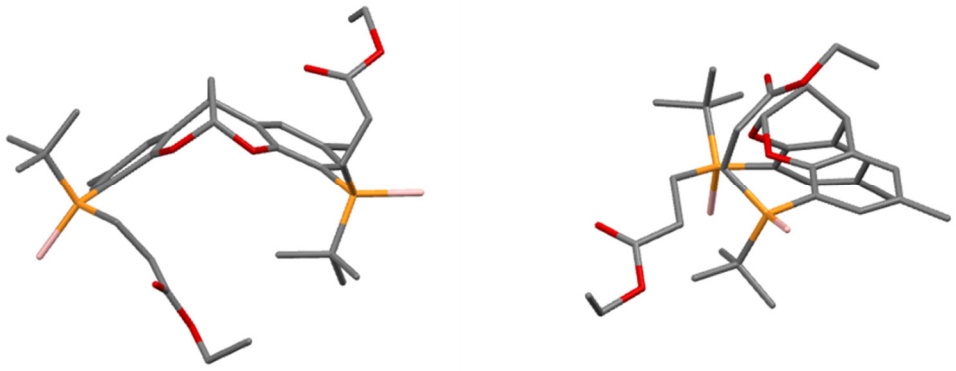

Figure 45: X-ray analysis of compound *rac* **40** shows the *rac* form. Non-relevant hydrogen atoms have been hidden for the sake of clarity.

As expected, during the subsequent reduction with lithium aluminium hydride followed by the mesylation of the product alcohol, no change in the stereoinformation of the phosphorus atoms was observed (Scheme 40). *Rac* **40** (5 g, 7.62 mmol) dissolved in 300 mL dry THF was added to 4 eq. of lithium aluminium hydride (2.2 g, 30.48 mmol) dissolved in 200 mL dry THF at 0 °C dropwise under vigorous stirring; after addition was completed the mixture was allowed to warm up slowly and stirred further 1.5 h at room temperature. Subsequently the reaction was quenched using the method as described previously, filtered, washed and extracted, followed by removal of the solvent to yield in a white powder of 82 % (**60**). The ^{13}C–NMR($CDCl_3$) in Figure 46 shows clearly that the stereoinformation on the phosphorus atoms did not change during the reduction to the alcohol **60**. This result confirms the expectation that a functionalization at the chain-end is unlikely to change the stereoinformation at the phosphorus atoms.

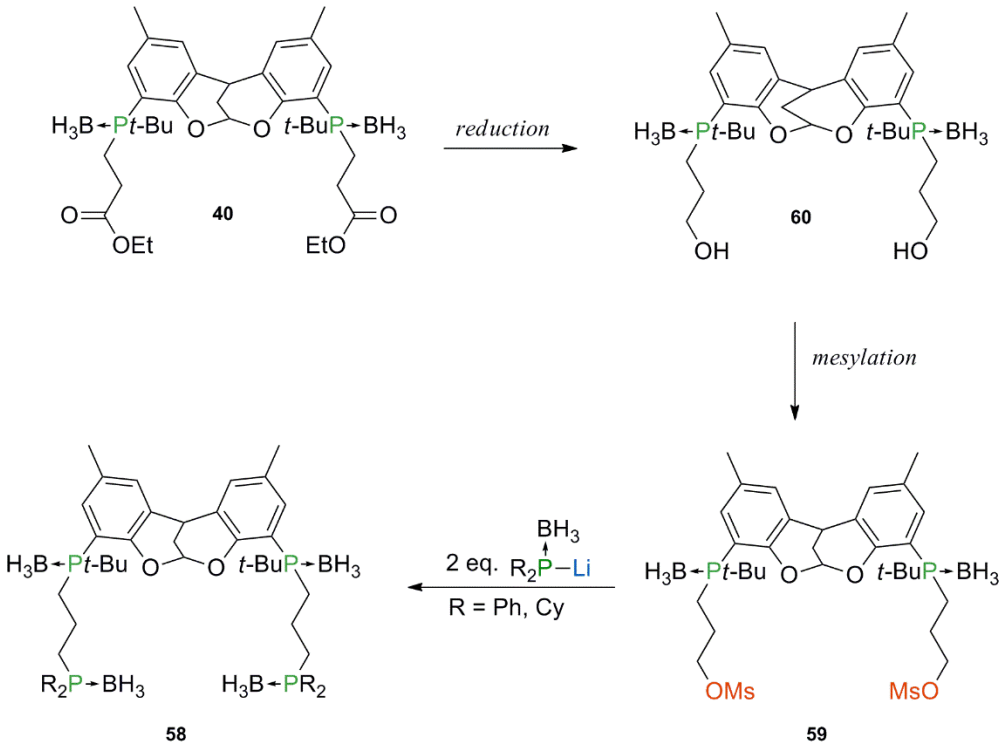

Scheme 40: Generation of tetraphosphine boranes *rac* **58** from *rac* **40**. The process involves reduction with lithium aluminium hydride (**60**), followed by mesylation with MsCl (**59**) and substitution of the backbone-side-arm ester **40**. All steps could be achieved with retention of configuration.

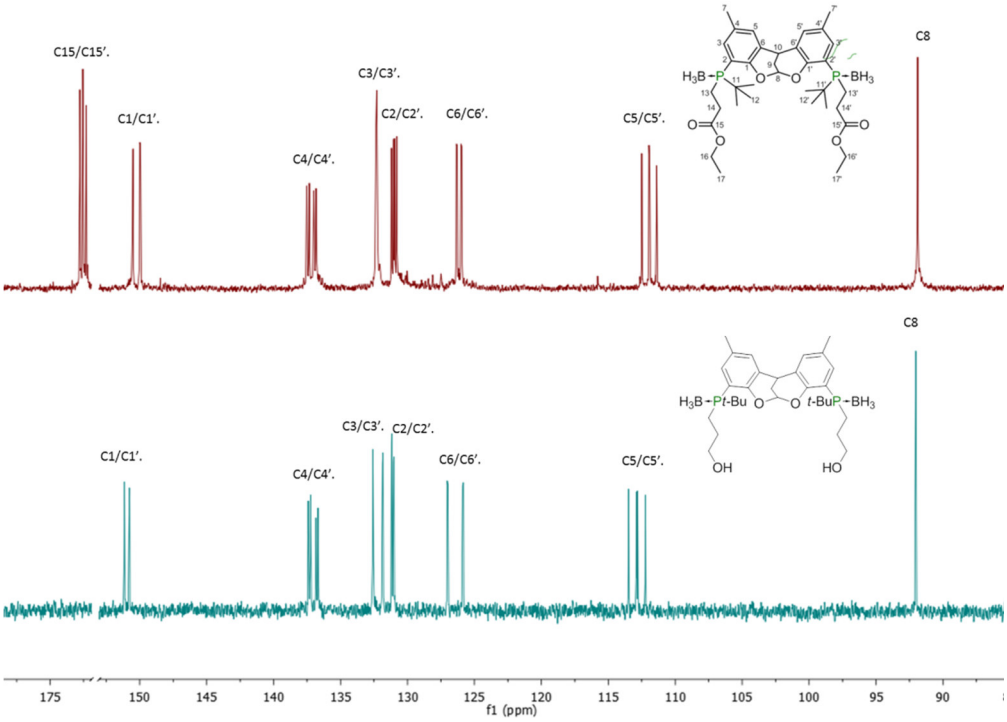

Figure 46: $^{13}C\{^{1}H\}$–NMR spectra of the aromatic region of compounds **40** and **60**. The reduction of **40** with lithium aluminium hydride to **60** does not change the stereoinformation on the phosphorus atoms (only one resonance at C8 and the same pattern in the aromatic region), cut between C15 and C1.

The mesylation was performed as previously; *rac* **60** (5 g, 8.74 mmol) was dissolved in 300 mL dry DCM and 2.6 eq. freshly distilled Et_3N (3.2 mL, 22.71 mmol) and cooled down to 0 °C, subsequently mesyl chloride (2.4 eq., 8.9 mL, 20.98 mmol) was added dropwise, after 1 h at 0 °C the reaction mixture was allowed to warm up to room temperature and stirred further 30 min. The reaction mixture was quenched with 20 mL of a 2 M NH_4Cl solution, washed with sodium bicarbonate (2 x 60 mL) and then dried over $MgSO_4$ and filtered, after the removal of the solvent a white powder of 96 % (**59**) was obtained. As expected the ^{13}C–NMR($CDCl_3$) displayed the desired patterns in the aromatic region and a single C8 resonance, maintaining the *rac* configuration, furthermore the $^{31}P\{^{1}H\}$–NMR($CDCl_3$) spectrum displays two equally intense resonances at 39.09 and 37.55 ppm (Figure 47).

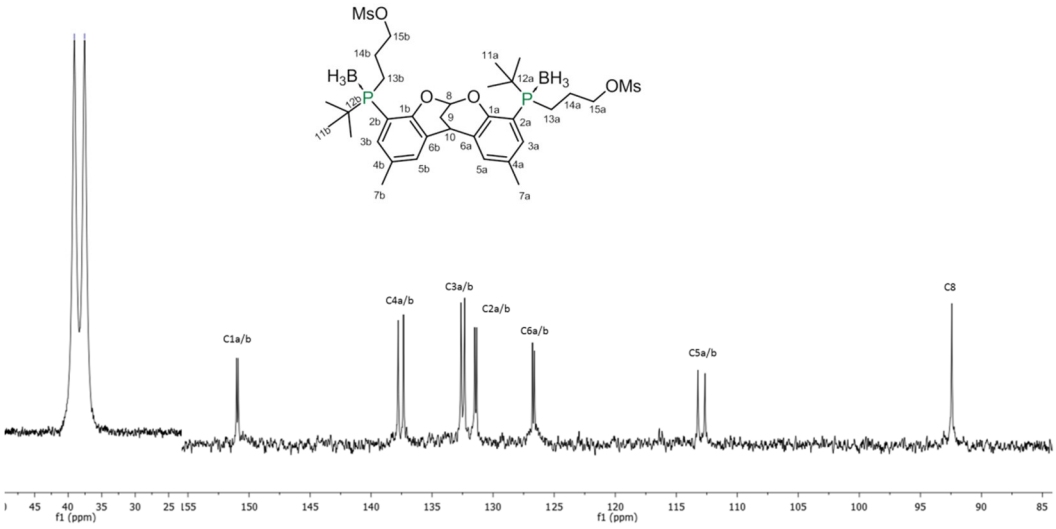

Figure 47: NMR spectra of the DBDOC backbone functionalized with two P(BH_3)*t*-Bu(CH_2)$_3$OMs groups. In the $^{31}P\{^1H\}$–NMR (left) the two peaks characteristic of the *rac*- formulation, as in the starting material *rac* **40** are maintained as equally intense resonances in *rac* **59**. The $^{13}C\{^1H\}$–NMR spectrum (right) of the aromatic region of compound **59** displays no change in the stereochemistry at the phosphorus atoms (only one resonance at C8 and the same pattern in the aromatic region).

As a conclusion this reaction sequence is efficient in the synthesis of an electrophilic side-arm connected to the chiral phosphines over three steps without modifying the stereoinformation of the starting molecule *rac* **38c.**

2.7.1 Synthesis of Tetraphosphines Using Cyclic Sulfates

A further approach to tetraphosphines was evaluated, which uses cyclic sulfates as dielectrophiles. Cyclic sulfates provide a convenient alternative to the electrophilic side-arms: not only are they straightforward[211,227] in their synthesis, they are also very versatile in their electrophilic behavior, and can introduce chirality in the carbon chain if desired. Cyclic sulfates have enhanced reactivity relative to acyclic sulfates, this might be due to the ring.[228,229] They are normally prepared by reaction of a diol[a] with thionyl chloride forming cyclic sulfites, followed by ruthenium-catalyzed oxidation of sulfur. The principal advantage of this one-pot procedure introduced by *Sharpless et al.* is the ability to use alcohols as starting materials, thus opening up a large range of enantiopure products. Only a small amount of transition metal catalyst is required, limiting the risks associated with the highly dangerous and toxic RuO_4 oxidant.[144,211]

[a] Enantioresolved or not, as desired.[211,336]

Cyclic sulfates are electrophilic and ring-open during a nucleophilic attack[a,228] (1 eq.) forming monoanionic sulfates which cleave much less easily than the cyclic sulfate precursors. However, sulfates hydrolyze quite easily in the presence of water with catalytic amount of acid[144,229], so that dry and inert conditions should be maintained during the reaction (Scheme 41).

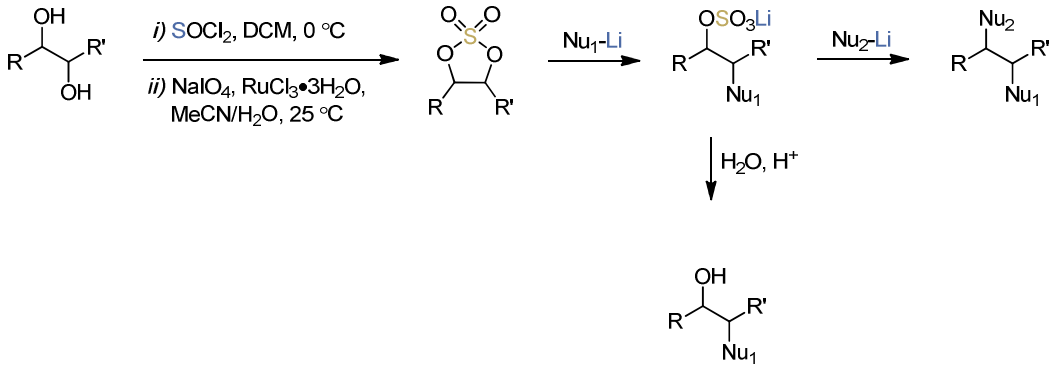

Scheme 41: Synthesis of cyclic sulfates. These compopunds undergo clean, sequential reactions with nucleophiles.[144,229]

Cyclic sulfates are well- investigated in the synthesis of organophosphorus compounds, especially the synthesis of enantiopure phospholanes;[228] a major asset is that they are commercially available, if not, their synthesis is facile and fast. Werner and co-workers used cyclic sulfates to synthesise unsymmetrical[b] bidentate ligands with bulky substituents (Cy, *t*-Bu, *i*-Pr, and Ph as comparison or combination) at the phosphorus atom donor centers of of C2 and C3 linked dissymmetric diphosphines. Werner's group worked with free phosphines to synthesize these symmetric and unsymmetrical diphosphines;[211] Dr. F. Heutz[230,231] from the group of *Kamer et al*. used phosphine boranes in the ring-opening step for the synthesis of his to resin- bound diphosphines. This phosphine borane approach suits our methods better, in enabling the use of the secondary phosphine borane backbone *rac* **38c**. Phosphine boranes are anticipated to retain configuration as described previously; hence the use of cyclic sulfates is very attractive maintaining the stereoinformation of the two phosphorus atoms in *rac* **38c**. The intermediate could not be isolated due to the 'detergent' nature of monoanionic sulfate anions connected to a carbon-chain (**61**) in aqueous solutions; as a consequence only after addition of the second phosphine and protection with boranes (in **62**) changes in the stereoinformation could be observed. Nevertheless this was not a major problem, since the reaction time is very short (2 h).

[a] A wide variety of nucleophiles are suitable, like hydride, azide, fluoride, benzoate, amines, and phosphides, etc.[228]

[b] Bearing two electronically different end groups.

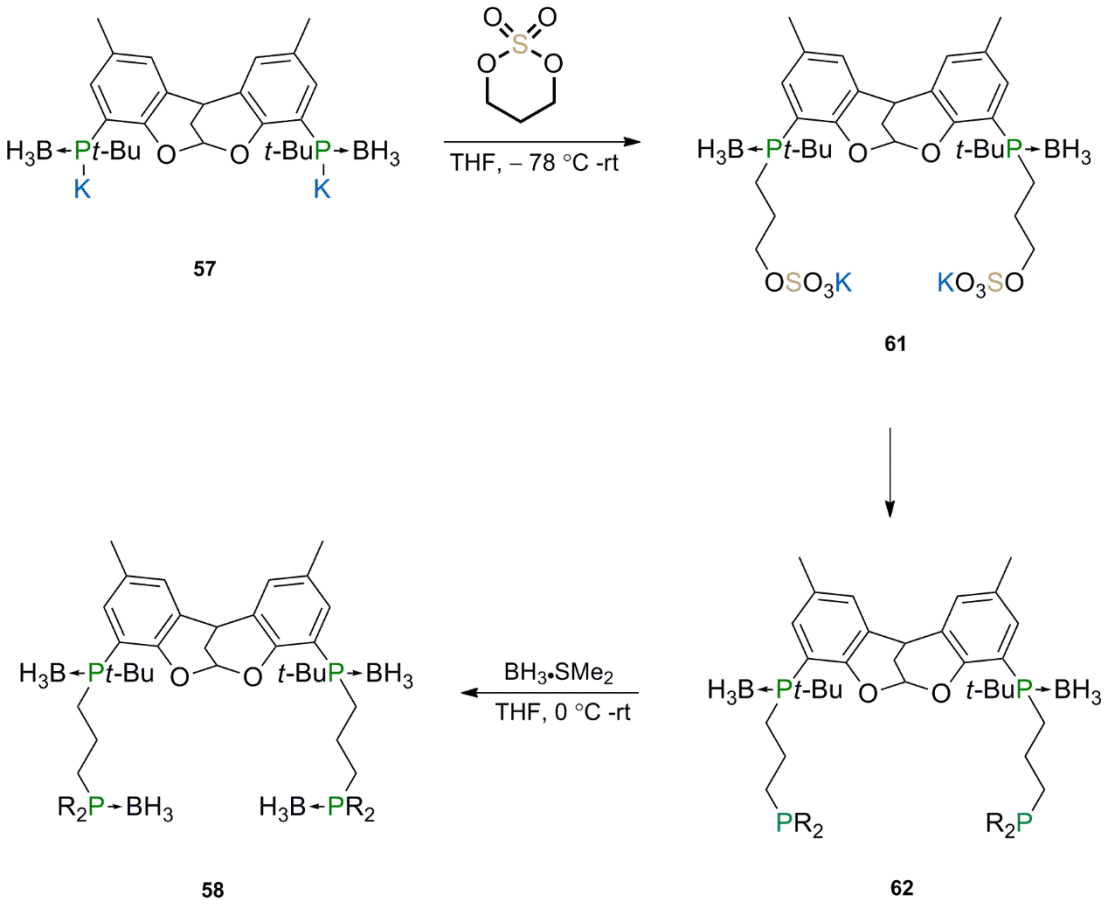

Scheme 42: Projected synthesis of the tetraphosphines using cyclic sulfate electrophiles. The resulting tetraphosphine **62** can be protected by boranes for purification purposes. The boranes can be removed in the next step.

In the first step *rac* **38c** (0.3 g, 0.69 mmol) dissolved in 80 mL dry THF was metallated at room temperature with KO*t*-Bu (2.3 eq., 0.18 g, 1.59 mmol). The crude metallated product **57** was subsequently added at – 78 °C to the cyclic sulfate (2.1 eq., 0.2 g, 1.45 mmol) dissolved in 10 mL dry THF, which gave ring opening and the formation of potassium salts of the bis(phosphineborane-ω-propionylsulfate) (**61**). This step, when monitored by $^{31}P\{^{1}H\}$–NMR displayed a change from the metallated phosphide borane **57** at –37.13 ppm to the tertiary phosphine borane **61** at +35.34 ppm. Only one broad signal appears after the formation of the tertiary phosphine boranes, so no useful indication concerning stereocontrol in this step is available at this stage.

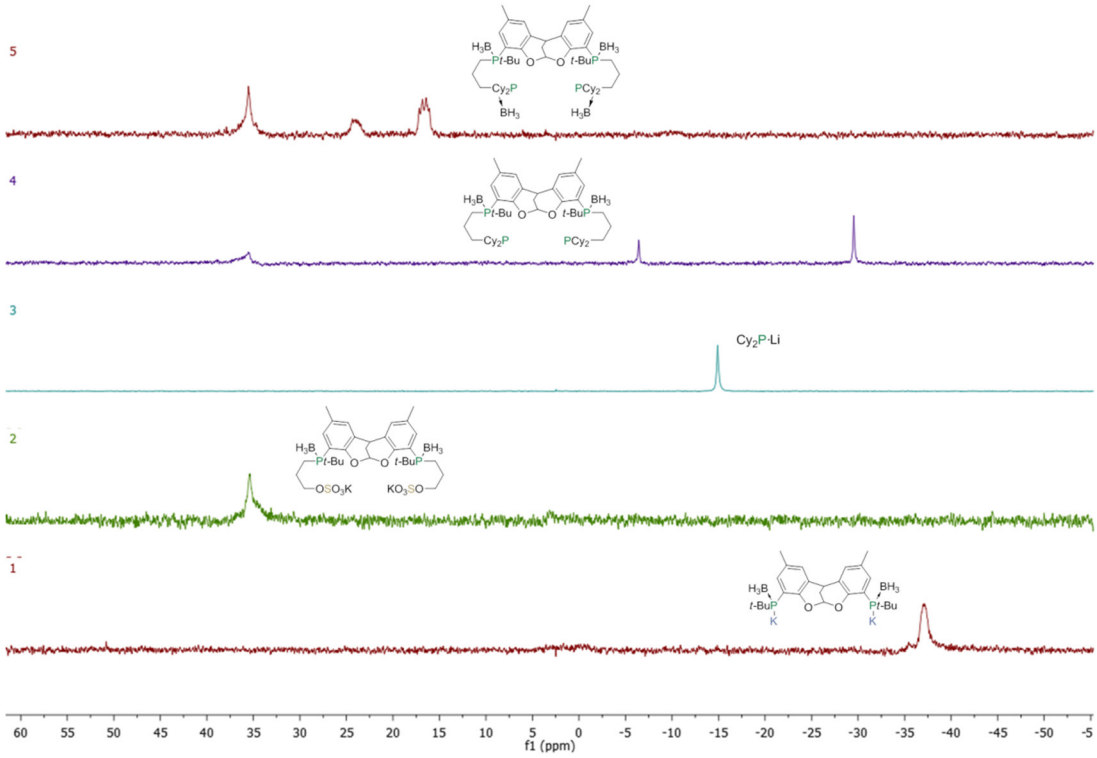

Figure 48: The $^{31}P\{^{1}H\}$ NMR spectra for the synthesis of tetraphosphine boranes from *rac* **38c.** After metallation of *rac* **38c** by KO*t*-Bu (spectrum 1), the mixture is allowed to open the cyclic sulfate to form di(tertiaryphosphineborane) **61** (spectrum 2). Separately, $LiPCy_2$ is prepared from $HPCy_2$.and *n*-BuLi (spectrum 3) and this mixture is added to the crude solution of **62** (spectrum 4). Boronation provides the tetra(phosphine borane) **58** and $HPCy_2{\cdot}BH_3$.

The product was not isolated, but was further treated *in situ* with a solution of $LiPCy_2$ that had been freshly prepared from $HPCy_2$.[a] An excess of phosphide reagent was necessary (4 eq.), because in addition to the formation of the presumed product **62** ($^{31}P\{^{1}H\}$–NMR = –6.44 and + 35.39 ppm), quenching (to Cy_2PH: $^{31}P\{^{1}H\}$–NMR = –29.54 ppm) was observed when stoichiometric amounts of phosphide were used. This quenching probably results from the use in the first step of the base KO*t*-Bu, whose by-product *t*-BuOH is likely to protonate $LiPCy_2$.[b]: As a consequence, two equivalents of $HPCy_2$ are also generated. It should be noted that the PCy_2 endgroups in **62** seem to appear in the $^{31}P\{^{1}H\}$–NMR as a singlet. Whilst unexpected, this feature also appears in the corresponding fully deboronated analogue (R=Cy) *vide infra*. Finally **62** was protected *in situ* with $BH_3{\bullet}SMe_2$ (4.2 eq.) to give the tetra(phosphine borane) **58** which shows shifts in the $^{31}P\{^{1}H\}$–NMR in the expected regions of to +24.1 and +35.4 ppm, and the

[a] The greater nucleophilicity of the free phosphide relative to the phosphide borane is necessary to compensate for the low reactivity of the potassium alkanesulfate functionalities.

[b] p*K*a of *t*-BuOH = 32.2, and estimate dialkylphosphines = 35 in DMSO.[337]

by-product $Cy_2PH(BH_3)$ at + 16.6 ppm. The lack of two distinct peaks in the 35 ppm region suggests the presence of some impurities.

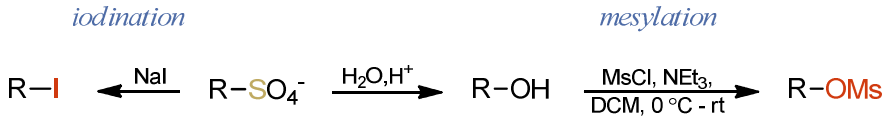

Scheme 43: Displacement of the sulfate-group to produce the corresponding iodide or mesylate.

Since the yield of the desired tetraphosphine **58** was low, alternative methods were again explored. The sulfate group can be transformed into different leaving group (Scheme 43). Iodination and mesylation were considered, but the mesylate would require transformation into the corresponding alcohol, followed by mesylation as described in previous experiments. Since this would imply a three step procedure this method was rejected. Direct displacement of the sulfate group with iodide would reduce the synthetic electrophile procedure by one step to a two-step procedure, and thus this was attempted. However no clean reaction was obtained and purification proved to be difficult, hence this method was dismissed.

The use of cyclic sulfates has great advantages, because of their short and easy reaction sequences, straightforward reaction conditions, and the availability of commercial starting material. The problem concerning any inversion at phosphorus cannot be monitored after the first step by ^{31}P–NMR, hence all steps have to be finished and a proper work-up has to be done to obtain any information regarding inversion and the generation of multiple distereomers at the backbone. Consequently, we did not focus on this method, because of the already more efficient working protocol described previously. Nonetheless, we believe after optimization this method may be a good alternative.

2.8 Synthesis of Tetraphosphines: A Comparison of Stepwise Synthetic Routes

To conclude, Scheme 44 shows the three main approaches used to synthesize the tetraphosphines. All are based on the use of *rac* **38c**, and are intended to retain its stereoinformation. As previously mentioned the metalation of a secondary phosphine boranes (*rac* **38c**) should be

very stable, even with an anisole-type moiety in the molecule, and undergoes the addition reaction with retention of configuration.[167] Consequently in theory all nucleophilic substitution reaction using metallated *rac* **38c** should maintain the diastereoselectivity, leading directly to the *rac* tetraphosphine boranes **58**.

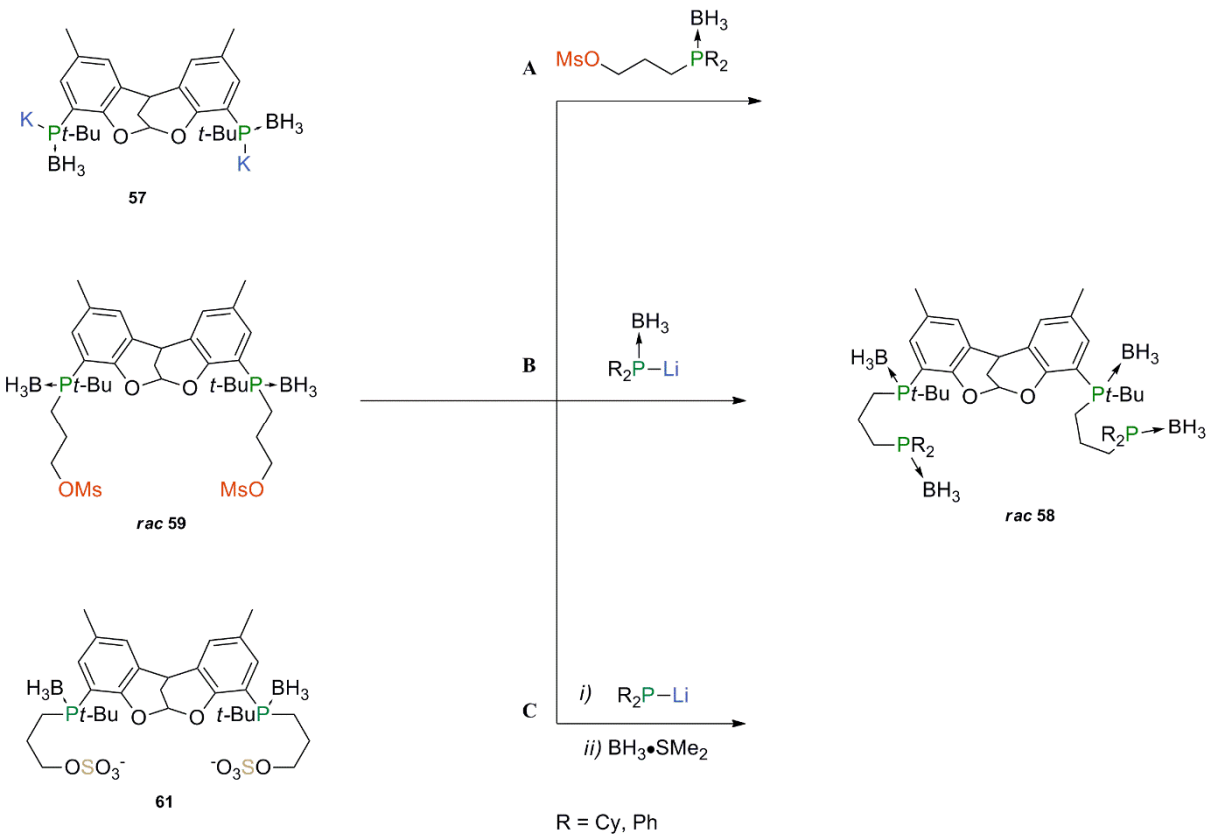

Scheme 44: Three potentially diastereoselective methods to synthesize tetraphosphine boranes *rac* **58**. Method **A** requires the use of pre-synthesized phosphorus containing electrophiles, method **B** and **C** transform the backbone by adding a chain of the desired length which is elaborated with an electrophile, **B** through Michael addition and **C** through cyclic sulfates.

Scrambling (4-10 % *meso*) was observed during the substitution reaction using side-arm mesylates (method **A**, Scheme 44). Since diastereomers have different physical properties their separation was attempted by simple washings and recrystallizations of the diastereo-enriched product mixture. The initial challenge associated with diastereomeric crystallization is the choice of the nature and composition of the solvent. After screening many solvents the most suitable were MeOH, EtOH and THF for washings or trituration; proper recrystallization has proven to be inefficient since an insoluble and unidentifiable solid was present even after filtration and the products have a tendency to form oils. No solvent could separate the *meso* from the *rac* phosphine boranes, but the ratio could be optimized slightly (< 4 % *meso*). After each

washing, ^{13}C–NMR was necessary to detect the number of diastereomers, which made the process quite time consuming. Due to the poor solubility of **58** (R = Cy[a]) the ^{13}C–NMR has proven to be a challenge[b]. The washings improved the purity of the mixture; nevertheless we dismissed this method. A spectrum of crude **58**, bearing Cy-groups at the non-chiral phosphine boranes, is ^{31}P{^{1}H}–NMR displayed in Figure 49 which shows the formation of the tetraphosphine borane **58** with the chiral phosphine boranes at +31.61 and +29.96 ppm and the chain-end non-chiral phosphine boranes at +20.83 ppm.

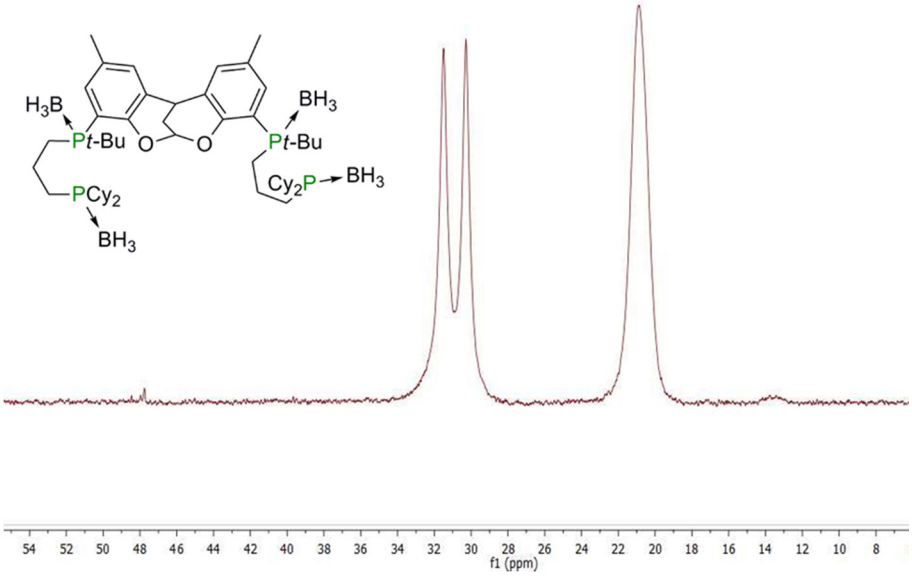

Figure 49: Synthesis of the tetraphosphine borane **58** (R= Cy) by nucleophilic substitution of metallated ***rac* 38c**. This synthesis using the dicycohexanylphosphine- substituted side-arm showed 15 % formation of a sideproduct suspected to be the *meso*-form.

In method **B** (Scheme 44) *rac* **59** bears a mesylate group at one terminus. As described previously, Michael addition of ethyl acrylate to *rac* **38**c led exclusively to *rac*- **40** (Figure 42, Figure 43). No stereoinformation was lost in the following steps, so *rac* **58** could be synthesized in a simple four step reaction sequence, with R = Cy, Ph. About 10 % of an unidentifiable by-product appears at +29.2 ppm in the ^{31}P{^{1}H}–NMR displayed in Figure 50.

[a] R = Ph displayed a similar behaviour.

[b] Overnight in general.

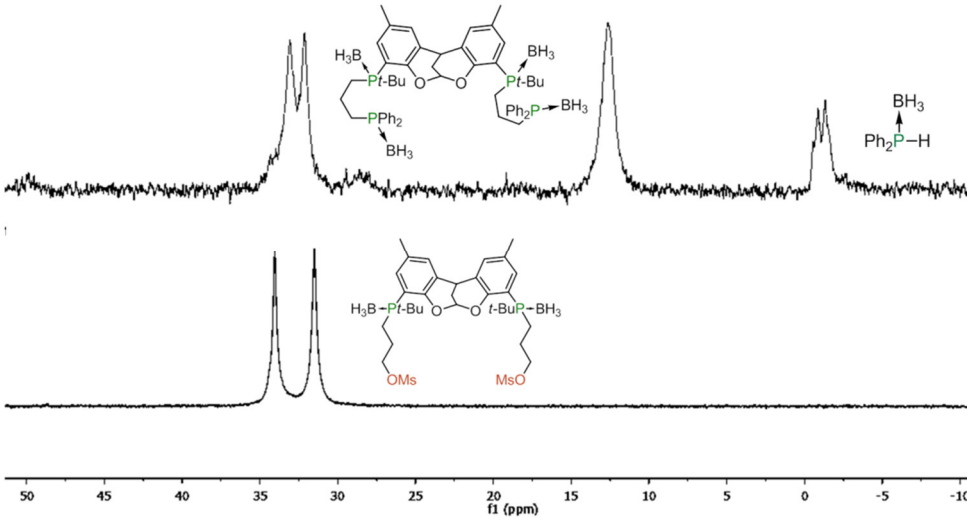

Figure 50: Synthesis of the tetraphosphine borane **58** (R = Ph) through the Michael addition approach.

The synthesis giving a side-arm bearing Cy-groups led to 95 % *rac* **58** and 5 % unidentified by-product, apparent in the $^{31}P\{^{1}H\}$–NMR (Figure 51). Removal of excess phosphine boranes $R_2PH(BH_3)$ is easily achieved by short column chromatography (9/1, PE/EtOAc), since the polarities are very different from the tetraphosphine.

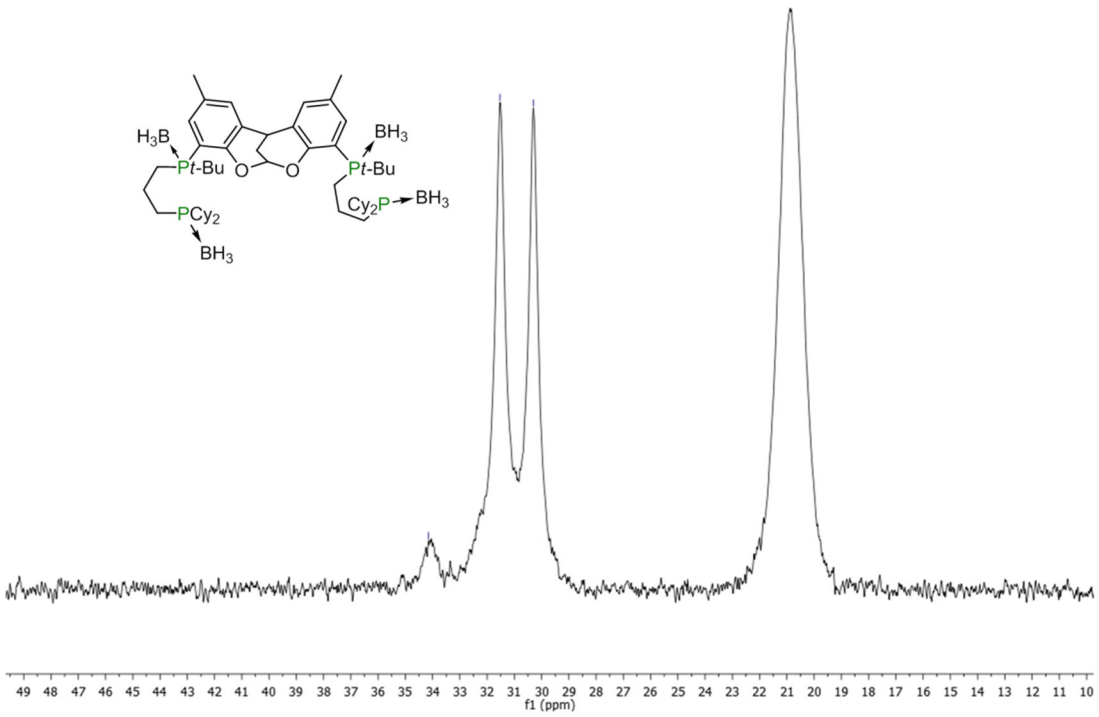

Figure 51: The synthesis of **58** employing the reaction of the metallated compound *rac* **38c** with an electrophilic side-arm bearing Cy-groups. This led to 95 % *rac* **58** and 5 % unidentified by-product.

Method **C** uses cyclic sulfates as mentioned in section 2.7.1. Besides the difficulties in detecting the stereoinformation of the phosphorus atoms after ring opening, the main problem was the poor yield of tetraphosphine, which was confirmed by the appearance of multiple backbone containing components in its ^{1}H–NMR. This method was therefore not developed further.

To summarize, we could successfully synthesize tetraphosphines through scaleable, diastereoselective syntheses. Some reactions could certainly be optimized, particularly those involving **38c**, where precise controlling of addition rate and temperature are likely to be beneficial; if the reaction warms up to fast during the nucleophilic addition[a] of the stereogenic phosphide to an electrophile, the stereoinformation will probably be diluted. Nonetheless the best results to date were clearly obtained by method B, the excess $R_2PH(BH_3)$ (R = Ph, Cy) could easily be separated from **58** by a short column, but the still unidentified by-products have to be determined and if possible avoided to maintain a straightforward and diastereoselective synthesis through all steps.

[a] The low solubility of *rac* **39c** requires a significant amount of solvent (10 g product/400-500 mL THF) to dissolve the entire compound.

2.8.1 Removal of the Borane-Groups from Compound 58

Once the tetraphosphine borane complexes are available, the borane groups have to be removed. In the literature, two methods are widely used to cleave the P–B bond; these use amines or acids ($HBF_4 \cdot Et_2O$). As mentioned in section 2.5.1, amines like NEt_3, DABCO, etc. undergo a S_N2 reaction at boron at high temperatures, whilst acids ($HBF_4 \cdot Et_2O$) provoke a faster reaction requiring lower temperatures. Both methods proceed under retention of configuration at phosphorus.[167,170,209,214,232–236]

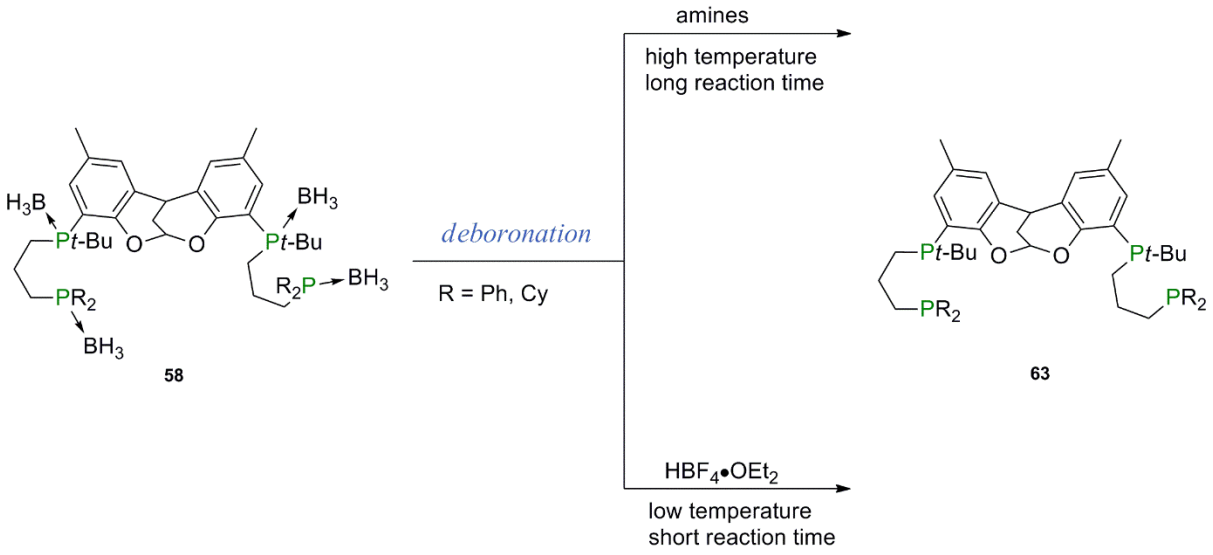

Scheme 45: Deboronation of tetraphosphines. P–B cleavage using either amines, requiring high T and long reaction times, or acidic conditions, requiring low T and short reaction times.[214]

McKenstry and *Livinghouse* introduced the use of tetrafluoroboric acid ($HBF_4 \cdot Et_2O$) as a convenient method to cleave the P–B bond of those phosphine–boranes[214] that are resistant towards deprotection by amines. Its mechanism is not fully clear, but according to *McKinstry et. al.*,[214,237] NMR data indicates that a phosphine fluoroborane is formed (Scheme 46).

This acid- deprotection method is especially suited to electron-rich phosphine-boranes,[170] and the combination of a *t*-Bu-group, an alkyl-chain and the aromatic scaffold at our chiral phosphine boranes makes them quite electron-rich. Hence the use of amines requires a long time at high temperatures to remove the borane. The amines with which we attempted to deboronate the tetraphosphine boranes bearing R = Cy were diethylamine and DABCO. With excess diethylamine (degassed, ca. 10 eq.), heating at 40 °C 12 h in DCM did not lead to any visible deprotection, on the other hand excess DABCO (10 eq.) in toluene heating at 100 °C 12 h lead

to partial deprotection of the phosphine boranes bearing Cy-groups first and also some of the chiral phosphine boranes. After heating for 3 d no further change was observed.

The decomplexation using $HBF_4 \cdot Et_2O$ proved to be more efficient: excess acid (25 eq.) in DCM at 0 °C cleaved all P–B bonds in less than 1 h and, after quenching with degassed, aqueous $NaHCO_3$ solution, the free phosphines were released.

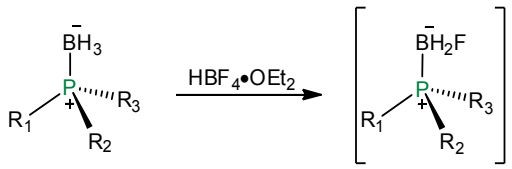

Scheme 46: Decomplexation of phosphine boranes using $HBF_4 \bullet OEt_2$. The reaction is reported to go through the formation of a phosphine fluoroborane intermediate.[214,237]

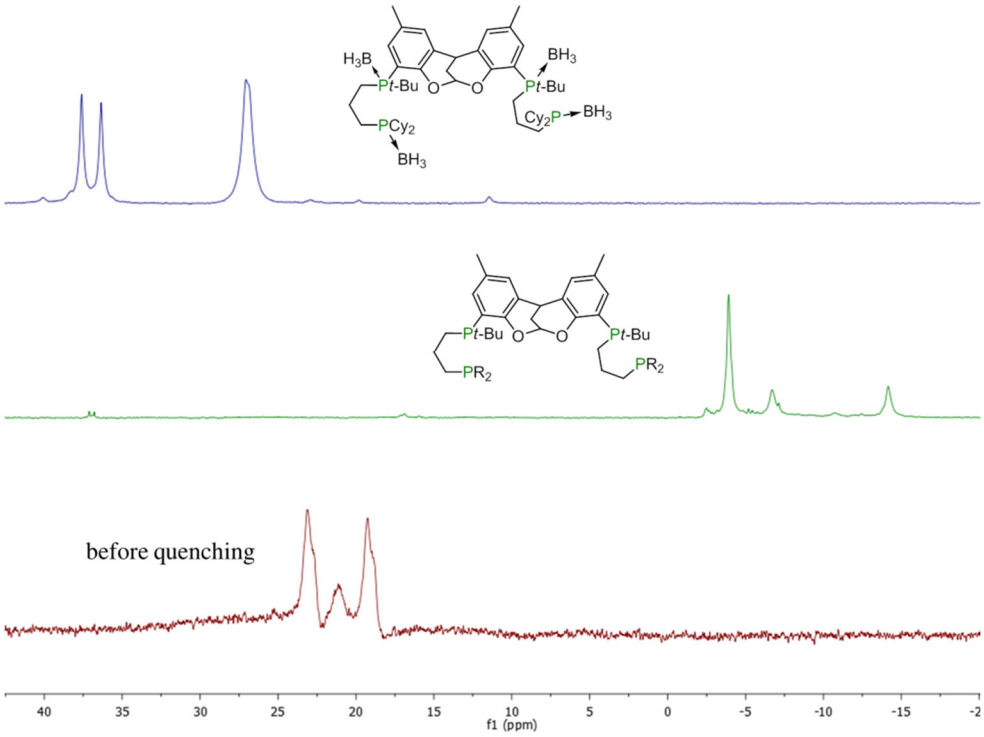

Figure 52: Deboronation of tetraphosphine **58** (R= Cy). The ^{31}P-NMR spectra before treating with acid (top), before the quench (bottom) and after quench (middle) are illustrated.

2.9 Conclusion

In summary we have optimized the synthesis of the backbone precursor DBDOC and the corresponding 4,8-dibromo derivative **36** to allow medium scale synthesis using simple purifications by washing or recrystallization rather than chromatography. Introduction of phosphines stepwise allowed a potentially modular approach to tetraphosphines be developed. In all cases the backbone was phosphinated in the first step. In this step, three diastereomers of the corresponding di(secondary phosphineborane) are theoretically formed but, in the particularly favorable case of **38**, where *t*-Bu substituents are present, only two are isolated, and the *rac* form is obtained very preferentially. This synthesis is a straightforward three step reaction without isolation of intermediates, it is scalable, and the work-up to the *rac* phosphine boranes (*rac* **38c**) is accomplished through simple trituration in EtOAc. Consequently we decided to focus on this backbone bis(phosphine) as a precursor. The phosphine boranes have many advantages, they are air-stable, hence easily handled, and the metalation of the secondary phosphine boranes proceeds retention of configuration.[167] This is important in as much as once resolution of diastereomers is achieved, the stereochemical information should be carried straight through to product; this is particularly advantageous for the series of phosphines targeted here, because the early resolution of diastereomers at the *bis*-(*sec*-phosphine) stage means that modular approaches can be applied to both the chelate chain length and the terminal phosphine groups without any need for further separation of diastereomers. Our focus was initially on electrophilic 'preformed' side-arm phosphine boranes that featured an electrophilic functionality at the end of what was to become the sidearm chain, but later, and more successfully, **38c** was first functionalized first with a Michael acceptor and then converted into tetraphosphines by functional group elaboration. Both methods allowed diastereoselective tetraphosphine borane syntheses, but the Michael addition showed a better and reproducible selectivity. All other methods led to a mixture of the diastereomers, for which a separation method has not yet been perfected.

Chapter 3 Introduction of Diphosphine Chains directly onto the DBDOC backbone

These methods have been found to be significantly less easy to operate than the stepwise introduction of phosphines to the DBDOC backbone that has been described in Chapter 2, and they have not yet led to the production of tetraphosphines. They are nonetheless described here.

As noted in section 2.3.1, there are two main methods to connect diphosphine chains to the backbone: one is a substitution reaction employing a nucleophilic backbone and an electrophilic diphosphine (**A**), the other method involves an electrophilic backbone and requires transition metal induced coupling of a nucleophilic diphosphine to it (**B**)[135–142] (Scheme 13). In the first case the diphosphine would need a suitable leaving group like Cl, Br, I, etc., and these types of diphosphines are not readily available. Coupling reactions require a secondary phosphine functionality, and these are also not commercially available for dissymmetrical diphosphines. In each of these approaches, a secondary phosphine on one of the P-moieties could be a key intermediate: in approach **A** the P-H functionality can- at least theoretically- be "umpoled" to give a suitable leaving group; approach **B** uses the secondary phosphine directly.

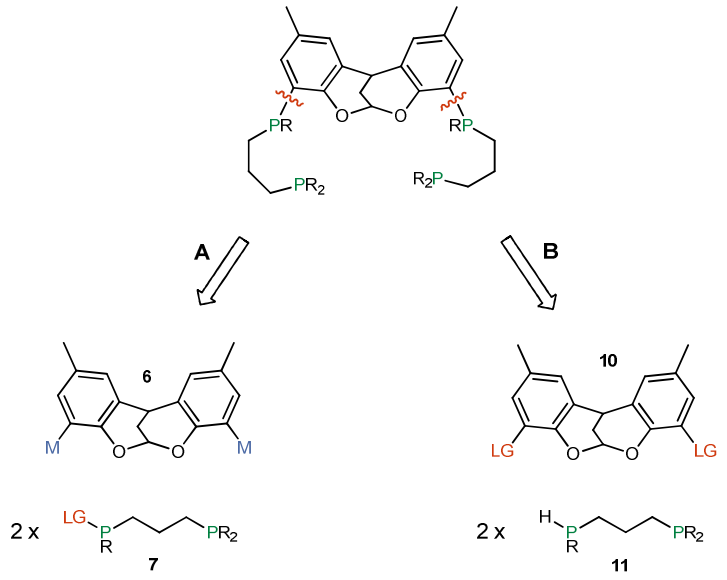

Scheme 47: Retrosynthesis of the tetraphosphine through breaking the bond between the aromatic backbone and the diphosphine component. Two different synthetic methods; **A** which would require substitution reactions, **B** cross-coupling or similar reactions, are possible.[135–142]

3.1 Analysis and Synthesis of Unsymmetric Bisphosphines

Generating a secondary phosphine on one P-moiety of the diphosphine chain can be accomplished through two different approaches (Scheme 48). The first employs methods such as **I**[238], which selectively cleaves commercially available diphosphines of type $R_2P(CH_2)_nPArR$ (n = 2-5, R = aryl), whilst the second involves the synthesis of a non-symmetrically substituted diphosphine from two different P-fragments (**II**)[167,171,176,209,210,239–241].

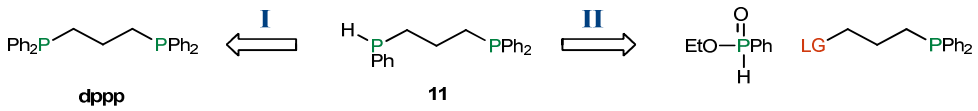

Scheme 48: Retrosynthetic analysis of the secondary diphosphine reactant.[242]

3.1.1 Reductive Cleavage of a P–Ar bond in bis(diphenylphosphanyl)alkanes

Cleavage of a P–C bond can be effected with alkali metals directly or in the presence of electron carriers like naphthalene or liquid ammonia (Scheme 49).[157,243,244]

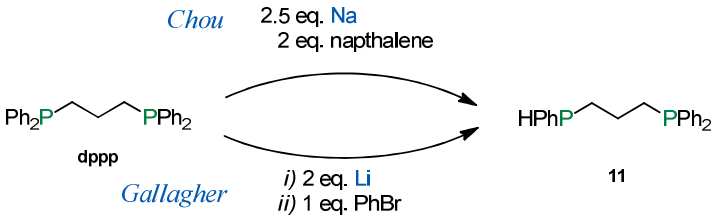

Scheme 49: Potential syntheses of unsymmetrical secondary- tertiary bis(phosphines). Selective cleavage of one aryl-group[242], or cleaving two aryl groups and subsequently reattaching an aryl-group are possible.[242]

Reductive cleavage of *bis*(phosphine)s often leads to double cleavage, with loss of one Ar-group from each P-terminus. If the objective is to generate unsymmetric bisphosphines, two different approaches have been reported, *Chou et al.* used a combination of sodium (2.5 eq.) and naphthalene (2 eq.) and observed a quite selective cleavage of an aryl-group from one P-moiety [242], *Gallagher* on the other hand cleaved an aryl-group with lithium on both P-moieties, followed by selective arylation[245] to produce the targeted bis(phosphine). The selective cleavage seems to be a very attractive method to produce the secondary phosphine on one P-moiety directly, reducing the overall number of reaction steps in theory.[a]

[a] Could be used directly for a cross-coupling reaction or chlorinated and used for a substitution reaction.

The conditions introduced by *Chou* were implemented with dppp, and multiple experiments were run. However, as might be expected for a reaction involving the surface of an electropositive metal, the reproducibility of the reaction was relatively poor. As a consequence, monitoring of the ongoing reaction by ^{31}P NMR is required. In most reactions, di-cleavage of 4-10 % was observed, and some unreacted starting material is also normally present. This might be expected given the lack of any obvious electronic communication between the two phosphine termini. The separation of the mono-cleaved desired product from the di-cleaved by-product will be crucial for all subsequent reactions, since the by-product is likely to interfere, especially in catalytic couplings (Scheme 50). The mixtures obtained under Chou conditions could not be purified successfully using Kugelrohr distillation, recrystallization or column chromatography of the corresponding phosphine oxides. Given that boronated *sec*- phosphines are likely to be much better precursors for transition metal catalysed couplings than the corresponding phosphines themselves[246], and have also been shown to be susceptible to umpolung[134,168,171,247], the crude mixture was boronated, and subjected to an attempted purification by column chromatography. The monocleaved diborane complex ran at a very similar rate to the noncleaved diboronated compound, so these compounds could not be separated in a satisfactory way. The noncleaved diboronated compound (dppp•2BH_3) is highly crystalline, which allowed a large part of it to be removed. However, the monocleaved diborane complex ($Ph_2P(CH_2)_3$ PHPh•2BH_3) was found to be an oil which retains solvent strongly and resists crystallization, so this compound could not be obtained clean in operationally useful quantities.

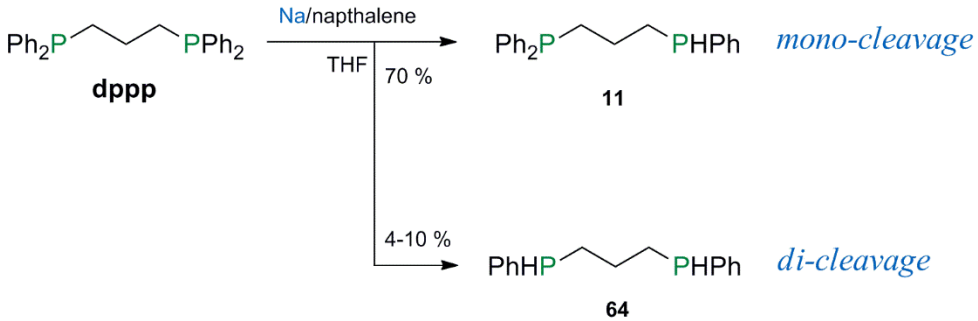

Scheme 50: The reductive P–C bond cleavage of dppp. Typically, this results in 70 % mono-cleaved product and 4-10 % di-cleaved by-product, with conversion being around 70-80 %.[242]

3.1.2 Synthesis of the Unsymmetric Bis(phosphine)s from two different P-fragments

Given the not- unexpected difficulties in generating clean precursors by selective cleavage, it was decided to attempt the longer, but probably cleaner, approach of employing syntheses that were specifically oriented towards the preparation of dissymmetrical compounds. *H*–phosphinates were applied to generate unsymmetric bisphosphines (section 2.5.4.1).

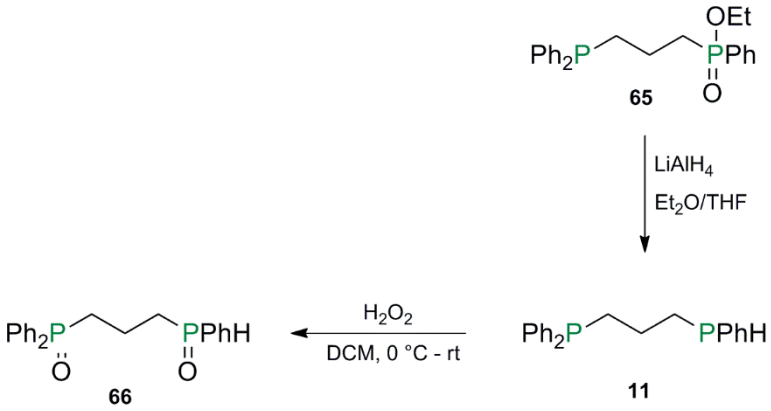

Scheme 51: Potential synthesis of mixed secondary-tertiary phosphine oxides. Upon reduction, 3-diphenylphosphinylpropylphosphinates- could lead, depending on the number of equivalents of reducing agent applied, to the cleavage of the ethoxy group or to a complete reduction. Subsequent oxidation by hydrogen peroxide could form phosphine oxides.

The methods attempted to produce unsymmetric bisphosphines using compound **15** are displayed in Scheme 52. Method I uses compound **17** which is suitable to undergo a radical addition with a radical starter like AIBN. Method II involves a substitution reaction with a compound bearing a leaving group (**18**).[167,171,176,209,210,239–241]

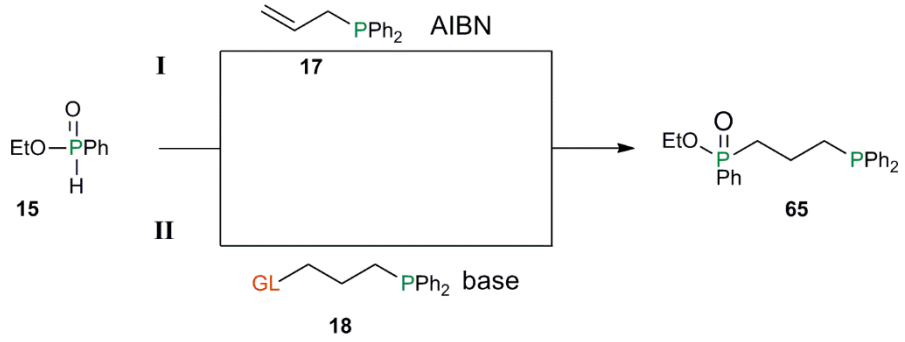

Scheme 52: Potential synthesis of a mixed secondary phosphine oxide/tertiary phosphine. Two electrophiles were attempted, one with a typical leaving group (II), and the other with a non- activated olefin (I).[167,171,176,209,210,239–241]

Direct alkylation (method **II**, Scheme 52) using a strong base to deprotonate the phosphinate did not give the desired substitution reaction. Instead of the formation of compound **65**, a second P–H coupled moiety was observed in the ^{31}P–NMR, so this method was not pursued further. The radical addition (**I**) was run as a neat reaction at 80 °C and, after approximately 20 h, the product was obtained in a yield of 60 %. This reaction was straightforward, but the yields were only moderate, so the method was rejected after moving to Palaiseau and focusing on the phosphine borane approaches.

3.1.3 Chlorination of Unsymmetric Bisphosphines

Diphosphines bearing a leaving group such as chloride at phosphorus can theoretically undergo a substitution reaction with the dilithiated backbone to provide tetraphosphines. This is a straightforward and very intuitive approach (Scheme 53) that has similarities to the synthesis of **38a**. As a result, because many reactions are described using chloride leaving groups,[140,248–250] it was attempted to transform the secondary phosphine of the unsymmetric bisphosphine **11** into the corresponding chloride. However, the secondary phosphine that is required to synthesize the corresponding *sec*-chlorophosphine was difficult to obtain pure.

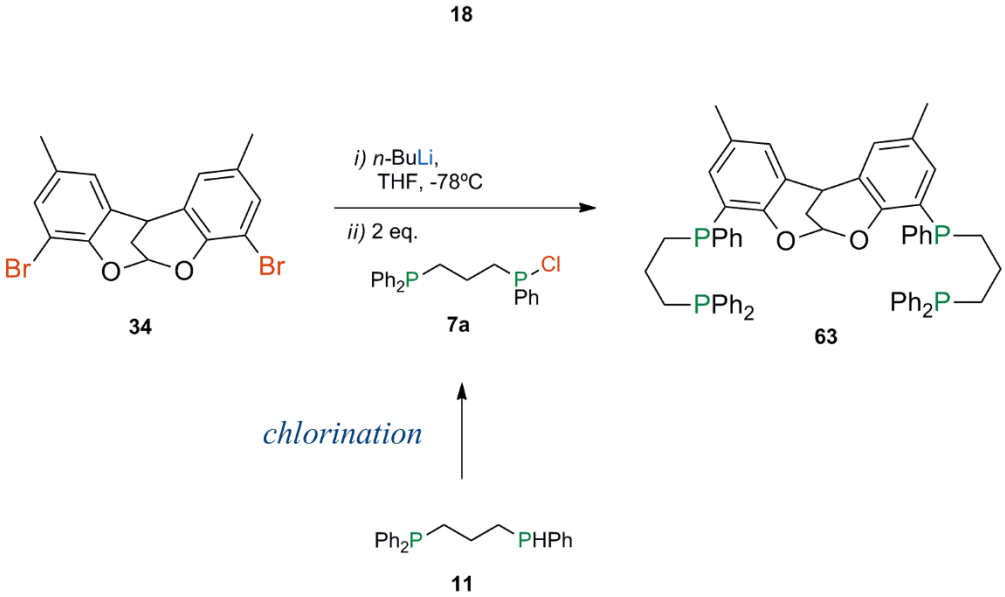

Scheme 53: Potential S_N2 reaction at a P-chlorodiphosphine as a route to tetraphosphines. The chlorinated phosphine can theoretically be synthesized from the corresponding secondary phosphine.

Despite reservations concerning problems in purification, the simplicity of method A was thought to be interesting enough to justify some, at least exploratory, efforts to prepare an electrophilic diphosphine synthon. In the literature, many chlorination methods to synthesize phosphine-chlorides are described.[251–255] The "best" reagent, phosgene, was rejected out- of- hand for reasons related to its toxicity. Various other chlorination reagents were tested, but none worked well; in each case multiple chlorinated compounds were detected in the ^{31}P–NMR. This is partly due to impure starting material (di-cleavage); this complicates what are already delicate reactions because imprecise stoichiometries can be expected to provide either insufficient oxidation (giving 1,1'-biphosphines) or overoxidation to P(V) compounds. All methods were indeed found to result in very significant amounts of by-products. The best, but poor, chlorination method suitable for our phosphine was phosphorus trichloride with a base (Et_3N), which led to an estimated yield of 35 %. However the product could not be isolated. Given the problems already associated with the synthesis of clean unsymmetric *sec- tert-* diphosphine starting material, these additional difficulties lead to the abandon of this approach with some alacrity.

3.2 Coupling Reactions

As mentioned in the retroanalyses presented in section 2.3.1, two types of reactions were considered for producing tetraphosphines. One (retrosynthesis A) uses a leaving group and a classical nucleophilic substitution; the other (retrosynthesis B)[135–142] is based on transition metal catalyzed or metal induced reactions. Retrosynthesis A was unsuccessful, because the required bisphosphine bearing a leaving group (**7a**) could not be obtained. When attempting the second approach, using the intermediate secondary/tertiary bisphosphine (**11**) for cross-coupling reactions, an important factor is to protect the lone pair(s) that might otherwise block the catalyst. The oxidized bis(phosphine) **66** was applied in cross-coupling reactions. There are various methods known in the literature to couple phosphines with carbon, the majority of which use Pd, Ni or Cu catalysts.[135–142] Here, the focus was on Pd and Cu.

3.2.1 Copper Induced P–C Bond Formation

Cross-coupling using copper iodide, caesium carbonate and an *N,N'*-dimethylenediamine ligand in toluene using **66** and DBDOC-diiodide (**67**) as reactants gave preliminary data that suggest that the reaction might have worked well (Scheme 54). The acetal-protons in the ^{1}H–NMR

suggest two major backbone containing species in the product mixture; however the reaction was not clean, and purification was unsuccessful. In the $^{31}P\{^{1}H\}$–NMR four resonances seem to overlap around +35.0 ppm, however it could not be determined if mono-or/and di-functionalization occurred, or which products were obtained. This reaction appears to be reasonably promising, but even if the $^{31}P\{^{1}H\}$–NMR indicates a satisfactory transformation into product (note that four signals would be expected, see section 2.2) a potential significant problem in the separation of diastereomers remains.[a]

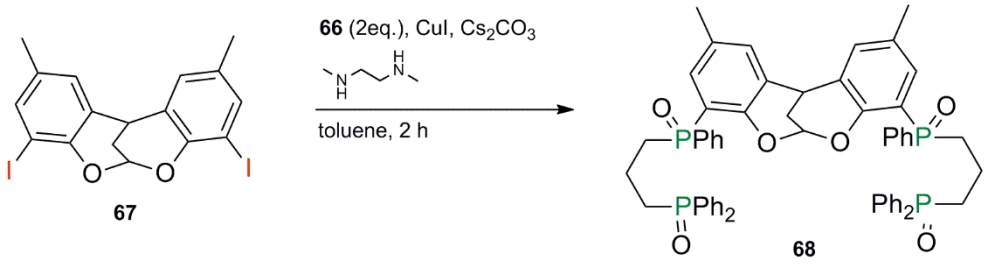

Scheme 54: A copper coupled approach to tetraphosphine tetraoxide **68** through reaction of **66** with $DBDOCI_2$.

3.2.2 Palladium Catalyzed Cross-Coupling

A very common tool for P–C bond formation is Pd catalyzed cross-coupling and, as previously mentioned, it has proved to be effective in the phosphorylation of the backbone.[138,140,184,256–259] Various palladium couplings were attempted of bis(phosphine oxides) (**66**) with DBDOC diiodide (**67**) or dibromide (**35**); general conditions included as precursors 0.5 mol% $Pd(OAc)_2$ or Pd_2dba_3, as ligands 1 mol% PCy_3, Xantphos[97,179] or Nixantphos.[186,260] Aprotic solvents like 1,4-dioxane, DMAc or toluene, and different bases like the Hünig base, Cs_2CO_3, KOAc, and various diamines were employed, but none of the standard reactions led to satisfactory results. Microwave assisted[261] cross coupling without and with a ligand were attempted as well, but gave little advantage over the more traditional methods. A mixture of backbone- containing compounds was invariably obtained, and these could not be isolated.

3.3 Conclusion

[a] The work-up and separation from the starting materials and mono-functionalized by-products has proven to be difficult, no clean spectra (NMR, Mass spectrometry) were obtained.

The introduction of preformed bis(phosphine) fragments to the DBDOC backbone is probably the most intuitive tetraphosphine synthesis to the non- specialist in phosphorus chemistry, and the nucleophilic substitution of the chlorinated bisphosphine with the metallated backbone appears especially promising. However, it presents a number of significant synthetic difficulties; all attempted methods to obtain the required bis(phosphine) synthons were not straightforward and have proven to be very problematical in their separation and purification. The reductive cleavage was a very attractive idea but it led partly to di-cleavage (**64**). Upon quenching, it was possible to obtain impure secondary/tertiary bisphosphine **11**, (Scheme 55). Whilst these routes are probably feasible, the very clean synthesis of the targets with two different P-moieties seems to be a prerequisite for success. If the phosphines had been protected by a borane group and the desired bis(phosphine) could have been produced cleanly, this would have meant that only the problem with diastereomers would remain. However, all coupling reactions and nucleophilic substitutions were inconclusive, it was not evident if different diastereomers or simply different backbone-based products were obtained.

Chapter 4 Coordination Chemistry

Despite the increasing uses of phosphorus compounds in optoelectronics[262–264] (especially black phosphorus[265]) and organocatalysis,[265,266] their principal area of application remains coordination chemistry. The affinity of the lone pair in phosphorus (III) compounds for metals has led to a particularly widespread use of phosphines in coordination compounds. This chapter provides some data relating to the coordination chemistry of wide bite angle ligands at Pt and Pd centers. Pd(II) and Pt(II) form complexes that are isoelectronic in their valence shells.

Metal phosphine complexes exhibit a wide range of reactivity and selectivity.[2] Phosphines are very versatile and allow the rational design[2,36,98] of organometallic compounds for specific procedures. As described in chapter **1.1**, the groups attached to phosphorus alter the character of phosphines strongly.[2,36,98] An important parameter not yet discussed in detail is the position of the phosphines in a complex relative to the remaining ligands coordinated to the transition metal. To constrain geometric degrees of freedom, and therefore control geometry directly at the metal or within space, bidentate ligands can be employed. However, it should be noted that the bite angle of the employed chelating diphosphine has a great effect on the formation of the desired species, in that the PMP angle influences the capacity of the metal center to back-donate into the ligand significantly.[267] From the geometric standpoint, ligands having small bite angles and rigid backbones will most likely result in a monometallic chelating *cis* conformation; those with wide bite angles, if containing flexible backbones, might result in non- chelated *trans*- or *cis*- compounds or/and bimetallic complexes. The latter was observed with SPANphos[34,95,100,101]. Moreover in SPANphos the flexibility of the coordination mode was demonstrated by the formation of bimetallic complexes by changing the metal-to-ligand ratio as noted in Table 2 and Figure 12 in chapter 1.

This chapter deals principally with phosphines coordinated to group 10 metals in the +2 oxidation state, and within this context a short analysis of ^{31}P–NMR data provided by this kind of complex is necessary. For our study we focused principally on complexes containing Pd and Pt. The principal naturally occurring NMR-active isotope of palladium, ^{105}Pd, has a moderate natural abundance (22.2 %), but is a quadrupolar nucleus with low sensitivity to detection by NMR, low resonance frequencies a negative magnetocyric ratio, and extremely fast relaxation times ($<10^{-5}$ s), which make it essentially 'invisible' in the ^{31}P–NMR spectra.[268] ^{195}Pt, on the other hand,[269] is a reasonably sensitive nucleus for NMR detection with a natural abundance of 33.7 % and receptivity relative to ^{13}C of 19.1 %[270].[268] The $^{1}J_{P-Pt}$ coupling constant increases

broadly with increasing *s*-character of the M–P bond, decreases with increased Pt oxidation state, and correlates well to the Pt–P bond length within a structurally related series.[271] The ^{31}P–NMR spectra of square-planar *cis*-Pt(II) dichloride complexes containing phosphine and phosphite ligands normally display ^{31}P–^{195}Pt coupling constants[a] of 3000–6000 Hz[272], *trans*-Pt(II) dichloride complexes generally display a smaller coupling constant than *cis*-complexes, with the variation in these constants being well understood and quite useful for interpreting the coordination geometry in Pt(II) complexes.[273]

1.1 Coordination Chemistry with DBDOCphos at Pd(II) and Pt(II) centers

Before discussing tetraphosphines, it is interesting to consider the chemistry of the DBDOCphos series in a little more detail. The declared objective[34] with this class of compounds is to prepare bimetallic complexes that can show reversible inter-metal cooperativity, rather than generating the kind of highly stable binuclear species that are formed using ligands such as dppm.[84] Thus different and potentially interconverting binding modes can occur at any given metal center.

Given our overall interest in palladium-based species, our initial target was to develop the chemistry of the palladium(II) center at the DBDOCphos type of ligand skeleton. A very comprehensive earlier publication on the DBDOCphos ligand class[34] has treated coordination to the isoelectronic rhodium(I), where a variety of different coordination modes were observed. The chloride bridged rhodium complex (**69**) was formed in a clean reaction with a ^{31}P{^{1}H}–NMR($CDCl_3$) resonance of 45.7 ppm with a $^{1}J_{Rh\text{-}P}$ of 182 Hz, whilst the dimeric bimetallic structure (**70**[b]) on the other hand showed two resonances: a doublet at 22.6 ppm with a $^{1}J_{Rh\text{-}P}$ of 130 Hz and another doublet at 25.7 ppm with a $^{1}J_{Rh\text{-}P}$ of 128 Hz; at different temperatures however several isomers of the dimeric dirhodium species could be confirmed.[34] An initial objective of our investigation was to transfer this coordination chemistry from rhodium to palladium and platinum centers (Figure 53).

[a] Given by the ^{195}Pt satellites, whose separation represents $^{1}J_{(Pt–P)}$, a very useful tool.[275]

[b] In the study of the wide bite angle diphosphines towards rhodium, several dirhodium isomers were obtained at different temperatures. These will not be discussed here.

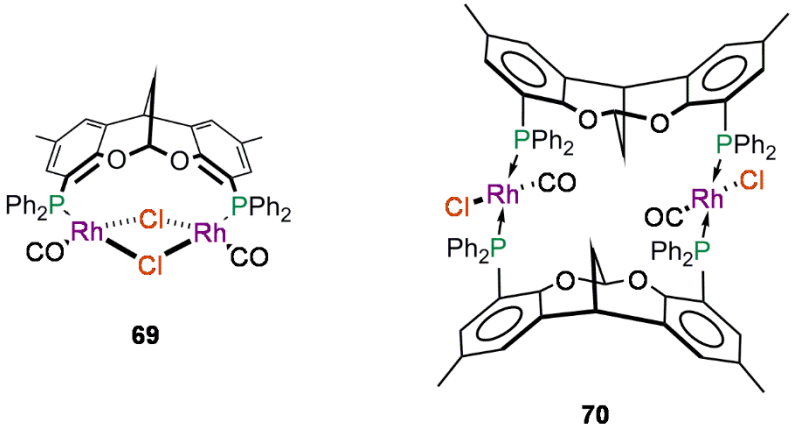

Figure 53: Structures of the rhodium complexes **69** and **70** obtained in previous work of *van Leeuwen et al*.[34]

Preliminary experiments conducted by Josep M. López-Valbuena, during the development of wide bite angle ligands, described their coordination to Rh centers[34]. In other work, he also showed that the type of geometry observed in the chloride bridged Rh complex **69** could also be generated with Pd centers. His experiment, which led to the crystallization of the chloride bridged complex **72** (

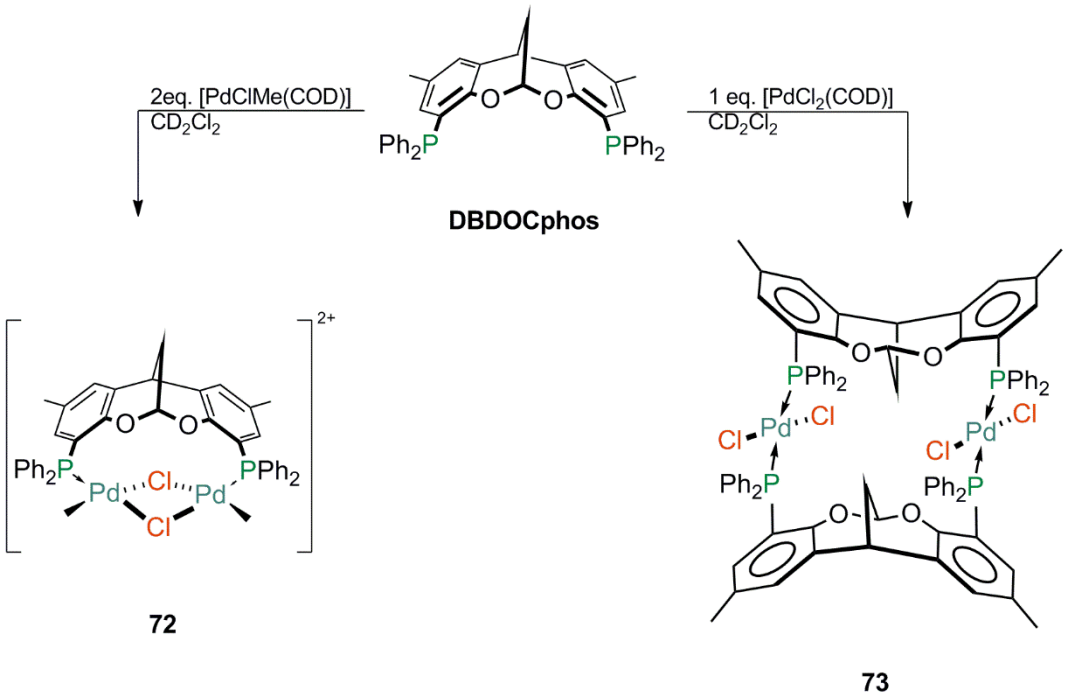

Scheme 57), was conducted in an NMR tube using as precursor [PdMeCl(COD)] in 4 mL $CDCl_3$ and a M:L ratio of 2:1, with 16 µmol DBDOCphos (ligand). We were interested to look into the potential for multiple binding modes in this sort of system. Initially, the Valbuena system was reinvestigated. The $^{31}P\{^1H\}$–NMR($CDCl_3$) displayed essentially a clean AB pattern: 20.5 ppm, 22.7 ppm, 25.8 ppm and 27.9 ppm (Figure 54), that showed a very large $^2J_{P-P}$ of

441.7 Hz that would normally be considered to be characteristic of a *trans*-coupling across Pd.[274–276] Such an NMR signature is clearly not compatible with the structure that is crystallographically observed and, surprisingly given the structure of **69**, few or no other complexes were present. It suggests that the predominant solution complex is a dimeric bimetallic structure similar to that found for Rh in **70**, and that crystallization causes the isolation of what is at best a minority mono-ligand form in solution. Given the small scale measurements of the component starting materials, it seems reasonable to assume that **71** is the near-exclusive product of the reaction.

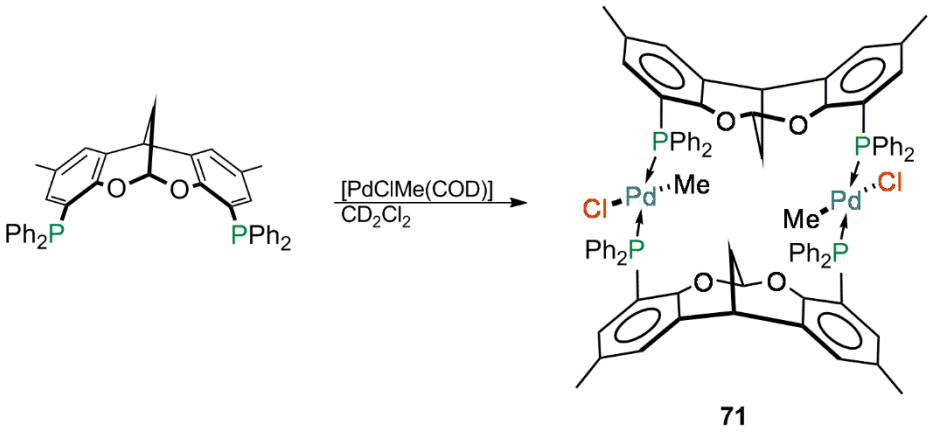

Scheme 56: Reaction of DBDOCphos with PdClMe(COD).[a] Study of solution spectra under the coordination conditions employed by Valbuena to obtain the μ^2-chloro complex **72**, showed the majority formation of the dimeric dipalladium trans-configured complex **71**.

[a] Unpublished results from former co-worker *López-Valbuena et al.*

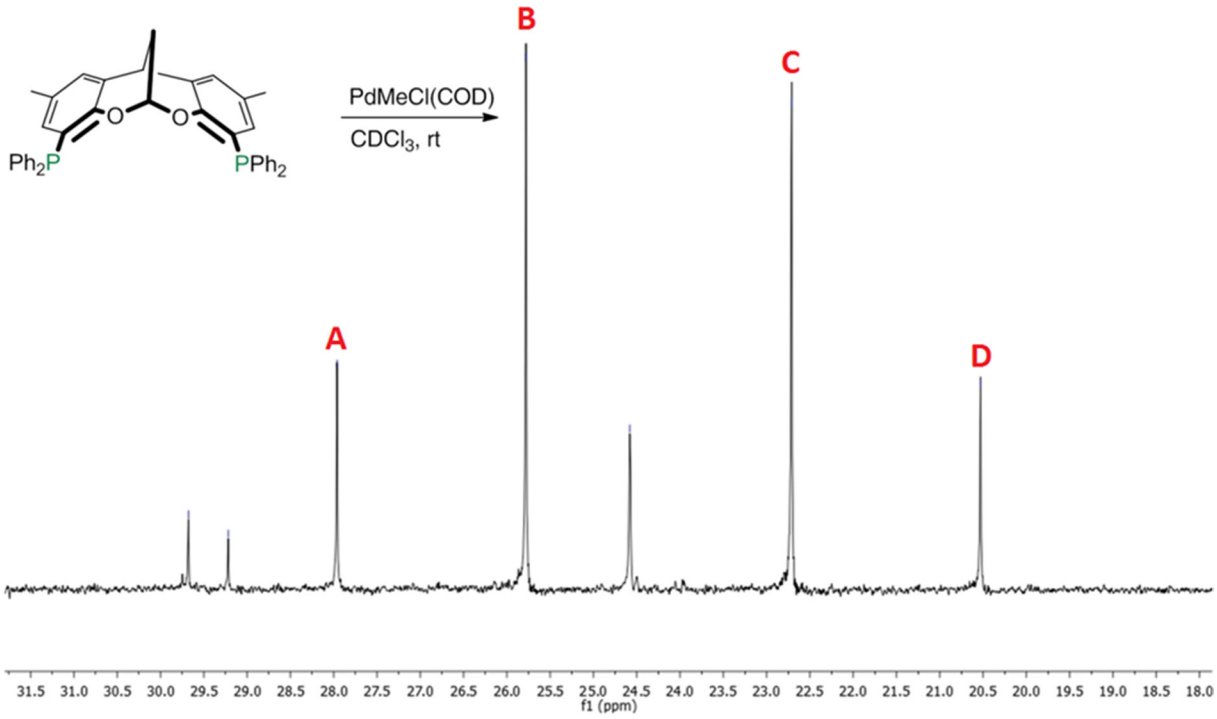

Figure 54: The coordination of DBDOCphos towards PdMeCl(COD) (M:L = 1:1.2). $^{31}P\{^{1}H\}$–NMR spectrum showing a clean AB pattern indicating the formation of a dimeric bimetallic species **71** in which the coordinating phosphines are *trans*- configured. No crystals could be obtained. Conditions: M:13 µmol, L: 16 µmol in 4 mL solvent.

To investigate the area further, we chose to evaluate the coordination chemistry of the same ligand towards a different precursor [$PdCl_2$(COD)] under identical conditions here. This led to the formation of a dimeric dipalladium species **73** (

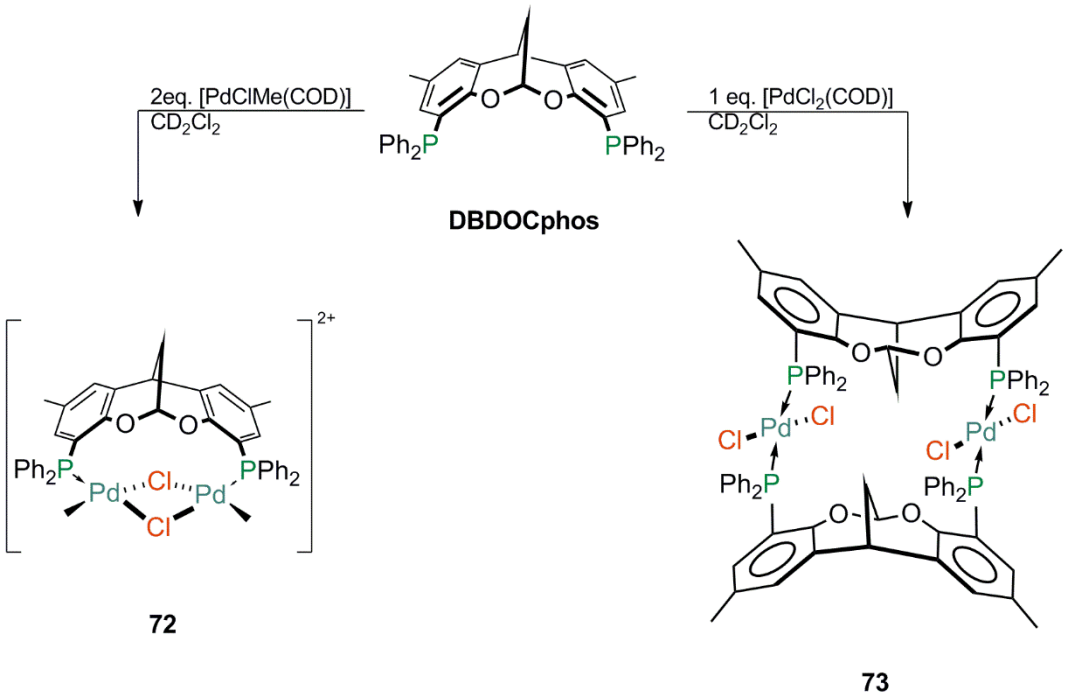

Scheme 57). Orange colored needles crystallized through evaporation in the NMR tube, and a crystal structure could be obtained (Figure 56).

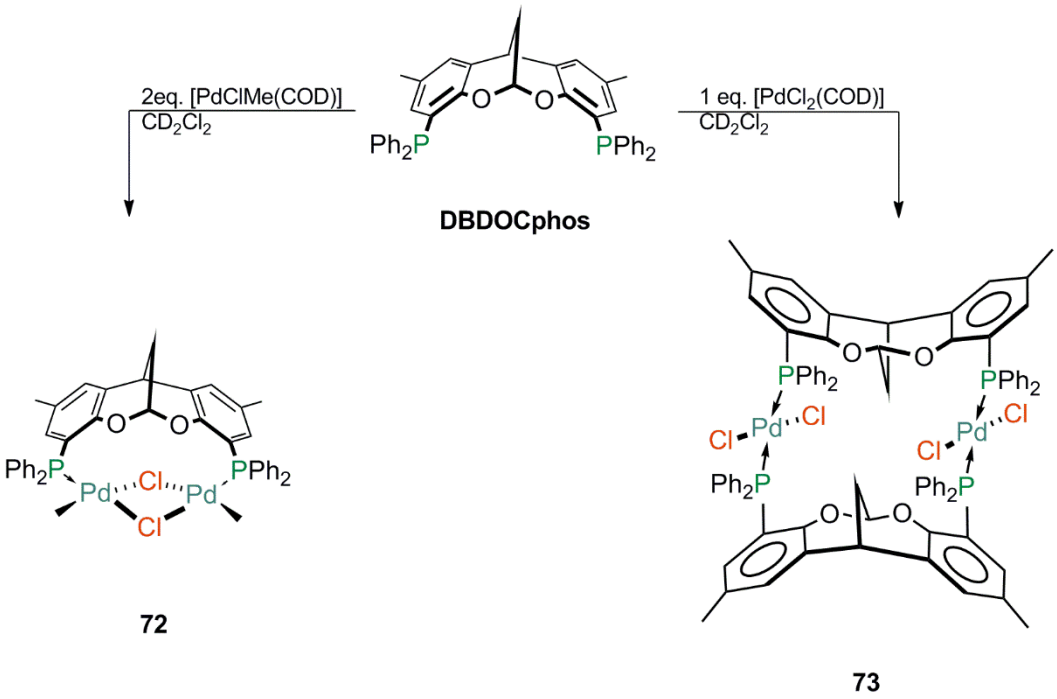

Scheme 57: Syntheses of the dipalladium complexes **72** and **73**. A change in the precursor and its stoichiometry leads to two different bimetallic coordination modes: **72**, a chloride bridged mono-ligand dipalladium species and **73**, a dimeric dipalladium species.

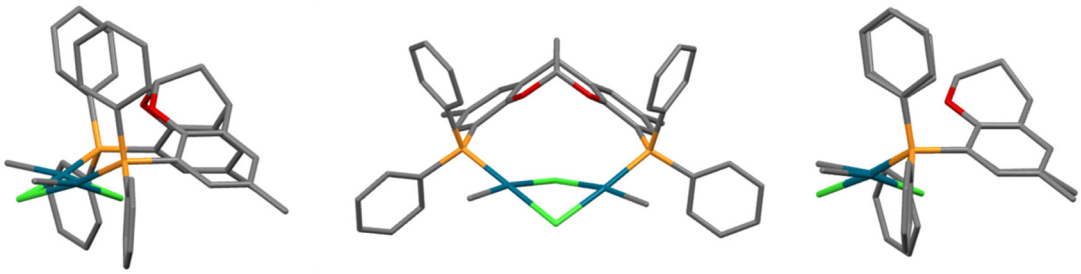

Figure 55: X ray views of the dipalladium chloride bridged complex [$Pd_2Me_2\mu$-$(Cl)_2$DBDOCphos] **72**, which bears one methyl-group on each palladium atom. **72** is C_s symmetric. Non-relevant hydrogen atoms have been hidden for the sake of clarity.

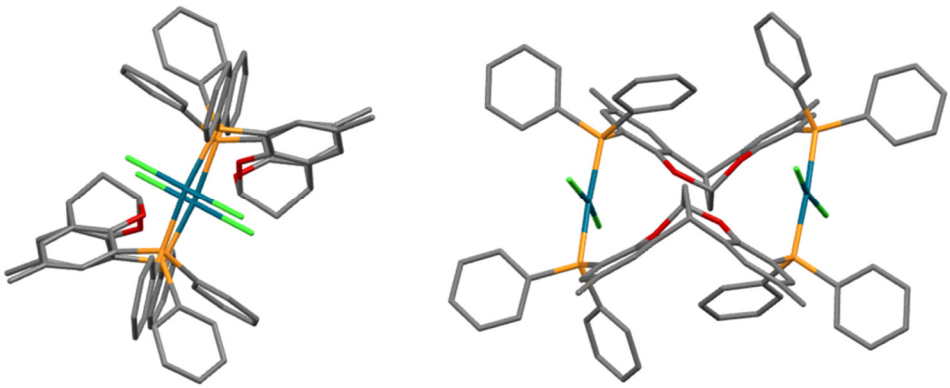

Figure 56: The dimeric dipalladium tetrachloro complex of DBDOCphos: *trans*-[Pd_2Cl_4(DBDOCphos)$_2$] **73**.

The product dimeric dipalladium complex **73** displays *trans* configured phosphines and is highly symmetrical; both DBDOCphos ligands display the same configuration of the bridge-head and their measured angles (69.24°) and torsion angles (A: 47.73°, B: 11.3°, described in Table 6) are identical in both ligands (equally measured as described in section **2.5.3**), the Pd–Pd distance is 7.516 Å and the P–P distance in one DBDOCphos molecule is 7.377 Å and between the phosphorus atoms coordinated to one palladium atom 4.671 Å (Figure 56). On the other hand the chloride bridged dipalladium complex **72** has an angle of 72.0°, torsion angles of A: 33.5° and B: 33.9°, the Pd–Pd distance is 3.38 Å and the P–P distance of DBDOCphos is 6.57 Å. Complex **73** shows the highest symmetry of all crystal structures obtained containing the DBDOC scaffold, and nearly no distortion (the torsion angles are nearly identical). A side-view of the crystal structure in Figure 55 shows that the two halves of the molecule are overlaid, which was not the case with more twisted scaffolds such as the ones described in section 2.5.3.

Compounds	Pd-Pd distance / Å	P-P distance / Å	Angle / °	Torsion Angle / ° A	B
DBDOC		--	67.5	35.59	25.96
38c		6.52	79.06	27.06	41.36
40		7.913	62.84	36.96	16.32
		7.366[a]			
73	7.516	4.671[b]	69.24	42.73	11.30
72	3.378	6.567	71.99	33.48	33.86

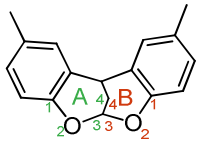

Table 6: Selected geometrical data for the four different compounds **38c**, **40**, **73**, and **72**. The data show indicates a strong dependency on the steric interaction in the molecule and the torsion angles indicating the twist (strong inequality in the torsion angles of A and B leads to a stronger twist) depending of the steric interaction. Depending on these parameters the P–P distance is influenced strongly, and dependent on the coordination form the Pd–Pd distance varies tremendously. [a] P–P distance in one molecule. [b] P–P distance of two P-atoms coordinated to one Pd-atom.

Various precursors and different M:L ratios were tested in the synthesis of **73** as shown in Table 6. All dichloro- bearing precursors led to the formation of similar $^{31}P\{^{1}H\}$–NMR($CDCl_3$) spectra, which differed mainly in terms of line intensity. Two singlets at + 26.0 ppm and + 17.0 ppm dominate, as is shown in Table 7 which indicates their intensity as a function of the metal-to-ligand ratio. The major contaminant was the starting material: in the table the estimated yields of each resonance are listed. The nature of the interconversion process between two species makes it difficult to assign the chemical shift of **73** with certainty, although the inability to obtain crystals of this compound from entry 5 (Table 7) suggest that the crystallographically observed structure corresponds to the resonance at 26.0 ppm. The nature of the species giving rise to the 17.0[a] ppm peak is undetermined at this stage, although a tetrachloro- analogue of **72** wherein the two methyl groups are replaced by two halo functionalities would perhaps not be unexpected. However, interestingly in the majority of the complexation reactions in which both resonances appeared in solution, crystals of **73** were obtained (as verified by crystallographic cell dimension).

Entry	Precursor	$^{31}P\{^{1}H\}$–NMR intensities 26.0 ppm[a]	17.0 ppm[a]	M:L	Crystal

[a] ^{31}P–NMR of DBDOCphos appears at $\delta = -11.4$ ppm.[34]

1	$PdCl_2(PPh_3)_2$	87	13	2:1	**None**
2		27	73	1:1.5	**73**
3		No, NMR data, but crystal structure		1:2	**73**
4	$PdCl_2(PhCN)_2$	27	73	2:1	**73**
5		0	100	1:1.5	**None**
6	$PdCl_2(COD)$	24	76	2:1	**73**
7		0	100	1:1.5	**None**
8	PdClMe(COD)	*AB pattern*: 20.5 ppm, 22.7 ppm, 25.8 ppm and 27.9 ppm		1:1.2	**None**

Table 7: Conditions for the generation of complex **73**. The change of the M:L ratio has a direct effect on the formation of the coordinated species. [a]Estimated by $^{31}P\{^1H\}$–NMR ($CDCl_3$). Data in the table correspond to the relative ratios of 26 and 17 ppm peaks (excluding any other species), given in percent.

A few experiments were conducted using platinum precursors. For $PtMe_2(COD)$ with a M:L ratio of 1:1 in 4 mL $CDCl_3$ and 16 µmol ligand scale, quite different $^{31}P\{^1H\}$–NMR patterns were displayed to the Pd complexes. Two resonances at 24 ppm with a $^2J_{P-P}$ = 10.7 Hz and a $^1J_{Pt-P}$ = 1933.6 Hz and at 18 ppm with a $^2J_{P-P}$ = 10.8 Hz and a $^1J_{Pt-P}$ = 1989.8 Hz were obtained.

These resonances strongly suggest the formation of a dimeric diplatinum complex (**74**, Figure 57**)**, in which the phosphines are *cis*-configured, because of the small $^2J_{P-P}$ constants of around 10.7 Hz.[271] The observed $^1J_{Pt-P}$ couplings of less than 2000 Hz are only compatible with phosphines *trans*- to very strong trans- influence groups such as hydride or alkyl.[277] In the ^{1}H–NMR (Figure 57) two methyl groups at 0.26 ppm and at 0.15 ppm each show a distinct doublet of doublets pattern (dd) with $^2J_{H-P}$ coupling constants of 9.4 Hz and 9.1 Hz; the non-equivalence of these couplings can only reasonably be explained by a mutually *cis* configuration of the phosphines[278] (Scheme 58). These data constrain the number of potential structures that can be drawn for the product, with a *cis*-configured dimeric diplatinum species, wherein the two ligands are desymmetrized by their arrangement in space, being one of the most feasible options. A structure such as given in Figure 58 where the DBDOCphos has the bridgehead in the cavity made by the second DBDOCPhos (whose bridgehead is in essentially “open” space) desymmetrises the phosphorus atoms and would adequately satisfied the observed spectrum.

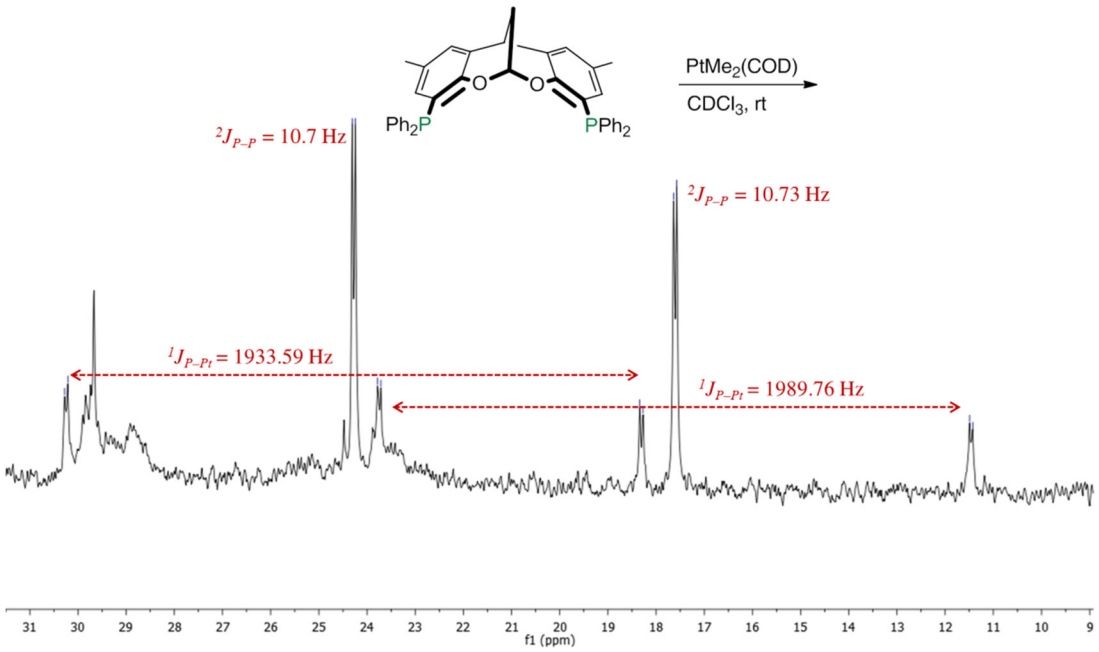

Figure 57: Coordination reaction of DBDOCphos with $PtMe_2(COD)$ (M:L = 1:1). The $^{31}P\{^1H\}$–NMR spectrum shows two distinct doublets with $^3J_{P-Pt}$ of 1933.6 Hz at 24.3 ppm and 1970.4 Hz at 17.6 ppm, which are an indication of a *cis*-configured complex such as **74**. Conditions: 16 µmol in 4 mL solvent.

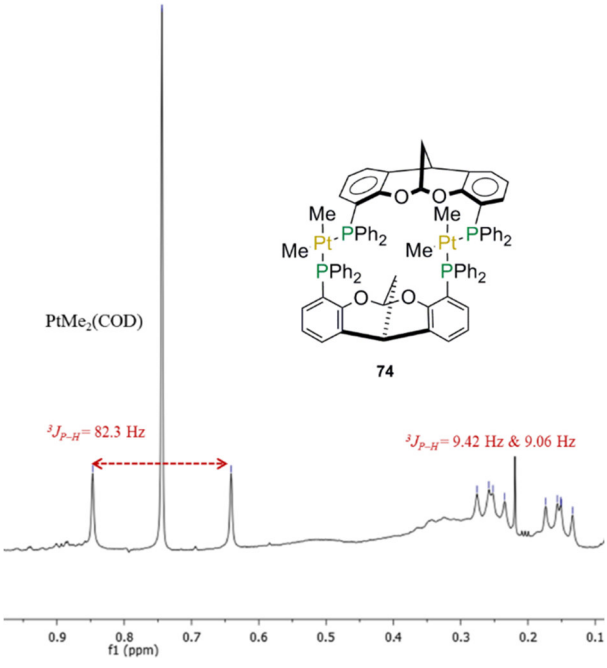

Figure 58: Coordination of DBDOCphos with $[PtMe_2(COD)]$. The ^1H–NMR spectrum ($CDCl_3$) shows the $[PtMe_2(COD)]$ starting material at 0.7 ppm with a $^2J_{Pt-H}$ = 82.3 Hz[279] and two dd at 0.26 ppm with a $^2J_{Pt-H}$ = 9.5 Hz and 0.15 ppm with a $^2J_{Pt-H}$ = 9.1 Hz, indicating non-equivalent methyl groups which have couplings to two phosphorus atoms in non-equivalent coordination environments.

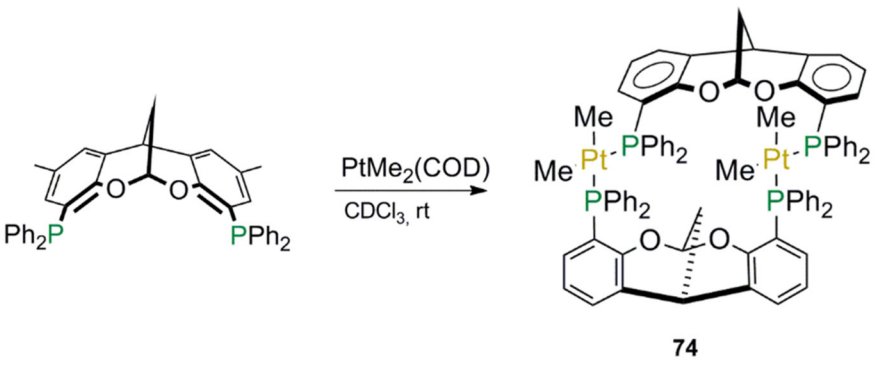

Scheme 58: Coordination of DBDOCphos with [$PtMe_2$(COD)]. Reaction conditions: 16 µmol DBDOCphos and 16 µmol $PtMe_2$(COD) in 4 mL solvent, leads to the formation of *cis* complexes.

1.1.1 Conclusion

The previously described diphosphine ligands synthesized by the group of *van Leeuwen* are able to stabilize dimeric complexes for rhodium metal centers. Complexation studies undertaken towards Pd(II) and Pt(II) metal centers confirmed the binucleating nature of the ligands. The out-come of the reactions of these ligands with [$PdCl_2(PPh_3)_2$], [$PdCl_2$(COD)] or [$PdCl_2$(COD)] at different metal-to-ligand ratios were investigated, and it was found that the metal-to-ligand ratios have relatively little effect on the formation of the bimetallic face-to-face complex **73** which crystallized exclusively with two ligands occupying mutually *trans* positions where each acts as a support for both metals. Valbuena has shown that a low ligand-to-metal ratio (1:2) using [PdMeCl(COD)] as precursor led to the formation of a halide-bridged dimer **72**, but experiments here show that higher stoichiometries of ligand appear to give rise to binuclear *trans*- coordinated complexes **71**. The use of the precursor [$PtMe_2$(COD)] appears to lead to the formation of a *cis*-configured dimeric diplatinum species **74**, whose structure is proposed on the basis of $^{31}P\{^1H\}$–NMR($^2J_{P-P}$, $^1J_{Pt-P}$) and ^{1}H–NMR ($^2J_{Pt-H}$), in the absence of a crystal structure determination. Wide bite angle diphosphines like DBDOCphos appear to have a wide variety of binding modes available for their coordination towards metal centers.

1.2 Coordination Chemistry of Tetraphosphines at Pd(II) and Pt(II) centers

A second series of reactions treated the new tetraphosphines prepared in this work. The objective at this stage was to establish that the tetraphosphines are capable of forming bimetallic complexes with the late transition metals, and that they can reliably provide pre-catalysts that have predictable structures. Coordination to both palladium and platinum centers was attempted. Multiple attempts at crystallization failed to give single crystals suitable for X-ray analysis and, as a result, the formulation of the products currently rests exclusively upon NMR data. For this reason, the platinum complexes are presented in greater detail than the palladium, because there is significantly more information in their spectra. The choice of Pt centers for the study reflects the immense body of data concerning platinum(II) dihalide complexes, the nature of the $^{1}J_{Pt-P}$ platinum phosphorus coupling constant, which varies predictably as a function of the coordination sphere of platinum, and the general understanding of the Pt–P interaction that has grown out of sustained interest in the nature of the *trans*- influence in this class of compound.[277,280–283]

The experiments were conducted in a Schlenk tube with a M:L ratio of 2:1[a] of ligand ***rac* 63** towards $PdCl_2$(COD) and $PtCl_2$(COD). Each reaction was stirred 30 – 60 min at room temperature. The formation of two different types of compound can be envisioned, either a complex **75** (Scheme 59), in which the two halves of the ligand coordinate independently towards the metal centers, or the formation of a chloride bridged species such as **76**[b] (Figure 59), in which the two metal centers face to one another and share chlorides.

[a] M: 0.552 mmol, L: 0.276 mmol in 4.5 mL DCM.

[b] The formation of a μ^2-chloro complex could possibly be effected by abstracting two chlorides of compound **81** employing silver triflate

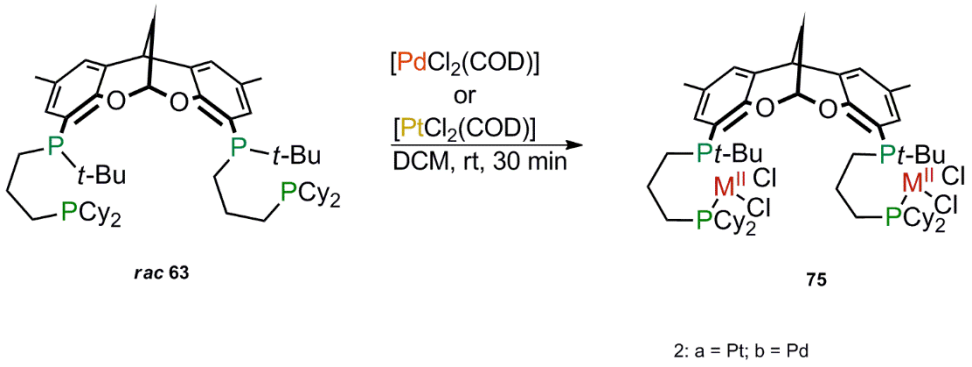

Scheme 59: Coordination of tetraphosphines to $PtCl_2$ centres. Treatment of the free *rac*-tetraphosphine ligand with 2 eq. $[MCl_2(COD)]$ (M = Pt, Pd) probably leads to a homobimetallic complex with square planar 16 VE coordination (d^8).

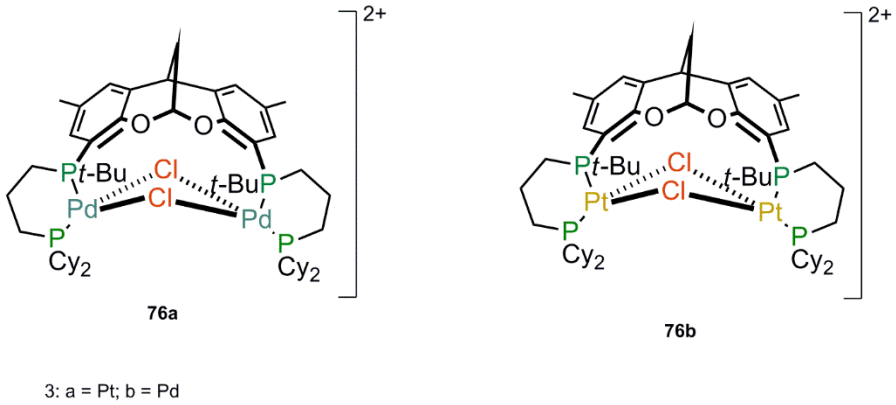

Figure 59: Coordination of tetraphosphines to $PtCl_2$ centres. Chloride-bridged possibilities can not be definitively eliminated by ^{31}P–NMR spectra.

The $^{31}P\{^1H\}$–NMR spectrum in the case of M= Pt is given in Figure 60 The major pattern is clearly of four different phosphorus resonances, each of which appears as a doublet with satellites. The four resonances appear as two sets of pairs that have quite similar chemical shifts, as might be expected given that the *rac* tetraphosphine that was used as the starting material has two different PCy_2 groups and two different P*t*-Bu(Ar) groups. Two resonances at 24.3 ppm with a $^2J_{P-P}$ = 17.6 and 23.8 Hz with a $^2J_{P-P}$ = 18.1 Hz and two resonances at 18.3 ppm with a $^2J_{P-P}$ = 17.8 Hz and 17.6 Hz with a $^2J_{P-P}$ = 18.1 Hz, their respective $^1J_{Pt-P}$ is 3684.4 Hz, 3702.0 Hz, 3432.0 Hz and 3425.2 Hz[a]. These values of $^1J_{Pt-P}$ are typical of Pt(II) complexes having two *cis*- chloride ligands;[281] equally, the values of $^2J_{P-P}$ imply simple *cis*-$[PtCl_2PP']$ centers. These are consistent with the formation of the two different coordination spheres that would be expected for the dimeric diplatinum complex **75** (Scheme 59). The data are therefore

[a] The $^1J_{Pt-P}$ of around 3560.9 Hz in complex **75a** matches the $^1J_{Pt-P}$ of $PtCl_2$ dppp platinum of around 3512 Hz.[128]

capable of defining the nature of the product quite tightly, despite the very limited information available.[a] The proposed diplatinum complex contained only one clean acetal backbone proton resonance according to the ^{1}H–NMR spectrum, as would be expected for the formulation given (Figure 61).

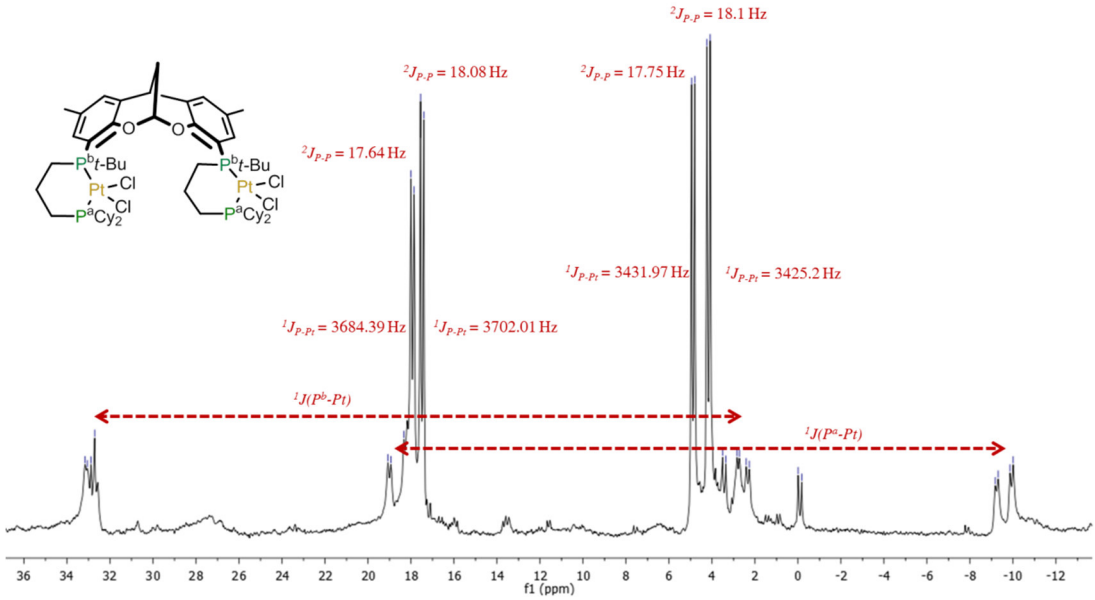

Figure 60: ^{31}P{^{1}H}–NMR spectrum of the homobimetallic diplatinum complex **75a**.

[a] The major uncertainty at this stage concerns the possibility of an auto-ionization process that could give rise a dicationic structure having two μ^{2}-chloro ligands bridging the two platinum (II) centers and two free chloride ions (or an intermediate triply chlorosubstituted monocation). Whilst this cannot be excluded definitively, the absence of any obvious long- range Pt-P couplings argues against such a formulation. Equally, the values of 3684.4 Hz, 3702.0 Hz, 3432.0Hz and 3425.2 Hz are very typical of complexes such as **75**; bridged dimers often give values which are somewhat larger.[277,282]

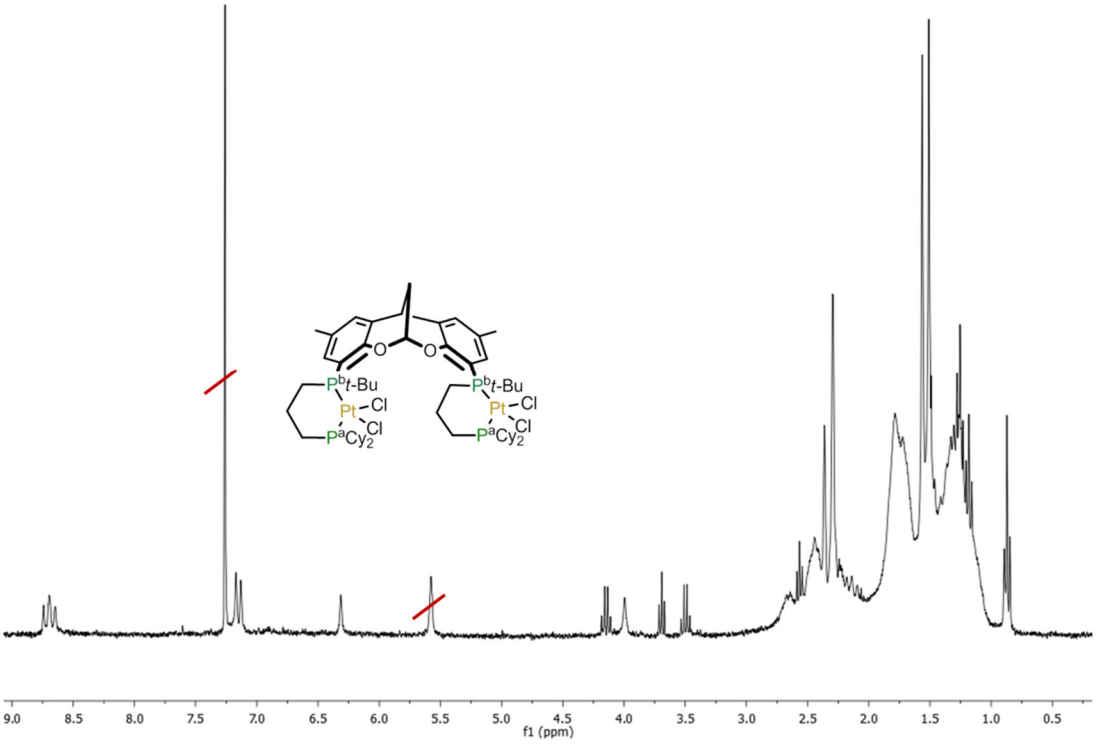

Figure 61: ^{1}H–NMR from the tetraphosphine *rac* **63** coordinated to two Pt centers. Some residual ethyl ethoxy-propionate is present.

The coordination with palladium led to similar ^{31}P{^{1}H}–NMR patterns, two resonances at 40.7 and 40.6 ppm and two resonances at 29.9 and 29.7 ppm (Figure 62), justifying the formation of a dipalladium complex forming two identical halves (**75b**).

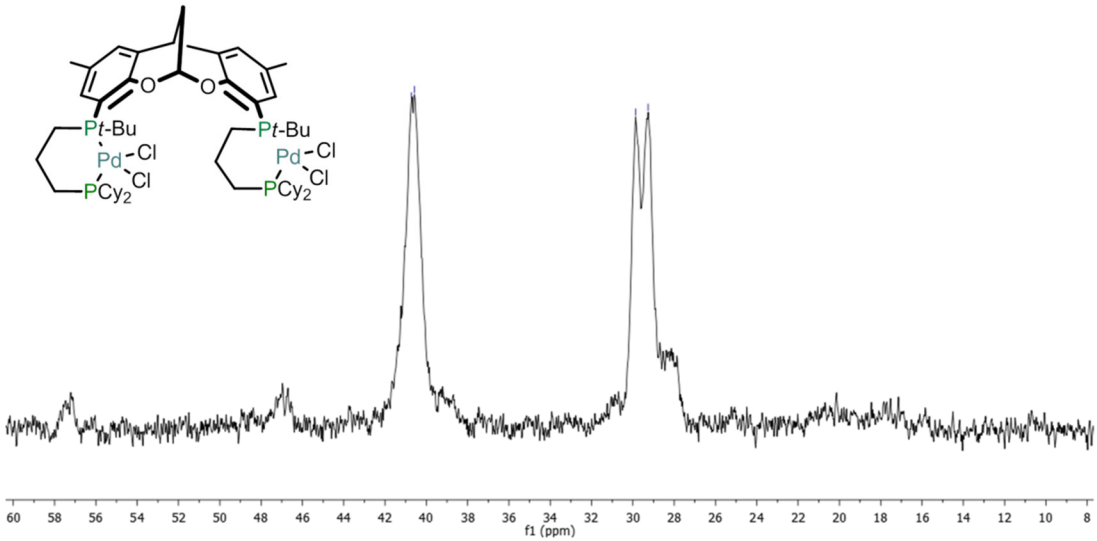

Figure 62: ^{31}P{^{1}H}–NMR of the proposed homobimetallic dipalladium complex **75b**.

1.3 Conclusion

A preliminary coordination study of DBDOCphos was conducted towards Pd(II) and Pt(II) in an attempt to transpose some of the results reported for its dirhodium complexes to the platinum and palladium class.[34] The formation of two bimetallic species towards Pd(II), a dimeric bimetallic one, **73,** the other a chloride bridged bimetallic species **72** having two non-equivalent phosphorus atoms, could be confirmed by X–ray crystal structure analysis.

A test reaction with Pt(II) using [$PtMe_2$(COD)], a precursor without chlorides, led to the formation of what is probably the *cis* configured diliganded bimetallic complex **74** whose structure could be proposed with some degree of confidence from $^{31}P\{^1H\}$–NMR($^2J_{P-P}$, $^1J_{Pt-P}$) and ^1H–NMR($^2J_{Pt-H}$), although crystallization was not successful. Thus, wide bite angle diphosphines like DBDOCphos proved to provide a number of coordination modes towards metal centers.

In case of the new tetraphosphine ligand ***rac* 63**, the initial objective was to obtain bimetallic complexes; furthermore we were interested to determine if a certain coordination mode was preferred. The nature of the coordination of the *rac* tetraphosphine ligands (***rac* 63**) towards Pd(II) and Pt(II) could not be demonstated by X- ray crystal structures but the $^{31}P\{^1H\}$–NMR study of the platinum complex delivered enough information for a preliminary conclusion to be drawn. The NMR implies that the two chelating arms each coordinate independently to a different metal center (**75**), with both of these coordinated metals appearing to be classically *cis* coordinated according to the coupling constants obtained from the $^{31}P\{^1H\}$–NMR ($^2J_{P-P}$, $^1J_{Pt-P}$). As expected, all phosphorus atoms are non-equivalent in this coordination form. It should be noted that a c*is* formulation having chloride bridged coordination is conceivable and, given that the changes in the value of $^1J_{Pt-P}$ between such dimers and the simple terminal chloride complexes are likely to be small, this kind of structure cannot be definitively eliminated with the data available at present.

As a conclusion it could be determined by attaching two chelating arms to the DBDOC scaffold exclusively one coordination species from the *rac* form could be obtained. The tetraphosphine complexes crystallize less easily than those of the DBDOCphos series, and as a result all current information has only been obtained through NMR analysis. To obtain definitive results a more in-depth study will have to be conducted. The application of these ligands to reactions that may benefit from the cooperative effect of two metal centers in close proximity is currently under study.

Chapter 5 Palladium Catalyzed Carbonylation and Related Reactions

The synthesized tetraphosphine ligands were evaluated in catalytic reactions in collaboration with Prof. PCJ Kamer and his group at the University of St. Andrews (UK). The initial objective of this study was to test the efficiency of the catalysts formed from the synthesized ligand system coordinated towards palladium- catalyzed carbonylation reactions. For this reason a short overview of palladium catalyzed hydroformylation will be discussed prior to the experimental procedure and obtained results.

5.1 General Introduction

The heterogeneous catalysis of conversion of carbon monoxide and hydrogen to hydrocarbons and oxygenated products was first described by Fischer and Tropsch in 1922.[284] Numerous homogeneous and heterogeneous catalyzed reactions were developed with carbon monoxide and organic compounds.[1,34,48,50,65,100,107,115,131,159,285–296] Carbon monoxide is predisposed to undergo nucleophilic attack at the carbon and electrophilic attack at the oxygen, and it has a polarizing effect on its neighboring atoms and functional groups once incorporated into a molecule.[297,298] Moreover the carbonyl group has the ability to stabilize a neighboring carbanion by delocalization into the CO double bond. CO is a readily available one-carbon feedstock and it is feasible to introduce it as an additional/alternative functionality into alkenes, specifically α-olefins. In most carbonylation reactions applied in practice the catalyst systems are not based on palladium, and therefore a short description of palladium catalyzed carbonylation reactions in homogeneous catalysis will be given. The focus here will be on hydroformylation.

5.2 Hydroformylation

Hydroformylation, also known as "the oxo process"[1] is the transition-metal catalyzed conversion of olefins to aldehydes using carbon monoxide and hydrogen (Scheme 60). Important factors in this process are the catalytic activity, chemoselectivity and regioselectivity. Linear aldehydes are desired products for bulk applications like butyraldehydes, the starting material for the production of dialkyl phthalates.[299] Branched aldehydes are of interest for the synthesis of pharmaceutical and fine chemicals because of the potential formation of a stereogenic center.

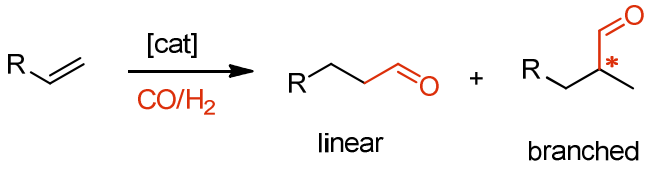

Scheme 60: The Hydroformylation of terminal olefins can lead to linear or branched, chiral, aldehydes.

In 1938 Otto Roelen discovered the hydroformylation reaction.[300–302] The first generation of Co-catalyzed hydroformylation processes (BASF, ICI, and Ruhrchemie) was performed at high temperature (150-180°C) and pressure (200-350 bar). In 1950 Shell introduced a phosphine based catalyst for the synthesis of detergent alcohols that is still used today.[107,288] The original cobalt based process suffers from low chemo- and regioselectivity, as significant amounts of undesired by-products were obtained. In 1965 Wilkinson introduced rhodium triphenylphospine catalyzed hydroformylation under mild conditions which gave superior chemo- and regioselectivity.[303] Subsequently rhodium-based systems gained considerable attention and significant progress in terms of chemo- and regioselectivity has been made. In 1980 Ruhrchemie/ Rhone-Poulenc introduced a water-soluble rhodium catalyst employed in a two-phase hydroformylation process based on an Rh/TPPTS (TPPTS = tri-sodium salt of *meta*-trisulfonated triphenylphosphine).[304] Problems in the hydroformylation of internal olefins or longer chain olefins were overcome using bulky bidentate diphosphines.[305–307]

Due to the success of rhodium-based hydroformylation, academic and industrial research has focused on this area since the 1970s. The increased demand for rhodium for chemical and technical processes elevated the price of this already expensive precious metal. This led eventually to the search for more readily available alternative transition metal-catalysts (e.g. Ru, Ir, Pd, Pt, and Fe).[288]

5.3 Palladium Catalyzed Hydroformylation

Transition metal catalyzed hydroformylation represents an outstanding example of homogeneous catalysis on an industrial scale. The aldehydes formed from cheap feedstock serve as major building blocks for numerous chemical products. Aldehydes serve as highly versatile intermediates in the fine chemical and pharmaceutical industry; they are as well used as plasticizers,

detergents and surfactants and produced on a million ton scale. Today most of the bulk hydroformylation processes rely on rhodium-based catalysts. The rhodium catalyst demand and the resulting high cost have resulted in the investigation of alternative transition-metal catalysts. Palladium has many advantages; it is one of the most versatile transition metals for organometallic catalyzed organic reactions, especially in the C−C bond formation.[308] Moreover Pd tolerates many functional groups like carbonyl or hydroxyl groups.[69] Many palladium complexes can also tolerate to some degree oxygen, moisture or acids, and this makes it very flexible in different reactions. The high price of palladium is challenging (still cheaper than Rh), but if the catalyst is efficient it is tolerable.[309] Palladium has posed no problem with respect to ecological standards.[310]

Shell discovered a catalyst system that produces commercial polyketones[311,312] and comprises a Pd(II) species having a weakly coordinating anion together with an equimolar quantity of a suitable bidentate phosphine ligand. Palladium(II) diphosphine complexes bearing weakly or non-coordinating anions proved to be useful catalysts for hydroformylation.[131] *Drent et al.* discovered at Shell that Pd-based carbonylation catalyst demonstrate excellent catalytic performance of cationic palladium catalysts in highly efficient alternating copolymerization of olefins with carbon monoxide.[311] They also developed a process for the preparation of aldehydes by hydroformylation in the presence of a palladium based catalyst with bidentate phosphine ligands.[131,313,314] Palladium catalysts are used in hydrocarboxylation[131,285,311,315,316], hydroesterification and the copolymerization[311] of olefins with carbon monoxide.

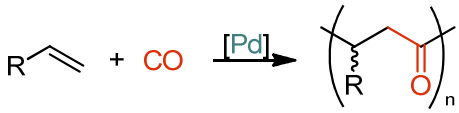

Scheme 61: Palladium catalyzed olefin/CO copolymerization.[311]

After this discovery, research focused on the selective interruption of the polymerization process so as to target the efficient formation of aldehydes and ketones; and within the last decade progress has been achieved in regard to chemoselectivity.[317,318] The essential steric and electronic properties of the metal complex, described as $[PdL_2X_2]$ (L_2 = bidentate ligand), determine the distribution of alcohols, aldehydes, ketones, or oligoketones in the product. The catalyst characteristics can be controlled by the appropriate choice of ligands, solvents, acids, base additives, and counter-ions.[131] For hydroformylation catalyzed by palladium complexes, strongly

coordinating counter-ions and basic ligands are favored.[131,305,319] In Scheme 62 the proposed mechanism is shown.[123,131,291,320,321] Most authors have postulated that the catalytically active species is the Pd-hydride complex [PdL_2HX] (**77**),[294] which is probably formed by an anion-assisted heterolytic cleavage of dihydrogen. Then coordination of the olefin to complex **77** and its migration is generating the Pd-alkyl bond (**78**). Carbon monoxide inserts into the Pd-alkyl bond and forms the Pd-acyl complex **79**, which is the key intermediate of the hydrocarbonylation sequence. This intermediate **79** leads to various pathways, in case of the hydroformylation direct hydrogenolysis of Pd-acyl **79** species leads to aldehydes. Hydroacylation occurs by insertion of a second olefin into **79**, in which the carbonyl group coordinates to the metal center.[320] The active catalyst can be regenerated by hydrogenolysis to form ketones-aldehydes, or after olefin CO copolymerization *α, β*-unsaturated ketones through *β*-hydride elimination.[123,131,291,320,321]

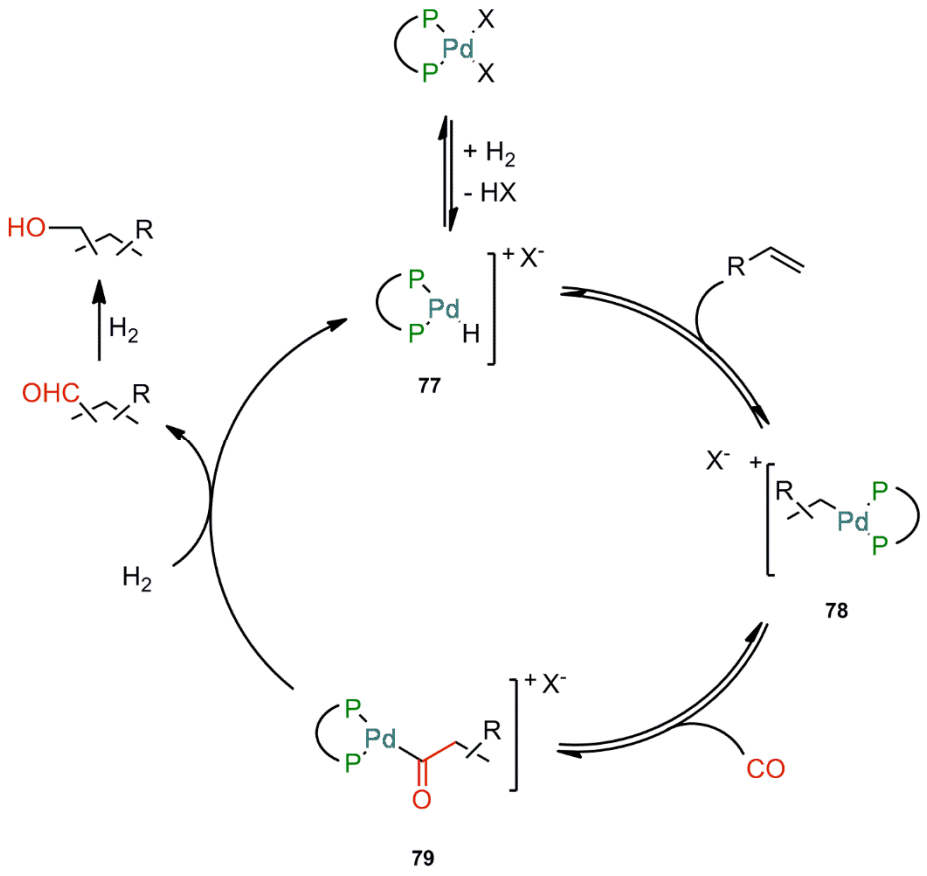

Scheme 62: Proposed mechanism for palladium-catalyzed hydroformylation reaction.[123,131,291,320,321]

Further research by *Drent et al.* led to cutting-edge studies on chemoselective palladium-catalyzed formylation.[131] Adjustment of the chelating phosphine ligands with the general formula

$R_2P(CH_2)_nPR_2$ and the appropriate choice of counter-ions X^- allowed either the hydroformylation or the hydroacylation products to be selectively obtained. The active complexes were generated *in situ* through ligand complexation/anion displacement sequence starting from $Pd(OAc)_2$. The reaction was performed at 30 bar syngas pressure (CO/H_2 = 1/1) at temperatures between 80 and 125 °C. Turnover frequencies up to 800^{-h} have been achieved under these reaction conditions. Higher rates resulted in poor chemoselectivity, which was mostly affected by the nature of the used acid. A comparison of TFA (trifluroacetic acid, $pK_a = -0.7$) and TsOH (trifluoromethanesulfonic acid, $pK_a = -5.1$) shows that TFA led to the selective synthesis of aldehydes, whereas TsOH formed ketones. The use of *p*-TsOH (para-toluenesulfonic acid, pK_a = -2.7) combined with an increased hydrogen pressure altered the chemoselectivity in favor of the alcohol products.[131] Weaker acids affected the regioselectivity, resulting in a reduced electrophilicity of the metal center upon coordination, and the proximity of the anion to metal center led to enhanced regiocontrol. The use of basic *cis*-chelating phosphines led favorably to the linear hydroformylation product. In contrast stronger acids and less basic ligands decreased the *n*-selectivity. Another important aspect is the polarity of the solvents, since the coordination strength of anions depends on it. The best results in the study of *Drent et al.* were obtained in relatively low polarity solvent like diglyme.[131]

In industry, the selective conversion of miscellaneous internal alkenes to linear carbonylation products is of great interest. The current methods still lack chemoselectivity. Simple carbonylcobalt complexes are suitable for isomerization/hydroformylation but give a significant amount of alkane by-product.[322] Regioselectivity can be achieved with rhodium-based catalysts requiring often expensive and sophisticated ligands.[1] *Konya et al.* reported a highly selective anion promoted palladium-catalyzed isomerization-hydroformylation sequence allowing the efficient conversion of internal alkenes into linear aldehydes and alcohols.[305]

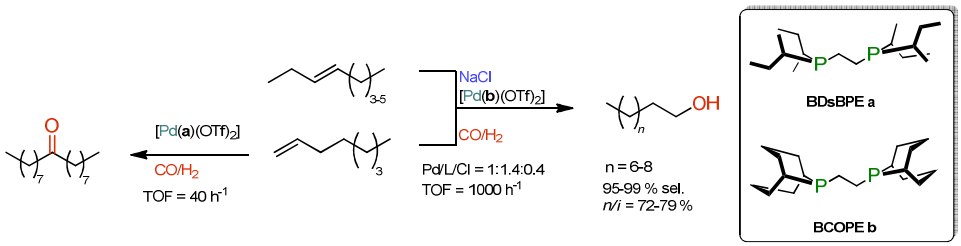

Scheme 63: The effect of the ligand structure on (P-P)$Pd(OTf)_2$-catalyzed hydrocarbonylation of higher alkenes.[305]

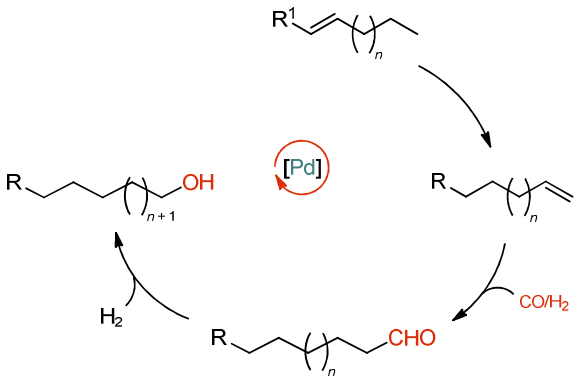

Scheme 64: Efficient halide anion promoted Pd-catalyzed hydroformylation of internal alkenes to linear aldehydes or alcohols.[305]

A domino isomerization-hydrocarbonylation-hydrogenation reaction sequence (Scheme 64) was achieved using the catalyst [Pd(OTf)$_2$-(bcope[a])], ligand **b** displayed in Scheme 63, and a stoichiometric amount of a halide anion (Pd/L/Hal = 1:1.4:0.4) promoted efficient conversion of a conglomerate of *i*-C$_8$ – C$_{10}$ internal olefins into terminal alcohols.[305] They proved that halide anions have a significant influence on the thermal equilibration of internal alkenes. Their best example was NaCl as halide source leading to an enhanced regioselectivity and increased overall reaction rate. Moreover the authors also claimed that the Pd-acyl species underwent an accelerated hydrogenolysis upon addition of NaCl. The chemoselectivity on the other hand was ligand-dependent, but not influenced by the addition of an anion. A comparison of ligand **a** and **b** showed that although these two ligands are structurally very similar ligand **a** yielded mainly hydroacylation products and showed no activity in terms of the conversion of internal olefins. Ligand **b** converted the mixture of internal *i*-C$_8$ – C$_{10}$ alkenes successfully into their corresponding higher linear alcohols.[305,313]

Beller et al. investigated Pd-catalyzed hydroformylation reactions using a catalytic system of [Pd(acac[b])$_2$], a bidentate ligand derived from 1-(naphthalene-1-yl)-1H-pyrrole (**c**), and *p*-TsOH at 60 bar total pressure in diglyme solution (Scheme 65). Reactions using degassed water or methanol resulted in hydroxy and methoxy alkylation products.[123,319]

[a] bcope = bis(cyclooctyl)phosphinoethane, shown as ligand **b**, Scheme 63.

[b] acac = acetylacetonyl

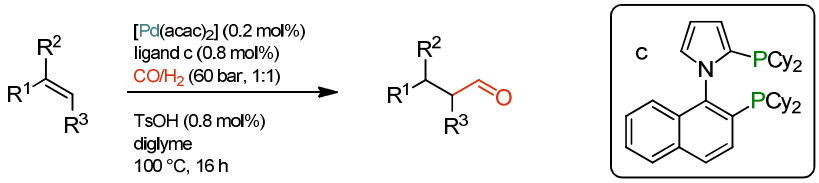

Scheme 65: Palladium catalyzed hydroformylation.[123,319]

The Pd-catalyzed hydroformylation of vinyl substrates showed impressive regioselectivity for linear aldehydes. For instance, N-vinylphthalimide was transformed to the corresponding aldehyde in 95% yield and 98% *n*-selectivity, the best selectivities known for this substrate (Scheme 66).[123,319]

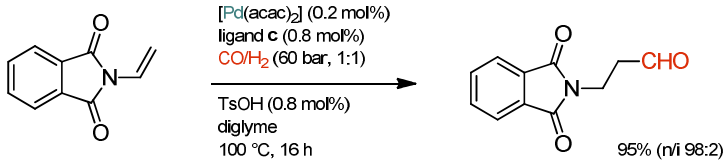

Scheme 66: *N*-selective palladium catalyzed of *N*-vinylphthalimide.[123,319]

In conclusion, effective Pd-catalyst for hydroformylation can be designed from basic bidentate phosphine ligands in combination with an acid co-catalyst. However, it has still received little attention from the chemical community, which is why our intention was the synthesis of basic ligands to obtain active and efficient Pd-catalysts for hydroformylation.

5.4 Palladium-Catalyzed Hydroformylation of *α*-Olefins

The catalysts, in the conducted experiments, were formed by a combination of a suitable bidentate ligand (L_2) with a Pd(II) species and generated *in situ*, e.g. $Pd(OAc)_2$ and an acid containing weakly or non-coordinating anions (X^-). The catalyst system L_2PdX_2 is formed by a ligand complexation and anion displacement reaction sequence:

$$L_2 + Pd(OAc)_2 + 2\,HX \rightarrow L_2PdX_2 + 2\,HOAc$$

The effect of variations of ligand, acid and solvent on the product formation will be described in detail of the results obtained below. Since only preliminary studies were conducted, yields of the products of interest, here mono-functional C-9 aldehydes were calculated according to the conversion of olefin into the product. Undesired by-products include oligomeric ketones

and other "heavy" species resulting from aldol condensation reactions of the mono-functional aldehydes and ketones under the reaction conditions. The preliminary results are only qualitatively discussed here, because internal standards were not used in any reaction. It has to be noted that this is not a full study, and is based on a few experiments only. As a consequence, no kinetic or mechanistic studies have been conducted.

5.5 DBDOCphos System in Palladium-Catalyzed Hydroformylation

Preliminary catalytic experiments were conducted with DBDOCphos coordinated *in situ* to palladium. As previously mentioned, this may not be an ideal system for Pd-catalyzed hydroformylation, since basic ligands are reported to form the most active Pd catalysts.[123] However, our intention was to prove DBDOC based ligands bearing only aromatics are not efficient and to rationalize the ligand design towards Pd systems.

The reactions were performed in a Hastelloy C® autoclave in diglyme with a $Pd(OAc)_2$ precursor, a CO/H_2 (1:1) pressure of 60 bar, and the reaction was conducted 5 h at 125 °C, these conditions have proven to be the most efficient in the systems introduced by Drent[123,305] and Beller[123,321]. A screening of several acids (TFA, TfOH, *p*-TsOH, acetic acid, CH_3COOH) was conducted (Table 8). Intriguingly no reaction at all took place, which is why we decided to do a second screening of the solvents.

		Selectivity (%)		
Acid	**1-octene**	**Ald**	**Iso**	**'Heavy'**
TFA	100	0	0	0
p-TsOH	100	0	0	0
TfOH	100	0	0	0
CH_3COOH	100	0	0	0

Table 8: Conditions: acid: 0.22 mmol, 1-octene: 4.4 mL, $Pd(OAc)_2$ (12 mg, 55 µmol), ligand DBDOCphos (82 mg, 132 µmol), T = 125 °C, $CO:H_2$ (1 :1) = 60 bar, L/Pd = 2.4, V_{tot} = 15 mL, 5 h .

The same conditions as described above were applied for a screening of the solvents. The solvents diglyme, THF, toluene, chlorobenzene and 1,2-dichlorobenzene were tested in parallel in a robotic system by AMTEC® in which multiple reactions could be performed at once, under the same pressure and temperature (Table 9). Unfortunately, again, no conversion occurred.

		Selectivity (%)		
Solvent	**1-octene**	**Ald**	**Iso**	**'Heavy'**
Diglyme	100	0	0	0
THF	100	0	0	0
Toluene	100	0	0	0
1,2 -dichlorobenzene	100	0	0	0
Chlorobenzene	100	0	0	0

Table 9: Conditions: *p*-TsOH: 0.22 mmol, 1-octene: 4.4 mL, $Pd(OAc)_2$ (12 mg, 55 µmol), ligand DBDOCphos (82 mg, 132 µmol), T = 125 °C, $CO:H_2$ (1 :1) = 60 bar, L/Pd = 2.4, V_{tot} = 15 mL, 5 h.

These catalytic reactions were performed in Tarragona; to ensure the validity of the results, a repetition of the solvent screen using TFA as the acid was performed at a later point in the laboratory of Prof. Paul Kamer at the University of St. Andrews. The reactions were performed in parallel in the same autoclave, with each reaction mixture being contained in a vial of a total volume of 1.2 mL filled to avoid leaking. The newer results, performed in TFA, were slightly different from those obtained previously, which were done on a larger scale and with *p*-TsOH as the acid. The combination of diglyme and DBDOCphos with TFA, a L/M ratio of 2.4 after 12h at 60 bar syngas mixture (CO/H_2, 1:1) appeared to indicate an isomerization of 61 % and some heavy species (aldol products). However this result is questionable, given what appears to have been some contamination of the GC instrument used. The following results, performed with the tetraphosphine *rac* **63** (R = Ph) were analyzed using a different machine. The main difference from the previous experiments was the observation of isomerization when we employed diglyme, the best solvent as reported by Drent[123,305] and Beller.[123,321] Nonetheless this non-basic bidentate ligand forming has proven not to provide a very efficient catalyst for Pd-catalyzed hydroformylation.

		Selectivity (%)		
Solvent	**1-octene**	**Ald**	**Iso**	**'Heavy'**
Diglyme	23	0	61	16
Toluene	99	0	1	0
1,2 -dichlorobenzene	99	0	1	0
Chlorobenzene	97	0	3	traces

Table 10: Conditions: TFA: 12 µL, 1-octene: 0.4 mL, $Pd(OAc)_2$, ligand DBDOCphos (7 µmol), T = 125 °C, $CO:H_2$ (1 :1) = 60 bar, L/Pd = 2.4, V_{tot} = 1.2 mL, 12 h.

5.6 Tetraphosphine Systems in Pd-catalyzed Hydroformylation

The design of the tetraphosphine ligand bearing a C3 chain is particularly interesting for palladium catalyzed hydroformylation, because Drent and co-workers discovered that 1,3-bis(diphenylphosphino)propane (dppp) in combination with trifluoroacetic acid gave the best results,[131] and this was confirmed by Beller and co-workers.[319] Our ligand design bears two chelating arms that mimick dppp-moieties which might, if it were possible to induce metal cooperativity, improve the catalytic reaction.

A number of experiments were conducted using the tetraphosphine *rac* **63** (R=Ph) shown in Scheme 67, which is assumed to form a Pd(II) bimetallic complex **75b**. The catalysts were generated *in situ* using a combination of palladium acetate and an acid, and used for the hydroformylation of 1-octene. In some reactions, NaCl was added as halide source, because of the improved results that it gave in the protocols described by *Almeida Leñero et al.* and *Drent et. al*.[305]

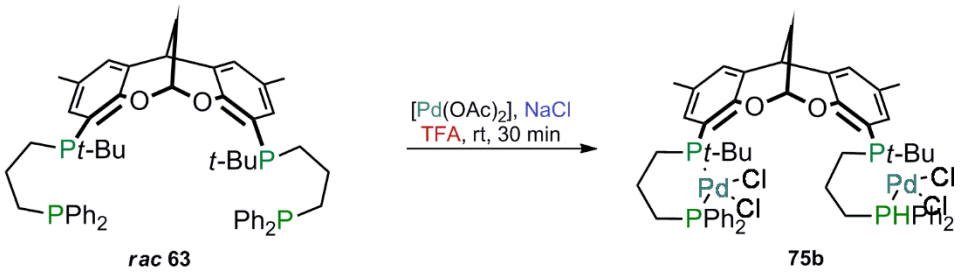

Scheme 67: Tetraphosphine *rac* **63** was used to form *in situ* the catalyst, which probably has the configuration of complex **75b**.

As shown in Figure 63 an investigation of propene hydrocarbonylation by Budzelaar and Drent gave a correlation between the chemoselectivity, ligand basicity and the employed acid strength.[131]

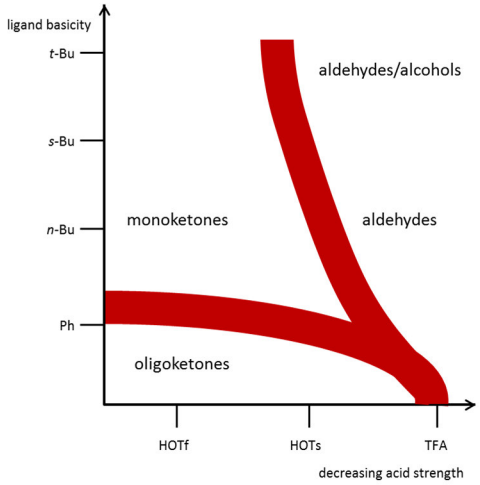

Figure 63: Schematic discription of chemoselectivity as a function of ligand and acid properties. X-axis shows increasing pK_a: HOTf (- 5.1) < HOTs (- 2.7) < TFA (- 0.7) and Y-axis: Increasing ligand basicity: DPPP < DcBPP < DsBPP < DtBPP.[131]

The catalytic experiments were conducted upon α-octene, which was filtered through an aluminum pad prior to the experiment.

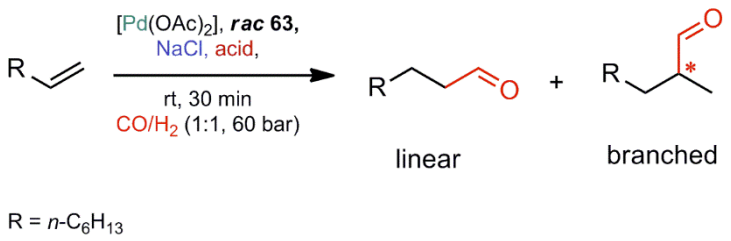

Scheme 68: Palladium-catalyzed hydroformylation of 1-octene with the in situ formed catalyst *rac* **63**.

5.6.1 The Effect of Anions on Palladium-catalyzed Hydroformylation

The study of the effect of anions on the palladium-catalyzed hydroformylation of 1-octene led to inconclusive results. For this study two different acids, TFA and *p*-methane sulfonic acid were employed and different solvents (diglyme, *o*-dichlorobenzene, chlorobenzene and toluene) were screened (Table 11). The combination of TFA and a preformed complex $Pd(OTf)_2$ with ligand *rac* **63** led to inconclusive results.

The first test involved a preformed precursor $Pd(OTf)_2$, which features weakly coordinating anions, with L/Pd of 0.5, CO/H_2 (1:1) 60 bar, 125 °C, 16 h. The precursor and ligand ***rac* 63**

were loaded in the glove box and stirred in the dry solvents for 30 minutes prior to the loading of the autoclave and pressurizing the system with syngas.

This catalytic system showed mainly isomerization in diglyme, chlorobenzene and o-dichlorobenzene. Unfortunately, under these conditions internal olefins (70-98 %) were predominantly produced as main products. The *in situ* formed palladium hydride complex isomerizes 1-octene much faster than catalyzing the desired hydroformylation reaction, which is in accordance with the study of *Beller* and co-workers, who observed isomerization of 1-octene without any hydrogen pressure even at room temperature.[319] In case of toluene only 'heavy' products were observed; these are products that result from the evolution of aldehydes and ketones.

The change of the anion had a huge impact on the catalytic results (Table 11), the conditions were identical to the previously described reaction, a L/Pd 0.5, CO/H_2 (1:1) 60 bar, 125 °C, 16 h, but the anion was formed *in situ* from $Pd(OAc)_2$, ligand ***rac* 63** and TFA (0.8 mol%). The ligand complex was formed upon stirring for 30 min in the glovebox without the acid prior to pressurizing the system with syngas. Since the first screening showed mainly isomerization which, according to the observations of *Almeida Leñero et al.* is at least an order of magnitude faster than the conversion to hydrocarbonylation products,[305] we decided to add NaCl which was found by the same authors to accelerate the hydroformylation reaction.[305]

As in the first screening with the preformed anion attached to the precursor, the main products were internal olefins (isomerization), especially in diglyme. However, in contrast to the first screening in the solvents toluene, *o*-dichlorobenzene and chlorobenzene, three peaks around 9-10 min appeared in the GC, these products could not be isolated because of the small scale of the reaction (Figure 64). Nonetheless, it proves that halides accelerate the catalytic reaction that gives hydroformylation products. Even so these signals are not the expected aldehydes, but most probably further reactions of these products, and since they appear around the same retention time they are most probably chemically very similar.

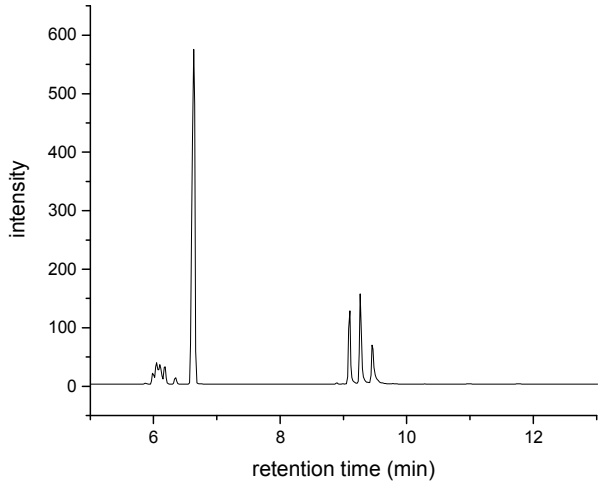

Figure 64: GC analysis of probe 8 shows the formation of three products which appear between 9-10 min. They could not be identified, but it can be assumed that these reflect the formation of ketones. The other signals are isomers and the solvent peak, the 'heavy' species is not displayed here.

		Acid/		Selectivity (%)[c]			
Entry	**Solvent**	**preformed anion**	**1-octene**	**Ald**	**Iso**	**'Heavy'**	**Ret t:10min**
1	Diglyme[a]	$Pd(OTf_2)$	30	0	70	0	0
2	Toluene[a]	$Pd(OTf_2)$	0	0	0	100	0
3	*o*-dichlorobenzene[a]	$Pd(OTf_2)$	2	0	98	0	0
4	Chlorobenzene[a]	$Pd(OTf_2)$	3	0	97	0	0
5	Diglyme[b]	TFA	2	0	92	6	0
6	Toluene[b]	TFA	0	0	20	0	80
7	*o*-dichlorobenzene[b]	TFA	0	0	8	0	92
8	Chlorobenzene[b]	TFA	3	0	0	1	96

Table 11: a) Conditions: 1-octene: 4 mL, $Pd(OTf_2)$ (0.05368 mmol), ligand ***rac* 63** (0.02838 mmol), T = 125 °C, $CO:H_2$ (1 :1), P = 60 bar, L/Pd = 0.5, V_{tot} = 1.2 mL, 16 h . b) Conditions: 1-octene: 4 mL, $Pd(OAc)_2$ (0.05368 mmol), ligand ***rac* 63** (0.02838 mmol), T = 125 °C, $CO:H_2$ (1 :1), P = 60 bar, L/Pd = 0.5, Cl/Pd = 0.016, V_{tot} = 1.2 mL, 16 h, acid (0.8 mol%, 0.07 mL). c) The yields were determined by GC. (Ald= aldehyde; Iso = isomerization)

5.6.2 Acid Affecting the Ligand and Hydroformylation

As described in section 2.3.3 phosphines can be protonated by acids. In the palladium-catalyzed hydroformylation two equivalents of acid are required to activate the precursor $Pd(OAc)_2$.[a] Excess acid in the reaction mixture accelerates the conversion of any Pd(0) to the Pd-hydride[1,8,131,294,305,319,323] species, the active catalyst. In the presence of excess acid the palladium complex becomes unstable and palladium metal precipitates**.**

5.6.3 Influence of the Metal-to-Ligand Ratio on Hydroformylation

Little is known in the literature about the effect of the catalyst loading on palladium-catalyzed hydroformylation, which is why we decided to study this briefly. Chlorobenzene was chosen as the solvent, due to the result of entry **7** in in Table 11. The catalytic conditions were those of entries **5-8**, but the metal-to-ligand ratio and the amount of acid were changed and the reaction time was shortened to 5 h from 16 h. The [(***rac* 63**)$Pd(OAc)_2$] was formed in the glovebox prior to the hydroformylation in the autoclave.

A higher catalyst loading and an excess of acid produced 96 % of the products having retention times of around 9-10 min in entry **8**. Since we were not able to identify these three products, it can only be assumed that these are products evolved from the hydroformylation products. The reduction of the catalyst loading and amount of acid resulted in entries **9-12** to a conversion of 98 %. Isomerization was the main product in all cases and the average formation of *iso*-octene was 93 %. In contrast to the previous experiment aldehydes could be detected and their average formation was 4 % with a branched-to- linear ratio of 3 in entries **9**, **10** and **12** and 2 in entry **11**. Since no formation of the products around 9-10 min was observed in these reactions, it can be assumed that the products are formed as a result of the excess of acid used in reaction **8**. It seems that the L/M ratio does not influence the system, as no great changes were observed upon changing this parameter.

				Selectivity (%)					
					Ald				
Entry	**[Pd]/mmol**	**L/Pd**	**TFA/µL**	**1-octene**	**lin**	**br**	**Iso**	**'Heavy'**	**Ret t:10min**
8	0.054	0.5	70 (0.938 mmol)	3	0	0	0	1	96
9	0.005	0.6	1.5 (0.019 mmol)	2	1	3	93	traces	0

[a] Otherwise unreactive in hydroformylation.

10	0.004	0.75	1.2(0.017 mmol)	2	1	3	93	traces	0
11	0.003	1	0.9(0.012 mmol)	2	2	4	92	traces	0
12	0.002	1.5	0.6(0.008 mmol)	2	1	3	93	traces	0

Table 12: Conditions: 1-octene: 4 mL, $Pd(OAc)_2$, TFA, ligand ***rac* 63** (0.003 mmol), T = 125 °C, $CO:H_2$ (1 :1), P = 60 bar, L/Pd = 0.5, NaCl = four grains, V_{tot} = 1.2 mL, 5 h .

It remains questionable if these results would have changed after 16 h. At this point no conclusion can be reached. What is clear is that the synthesized ligand ***rac* 63** is forming an active catalyst system with palladium.

5.6.4 Rhodium catalyzed hydroformylation[1,324]

Control experiments were conducted with ligand ***rac* 63** in rhodium-catalyzed hydroformylation. In contrast to palladium neither an acid nor a halide source is needed. The reaction was performed under 20 bar syngas pressure at 60 °C in toluene with $Rh(CO)_2acac$ as precursor forming the catalyst *in situ*.

In all reactions isomerization and the formation of aldehydes was observed, moreover complete conversion occurred (Table 13). It appears that ligand ***rac* 63** forms also an active catalyst with rhodium. Isomerization is the main product in all cases but, in contrast to the Pd-catalyzed reactions, more aldehydes were formed and a preference of branched aldehydes over linear ones was observed. A control experiment without metal with ligand ***rac* 63** was performed in parallel which gave aldehydes in the absence of metal, but with a reversed selectivity towards linear aldehydes (entry **5**).

			Selectivity (%)			
			Ald			
Entry	**L/Rh**	**1-octene**	**lin**	**br**	**br/lin**	**Iso**
1	0.9	0	6	16	2.7	78
2	1.65	0	6	16	2.7	78
3	7.5	0	7	16	2.3	77
4	12	0	9	23	2.6	68

	L				**lin/br**	
5	0.003	2	11	4	2.8	82

Table 13: Conditions: 1-octene: 1 mL, $Rh(CO)_2acac$, ligand ***rac* 63**(0.003 mmol), T = 60 °C, $CO:H_2$ (1 :1), P = 20 bar, V_{tot} = 1.2 mL, 3:45 h .

5.7 Conclusion

We have performed experiments testing the effect of the basicity of the employed ligand, the effect of the anion, M/L ratio and the addition of a halide, as well control experiments with Rh and without any metal present. All experiments could only be interpreted qualitatively; the yields are only estimated by GC, since a reference was not employed in all samples.

Our initial study with DBDOCphos as ligand in palladium-catalyzed hydroformylation confirmed the literature results that non-basic ligands do not form active catalysts with Pd. No conversion at all was observed in the majority of the reactions performed, only in diglyme did isomerization occur along with the formation of some 'heavy' species, which might support the choice of diglyme as reaction solvent as mentioned in the literature.[131,319]

Our ligand ***rac* 63** showed activity, mainly in the form of isomerization. The first screening in a preformed anion containing precursor $Pd(OTf)_2$, showed isomerization in all solvents except toluene, in which a complete conversion to 'heavy' products occurred. This is quite curious, since no similar outcome was observed in any other reaction, and the only possible assumption is that poor solubility of the complex led to this result. A comparison with another anion was conducted, when TFA and was employed directly without preforming the precursor. Here in all solvents except diglyme the formation of three products around 9-10 min in the GC was observed in more than 95 % yield. It might be that these are ketones, given to the correlation proposed for dppp by Drent and Budzelaar.[131] Unfortunately we were unable to isolate the products, because of the small scale employed here, and hence no firm assumptions can be made about these products. It proves though that the employed anion has a great effect on the formation of the products. A third screening was done in chlorobenzene and the effect of the change of the amount of TFA, as well as the catalyst loading was tested. Excess of acid led to the formation of three unidentified products as mentioned above; the use of less acid again gave isomerization as the main products, but also some formation of aldehydes. It seems that the formation of linear aldehydes is preferred. A change in the catalyst loading did not seem to affect the reaction outcome.

Control experiments with Rh and without metal showed surprisingly also activity in hydroformylation. In Rh-catalyzed reactions complete conversion with mainly isomerization occurred and aldehydes with a preference of branched aldehydes were obtained. These reactions display an inverted selectivity in comparison to palladium-catalyzed reactions. Much to our surprise the ligand ***rac* 63** in the absence of a metal showed activity in hydroformylation! This may be due to metal impurities in the autoclave. Here, the main product was isomerization with the appearance of aldehydes showing a similar selectivity towards the linear aldehydes like in the palladium-catalyzed case.

In conclusion these preliminary experiments show promising results and prove that our tetraphosphine ligand forms active catalysts for palladium-catalyzed hydroformylation. It seems that our ligand accelerates the isomerization of 1-octene, which is an interesting result in terms of the potential for employing internal olefins to form terminal aldehydes.

Chapter 6 Experimental Section

6.1 General procedures

Throughout this project similar reactions were performed, hence the order of the products is not strictly chronological. Unless otherwise noted, all preparations were carried out under an inert atmosphere of argon or nitrogen using standard Schlenk techniques or glove boxes, unless noted otherwise. All used glassware was oven dried and flamed out.

6.1.1 Solvents and Reagents

All reagents were in-house made using literature protocols or from commercial suppliers and used without further purification, unless noted otherwise. Deuterated solvents ($CDCl_3$, C_6D_6, C_6D_{12}, CD_3CN, CD_2Cl_2 Tol-d_8 and THF-d_8) purchased from Sigma-Aldrich were stored over activated 4 Å molecular sieves. THF and diethyl ether were distilled from sodium benzophenone ketyl. DCM, pentane, hexane, PE, DMF and toluene were taken from the Braun MB-SPS-800 system or the solvent purification system SPS-400-6 from Innovative Technologies, inc. All solvents were degassed by three freeze-pump-thaw cycles prior to use or by purging when large quantities were required. Room temperature refers to 20-25 °C.

6.2 Experiments conducted inTarragona

NMR Spectroscopy

Routine ^{1}H, $^{13}C\{^{1}H\}$ and $^{31}P\{^{1}H\}$ spectra were recorded on a Bruker Avance 400 Ultrashield spectrometer (400.1 MHz for ^{1}H NMR, 100.6 MHz for $^{13}C\{^{1}H\}$ and 162.0 MHz for $^{31}P\{^{1}H\}$). The deuterated solvents[325] used are indicated in the experimental part; chemical shifts, δ, are given in ppm, relative to TMS (^{1}H, ^{13}C) and 85 % H_3PO_4 (^{31}P). Coupling constants, J, are given in Hz.

Gas chromatographic analyses were performed on an Agilent 6890N using FID detector. When coupling GC-MS, a mass selective detector with EI ionization source was used (5973).

Single crystal X-ray diffraction

Crystal structure determination was carried out using a Bruker-Nonius diffractometer equipped with a APPEX 2 4K CCD area detector, a FR591 rotating anode with $Mo_{K\alpha}$ radiation, Montel mirrors as monochromator and a Kryoflex low temperature device (T = 100 K). Fullsphere data collection omega and phi scans. Programs used: Data collection Apex2 V. 1.0-22 (Bruker- Nonius 2004), data reduction Saint + Version 6.22 (Bruker- Nonius 2001) and absorption correction SADABS V. 2.10 (2003). Crystal structure solution was achieved using direct methods as implemented in SHELXTL Version 6.10 (Sheldrick, Universität Göttingen (Germany), 2000) and visualized using XP program. Missing atoms were subsequently located from difference Fourier synthesis and added to the atom list. Least-squares refinement on F2 using all measured intensities was carried out using the program SHELXTL Version 6.10 (Sheldrick, Universität Göttingen (Germany), 2000).

Mass Spectrometry

Electron spray ionization (ESI) mass spectra were recorded on a Waters LCT Premier ESI-TOF spectrometer or in a Waters GTC spectrometer. The detected ion masses are reported as mass-to-charge ratio (m/z) and refer to the isotope with the highest natural abundance. The isotope patterns of the reported signals are in agreement with the expected isotope distribution.

6.3 Experiments conducted in Palaiseau

NMR Spectroscopy

NMR measurements were obtained using a Bruker 300 Avance spectrometer operating at 300 MHz for ^{1}H, 75.5 MHz for ^{13}C and 121.5 MHz for ^{31}P. The spectra were recorded at 20 °C unless mentioned otherwise. Chemical shifts δ are reported in parts per million (ppm) relative to $SiMe_4$ (internal reference) for ^{1}H and ^{13}C and relative to 85% H_3PO_4 (external reference) for ^{31}P. The following abbreviations are used for the description of the NMR spectra: *s* (singlet), *d* (doublet), *t* (triplet), *m* (multiplet), *br* (broad).

Single crystal X-ray diffraction

Data were collected at 150.0-(1) K on a Nonius Kappa CCD diffractometer using a Mo Kα (λ= 0.71070 Å) X-ray source and a graphite monochromator. All data were measured using phi and omega scans. The crystal structures were solved using SIR 97 and Shelx-97. ORTEP drawings were made using ORTEP III for Windows. Mercury drawings were made using Mercury 3.6.

Elemental analysis

Microanalysis was obtained from the London Metropolitan University, UK.

Mass Spectrometry

High-resolution mass spectra were recorded by electron impact ionization (EI) in positive mode on a Q-TOF Premier mass spectrometer (Waters, France). Ion source parameters were adjusted as followed: cone voltage (Vcone) was set at 20 V while the capillary voltage was set at 3 kV. Typical values for the other source parameters were 2 V for the extraction cone and 2.4 V for the ion guide. Source and desolvatation temperatures were set to 80 °C and 250 °C, respectively. Nitrogen was used as both nebulizing and desolvation gas. Argon was used as collision gas at a flow rate of 0.28 mL min^{-1} corresponding to a pressure of ca. 4 10^{-3} mBar. Sample solutions at 10^{-5} M were prepared in MeOH with LiCl to allow the formation of MLi^{+}. Solutions were infused into the ion source at a flow rate of 10 μL/min.

6.4 Experiments conducted in Saint Andrews

Gas Chromatography

The hydroformylation selectivity was monitored with an Agilent 7820A GC instrument with an Agilent HP-5 column (model 19091J-413, 320 μm, 30 m, 0.25 μm) and FID detector.

6.5 Syntheses

Procedure to prepare 2,10-dimethyl-12H-6,12-methanodibenzo[d,g][1,3]di-oxocine (DBDOC)

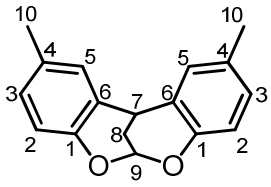

p-Cresol (50 mmol), and malonaldehyde tetramethyl acetal (4.0 mL, 25 mmol) and trifiuoroacetic acid (10-15 mL) was stirred 4-48 h at room temperature. The reaction mixture solidified. After addition of acetic acid (20-30 mL), the crude product was filtered and washed with hot water. The product was purified by recrystallizing from ethanol to give white crystalline needles.

Yield: 64 %. Lit. yield[132]: 91 %

^{1}H NMR (300 MHz, Chloroform-d) δ 7.06 – 7.00 (m, 2H, Ph), 6.97 – 6.88 (m, 2H, Ph), 6.82 (d, *J* = 8.2 Hz, 2H, Ph), 6.13 (q, *J* = 2.1 Hz, 1H, **C9**), 3.89 (q, *J* = 2.7 Hz, 1H, **C7**), 2.28 (s, 6H, **C10**), 2.23 (dd, *J* = 3.0, 2.2 Hz, 2H, **C8**).

^{13}C{^{1}H} NMR (100 MHz, $CDCl_3$) δ 149.08 (**C1**), 130.84 (C_{Ar}), 128.88 (C_{Ar}), 128.08 (C_{Ar}), 126.74 (C_{Ar}), 116.57 (C_{Ar}), 92.49 (**C9**), 32.09 (**C8**), 26.01 (**C7**), 20.85 (**C10**).

Procedure to prepare 4,8-dibromo-2,10-dimethyl-12H-6,12-methanodibenzo-o[2,l-d:l',2''-g][1,3] dioxocine

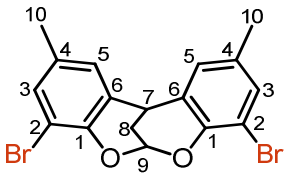

2,10-dimethyl-12H-6,12-methanodibenzo[d,g][1,3]dioxocine (12.62 g, 50 mmol) and N-bromo-succinimide (3 eq., 26.7 g, 150 mmol) were dissolved in 200 mL acetone. Then 4 mL

concentrated HCl was added. The solution turned deep orange and after a few seconds the reaction mixture solidified. The reaction was stirred 2 min at room temperature. The end of the reaction was indicated by the change from orange to yellow of the solution. The reaction was filtered and was washed with hot water to remove succinimide. The product was purified by recrystallizing from acetone to give white crystalline solid.

Yield: 14.76 g (36 mmol, 72 %). Lit. yield[159]: 87 %

^{1}H NMR (300 MHz, Chloroform-d) δ 7.23 – 7.13 (m, 2H, **C3**), 6.96 – 6.86 (m, 2H, **C5**), 6.33 (q, *J* = 2.1 Hz, 1H, **C9**), 3.89 (q, *J* = 2.9 Hz, 1H, **C7**), 2.35 – 2.18 (m, 8H, **C10** and **C8**).

^{13}C{^{1}H} NMR (100 MHz, $CDCl_3$): d 20.4 (s, **C10**), 25.4 (s, **C8**), 32.2 (s, **C7**), 92.9 (s, **C9**), 110.3 (s, **C$_{Ar}$**), 127.2 (s, **C$_{Ar}$**), 127.3 (s, **C$_{Ar}$**), 132.2 (s, **C$_{Ar}$**), 132.5 (s, **C$_{Ar}$**), 145.8 (s, **C1**).

Procedure to prepare 2,10-Dimethyl-4,8-diphenylphosphino-6,12-methano-12H-di-benzo [2,1-d:l¢,2¢¢-g][l,3]dioxocin (DBDOCphos)

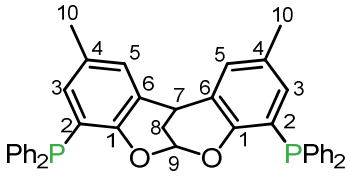

At –78 ◦C *n*-BuLi (10.9 ml, 1.6 M in THF, 17.5 mmol) was added dropwise to a stirred solution of DBDOC (3.44 g, 8.1 mmol) in dry THF (350 ml). The reaction mixture was stirred for 1 h and then was allowed to warm to -40 ◦C. At this temperature chlorodiphenylphosphine (3.1 ml, 17.3 mmol) was added and the reaction mixture was allowed to warm to room temperature. The solvent was removed *in vacuo* and recrystallized from deoxygenated methanol to give an air-stable white solid.

Yield: 3.62 g (5.83 mmol, 72%). Lit. yield[159]: 86 %

^{1}H NMR (400 MHz, $CDCl_3$): δ 2.09 (2H, *t*, $^{3}J_{H-H}$ = 2.48 Hz, CH_2), 2.11 (6H, *s*, CH_3), 3.89–3.92 (1H, *m*, CH), 5.88–5.90 (1H, *m*, CH), 6.32 (2H, *dd*, $^{3}J_{H-P}$ = 4.8 and $^{4}J_{H-H}$ = 1.9Hz, Ar), 7.02 (2H, *d*, $^{4}J_{H-H}$ = 1.72 Hz, Ar), 7.19 – 7.35 (20H, *m*, Ar).

^{13}C{^{1}H} NMR (100 MHz, $CDCl_3$): δ 20.8 (s, **C10**), 25.7 (s, **C8**), 32.2 (s, **C7**), 92.2 (s, **C9**), 124.6 (d, J_{C-P} = 15.4 Hz, **C$_{Ar}$**), 126.1 (d, J_{C-P} = 2.2 Hz, **C$_{Ar}$**), 128.4 (d, J_{C-P} = 4.9 Hz, **C$_{Ar}$**),128.5

(d, J_{C-P} = 3.6Hz, **C_{Ar}**), 128.6 (s, **C_{Ar}**), 129.0 (s, **C_{Ar}**), 130.6 (d, J_{C-P} = 1.5 Hz, **C_{Ar}**), 133.0 (d, J_{C-P} = 1.5 Hz, **C_{Ar}**), 33.8 (d, J_{C-P} = 19.8 Hz, **C_{Ar}**), 134.1 (d, J_{C-P} = 20.5 Hz, **C_{Ar}**), 136.8 (d, J_{C-P} = 11.3 Hz, **C_{Ar}**), 137.1 (d, J_{C-P} = 11.4 Hz, **C_{Ar}**), 150.9 (d, J_{C-P} = 15.0 Hz, **C1**).

^{31}P {^{1}H} NMR (162 MHz, $CDCl_3$): δ –12.8 (*s*).

General procedure for the preparation of (2,10-dimethyl-12H-6,12-methano-dibenzo[d,g][1,3]dioxocine-4,8-diyl)bis(R-phosphine borane) 38 a-c

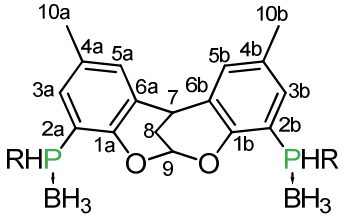

R = Ph (**a**), Cy (**b**), *t*-Bu (**c**)

The compounds were synthesized by four *in situ* steps, which were performed by following procedures: phosphination, reduction and protection of the phosphines.

34 (1 g, 2.44 mmol) was dissolved in in freshly distilled THF (60 mL). The solution was cooled to – 78 °C and *n*-BuLi (2.1 eq., 5.12 mmol, 3.2 mL) was added dropwise. The reaction was followed by ^{31}P NMR and finished immediately. Subsequently the reaction was allowed to warm up to 0 °C and dichloro-R-phosphine (2.2 eq., 5.36 mmol) was added and it was stirred further 30 min at room temperature. The reaction was followed by ^{31}P NMR and finished immediately. The obtained chloro-R-backbone phosphines were then reduced to the secondary backbone phosphines. Freshly crushed $LiAlH_4$ was dissolved in freshly distilled THF and was cooled to 0 °C. The Schlenk was equipped with a dropping funnel, filled via cannula with (2,10-dimethyl-12H-6,12-methanodibenzo[d,g][1,3] dioxocine-4,8-diyl)bis (chloro-R-phosphine) dissolved in dry THF. The chloro-backbone phosphines were added dropwise to the reducing agent. After the reaction finished the solution was allowed to warm up to rt and stirred further 30 min. The reaction was followed by ^{31}P NMR. The reaction mixture was recooled to 0 °C, and quenched with degassed water, and subsequently with degassed 15 % NaOH (aq.), both repeatedly 3x of the same amount degassed water was added, until the hydrogen gas production stopped. The reaction mixture was allowed to warm up to rt and stirred for further 30 min, so as to give microcrystalline aluminium salts, then the reaction mixture was filtered through celite

to give the desired secondary phosphines. The air-sensitive products were not isolated, but were then protected *in situ*. To a solution of (2,10-dimethyl-12H-6,12-methanodibenzo[d,g][1,3]dioxocine-4,8-diyl)bis(terbutylphosphine) dissolved in dry THF boran dimethylsulfide complex was added dropwise at 0 °C. The reaction finished immediately. The reaction mixture was poured onto crushed ice inside a crystallizing dish, and then 1 M HCl was added to neutralize the remaining $LiAlH_4$. The product was extracted with Et_2O or DCM, dried over $MgSO_4$ and filtered. The solvent was removed. The white powder was recrystallized in EtOAc. A white crystalline powder was obtained.

38a: Yield: 0.55 g (1.1 mmol, 45 %) of a diastereomeric mixture was obtained.

$^{31}P\{^1H\}$ NMR (121 MHz, $CDCl_3$) δ –18.90 (br m), – 21.04 (br m), – 21.33 (br m), – 52.49 (br m).

38b: Yield: 1.15 g (2.27 mmol, 93 %) of a diastereomeric mixture was obtained.

Anal. Calcd. for $C_{29}H_{44}B_2O_2P_2$: C, 68.53; H, 8.73. Found: C, 68.36; H, 8.84.

^1H NMR (300 MHz, Chloroform-d) δ 7.37 – 7.27 (m, 2H, **C3**), 7.21 – 7.09 (m, 2H, **C5**), 6.28 (dd, 1H, **C9**), 5.51 (br m, , $^1J_{P–H}$ = 382.15 Hz , 2H, P-H), 3.97 (dd, 1H, **C7**), 2.48 – 2.21 (m, 8H, **C8** and **C10**), 1.98 – 1.57 (m, 8H, Cy), 1.55 – 1.09 (m, 14H, Cy).

$^{31}P\{^1H\}$ NMR (121 MHz, $CDCl_3$) δ – 6.93 (br m), – 8.07 (br m), – 10.74 (br m), – 12.12 (br m).

Ms(FAB): *m/z* calcd = 515.32$[M+Li]^+$; found: 515.35; 1023.62 $[2M+Li]^+$; found: 1023.70

38c: Yield: 0.82 g (2.1 mmol, 86 %), after trituration in EtOAc pure *rac*-compound was obtained.

^1H NMR (300 MHz, Chloroform-d) δ 7.43 – 7.21 (m, 2H, **Ar**), 7.22 – 7.05 (m, 2H, **Ar**), 6.27 – 6.21 (m, 1H, **C9**), 5.62 (q, $^1J_{P-H}$ = 382.15 Hz, $^3J_{H-H}$ = 6.65 Hz, 1H, **P–H**), 5.49 (q, $^1J_{P-H}$ = 380.9 Hz, $^3J_{H-H}$ = 6.8 Hz, 1H, **P–H**), 4.02 – 3.94 (m, 1H, **C7**), 2.28 (s, 6H, **C10**), 2.24 (m, 2H), 1.13 (d, $^3J_{P-H}$ = 15.1 Hz, 9H, **C12**), 1.09 (d, $^3J_{P-H}$ = 15.3 Hz, 9H, **C12**).

$^{13}C\{^1H\}$ NMR (75 MHz, Chloroform-d) δ 149.93 (d, $^2J_{P–C}$ = 2.0 Hz, **C1**), 149.73 (d, $^2J_{P–C}$ = 2.5 Hz, **C1**), 134.45 (d, $^2J_{P–C}$ = 4.3 Hz, **C3**), 134.28 (d, $^2J_{P–C}$ = 3.6 Hz, **C3**), 131.98 (d, $^2J_{P–C}$ = 2.0 Hz, **C2**), 131.72 (d, $^2J_{P–C}$ = 3.8 Hz, **C5**), 131.56 (d, $^2J_{P–C}$ = 3.7 Hz, **C5**), 126.83 (d, $^2J_{P–C}$ =

4.0 Hz, **C6**), 125.99 (d, $^{2}J_{P-C}$ = 3.9 Hz, **C6**), 112.95 (d, $^{2}J_{P-C}$ = 15.8 Hz, **C4**), 112.31 (d, $^{2}J_{P-C}$ = 16.0 Hz, **C4**), 92.57 (s, **C9**), 32.15 (s, **C7**) , 29.65 (d, $^{2}J_{P-C}$ = 20.0 Hz, **C11**), 29.20 (d, $^{2}J_{P-C}$ = 19.7 Hz, **C11**), 26.88 (d, $^{2}J_{P-C}$ = 3.1 Hz, **C12**), 26.54 (d, $^{2}J_{P-C}$ = 3.1 Hz, **C12**), 25.29 (s, **C8**), 20.61 (d, $^{2}J_{P-C}$ = 3.3 Hz, **C10**).

$^{31}P\{^{1}H\}$ NMR (121 MHz, $CDCl_3$) δ 2.06 ppm (br m, $^{1}J_{H-P}$ = 382.15 Hz), − 0.55 ppm (br m, $^{1}J_{H-P}$ = 380.09 Hz).

General procedure for the preparation of (2,10-dimethyl-12H-6,12-methano-dibenzo[d,g][1,3]dioxocine-4,8-diyl)bis(chlorophenylphosphine) 36 a-c

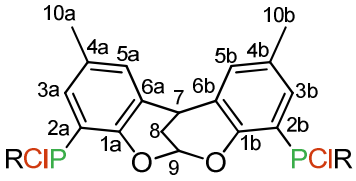

R = Ph (**a**), Cy (**b**), *t*-Bu (**c**)

36a: Yield (estimated by ^{31}P NMR): 40 %.

$^{31}P\{^{1}H\}$ NMR (121 MHz, $CDCl_3$) δ 77.58 (s), 76.82 (s), 76.55 (s), 75.78 (s), 74.46 (s).

36b: Yield (estimated by ^{31}P NMR): 100 %.

$^{31}P\{^{1}H\}$ NMR (121 MHz, $CDCl_3$) δ 101.28 (s), 100.67 (s), 99.59 (s), 97.44 (s).

36c: Yield (estimated by ^{31}P NMR): 100 %.

$^{31}P\{^{1}H\}$ NMR (121 MHz, $CDCl_3$) δ 103.41 (s), 103.03 (s), 99.67 (s).

General procedure for the preparation of (2,10-dimethyl-12H-6,12-methano-dibenzo[d,g][1,3]dioxocine-4,8-diyl)bis(r-phosphine) 37 a-c

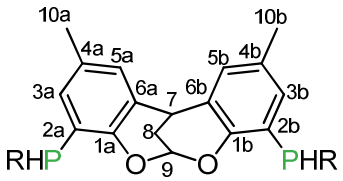

R = Ph (**a**), Cy (**b**), *t*-Bu (**c**)

37a: Yield (estimated by ^{31}P NMR): 100 %.

^{1}H NMR (300 MHz, $CDCl_3$) δ 7.30, 7.04, 6.35, 5.92, 3.93, 3.50, 2.34, 2.14.

^{31}P{^{1}H} NMR (162 MHz, $CDCl_3$) δ -31.74 (s), -32.10 (s), -32.41(s), -32.68 (s).

37b: Yield (estimated by ^{31}P NMR): 100 %.

^{31}P{^{1}H} NMR (121 MHz, $CDCl_3$) δ – 46.16 (s), – 48.14 (s), – 48.61 (s), – 49.26 (s).

37c: Yield (estimated by ^{31}P NMR): 100 %.

^{31}P{^{1}H} NMR (121 MHz, $CDCl_3$) δ –2 7.77 (s, $J_{P\text{-}H}$ = 192.17 Hz), – 28.90 (s, $J_{P\text{-}H}$ = 209.53 Hz), –31.17 (s, $J_{P\text{-}H}$ = 203.44 Hz), – 31.81 (s, $J_{P\text{-}H}$ = 210.58 Hz).

Procedure to prepare Diethyl (2,10-dimethyl-12H-6,12-methanodibenzo[d,g] [1,3]dioxocine-4,8-diyl)bis(phenylphosphinate) 41

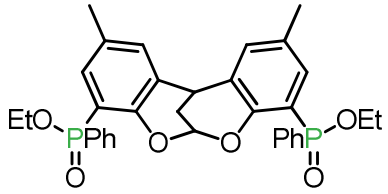

An oven-dried Schlenk, equipped with a stir bar, was charged with ethyl phenylphosphinate (2.1 eq. 0.39 mL, 2.56 mmol) and *i*-Pr_2EtN (4 eq., 0.84 mL, 4.88 mmol) and dissolved in dry DMAc (10 mL) under nitrogen atmosphere and stirred for 30 min. at rt. A separate Schlenk was filled with the precursor $Pd(OAc)_2$ (0.1 mol%, 82 mg, 0.12 mmol) and the ligand Xantphos (0.2 mol%, 145 mg, 0.25 mmol) in 0.5 mL dry DMAc and stirred 30 min. at rt to form the complex. In a third Schlenk DBDOCBr (0.5 g, 1.22 mmol) was dissolved in 20 mL dry DMAc and added

after 30 min. to the solution with the phosphinate and subsequently the catalyst was added and the reaction mixture was stirred for 3 d at 120 °C. After the reaction finished the solution was quenched with H_2O (5 mL) and diluted with 3 mL of ethyl acetate, filtered over a pad of $MgSO_4$ and silica. The solution was concentrated *in vacuo* to give a light brown-whitish solid was obtained.

Yield 1.02 g (68 %, 1.74 mmol).

^{31}P {^{1}H} NMR (162 MHz, $CDCl_3$): δ 32.87 (s), 32.57 *(s)*, 31.92 (s), 31.61 (s).

Procedure to prepare (2,10-dimethyl-12H-6,12-methanodibenzo[d,g][1,3] dioxocine-4,8-diyl)bis (phenylphosphinate) 39

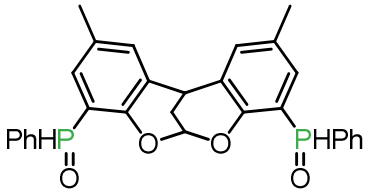

Yield (estimated by ^{31}P NMR): 94 % of a diastereomeric mixture.

^{31}P NMR (121 MHz, $CDCl_3$) δ 27.07 (s, J_{P-H} = 470.7 Hz), 21.28 (s, J_{P-H} = 562.39 Hz), 12.97 (s, J_{P-H} = 501.88 Hz), 9.37 (s, J_{P-H} = 517.02 Hz).

Procedure to prepare Dichlorocyclohexylphosphine

PCl_2Cy

Cyclohexylmagnesium chloride solution (1.8 M, 68 mmol) was added slowly during 2 h to a stirred and cooled (– 78 °C) solution of PCl_3 (68 mmol) in freshly distilled Et_2O (60 mL) and the solution was allowed to come back to room temperature. The solution turned yellow was concentrated and filtered. Then the remaining solvent was removed *in vacuo*. Complete conversion was estimated by ^{31}P–NMR resulting in 90 % desired product and 10 % by-product (PCy_2Cl).

$^{31}P\{^{1}H\}$ NMR (121 MHz, CD_2Cl_2) δ 192.59 ppm (s). Lit.: δ 196.29 (s).[326]

Procedure to prepare Dicyclohexylphosphine-borane

Dicyclohexylphosphine (0.23 g, 1 mol) was dissolved in degassed and freshly distilled THF (10 mL). The solution was cooled to 0 °C, and BH_3*THF (1.1 eq.) was slowly added. The reaction finished immediately resulting in a colorless solution. The reaction mixture was allowed to warm to room temperature and the solvent was carefully evaporated resulting in a crystalline white solid.[a]

Yield: 0.21 g (98%, 0.98 mmol).

^{1}H NMR (300 MHz, Chloroform-d) δ 4.11 (dd, $^{2}J_{H\text{-}H}$ = 5.6 Hz, $J_{P\text{-}H}$ = 351.5 Hz, 1H), 1.98 – 1.60 (m, 10H), 1.59 – 1.08 (m, 12H), 0.40 (dd, $J_{B\text{-}H}$ = 195.1, 91.7 Hz, 3H).

$^{31}P\{^{1}H\}$ NMR (121 MHz, Chloroform-d) δ 19.72 (br m, J = 95.2, 33.0 Hz).

General procedure to prepare di-R-phosphine-borane propionate 43

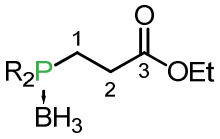

R = Ph (**a**), Cy (**b**)

Di-R-phosphine borane (9.7 g, 44.48 mmol, R =Ph, Cy) was dissolved in freshly distilled and degassed THF. The solution was cooled to – 78 °C and *n*-BuLi (1.1 eq., 5.7 mL) was added

[a] If excess BMS is present, the sample may sponaneously ignite.

dropwise. The lithiation finished immediately. To the lithiated phosphine ethyl-3-bromopropionate (6 mL, 44.48 mmol) was added at – 78 °C. The reaction mixture was allowed to warm up to room temperature. The reaction finished immediately resulting in a 50 % conversion with 100 % desired product. The purification was done by flash chromatography in pure pentane leading to a white solid.

43a: Yield: 10.15 g (76%, 33.8 mmol)

^{1}H NMR (300 MHz, Chloroform-d) δ 7.68 (m, 6H), 7.58 – 7.33 (m, 4H), 4.07 (q, *J* = 7.2 Hz, 2H), 3.80 – 3.62 (m, 2H), 2.71 – 2.44 (m, 2H), 1.33 – 1.11 (m, 3H).

^{31}P NMR (121 MHz, $CDCl_3$) δ 13.53 (br m).

43b: Yield: 7.8 g (24.98 mmol, 56 %).

$R_2PLi(BH_3)$: **^{31}P{^{1}H} NMR** (121 MHz, DMSO-d6) δ -37.99 (dd, *J* = 77.9 Hz, 37.7 Hz).
^{1}H NMR (300 MHz, Chloroform-d) δ 4.25 – 3.96 (m, 23H), 2.87 (t, *J* = 6.7 Hz, 2H), 2.52 (q, *J* = 7.7 Hz, 3H, J_{P-H} = 8.1 Hz), 2.30 (t, *J* = 7.8 Hz, 2H), 1.95 – 1.55 (m, H), 1.55 – 0.91 (m, H), 0.24 (dd, J_{B-H}= 180.9, 79.4 Hz, 1H).
^{31}P{^{1}H} NMR (121 MHz, Chloroform-d) δ 27.97 ppm (br m).

General procedure to prepare 3-hydroxy-propyldi-R-phosphine-borane 45

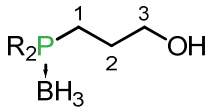

R = Ph (**a**), Cy (**b**)

$LiAlH_4$ (3.4 g, 90 mmol) was dissolved in 40 mL freshly distilled THF and cooled to 0 °C. Di-R-phosphine-borane propionate (7 g, 22 mmol, R = Cy, Ph) dissolved in 80 mL dry THF was added via cannula dropwise to the solution. The Schlenk was equipped with a needle connected to the Nitrogen line to equilibrate the H_2-gas production. After addition of the phosphine-borane the reaction mixture was allowed to warm up to room temperature and was stirred 30 min at room temperature. Subsequently the reaction was quenched with degassed water at 0 °C, slowly, and filtered. The solvent was removed. The crude product was purified by flash chromatography (3/7 EtOAc/pentane) resulting in a yield of a white solid.

45a: 5.45 g (96%, 21.12 mmol).

^{1}H NMR (300 MHz, Chloroform-d) δ 7.68 (m, 4H, Ph), 7.57 – 7.34 (m, 6H, Ph), 3.66 (t, *J* = 6.1 Hz, 2H, C3), 2.44 – 2.21 (m, 2H, C1), 1.88 – 1.61 (m, 2H, C2).

^{31}P NMR (121 MHz, $CDCl_3$) δ 13.43 (br m).

45b: Yield: 23.84 g (98%, 88.2 mmol).

^{1}H NMR (300 MHz, Chloroform-d) δ 3.68 (t, *J* = 6.0 Hz, 2H, H-7), 1.99 – 1.59 (m, 17H), 1.46 – 1.09 (m, 9H), 0.18 (q, 1H).

^{13}C{^{1}H} NMR (75 MHz, Chloroform-d) δ 63.65 (d, *J* = 12.7 Hz, **C-7**), 32.05 (d, *J* = 32.7 Hz, **C-1**), 27.18, 27.04 (d, *J* = 2.2 Hz), 26.92 (d, *J* = 2.5 Hz), 26.18 (d, *J* = 1.2 Hz), 15.86 (d, *J* = 32.6 Hz).
^{31}P{^{1}H} NMR (121 MHz, Chloroform-d) δ 27.97 ppm (br m).

Anal. Calcd. for $C_{15}H_{32}BOP$: C, 66.68; H, 11.94. Found: C, 66.54; H, 12.05.

Procedure to prepare 3-mesyloxypropyldi-R-phosphine-borane 46

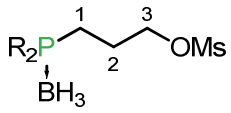

R = Ph (**a**), Cy (**b**)

3-hydroxy-propyldi-R-phosphine-borane (4.6 g, 22 mmol, R = Cy, Ph) was dissolved in 60 mL washing grade DCM and Et_3N (2.3 eq.) and cooled to 0 °C. MsCl (1.2 eq. 2.1 mL, 26.9 mmol) was added dropwise and stirred 1h maintaining the temperature. The solution turned from transparent to yellow. The reaction was quenched with 2M Ammonium chloride solution. The product was extracted with DCM and washed with brine, dried over $MgSO_4$, filtered and the solvent was removed. The crude product was purified by flash chromatography (9/1 pentane/EtOAc).

46a: 7.1 g (96%, 21.12 mmol).

^{1}H NMR (300 MHz, Chloroform-d) δ 7.75 – 7.60 (m, 4H, Ph), 7.60 – 7.34 (m, 5H, Ph), 4.24 (t, *J* = 6.0 Hz, 2H, C3), 2.97 (s, 3H, -CH_3), 2.45 – 2.26 (m, 2H, C1), 2.07 – 1.87 (m, 2H, C1).

^{13}C NMR (75 MHz, Chloroform-d) δ 132.32 – 131.96 (m, Ph), 131.51 (d, *J* = 1.5 Hz, Ph), 129.21 – 128.88 (m, Ph), 128.74 (s, C2), 70.29 – 69.52 (m, C3), 37.49 (s, CH_3), 23.35 (s, C2) 22.66 – 21.30 (m, C1).

^{31}P NMR (121 MHz, $CDCl_3$) δ 15.08 (br m).

46b: Yield: 7.13 g (93 %, 20.46 mmol).
^{1}H NMR (300 MHz, Chloroform-d) δ 4.26 (t, *J* = 5.9 Hz, 2H), 3.03 (s, 3H), 2.12 – 1.94 (m, 2H), 1.94 – 1.58 (m, 12H), 1.46 – 1.14 (m, 12H).

^{13}C{^{1}H} NMR (75 MHz, Chloroform-d) δ 70.49 (d, *J* = 12.7 Hz, **C-7**), 37.59 (s, **C-8**) , 31.90 (d, *J* = 32.7 Hz. **C-1**), 27.01 , 26.87 (d, *J* = 1.4 Hz), 26.73 (d, *J* = 2.6 Hz), 26.02 (d, *J* = 1.5 Hz), 24.21 (s, **C-6**) , 15.36 (d, *J* = 32.3 Hz, **C-5**).
^{31}P{^{1}H} NMR (121 MHz, $CDCl_3$) δ 27.74 (br m).
Anal. Calcd. for $C_{16}H_{34}BO_3PS$: C, 55.18; H, 9.84. Found: C, 55.01; H, 9.94.

Procedure to prepare 3-iodopropyldicyclohexylphosphine-borane 47

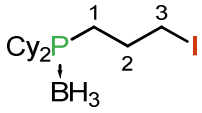

3-mesyloxypropyldicyclohexylphosphine-borane (0.5492 g, 1.58 mmol) and NaI (1g, 6.672 mmol) were dissolved in 20 mL dry acetone. The solution turned yellow and was refluxed 6 h. A white solid precipitated. The reaction was quenched with water and the product was extracted with pentane. Subsequently the organic phase was washed with water, $NaHCO_3$ and brine. The organic phase was dried over $MgSO_4$, filtered and the solvent was removed, resulting in a white solid.

Yield: 0.535 g (89 %, 1.41 mmol).
^{1}H NMR (300 MHz, Chloroform-d) δ 3.23 – 3.18 (m, 2H), 2.09 – 1.59 (m, 15H), 1.55 – 1.10 (m, 11H).

^{13}C{^{1}H} NMR (75 MHz, $CDCl_3$) δ 32.06, 27.82, 26.97, 26.84, 26.71, 26.00, 8.41.
^{31}P{^{1}H} NMR (121 MHz, $CDCl_3$) δ 22.59 ppm (bm).
Anal. Calcd. for $C_{15}H_{31}BIP$: C, 47.2; H, 8.22. Found: C, 47.52; H, 8.33.

Procedure to prepare *rac*- diethyl (2,10-dimethyl-12H-6,12-methanodibenzo [d,g][1,3] dioxocine-4,8-diyl)bis(*tert*-butylphosphine borane) propionate *rac* 40

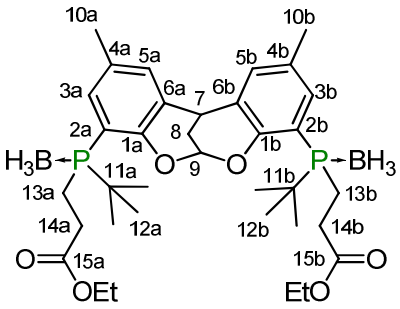

Rac **38c** (5g, 12.75 mmol) was dissolved in 400 mL degassed, dry THF and 20 mL degassed, dry EtOH and was cooled down to – 78 °C, subsequently sodium (600mg, 26.1 mmol) was added and stirred 30 min to form the base (NaOEt). Then acrylate was filtered through alumina and was added to the reaction mixture and was allowed to warm up to – 50 °C. The reaction was followed by ^{31}P–NMR and finished after 30 min. The reaction mixture was concentrated and subsequently washed with brine (100 mL) and the product was extracted with DCM (3x 200 mL), dried over $MgSO_4$, filtered and the solvent was removed. The product was recrystallized in EtOAc and a white powder of pure ***rac* 40** was obtained.

Yield: 11.17 g, (11.34 mmol, 89 %).

^{1}H NMR (300 MHz, Chloroform-d) δ 7.56 – 7.40 (m, 2H, **C3**), 7.21 (m, 2H, **C5**), 6.24 (q, *J* = 2.1 Hz, 1H, **C9**), 4.23 – 4.01 (m, 4H, -O-**CH$_2$**-CH$_3$), 3.96 (q, *J* = 2.3 Hz, 1H, **C7**), 2.81 – 2.69 (m, 2H, **C14**), 2.65 (m, 2H, **C13**), 2.28 (m, 8H, **C8**, **C10**), 2.06 (m, 2H, **C14**), 1.73 (m, 2H, **C13**), 1.39 – 1.00 (m, 24H, **C12**, -O-CH$_2$-**CH$_3$**).

^{13}C NMR (75 MHz, Chloroform-d) δ 173.11 (dd, *J* = 21.7, 16.9 Hz, **C15**), 150.91 (d, *J* = 2.4 Hz, **C1**), 150.27 (d, *J* = 3.1 Hz, **C1**), 138.01 (d, *J* = 14.3 Hz, **C3**), 137.37 (d, *J* = 13.3 Hz, **C3**), 132.52 (d, *J* = 2.2 Hz, **C4**), 131.64 (d, *J* = 12.0 Hz, **C5**), 131.37 (d, *J* = 11.6 Hz, **C5**), 126.60 (d, *J* = 4.2 Hz, **C6**), 126.09 (d, *J* = 4.1 Hz, **C6**), 112.76 (d, *J* = 38.4 Hz, **C2**), 112.19 (d, *J* = 37.9 Hz, **C2**), 92.19 (s, **C9**), 60.91 (s, **C7**), 60.80 (s, **C7**), 34.06 (s, **C8**), 30.69 (dd, *J* = 36.8, 33.4 Hz, **C11**), 29.02 (s, **C13/14**), 28.66 (s, **C13/14**), 26.37 (d, *J* = 2.4 Hz, **C12**), 26.15 (d, *J* = 2.6 Hz, **C12**), 16.28 (d, *J* = 18.3 Hz, -O-CH$_2$-**CH$_3$**), 15.80 (d, *J* = 18.0 Hz, -O-CH$_2$-**CH$_3$**), 15.16 (s, **C10**).

^{31}P NMR (121 MHz, $CDCl_3$) δ 40.21 (br m), 37.54 (br m).

Procedure to prepare (2,10-dimethyl-12H-6,12-methanodibenzo [d,g][1,3] dioxocine-4,8-diyl)bis(*tert*-butylphosphine borane)bis(3-hydroxy-propane) *rac* 60

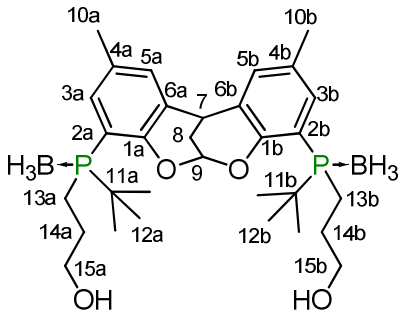

$LiAlH_4$ (4 eq., 1.73 g, 45.36 mmol) was dissolved in 50 mL dry THF and cooled to 0 °C. ***Rac* 40** (11.17 g, 11.34 mmol) dissolved in 300 mL dry THF and was added through a cannula dropwise to the solution. After the addition of ***rac* 40** was completed, the reaction mixture was allowed to warm up to room temperature and was stirred 30 min at rt. Subsequently the reaction was quenched with degassed water (25 mL) at 0 °C, slowly, and subsequently with degassed 15 % NaOH (aq., 10 mL), both repeatedly 3x of the same amount, until the hydrogen gas production stopped. Subsequently the reaction mixture was filtered over celite, dried over $MgSO_4$, filtered and the solvent was removed to give a white powder.

Yield: 21.55 g (83 %, 37.65 mmol).

^{1}H NMR (300 MHz, Chloroform-d) δ 7.53 – 7.49 (m, 1H, **C3**), 7.41 – 7.36 (m, 1H, **C3**), 7.22 – 7.16 (m, 2H, **C5**), 6.30 (m, 1H, **C9**), 3.94 (q, *J* = 2.7 Hz, 1H, **C7**), 3.67 (m, 4H, **C15**), 2.86 – 2.52 (m, 4H, **C13**), 2.29 (s, 3H, **C10**), 2.28 (s, 3H, **C10**), 2.08 (m, 2H, **C8**), 2.02 – 1.63 (m, 4H, **C14**), 1.08 (s, 9H, **C12**), 1.07 (s, 9H, **C12**).

^{13}C NMR (75 MHz, Chloroform-d) δ 151.14 (d, *J* = 1.5 Hz, **C1**), 150.77 (d, *J* = 2.5 Hz, **C1**), 137.27 (d, *J* = 13.0 Hz, **C3**), 136.74 (d, *J* = 11.7 Hz, **C3**), 132.57 (d, *J* = 2.4 Hz, **C4**), 131.84 (d, *J* = 2.3 Hz, **C4**), 131.15 (d, *J* = 1.3 Hz, **C5**), 131.00 (d, *J* = 1.9 Hz, **C5**), 126.99 (d, *J* = 4.4 Hz, **C6**), 125.85 (d, *J* = 4.1 Hz, **C6**), 113.15 (d, *J* = 43.6 Hz, **C2**), 112.48 (d, *J* = 43.9 Hz, **C2**), 92.01 (s, **C9**), 68.05 (s, **C15**), 31.97 (d, *J* = 9.7 Hz, **C7**), 31.35 – 29.84 (m, **C11**), 26.79 (d, *J* = 9.1 Hz, **C13**), 26.22 (d, *J* = 2.3 Hz, **C12**), 26.05 (d, *J* = 2.4 Hz, **C8**), 20.57 (s, **C10**), 17.34 (dd, *J* = 46.4, 35.8 Hz, **C14**).

^{31}P NMR (121 MHz, $CDCl_3$) δ 31.47 (br m).

Procedure to prepare (2,10-dimethyl-12H-6,12-methanodibenzo [d,g][1,3] dioxocine-4,8-diyl)bis(*tert*-butylphosphine borane)bis(3-mesyloxypropane) *rac* 59

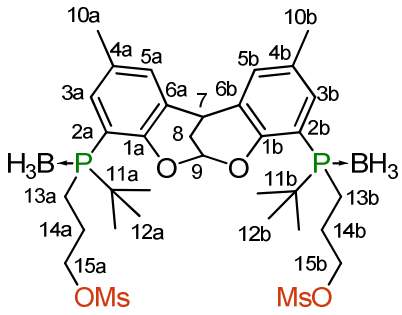

***Rac* 59** (11.17 g, 11.34 mmol) was dissolved in 250 mL dry DCM and dry Et_3N (4 eq., 6.33 mL, 45.36 mmol) and cooled to 0 °C. MsCl (2.4 eq. 2.1 mL, 27.22 mmol) was added dropwise under inert atmosphere and stirred 1-2 h at 0 °C. The reaction was quenched with 10 mL 2 M NH_4Cl (aq.). The product was washed with brine (100 mL) and extracted with DCM (2x 100 mL), dried over $MgSO_4$, filtered and the solvent was removed. A white powder was obtained.

Yield 7.68 g (93 %, 10.55 mmol).

^{1}H NMR (300 MHz, Chloroform-d) δ 7.48 (m, 2H, **C3**), 7.20 (m, 2H, **C5**), 6.34 (m, 1H, **C9**), 4.43 – 4.18 (m, 4H, **C15**), 3.94 (m, 1H, **C7**), 3.58 – 3.43 (m, 4H, **C13**), 3.04 (s, 3H, **-OMs**), 3.03 (s, 3H, **-OMs**), 2.29 (s, 6H), 2.08 (m, 2H), 1.72 (m, 4H, **C14**), 1.12 (s, 9H, **C12**), 1.12 (s, 9H, **C12**).

^{13}C NMR (75 MHz, Chloroform-d) δ 150.89 (d, *J* = 2.7 Hz, **C1**), 150.75 (d, *J* = 2.7 Hz, **C1**), 137.68 (d, *J* = 13.7 Hz, **C3**), 137.24 (d, *J* = 13.4 Hz, **C3**), 132.70 (d, *J* = 2.3 Hz, **C4**), 132.35 (d, *J* = 2.3 Hz, **C4**), 131.61 – 131.17 (m, **C5**), 126.66 (d, *J* = 4.2 Hz, **C6**), 126.43 (d, *J* = 4.1 Hz, **C6**), 112.50 (m, *J* = 43.7 Hz, , **C2**), 92.31 (s, **C9**), 71.48 (d, *J* = 15.5 Hz, **C15**), 70.96 (d, *J* = 13.7 Hz, **C15**), 68.09 (s, **C7**), 37.58 (d, *J* = 12.5 Hz, **-OMs**), 31.86 (s, **C8**), 30.82 (dd, *J* = 36.0, 33.2 Hz, **C11**), 26.23 (dd, *J* = 9.7, 2.5 Hz, **C12**), 25.33 (s, **C13**), 23.95 (s, **C14**) , 20.58 (d, *J* = 2.5 Hz, **C10**).

^{31}P NMR (121 MHz, $CDCl_3$) δ 39.16 (br m), 37.60 (br m).

Procedure to prepare (3-bromopropyl)diphenylphosphine oxide[327]

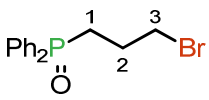

Diphenylphosphine oxide (1.2 g, 5.95 mmol) was dissolved in 10 mL DMSO and at 0 °C 2 mL of a 2M KOH solution was added. The solution turned from transparent to yellow. The solution was stirred further 30 min at rt to fully deprotonate. The reaction was added dropwise at 0 °C to a solution of dibromopropane (20 mL, 89.1 mmol, 10 eq.) dissolved in 20 mL DMSO. The solution turned lighter yellow. After 1 d the reaction was completed. The product was extracted with Et_2O (3 x 20 mL) and washed with water (2x 10 mL), dried over $MgSO_4$, filtered and the solvent was removed *in vacuo*.

Yield 1.46 g (4.52 mmol, 76 %).

^{1}H NMR (500 MHz, $CDCl_3$) δ 7.74 (m, 4H, **Ph**) 7.53 (m, 6H, **Ph**), 3.48 (t, 2H, **C3**), 2.45, 2.18(m, 2H, **C2**).

^{31}P{^{1}H} NMR (202 MHz, $CDCl_3$) δ 35.10.

Procedure to prepare (3-chloropropyl)diphenylphosphine[226]

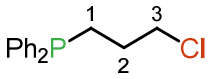

Diphenylphosphine (2.395 g, 12.873 mmol), 1-bromo-3-chloropropane (1.5 eq., 2 mL, 19.32 mmol), TEBA (0.11 eq, 323.7 mg, 1.42 mmol) and KOH pellets (2.5 eq. 1.822 g, 32.18 mmol) were dissolved in 20 mL dry MeCN in rt and stirred overnight (12 h). The color changed from transparent to slightly yellow. The product was extracted in 15 mL DCM and washed with iced water, the organic phase was dried over Na_2SO_4, filtered and the solvent was removed *in vacuo*. The oily product was dissolved in boiled dry hexane and put into the freezer 3 h. Subsequently the solution was filtered in inert atmosphere and the solvent was removed *in vacuo*. This was repeated two times. A yellow oil was obtained.

Yield: 2.43 g (9.27 mmol, 72 %).

^{1}H NMR (500 MHz, $CDCl_3$) δ 7.37 (m, 4H, **Ph**), 7.25 (m, 6H, **Ph**), 3.53 (t, 2H, **C3**), 2.13 (m, 2H, **C1**), 1.84 (m, 2H, **C2**).

^{31}P{^{1}H} NMR (202 MHz, $CDCl_3$) δ -14.05 ppm.

Procedure to prepare Ethyl (3-(diphenylphosphoryl)propyl)(phenyl) phosphinate

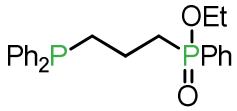

Ethyl phenylphosphinate (0.2 mL, 1.33 mmol) and KOH (1.1 eq., 82 mg, 1.46 mmol) were dissolved in 10 mL DMSO/H_2O (9/1) and stirred 30 min at rt, subsequently (3-chloropropyl)diphenylphosphine (0.349 g, 1.33 mmol). The reaction mixture was stirred overnight at rt and an transparent oil was obtained.

Yield (estimated by ^{31}P NMR): 63 % (345.5 mg, 0.84 mmol)

^{31}P NMR (162 MHz, $CDCl_3$) δ 11.90 (s), –13.90 (s).

Procedure to prepare Diphenyl(3-(phenylphosphino)propyl)phosphine

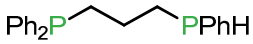

To a solution of naphthalene (327 mg, 1.95 mmol) in THF (10 ml) was added small cut sodium metal (60 mg, 2.5 mmol). The mixture was sonicated at room temperature, the change to a dark-green color indicated the formation of the naphthalene radical anion. After 30 min of stirring, the solution was filtered by cannula to remove the excess sodium metal. The resulting solution was added to a solution of a 1,3-bis(diphenylphosphino)propane (412.44 mg, 1 mmol) in THF (20 ml) at 0°C. The reaction mixture was then stirred at room temperature for 12 h, a dark red color developed gradually as the green color faded. The reaction mixture was cooled to -10 °C and saturated NH_4Cl solution (5 ml) was added dropwise. The stirring was continued for another 30 min. The reaction was filtered by a cannula filter and then THF was removed under reduced pressure. The resulting product was distilled first at 120°C/1 Torr to remove naphthalene and then redistilled with a Kugelrohr at 0.05 Torr to give the pure product, a transparent oil.

Yield (estimated by ^{31}P NMR): 70 % (235.45 mg , 0.7 mmol).

^{1}H NMR (400 MHz, Benzene-d6) δ 7.43 – 7.34 (m, 8H), 7.16 (m, 7H), 4.39 (dd, *J* = 7.6, 5.9 Hz, 2H), 3.87 (dd, *J* = 7.7, 5.9 Hz, 2H), 2.11 – 1.98 (m, 2H).

^{31}P{^{1}H} NMR (162 MHz, $CDCl_3$) δ – 14.26 (s), – 50.76 (s).

General procedure to prepare tetraphosphine boranes 58:

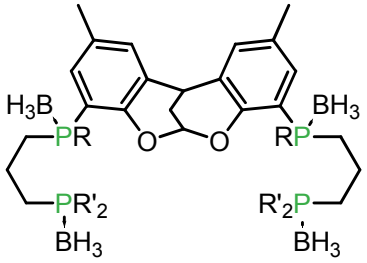

a: R = *t*-Bu, R' = Ph
b: R = *t*-Bu, R' = Cy
c: R = Cy, R' = Cy

Method A: 39 (1 g, 4.52 mmol) was dissolved in 120 mL degassed, dry THF and at 0 °C KO*t*-Bu (2.5 eq., 1.231 g, 11.5 mmol) was added. The reaction mixture was allowed to warm up and stirred 15 min at rt. The reaction was followed by ^{31}P–NMR (– 40.11 ppm, bm). The solution was added to the electrophile **46** (2.3 eq., 4.1 g, 12.19 mmol) dissolved in 20 mL degassed, dry THF at 0 °C. The reaction finished instantaneously. The reaction mixture was quenched with 5 mL degassed H_2O, subsequently washed with brine (30 mL), the product was extracted with DCM, dried over $MgSO_4$, filtered and the solvent removed *in vacuo*. The crude mixture consists of excess sidearm and tetraphosphine borane. The white crystalline powder was triturated in MeOH to remove excess of reactant **46**. A mixture of 95/5 *rac* to *meso* was obtained.

Method B: *Rac* 59 (0.16 g, 0.21 mmol) was dissolved in 40 mL dry THF, cooled down to – 78 °C and subsequently a cooled solution of lithiated $R_2PLi(BH_3)$ (2.2 eq., 0.47 mmol, R = Ph, Cy) was added. The reaction mixture was allowed to warm up to rt and stirred 30 min. The reaction was followed by ^{31}P–NMR, after completion, the reaction mixture was quenched with 5 mL degassed H_2O, washed with brine (20 mL), extracted with DCM (3x 20), dried over $MgSO_4$, filtered and the solvent removed *in vacuo*. The crude product was purified by column chromatography (9/1, PE/EtOAc) to remove excess $R_2PH(BH_3)$. A white crystalline powder of pure ***rac* 58** was obtained.

Method C: *Rac* 38c (0.2 g, 0.45 mmol) was dissolved in 60 mL dry THF, cooled down to 0 °C and KO*t*-Bu (2.1 eq., 0.1 g, 0.91 mmol) was added. The reaction mixture was allowed to warm up and stirred 15 min at rt. The reaction was followed by ^{31}P–NMR (– 37.13 ppm, bm). In another Schlenk 1,3-propanediol cyclic sulfate (2.1 eq., 0.13 g, 0.91 mmol) was dissolved in 10 mL dry THF and cooled down to 0 °C, to which the metallated ***rac* 38c** was added (**61**, + 35.34 ppm, bm). Subsequently compound **61** was reacted with R_2PLi (2.1 eq., 0.19 g, 0.91 mmol, R

= Ph, Cy) at – 78 °C, the reaction mixture was allowed to war up to rt and stirred 30 min to give a white crystalline powder. The crude product was purified by column chromatography (9/1, PE/EtOAc) to remove excess R_2PH. A mixture of 95/5 *rac* to *meso* was obtained.

58a: Yield: 5.54 g (96%, 4.38 mmol).

^{1}H NMR (300 MHz, Chloroform-d) δ 7.42 (t, *J* = 7.8 Hz, 8H), 7.05 – 6.77 (m, 16H), 6.17 (q, *J* = 6.7 Hz, 1H), 4.90 (q, *J* = 6.7 Hz, 1H), 4.20 (t, *J* = 6.0 Hz, 4H), 2.57 (m, 4H), 2.10 (s, 6H), 1.94 (m, 3H), 1.99 (m, 4H), 1.07 (m, 18H).

^{31}P NMR (121 MHz, $CDCl_3$) δ 37.75 (br m), 26.79 (br m).

Ms(FAB): *m/z* calcd = 942.54 $[M+Li]^+$; found: 943.56

58b: Yield: 5.64 g (97%, 4.38 mmol).

^{1}H NMR (300 MHz, Chloroform-d) δ 7.49 (t, *J* = 13.1 Hz, 2H), 7.20 – 7.12 (m, 2H), 6.19 (m, 1H), 3.91 (m, 1H), 3.65 (t, *J* = 6.5 Hz, 4H), 2.52 (t, *J* = 6.5 Hz, 4H), 1.99 (m, 8H), 1.91 – 0.99 (m, 66H).

^{31}P NMR (121 MHz, $CDCl_3$) δ 31.53 (br m), 30.30 (br m), 20.84 (br m).

58c: Yield: 4.26 g (93 %, 4.2 mmol), a diastereomeric mixture of **51**.

^{1}H NMR (300 MHz, Chloroform-d) δ 7.63 – 7.36 (m, 2H), 7.16 (m, 2H), 6.32 (m, 1H), 4.24 (t, *J* = 5.9 Hz, 4H), 3.94 (m, 1H), 2.24 (m, 8H), 2.12 – 1.47 (m, 8H), 1.43 – 0.99 (m, 74H).

^{13}C NMR (75 MHz, $CDCl_3$) δ 150.35, 136.41, 132.07, 131.56, 127.11, 126.11, 92.57, 70.38, 37.62, 34.10, 31.85, 27.01, 26.02, 25.68, 24.22, 20.46.

^{31}P NMR (121 MHz, $CDCl_3$) δ 24.60 (br m), 23.41(br m).

Ms(FAB): *m/z* calcd = 1026.77 $[M+2Li]^+$; found: 1027.62

Procedure to remove the borane group and form the tetraphosphine 63:

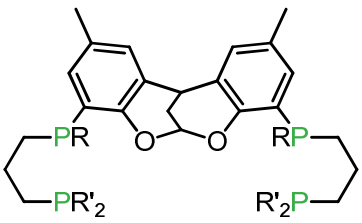

a: R = *t*-Bu, R' = Ph
b: R = *t*-Bu, R' = Cy
c: R = Cy, R' = Cy

58 (142.5 mg, 0.15 mmol) was dissolved in 5 mL dry, degassed DCM and cooled down to 0 °C, subsequently HBF_4•Et_2O (0.4 mL, 2.37 mmol) was added. The reaction mixrture was allowed to warm up to rt and stirred 30 min. The reaction was followed by ^{31}P–NMR. After completion the reaction was cooled to 0 °C and quenched with 10 mL degassed $NaHCO_3$ (aq.) and stirred 10 min. The organic phase was transferred by cannula to another Schlenk and the solvent was removed to give a white crystalline powder.

63a: Yield: 0.17 mg (94 %, 0.14 mmol).
^{31}P NMR (121 MHz, CD_2Cl_2, before quench); δ 9.13 (br s), 8.82 (br s), 7.04 (br s), 6.64 (br s), (after quench) δ – 18.17 (s), – 19.23 (s), – 19.34 (s).

63b: Yield: 0.178 g (96 %, 0.14 mmol)

^{1}H NMR (300 MHz, CD_2Cl_2) δ 7.08 – 6.91 (m, 4H), 6.19 (m, 1H), 3.89 (q, *J* = 2.8 Hz, 1H), 3.70 – 3.60 (m, 4H), 2.52 (m, 4H), 2.35 – 2.03 (m, 8H), 1.92 – 0.79 (m, 66H).

^{31}P NMR (121 MHz, CD_2Cl_2, before quench); δ 21.33 (br s), 20.92 (br s), (after quench) δ – 3.93 (s), – 16.4 (s), – 19.74 (s).

63c: Yield: 134 mg (94 %, 0.14 mmol)
^{1}H NMR (300 MHz, Chloroform-d) δ 7.63 – 7.36 (m, 2H), 7.16 (m, 2H), 6.32 (m, 1H), 4.24 (t, *J* = 5.9 Hz, 4H), 3.94 (m, 1H), 2.24 (m, 8H), 2.12 – 1.47 (m, 8H), 1.43 – 0.99 (m, 74H).

^{31}P NMR (121 MHz, CD_2Cl_2) δ – 4.48 (s), – 4.58 (s), – 4.85 (s), – 4.91 (s).

6.6 Coordination Chemistry

In the following part the synthesized coordination compounds will be described.

Procedure to prepare precursor η^2,η^2-(cycloocta-1,5diene)(chloro)methyl-palladium(II) [PdClMe(COD)][328]**:**

[$PdCl_2$(COD)] (0.504 g, 1.764 mmol) was dissolved in 50 mL dry DCM and $SnMe_4$ was added dropwise. After 36 h a grey solid precipitated from the yellow solution. The reaction mixture was filtered over celite and the solvent removed *in vacuo*. The greyish powder was washed 3x with 10 mL Et_2O. An off-white powder was obtained.

Yield: 0.2697 g (60 %, 1.06 mmol).

^{1}H NMR (400 MHz , CD_2Cl_2) δ 1.13 (s, 3H, CH_3), 2.50 (m, 8H, 4x CH_2), 5.14 (m, 2H, =CH *cis* to CH_3), 5.87 (m, 2H, =CH *trans* to CH_3).

Procedure to prepare complex 72:

DBDOCphos (10 mg, 16 μmol) and ([$PdMe_2$(COD)] (1.2 eq., 13 μmol) precursor were dissolved in 4 mL $CDCl_3$, dried over 4 Å molecular sieves, in a NMR tube and stirred 30 min at rt. The solution turned orange instantaneously, but no crystals were obtained.

Yield (estimated by ^{31}P NMR): 72.1 % (27.07 mg, 16 μmol).

^{31}P NMR (202 MHz, $CDCl_3$) δ 27.96 (AB, $^{2}J_{P-P}$ = 441.7 Hz), 25.78 (AB, $^{2}J_{P-P}$ = 441.7 Hz), 22.71 (AB, $^{2}J_{P-P}$ = 441.7 Hz), 20.53(AB, $^{2}J_{P-P}$ = 441.7 Hz).

Procedure to prepare complex 73:

DBDOCphos (10 mg, 16 μmol) and a Pd(II) (1/1.5/2 eq., 16/24/32 μmol) precursor ([$PdCl_2$(COD)], [$PdCl_2$ (PPh_3)$_2$], [$PdCl_2$(PhCN)$_2$]) were dissolved in 4 mL $CDCl_3$, dried over 4 Å molecular sieves, in a NMR tube and stirred 30 min at rt. The solution turned orange instantaneously and, orange needles were obtained by evaporation at rt.

Yield: 25.5 mg (100 %, 16 μmol).

^{31}P NMR (162 MHz, $CDCl_3$) δ 26.0.

Procedure to prepare complex :

DBDOCphos (10 mg, 16 μmol) and [$PtMe_2$(COD)] (5.33 mg, 16 μmol) were dissolved in 0.4 mL $CDCl_3$, dried over 4 Å molecular sieves, in a NMR tube. The solution was transparent. A *cis* configuration was obtained.

Yield (estimated by ^{31}P NMR): Not determined.

^{31}P NMR (162 MHz, $CDCl_3$) δ 26.0 ($^{2}J_{P-P}$ = 10.7 Hz, $^{1}J_{Pt-P}$ = 1933.59 Hz), 18.0 ($^{2}J_{P-P}$ = 10.73 Hz, $^{1}J_{Pt-P}$ = 1989.76 Hz).

Procedure to prepare complex 75b:

***Rac* 63b** (0.25 g, 0.28 mmol) and a Pd(II) (2 eq., 0.12 g, 0.56 mmol) [$PdCl_2$(COD)] were dissolved in 4.5 mL degassed, dry CD_2Cl_2 and stirred 30 min at rt. The solution turned orange.

Yield (estimated by ^{31}P NMR): 100 % conversion of ^{31}P resonances.

^{31}P NMR (121 MHz, unlocked) δ 40.73 (s), 40.58 (s), 29.87 (s), 29.26 (s).

Procedure to prepare complex 82b:

***Rac* 65b** (0.25 g, 0.28 mmol) and [$PtCl_2$(COD)] (2 eq., 0.17 mg, 0.56 mmol) were dissolved in 4.5 mL degassed, dry CD_2Cl_2 and stirred 30 min at rt. The solution was transparent. A *cis* configuration was obtained.

Yield (estimated by ^{31}P NMR): 100 % conversion of ^{31}P resonances.

^{31}P NMR (121 MHz, unlocked) δ 24.3 ($^2J_{P-P}$ = 17.64 Hz, $^1J_{Pt-P}$ = 3684.39 Hz), 23.8 ($^2J_{P-P}$ = 18.08 Hz, $^1J_{Pt-P}$ = 3702.01 Hz), 17.75 ($^2J_{P-P}$ = 18.3 Hz, $^1J_{Pt-P}$ = 3431.97 Hz), 17.6 ($^2J_{P-P}$ = 18.1 Hz, $^1J_{Pt-P}$ = 3425.2 Hz).

6.7 Batch Autoclave Procedure

All procedures were carried out in an autoclave 25 mL Hastelloy C®. The Amtec® robotic system was used by employing home-made Teflon® inlets. They contain a cylinder closed by a conic screw coupled with a digital or analogue pressure device. All catalytic hydroformylation reactions were performed in autoclaves that have a total volume of 10 mL using a glass inlet and a magnetic stirrer. In Tarragona 25 mL scale reactions were performed directly inside the autoclave, in Saint Andrews small scale reactions required home-made vial inlets to perform multiple experiments at once, the vials were equipped with needles to pressurize the vials.

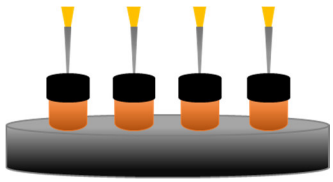

Figure 65: Vial inlet employed in St. Andrews to perform multiple small scale reactions in parallel in a hastelloy C®.

6.7.1 Palladium

Procedure A in Hastelloy C®: The autoclave was evacuated and then allowed to cool down under argon three times. In an argon glovebox or a Schlenk line, the catalyst components, 28 µmol (6.3 mg) $Pd(OAc)_2$, 83 µmol (52 mg) ligand and acid (0.111 mmol) were dissolved in 2.5 mL solvent and stirred 30 min. The solution was transferred to the autoclave prefilled with 0.3 mL solvent and 2.3 mL 1-octene. The transfer was carried out while a continuous stream of argon flowed through the autoclave. The autoclave was then pressurized to 15 bars with syngas ($CO:H_2$, 1:1) and heated to 125 °C. When the temperature stabilized the autoclave was pressurized to a final pressure of 60 bar. After a reaction time of 5 h the autoclave was allowed to cool, depressurized and opened. Selectivity data was obtained by GC.

Procedure B in Amtec®: The autoclaves were evacuated and then allowed to cool down under argon three times. In an argon glovebox or a Schlenk line, the catalyst components, 28 µmol (6.3 mg) $Pd(OAc)_2$, 83 µmol (52 mg) ligand and acid (0.111 mmol) were dissolved in 2.5 mL solvent and stirred 30 min. The solution was transferred to the autoclaves of the Amtec® prefilled with 0.3 mL solvent and 2.3 mL 1-octene. The transfer was carried out while a continuous stream of argon flowed through the autoclaves. The autoclaves were then pressurized to 15 bars with syngas ($CO:H_2$, 1:1) and heated to 125 °C. When the temperature stabilized the autoclave was pressurized to a final pressure of 60 bar. After a reaction time of 5 h the autoclave was allowed to cool, depressurized and opened. Selectivity data was obtained by GC.

Procedure C using glass vial inlet for Hastelloy C®: The autoclaves were evacuated and then allowed to cool down under argon three times. In an argon glovebox the catalyst components, 54 µmol $Pd(OAc)_2$, 28 µmol (52 mg) ligand and acid (0.8 mol%) were dissolved in 0.8 mL solvent and stirred 30 min. To the formed catalyst solution was added under a continuous flow of argon 0.4 mL 1-octene. The inlet with the reaction mixtures was subsequently put in the autoclave and then pressurized to 60 bars with syngas ($CO:H_2$, 1:1) and heated to 125 °C. After a reaction time of 5 h the autoclave was allowed to cool, depressurized and opened. Selectivity data was obtained by GC. Stocksolution: 52.86 mg ligand in 10 mL DCM.

6.7.2 Rhodium as catalyst

Generally the procedure given in C was used except that in the case of rhodium the catalyst system (25.8 mg Rh(acac)CO_2 in 10 mL toluene, 52.86 mg ligand in 10 mL DCM) and the substrate were heated to 80 °C and pressurized to 20 bar with syngas (CO:H_2, 1:1).

Appendix I: Crystallographic Data

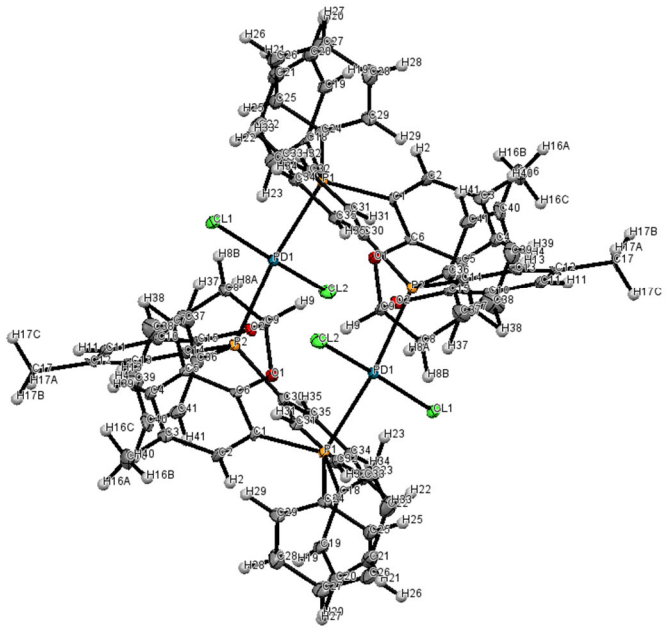

Identification code	**73**	
Empirical formula	C86 H72 Cl16 O4 P4 Pd2	
Formula weight	2073.31	
Temperature	100(2) K	
Wavelength	0.71073 Å	
Crystal system	Monoclinic	
Space group	P2(1)/c	
Unit cell dimensions	a = 12.8463(8)Å	α = 90°.
	b = 19.6193(12)Å	β =106.5207(14)°.
	c = 18.0803(11)Å	γ = 90°.
Volume	4368.8(5) $Å^3$	
Z	2	
Density (calculated)	1.576 g/cm^3	
Absorption coefficient	1.024 mm^{-1}	
F(000)	2088	
Crystal size	0.15 x 0.08 x 0.05 mm	
Theta range for data collection	1.57 to 34.87°.	

Index ranges	-19<=h<=20,-31<=k<=31,-25<=l<=28
Reflections collected	84362
Independent reflections	18147[R(int) = 0.0313]
Completeness to theta =34.868°	95.3%
Absorption correction	Empirical
Max. and min. transmission	0.951 and 0.885
Refinement method	Full-matrix least-squares on F^2
Data / restraints / parameters	18147/ 168/ 579
Goodness-of-fit on F^2	1.059
Final R indices [I>2sigma(I)]	R1 = 0.0310, wR2 = 0.0703
R indices (all data)	R1 = 0.0433, wR2 = 0.0796
Largest diff. peak and hole	1.016 and -1.361 e.$Å^{-3}$

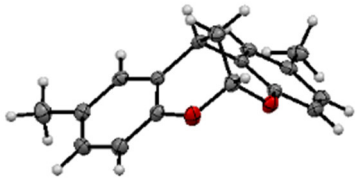

Compound	**DBDOC-H_2**
Molecular formula	'C_{17} H_{16} O_2'
Molecular weight	252.30
Crystal habit	colorless needle
Crystal dimensions(mm)	0.36 x0.14 x 0.12
Crystal system	orthorhombic
Space group	P n a 2_1
a (Å)	15.8494(10)
b (Å)	12.9442(9)
c (Å)	6.0638(4)
V ($Å^3$)	1244.04(14)
Z	4
d ($g\text{-}cm^{-3}$)	1.347
F (000)	536
μ (cm^{-1})	0.087
Absorption corrections	Kappa APEX II

Diffractometer	MoKa
X-ray source	MoKα
λ (Å)	graphite
Monochromator	150.0(1)
T (K)	phi and omega scans
Scan mode	29.445
Maximum θ	-21,18 ; -17,17 ; -8,8
h, k, l ranges	10325
Reflections measured	3337
Unique data	0.0624
Rint	2877
Reflections used	I > 2(I)
Criterion	I > 2σI)
Refinement type	constr
Hydrogen atoms	175
Parameters refined	16
Reflections / parameter	0.1317
wR2	0.0510
R1	-0.1(19)
Flack's parameter	0.0716 ; 0.0687
Weights a, b	1.054
GoF	0.358(0.058) / -0.239(0.058)
difference peak / hole (e $Å^{-3}$)	

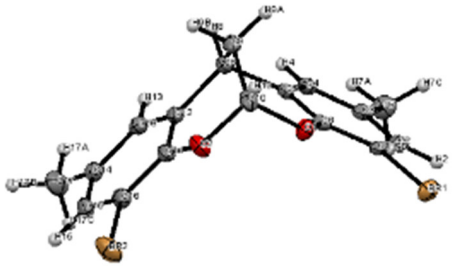

Compound **34**

Molecular formula	'C_{17} H_{14} Br_2 O_2'
Molecular weight	410.10
Crystal habit	colorless plate
Crystal dimensions(mm)	0.20 x 0.16 x0.04
Crystal system	orthorhombic
Space group	P b c a

a (Å)	13.2787(6)
b (Å)	9.0378(4)
c (Å)	25.1283(12)
V ($Å^3$)	3015.7(2)
Z	8
d ($g\text{-}cm^{-3}$)	1.807
F (000)	1616
μ (cm^{-1})	5.377
Absorption corrections	multi-scan;
Diffractometer	Kappa APEX II
X-ray source	MoKα
λ (Å)	0.71069
Monochromator	graphite
T (K)	150.0(1)
Scan mode	phi and omega scans
Maximum θ	30.188
h, k, l ranges	-18, 18; -12,11; -35,34
Reflections measured	25368
Unique data	4469
Rint	0.0622
Reflections used	3374
Criterion	I > 2σI)
Refinement type	Fsqd
Hydrogen atoms	constr
Parameters refined	192
Reflections / parameter	17
wR2	0.0930
R1	0.0335
Weights a, b	0.0457 ; 1.0140
GoF	1.029
difference peak / hole (e $Å^{-3}$)	0.772(0.105) / -0.943(0.105)

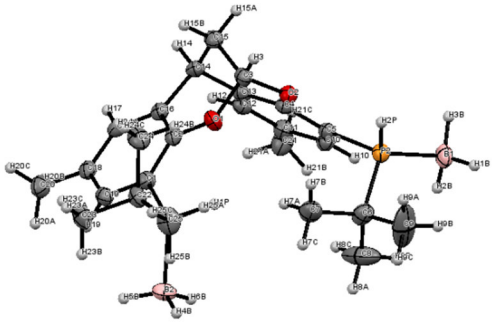

Compound	***rac* 38c**
Molecular formula	$C_{25}H_{40}B_2O_2P_2$
Molecular weight	456.13
Crystal habit	colorless block
Crystal dimensions(mm)	0.24 x 0.10 x 0.08
Crystal system	orthorhombic
Space group	P b c a
a (Å)	16.4344(3)
b (Å)	12.1938(3)
c (Å)	26.2750(7)
V (Å^3)	5265.5(2)
Z	8
d (g-cm^{-3})	1.151
F (000)	1968
μ (cm^{-1})	0.184
Absorption corrections	multi-scan; 0.792154 min, 1.19363 max
Diffractometer	Kappa APEX II
X-ray source	MoKα
λ (Å)	0.71069
Monochromator	graphite
T (K)	150.0(1)
Scan mode	phi and omega scans
Maximum θ	25.348
h, k, l ranges	-16,19; -14,14; -31,31
Reflections measured	28125
Unique data	4794
Rint	0.0940
Reflections used	3704
Criterion	I > 2σI)
Refinement type	Fsqd
Hydrogen atoms	mixed
Parameters refined	320

Reflections / parameter	11
wR2	0.1534
R1	0.0679
Weights a, b	0.0425 ; 11.389
GoF	1.078
difference peak / hole (e Å^{-3})	0.364(0.066) / -0.286(0.066)

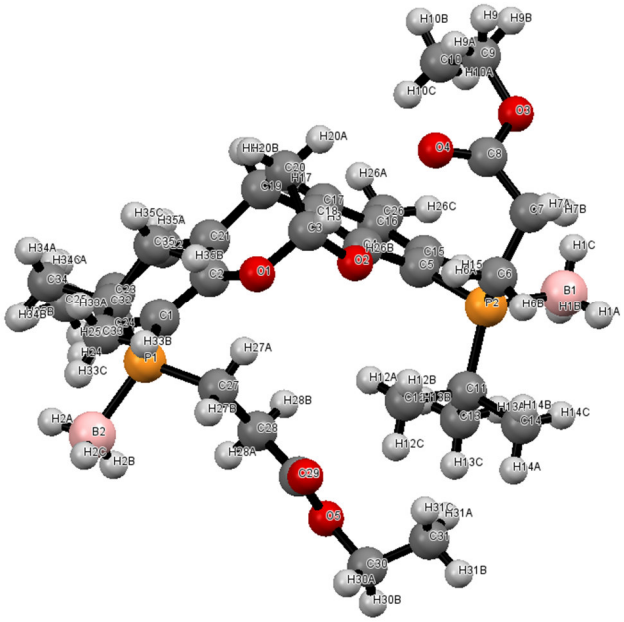

Compound	***rac* 40**
Molecular formula	'C_{35} H_{56} B_2 O_6 P_2'
Molecular weight	656.35
Crystal habit	colorless block
Crystal dimensions(mm)	0.30 x 0.22 x 0.20
Crystal system	monoclinic
Space group	P 2_1/n
a (Å)	8.5101(3)
b (Å)	24.6215(9)
c (Å)	17.6443(7)
α (°)	90
β (°)	93.439(2)
γ (°)	90
V(Å^3)	3690.4(2)
Z	4
d (g-cm^{-3})	1.181
F (000)	1416
μ (cm^{-1})	0.159

Absorption corrections	multi-scan;
Diffractometer	Kappa APEX II
X-ray source	MoKα
λ (Å)	0.71069
Monochromator	graphite
T (K)	150.0(1)
Scan mode	phi and omega scans
Maximum θ	25.680
h, k, l ranges	-9,10; -29,29; -21,21
Reflections measured	47413
Unique data	6880
Rint	0.0393
Reflections used	6087
Criterion	I > 2σI)
Refinement type	Fsqd
Hydrogen atoms	mixed
Parameters refined	461
Reflections / parameter	13
wR2	0.1824
R1	0.0648
Weights a, b	0.0846; 5.9769
GoF	1.090
difference peak / hole (e Å^{-3})	0.781(0.069) / -0.404(0.069)

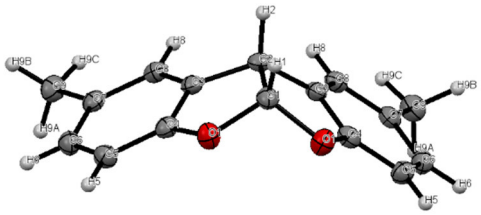

Compound	**BFBF-H$_2$**
Molecular formula	'C$_{16}$ H$_{14}$ O$_2$'
Molecular weight	238.27
Crystal habit	colorless block
Crystal dimensions (mm)	0.18 x 0.18 x 0.02
Crystal system	orthorhombic
Space group	P m n 2$_1$
A (Å)	20.5669(12)
b(Å)	5.7117(3)

c (Å)	4.8987(2)
V(Å^3)	575.46(5)
Z	2
d (g-cm^{-3})	1.375
F (000)	252
μ (cm^{-1})	0.090
Absorption corrections	multi-scan;
Diffractometer	Kappa APEX II
X-ray source	MoKα
λ (Å)	0.71069
Monochromator	graphite
T (K)	150.0(1)
Scan mode	phi and omega scans
Maximum θ	30.216
h, k, l ranges	-25,29; -7,8; -6,6
Reflections measured	14373
Unique data	1598
Rint	0.0789
Reflections used	1230
Criterion	I > 2σI)
Refinement type	Fsqd
Hydrogen atoms	constr
Parameters refined	87
Reflections / parameter	14
wR2	0.1136
R1	0.0480
Weights a, b	0.0579 ; 0.0723
GoF	1.045
difference peak / hole (e Å^{-3})	0.191(0.053) / -0.241(0.053)

Appendix II : Abstract

La réalisation de réaction chimiques de façon éco-compatible nécessite la synthèse de catalyseurs plus performants et plus modulables. Les systèmes catalytiques bimétalliques peuvent dans certains cas permettre la coopération entre deux centres métalliques afin d'en tirer parti pour activer les substrats. Le travail de thèse présenté dans ce manuscrit concerne la conception, la synthèse et la caractérisation de nouveaux ligands tétraphosphine aptes à réaliser une telle catalyse bimétallique. Bien que ces ligands puissent en principe être utilisés pour une large gamme de procédés, l'objectif principal de cette étude a concerné leur potentiel dans la réaction d'hydroformylation catalysée au palladium. En effet, l'hydroformylation fait partie des procédés de catalyse homogène les plus utilisés dans l'industrie, fournissant de nombreuses matières premières pour de multiples applications.

Quelques ligands bis(phosphorés) ont déjà été synthétisés à partir des squelettes méthanodibenzodioxocine et benzofurobenzofuranne, et ont déjà démontré leur intérêt pour la construction d'édifices bimétalliques dans lesquels chaque métal est coordiné à un seul atome de phosphore. Cependant, avec ces ligands, de multiples espèces bimétalliques sont en équilibre en solution, rendant difficile la détermination des structures formées dont la réactivité est difficile à contrôler. La synthèse des ligands tétraphosphines dans lesquels chaque métal sera coordiné par un bras phosphine chélatant devrait conduire à une coordination plus forte et mieux maitrisée, facilitant par la suite le contrôle de la réactivité de ces édifices.

Le défi synthétique tient à la stéréochimie de ces ligands tétraphosphine, qui peuvent exister sous 3 formes (2 *meso*- et une *rac-)*. Leur séparation s'est avérée très délicate nous conduisant à préférer une stratégie de synthèse diastérosélective. Différentes approches synthétiques ont été élaborées, les meilleurs résultats ont été obtenus en protégeant les phosphines par chélation au bore, pour faciliter les synthèses. La meilleure voie de synthèse passe par la préparation diastéreosélective des 4,8-bis(*sec*-phosphines) à partir du motif 6,12-methano-12H-dibenzo[l,3]dioxocines, conduisant majoritairement à la forme racémique. Un schéma réactionnel pouvant expliquer cette préférence a été proposé. La fonctionnalisation de ces phosphines (bis)-secondaires en dérivés di(R)phosphinopropyle à partir des éléctrophiles dérivés de propionates, $H_3BR_2P(CH_2)_3OMs$ (R= Ph, Cy), conduit à une inversion partielle de configuration, compliquant encore les étapes de séparation. C'est pourquoi une stratégie alternative a été mise au point. Elle utilise une réaction de Michael avec l'acrylate d'éthyle qui se fait avec une totale rétention de la configuration. Les étapes suivantes (réduction, mésylation et phosphination) n'affectant pas les stéréocentres, la préparation des *rac*-tétraphosphines a pu être réalisée de façon diastéréosélective.

Les premières études en coordination au $PdCl_2$ et $PtCl_2$ montrent une coordination forte des deux centres métalliques par le ligand tétraphosphine, rigide, permettant la formation de deux unités *cis*-M(II)P-P.

Enfin les premières études catalytiques ont été menées pour la réaction d'hydroformylation en présence de complexes de palladium(II) à ligand *rac*-tétraphosphine. Les réactions conduites *in situ* mettent en évidence une isomérisation facile mais une étape de carbonylation plus difficile. Cependant, l'isomérisation démontre que l'espèce active se forme ce qui est très prometteur en vue de futures études d'optimisation. C'est de plus particulièrement intéressant puisque les mélanges utilisés dans l'industrie sont riches en oléfines internes, qui peuvent donc subir une réaction isomérisation-hydroformylation pour former les produits désirés. En revanche, la nature de la sphère de coordination du palladium au sein de l'espèce active reste à étudier afin de déterminer s'il y a bien coopération entre les deux centres métalliques.

References

1. van Leeuwen, P. W. N. M. *Homogeneous Catalysis: Understanding the Art*. (Springer Berlin Heidelberg, 2004).
2. van Leeuwen, P. W. N. M. & Kamer, P. C. J. *Phosphorus(III) Ligands in Homogeneous Catalysis Design and Synthesis*. (John Wiley & Sons, Inc., 2012).
3. Strohmeier, W. & Müller, F. J. Klassifizierung phosphorhaltiger Liganden in Metallcarbonyl□Derivaten nach der π□Acceptorstärke. *Chem. Ber.* **100,** 2812–2821 (1967).
4. Van der Slot, S. C., Duran, J., Luten, J., Kamer, P. C. J. & Van Leeuwen, P. W. N. M. Rhodium-catalyzed hydroformylation and deuterioformylation with pyrrolyl-based phosphorus amidite ligands: Influence of electronic ligand properties. *Organometallics* **21,** 3873–3883 (2002).
5. Tolman, C. A. Electron donor-acceptor properties of phosphorus ligands. Substituent additivity. *J. Am. Chem. Soc.* **92,** 2953–2956 (1970).
6. Orpen, A. G. & Connelly, N. G. Structural Evidence for the Participation of P-X σ* Orbitals in MetaI-PX3 Bonding. *J. Chem. Soc., Chem. Commun* 1310–1311 (1985).
7. Marynick, D. S. π-Accepting abilities of phosphines in transition-metal complexes. *J. Am. Chem. Soc.* **106,** 4064–4065 (1984).
8. Van Leeuwen, P. W. N. M. Alcoholysis of acylpalladium(II) complexes relevant to the alternating copolymerization of ethene and carbon monoxide and the alkoxycarbonylation of alkenes: The importance of cis-coordinating phosphines. *J. Am. Chem. Soc.* **125,** 5523–5539 (2003).
9. Petitjean, M. Analytical algorithms for ligand cone angles calculations. Application to triphenylphosphine palladium complexes. *Comptes Rendus Chim.* (2015).
10. Schulz, A. On the steric hindrance of bulky substituents - determination of their cone angles. *Zeitschrift fur Anorg. und Allg. Chemie* **1970,** 2183–2192 (2014).
11. Bilbrey, J. A., Kazez, A. H., Locklin, J. & Allen, W. D. Exact ligand cone angles. *J. Comput. Chem.* **34,** 1189–1197 (2013).
12. White, D., Taverner, B. C., Coville, N. J. & Wade, P. W. Solid angles III. The role of conformers in solid angle calculations. *J. Organomet. Chem.* **495,** 41–51 (1995).
13. White, D., Tavener, B. C., Leach, P. G. L. & Neil, N. J. Solid angles I. The radial profile. *J. Organomet. Chem.* **478,** 205–211 (1994).
14. Bilbrey, J. A., Kazez, A. H., Locklin, J. & Allen, W. D. Exact Ligand Solid Angles. *J. Chem. Theory Comput.* **9,** 5734–5744 (2013).
15. Brown, T. L. & Lee, K. J. Ligand steric properties. *Coord. Chem. Rev.* **128,** 89–116 (1993).
16. Brown, T. L. A molecular mechanics model of ligand effects. 3. A new measure of ligand steric effects. *Inorg. Chem.* **31,** 1286 (1992).
17. Burello, E. & Rothenberg, G. Topological mapping of bidentate ligands: a fast approach for screening homogeneous catalysts. *Adv Synth Catal* **347,** (2005).

18. Fey, N. Stable fluorophosphines: Predicted and realized ligands for catalysis. *Angew. Chemie - Int. Ed.* **51,** 118–122 (2012).

19. Flener Lovitt, C., Frenking, G. & Girolami, G. S. Donor–Acceptor Properties of Bidentate Phosphines. DFT Study of Nickel Carbonyls and Molecular Dihydrogen Complexes. *Organometallics* **31,** 4122–4132 (2012).

20. Dierkes, P., van Leeuwen, P. W. N. M. & Leeuwen, P. W. N. M. Van. The bite angle makes the difference: a practical ligand parameter for diphosphine ligands. *J. Chem. Soc. Dalt. Trans.* 1519–1530 (1999).

21. Van Leeuwen, P. W. N. M., Kamer, P. C. J., Reek, J. N. H. & Dierkes, P. Ligand bite angle effects in metal-catalyzed C-C bond formation. *Chem. Rev.* **100,** 2741–2769 (2000).

22. Casey, C. P. & Whiteker, G. T. The Natural Bite Angle of Chelating Diphosphines. *Isr. J. Chem.* **30,** 299–304 (1990).

23. Koide, Y., Bott, S. G. & Barron, A. R. Alumoxanes as cocatalysts in the palladium-catalyzed copolymerization of carbon monoxide and ethylene: genesis of a structure-activity relationship. *Organometallics* **15,** 2213–2226 (1996).

24. Freixa, Z. & van Leeuwen, P. W. N. M. Bite angle effects in diphosphine metal catalysts: steric or electronic? *Dalt. Trans.* **77,** 1890 (2003).

25. Van der Vlugt, J. I. Cooperative catalysis with first-row late transition metals. *Eur. J. Inorg. Chem.* 363–375 (2012).

26. Maverick, A. W. *Catalysis by Di- and Polynuclear Metal Cluster Complexes*. (Wiley-VCH Verlag GmbH & Co. KGaA, 1998).

27. Van Den Beuken, E. K. & Feringa, B. L. Bimetallic catalysis by late transition metal complexes. *Tetrahedron* **54,** 12985–13011 (1998).

28. McCollum, D. G. & Bosnich, B. Cooperative bimetallic reactivity. *Inorganica Chim. Acta* **270,** 13–19 (1998).

29. Kember, M. R., Buchard, A. & Williams, C. K. Catalysts for CO_2/epoxide copolymerisation. *Chem. Commun. (Camb).* **47,** 141–163 (2011).

30. Cheng, M., Lobkovsky, E. B., Coates, G. W., V, C. U. & York, N. Catalytic Reactions Involving C1 Feedstocks : New High-Activity Zn(II)-Based Catalysts for the Alternating Copolymerization of Carbon Dioxide and Epoxides. *J. Am. Chem. Soc.* **120,** 11018–11019 (1998).

31. Finn, M. G. & Sharpless, K. B. Mechanism of Asymmetric Epoxidation. 2. Catalyst Structure. *J. Am. Chem. Soc.* **113,** 113–126 (1991).

32. Bhadra, S., Akakura, M. & Yamamoto, H. Design of a New Bimetallic Catalyst for Asymmetric Epoxidation and Sulfoxidation. *J. Am. Chem. Soc.* **137,** 15612–15615 (2015).

33. Jacobsen, E. N. Asymmetric catalysis of epoxide ring-opening reactions. *Acc. Chem. Res.* **33,** 421–431 (2000).

34. López-Valbuena, J. M. & Eduardo C. Escudero-Adan, Jordi Benet-Buchholz, Z. F. and P. W. N. M. van L. An approach to bimetallic catalysts by ligand design. *Dalton Trans.* **39,** 8363–76 (2010).

35. Gillespie, J. A., Zuidema, E., van Leeuwen, P. W. N. M. & Kamer, P. C. J. in *Phosphorus(III) Ligands in Homogeneous Catalysis: Design and Synthesis* (2012).

36. Gillespie, J. a, Dodds, D. L. & Kamer, P. C. J. Rational design of diphosphorus ligands-a route to superior catalysts. *Dalton Trans.* **39,** 2751–2764 (2010).

37. Castiglioni, M. Homogeneous hydrogenation of alkynes and of 1,4-cyclohexadiene in the presence of the clusters $Ru_3(CO)_7(\mu\text{-}PPh_2)_2(C_6H_4)$, $Ru_4(CO)_{11}(\mu^4\text{-}PPh)(C_6H_4)$, $Ru_3(CO)_7(\mu\text{-}PPh_2)_2(HC_2Ph)$ and $Ru_4(CO)_{11}(\mu^4\text{-}PPh)(C_2Ph_2)$. *J. Organomet. Chem.* **571,** 251–260 (1998).

38. Munetaka, A. Specific C–C coupling of the labile diruthenium bridging methylene complex, $Cp_2Ru_2(\mu\text{-}CH_2)(CO)_2(MeCN)$, with diazoalkanes ($R_2C{=}N_2$) leading to alkenyl complexes, $Cp_2Ru_2(\mu\text{-}CH{=}CR_2)(\mu\text{-}H)(CO)_2$, and alkenes, $CH_2{=}CR_2$. *J. Organomet. Chem.* **569,** 71–83 (1998).

39. Tanabe, Y. & Nishibayashi, Y. Catalytic Dinitrogen Fixation to Form Ammonia at Ambient Reaction Conditions Using Transition Metal-Dinitrogen Complexes. *Chem. Rec.* 1549–1577 (2016).

40. Keijsper, J. Ruthenium carbonyl 1,4-diaza-1,3-butadiene (R-DAB) complexes. Reactivity of $Ru_2(CO)_5$(R-DAB) toward molecular hydrogen. Molecular structure of $H_2Ru_4(CO)_8$(R-DAB)$_2$, containing an unique linear chain of four ruthenium atoms. *Organometallics* **4,** 2006–2012 (1985).

41. Yuki, M., Miyake, Y., Nishibayashi, Y., Wakiji, I. & Hidai, M. Synthesis and Reactivity of Tungsten - and Molybdenum - Dinitrogen Complexes Bearing Ferrocenyldiphosphines toward Protonolysis. *Organometallics* **27,** 3947–3953 (2008).

42. Hidai, M. Chemical nitrogen fixation by molybdenum and tungsten complexes. *Coord. Chem. Rev.* **185–186,** 99–108 (1999).

43. Hidai, M. & Mizobe, Y. in *Encyclopedia of Catalysis* (John Wiley & Sons, Inc., 2002).

44. Guochen, J., Morris, R. H. & Schweitzer, C. T. An acidic η^2-dihydrogen complex protonating coordinated dinitrogen. *Inorg. Chem.* **30,** 593–594 (1991).

45. Steinhagen, H. & Helmchen, G. Asymmetric Two-Center Catalysis - Learning from Nature. *Angew. Chemie Int. Ed. English* **35,** 2339–2342 (1996).

46. van, K. G. Asymmetric catalysis with chiral organocopper-copper arenethiolates. *Pure Appl. Chem.* **66,** 1455–1462 (1994).

47. Wilcox, D. E. Binuclear metallohydrolases. *Chem. Rev.* **96,** 2435–2458 (1996).

48. Ishii, Y. & Hidai, M. Carbonylation reactions catalyzed by homogeneous Pd–Co bimetallic systems. *Catal. Today* **66,** 53–61 (2001).

49. Noyori, R. & Kitamura, M. Enantioselective Addition of Organometallic Reagents to Carbonyl Compounds: Chirality Transfer, Multiplication, and Amplification. *Angew Chem Int Ed.* **30,** 49–69 (1991).

50. Raynal, M., Ballester, P., Vidal-Ferran, A. & van Leeuwen, P. W. N. M. Supramolecular catalysis. Part 1: non-covalent interactions as a tool for building and modifying homogeneous catalysts. *Chem. Soc. Rev.* **43,** 1660–1733 (2014).

51. Levin, M. D. Scope and Mechanism of Cooperativity at the Intersection of Organometallic and Supramolecular Catalysis. *J. Am. Chem. Soc.* **138,** 9682–9693 (2016).

52. Jahromi, E. Z. & Gailer, J. Probing bioinorganic chemistry processes in the

bloodstream to gain new insights into the origin of human diseases. *Dalton Trans.* 329–336 (2010).

53. Powers, D. C. & Ritter, T. Bimetallic Pd(III) complexes in palladium-catalysed carbon–heteroatom bond formation. *Nat. Chem.* **1,** 302–309 (2009).

54. Powers, D. C. & Ritter, T. Bimetallic redox synergy in oxidative palladium catalysis. *Acc. Chem. Res.* **45,** 840–850 (2012).

55. Powers, D. C., Geibel, M. a L., Klein, J. E. M. N. & Ritter, T. Bimetallic palladium catalysis: Direct observation of Pd(III)-Pd(III) intermediates. *J. Am. Chem. Soc.* **131,** 17050–17051 (2009).

56. Azerraf, C., Cohen, S. & Gelman, D. Roof-shaped halide-bridged bimetallic complexes via ring expansion reaction. *Inorg. Chem.* **45,** 7010–7017 (2006).

57. Pérez-Temprano, M. H., Casares, J. a. & Espinet, P. Bimetallic catalysis using transition and group 11 metals: An emerging tool for C-C coupling and other reactions. *Chem. - A Eur. J.* **18,** 1864–1884 (2012).

58. Paton, R. S. & Brown, J. M. Dinuclear palladium complexes-precursors or catalysts? *Angew. Chem. Int. Ed. Engl.* **51,** 10448–50 (2012).

59. Sankar, M. Designing bimetallic catalysts for a green and sustainable future. *Chem. Soc. Rev.* 8099–8139 (2012).

60. Astruc, D., Ornelas, C., Diallo, A. K. & Ruiz, J. Extremely efficient catalysis of carbon-carbon bond formation using 'Click' dendrimer-stabilized palladium nanoparticles. *Molecules* **15,** 4947–4960 (2010).

61. Karpmski, Z., Zhang, Z. & Sachtler, W. M. H. Hydroformylation of propene over palladium trimethylphosphinecarbonyl clusters encaged in zeolite Y. *J. Mol. Catal.* **77,** 181–192 (1992).

62. Tsukada, N., Setoguchi, H., Mitsuboshi, T. & Inoue, Y. Hydroalkenylation of Alkynes Catalyzed by Dinuclear Palladium Complexes via C–H Bond Activation. *Chem. Lett.* **35,** 1164–1165 (2006).

63. Christmann, U., Experimental and theoretical investigations of new dinuclear palladium complexes as precatalysts for the amination of aryl chlorides. *J. Am. Chem. Soc.* **128,** 6376–6390 (2006).

64. Wilkinson, M., van Leeuwen, P. W. N. M. & Reek, J. N. H. New directions in supramolecular transition metal catalysis. *Org. Biomol. Chem.* 2371–2383 (2005).

65. Maggini, S. Classification of P,N-binucleating ligands for hetero- and homobimetallic complexes. *Coord. Chem. Rev.* **253,** 1793–1832 (2009).

66. Tanase, T., Flexible, linear, tetranuclear palladium complexes supported by tetraphosphine ligands with electron-withdrawing groups. *Dalton Trans.* **42,** 15941–52 (2013).

67. Murahashi, T. & Kurosawa, H. Organopalladium complexes containing palladium-palladium bonds. *Coord. Chem. Rev.* **231,** 207–228 (2002).

68. Peters, R. *Cooperative Catalysis : Designing Efficient Catalysts for Synthesis*. (Wiley-VCH Verlag GmbH & Co. KGaA, 2015). doi:10.1002/9783527681020

69. Tsuji, J. *Modern Palladium Catalysis: New Perspectives for the 21st Century*. (Wiley-VCH Verlag GmbH & Co. KGaA, 2004).

70. McKenzie, C. J. & Robson, R. High turnover catalysis at bimetallic sites of the hydration of nitriles to carboxamides co-catalysed by acid. Highly specific hydration of acrylonitrile to acrylamide. *J. Chem. Soc. Chem. Commun.* 112 (1988).

71. Gabrielsson, A., Blanco-Rodríguez, A. M., Matousek, P., Towrie, M. & Vlček, A. Different Mechanisms of Photochemical Re−Me and Re−Et Bond Homolysis in [Re(R)$(CO)_3$(4,4‘-dimethyl-2,2‘-bipyridine)]. A Time-Resolved IR Spectroscopic Study Ranging from Picoseconds to Microseconds. *Organometallics* **25,** 2148–2156 (2006).

72. Fafard, C. M., Adhikari, D., Foxman, B. M., Mindiola, D. J. & Ozerov, O. V. Addition of ammonia, water, and dihydrogen across a single Pd-Pd bond. *J. Am. Chem. Soc.* **129,** 10318–10319 (2007).

73. Yanagimoto, Y., Negishi, Y., Fujihara, H. & Tsukuda, T. Chiroptical activity of BINAP-stabilized undecagold clusters. *J. Phys. Chem. B* **110,** 11611–4 (2006).

74. Muci, A. R. & Buchwald, S. L. Practical palladium catalysts for C-N and C-O bond formation. *Cross-Coupling Reactions* **219,** 131–209 (2002).

75. Canty, A. J. Development of organopalladium(IV) chemistry: fundamental aspects and systems for studies of mechanism in organometallic chemistry and catalysis. *Acc. Chem. Res.* **25,** 83–90 (1992).

76. Canty, A. J., Denney, M. C., Koten, G. Van, Skelton, B. W. & White, A. H. Carbon - Oxygen Bond Formation at Metal(IV) Centers : Reactivity of Palladium(II) and Platinum(II) Complexes of the [2,6-(Dimethylaminomethyl)phenyl-N,C,N]-(Pincer) Ligand toward Iodomethane and Dibenzoyl Peroxide ; Structural Studies of M(II) and M(IV) C. *Organometallics* **23,** 5432–5439 (2004).

77. Allison R. Dick, Jeff W. Kampf, and M. S. S. Unusually Stable Palladium(IV) Complexes: Detailed Mechanistic Investigation of C-O Bond-Forming Reductive Elimination. *J. Am. Chem. Soc.* **127,** 12790–12791 (2005).

78. Furuya, T. & Ritter, T. Carbon-fluorine reductive elimination from a high-valent palladium fluoride. *J. Am. Chem. Soc.* **130,** 10060–10061 (2008).

79. Pinkes, J. R., Steffey, B. D., Vites, J. C. & Cutler, A. R. Carbon Dioxide Insertion into the Fe-Zr and Ru-Zr Bonds of the Heterobimetallic Complexes $Cp(CO)_2$M-$Zr(Cl)Cp_2$: Direct Production of the μ-η^1(C)η^2(O,O’)-CO_2 Compounds $Cp(CO)_2$M-CO_2-$Zr(Cl)Cp_2$. *Organometallics* **13,** 21–23 (1994).

80. Steffey, B. D., Curtis, C. J. & Dubois, D. L. Electrochemical Reduction of CO2 Catalyzed by a Dinuclear Palladium Complex Containing a Bridging Hexaphosphine Ligand: Evidence for Cooperativity. *Organometallics* **14,** 4937–4943 (1995).

81. DUBOIS, D. L. Development of Transition Metal Phosphine Complexes as Electrocatalysts for CO, and CO Reduction. *Comments Inorg. Chem.* **19,** 307–325 (1997).

82. DuBois, D. L., Miedaner, A. & Haltiwanger, R. C. Electrochemical reduction of carbon dioxide catalyzed by [Pd(triphosphine)(solvent)]$(BF_4)_2$ complexes: synthetic and mechanistic studies. *J. Am. Chem. Soc.* **113,** 8753–8764 (1991).

83. Weiss, M. & Peters, R. Bimetallic Catalysis: Cooperation of Carbophilic Metal Centers. *Coop. Catal.* 227–262 (2015).

84. Broussard, M. E. A Bimetallic Hydroformylation Catalyst : High Regioselectivity and Reactivity Through Homobimetallic Cooperativity. *Science (80-.).* **260,** 1784–1788 (1993).

85. Matthews, R. C., Bimetallic hydroformylation catalysis: *in situ* characterization of a dinuclear rhodium(II) dihydrido complex with the largest Rh-H NMR coupling constant. *Angew. Chem., Int. Ed. Engl.* **35,** 2253–2256 (1996).

86. Hetterscheid, D. G. H., Chikkali, S. H., deBruin, B. & Reek, J. N. H. Binuclear cooperative catalysts for the hydrogenation and hydroformylation of olefins. *ChemCatChem* **5,** 2785–2793 (2013).

87. Aubry, D. A., Monteil, A. R., Peng, W. J. & Stanley, G. G. The unusual inhibition of a dirhodium tetraphosphine-based bimetallic hydroformylation catalyst by PPh_3. *Comptes Rendus Chim.* **5,** 473–480 (2002).

88. Patureau, F. W., Sulfonamido-phosphoramidite ligands in cooperative dinuclear hydrogenation catalysis. *J. Am. Chem. Soc.* **131,** 6683–6685 (2009).

89. Cornelissen, C., Erker, G., Kehr, G., Fro, R. & Mu, D.-. Chemistry of Metal - Metal-Bonded Early - Late Heterobimetallics : Cooperative Reactions of Functional Groups at a Persistent Organometallic Zr - Rh Framework. 214–225 (2005).

90. Cooper, B. G., Napoline, J. W. & Thomas, C. M. Catalytic Applications of Early/Late Heterobimetallic Complexes. *Catal. Rev. Sci. Eng.* **54,** 1–40 (2012).

91. Choukroun, R., Jaud, J., Kalck, I. P. & Data, S. d^0-d^8 Heterobimetallic Complexes as Catalyst: Molecular and Crystal Structure of a Zirconium-Dirhodium Complex, $Rh_2(\mu\text{-}t\text{-}BuS)_2[(\mu\text{-}Ph_2PCH_2)_2Zr(\eta\text{-}C_5H_5)_2](CO)_2$. *Organometallics* **5,** 67–71 (1986).

92. Choukroun, R., Dahan, F., Gervais, D. & Rifai, C. Substituted cyclopentadienyl phosphinomethyl complexes of zirconium. Synthesis, chemical characteristics, complexation with rhodium complexes, and catalytic properties. Molecular and crystal structure of $(\eta^5\text{-}tert\text{-}BuC_5H_4)_2Zr(CH_2PPh_2)_2[Rh_2(\mu\text{-}S\text{-}tert\text{-}Bu)_2(CO)_2]$. *Organometallics* **9,** 1982–1987 (1990).

93. Ferguson, G. S., Wolczanski, P. T., Psrkdnyi, L. & Zonnevylle, M. C. Synthesis and reactivity of heterobimetallic 'A-frames' and Rh-Zr bonded complexes: structure of $Cp^*Zr(\mu\text{-}OCH_2Ph_2P)_2RhMe_2$. *Organometallics* **7,** 1967–1979 (1989).

94. Esteruelas, M. A., Garcia, M. P., Lopez, A. M. & Oro, L. A. Indirect cooperative effects leading to synergism in bimetallic homogeneous catalysts containing azolates as bridging ligands. *Organometallics* **10,** 127–33 (1991).

95. van Leeuwen, P. W. N. M. & Freixa, Z. in *Modern Carbonylation Methods.* **59,** 6221–6226 (Wiley-VCH Verlag GmbH & Co. KGaA, 2011).

96. Rivillo, D., Catalysis by design: Wide-bite-angle diphosphines by assembly of ditopic ligands for selective rhodium-catalyzed hydroformylation. *Angew. Chemie - Int. Ed.* **46,** 7247–7250 (2007).

97. van Leeuwen, P. W. N. M., Reek, J. N. H. & Kamer, P. C. J. Wide Bite Angle Diphosphines: Xantphos Ligands in Transition Metal Complexes and Catalysis. *Acc. Chem. Res.* **34,** 895 (2001).

98. Leeuwen, P. W. N. M. Van, Kamer, P. C. J. & Reek, J. N. H. The bite angle makes the catalyst. *Pure Appl.Chem.* **71,** 1443–1452 (1999).

99. Leñero, K. Q. A., Heterolytic activation of dihydrogen by platinum and palladium complexes. *Dalton Trans.* **42,** 6495–512 (2013).

100. Freixa, Z., Kamer, P. C. J., Lutz, M., Spek, A. L. & Van Leeuwen, P. W. N. M. Activity of SPANphos rhodium dimers in methanol carbonylation. *Angew. Chemie - Int. Ed.* **44,** 4385–4388 (2005).

101. Freixa, Z., SPANphos: a C_2-symmetric trans-coordinating diphosphane ligand. *Angew. Chem. Int. Ed. Engl.* **42,** 1284–7 (2003).

102. van der Vlugt, J. I., New diphosphane ligands based on Bisphenol A backbones - synthesis and coordination chemistry. *Eur. J. Inorg. Chem.* 4361–4369 (2003).

103. Laurenti, D., Feuerstein, M., Pèpe, G., Doucet, H. & Santelli, M. A New Tetratertiary Phosphine Ligand and Its Use in Pd-Catalyzed Allylic Substitution. *J. Org. Chem.* **66,** 1633–1637 (2001).

104. Azerraf, C., Cohen, S. & Gelman, D. Roof-Shaped Halide-Bridged Bimetallic Complexes via Ring Expansion Reaction. *Inorg. Chem.* **45,** 7010–7017 (2006).

105. Heck, R. F. & Breslow, D. S. Acylcobalt Carbonyls and their Triphenylphosphine Complexes. *J. Am. Chem. Soc.* **84,** 2499–2502 (1962).

106. Aubry, D. A., Laneman, S. A., Fronczek, F. R. & Stanley, G. G. Separating the Racemic and Meso Diastereomers of a Binucleating Tetraphospine Ligand System through the use of Nickel Chloride. *Inorg. Chem.* **40,** 5036–5041 (2001).

107. Beller, M., Cornils, B., Frohning, C. D. & Kohlpaintner, C. W. Progress in hydroformylation and carbonylation. *J. Mol. Catal. A Chem.* **104,** 17–85 (1995).

108. Berben, L. A. & Peters, J. C. Dimanganese and Diiron Complexes of a Binucleating Cyclam Ligand: Four-Electron, Reversible Oxidation Chemistry at High Potentials. *Inorg. Chem.* **47,** 11669–11679 (2008).

109. Boranes, A., Johnson, H. C. & Weller, A. S. P–C-Activated Bimetallic Rhodium Xantphos Complexes: Formation and Catalytic Dehydrocoupling of Amine – Boranes. 10173–10177 (2015).

110. Collins, R. A., Russell, A. F. & Mountford, P. Group 4 metal complexes for homogeneous olefin polymerisation : a short tutorial review. *Appl. Petrochem. Res.* **5,** 153–171 (2015).

111. Diebolt, O., Tricas, H., Freixa, Z. & van Leeuwen, P. W. N. M. Strong π-Acceptor Ligands in Rhodium-Catalyzed Hydroformylation of Ethene and 1-Octene: Operando Catalysis. *ACS Catal.* **3,** 128–137 (2013).

112. Dufaud, V., Bimetallic Activation in Homogeneous Catalysis. 3. Mechanistic Study of the Methoxycarbonylation of Tricarbonyl(chlorobenzene)chromium: Isolation and Reactivity of Possible Reaction Intermediates. *Organometallics* **10,** 4005–4015 (1991).

113. Feliz, M., Freixa, Z., van Leeuwen, P. W. N. M. & Bo, C., Revisiting the methyl iodide oxidative addition to rhodium complexes: A DFT study of the activation parameters. *Organometallics* **24,** 5718–5723 (2005).

114. Hunt, C., Fronczek, F. R., Billodeaux, D. R. & Stanley, G. G. A monometallic Rh(III) tetraphosphine complex: Reductive activation of DCM and selective meso to racemic tetraphosphine ligand isomerization. *Inorg. Chem.* **40,** 5192–5198 (2001).

115. Konrad, T. M., Fuentes, J. a., Slawin, A. M. Z. & Clarke, M. L. Highly enantioselective hydroxycarbonylation and alkoxycarbonylation of alkenes using dipalladium complexes as precatalysts. *Angew. Chemie - Int. Ed.* **49,** 9197–9200 (2010).

116. Leenders, S. H. A. M., Gramage-Doria, R., de Bruin, B. & Reek, J. N. H. Transition metal catalysis in confined spaces. *Chem. Soc. Rev.* **44,** 433–448 (2015).

117. Liu, X., Wang, D. & Li, Y. Synthesis and catalytic properties of bimetallic nanomaterials with various architectures. *Nano Today* **7,** 448–466 (2012).

118. López-Valbuena, J. M., Escudero-Adan, E. C., Benet-Buchholz, J., Freixa, Z. & van Leeuwen, P. W. N. M. An approach to bimetallic catalysts by ligand design. *Dalton Trans.* **39,** 8560–74 (2010).

119. Maris, E. P., Ketchie, W. C., Murayama, M. & Davis, R. J. Glycerol hydrogenolysis on carbon-supported PtRu and AuRu bimetallic catalysts. *J. Catal.* **251,** 281–294 (2007).

120. Moulijn, J. A., van Leeuwen, P. W. N. M. & van Santen, R. A. *CATALYSIS: An Integrated Approach to Homogeneous, Heterogeneous and Industrial Catalysis*. *Igarss 2014* (1993).

121. Peng, W.-J., Train, S. G., Howell, D. K., Fronczek, F. R. & Stanley, G. G. Bimetallic hydroformylation: a zwitterionic Rh (-I) Rh (I) tetraphosphine ligand-based bimetallic complex exhibiting facile CO addition and phosphine ligand rearrangement equilibrium. *Chem. Commun.* **882,** 2607 (1996).

122. Piesik, D. F. J., Range, S. & Harder, S. Bimetallic calcium and zinc complexes with bridged *β*-diketiminate ligands: Investigations on epoxide/CO_2 copolymerization. *Organometallics* **27,** 6178–6187 (2008).

123. Pospech, J., Fleischer, I., Franke, R., Buchholz, S. & Beller, M. Alternative metals for homogeneous catalyzed hydroformylation reactions. *Angew. Chem. (Int. ed.)Int. ed.)* **52,** 2852–72 (2013).

124. Rida, M. A. & Smith, A. K. A bimetallic hydroformylation catalyst: High regioselectivity through heterobimetallic cooperativity. *J. Mol. Catal. A Chem.* **202,** 87–95 (2003).

125. Schreiter, W. J., Synthesis and Characterization of a New Binucleating Tetraphosphine Ligand Based on 1,2-Phenylene Chelates and the Structures of Dinickel Tetrachloride Complexes of the Ligand. *Inorg. Chem.* 8–10 (2014).

126. Serra, D., Abboud, K. a., Hilliard, C. R. & McElwee-White, L. Electronic interactions in iron- and ruthenium-containing heterobimetallic complexes: Structural and spectroscopic investigations. *Organometallics* **26,** 3085–3093 (2007).

127. Torres, G. M., Frauenlob, R., Franke, R. & Börner, A. Production of alcohols via hydroformylation. *Catal. Sci. Technol.* **5,** 34–54 (2015).

128. Tsutsumi, H., Sunada, Y., Shiota, Y., Yoshizawa, K. & Nagashima, H. Nickel(II), Palladium(II), and Platinum(II) η3-Allyl Complexes Bearing a Bidentate Titanium(IV) Phosphinoamide Ligand: A Ti←M2 Dative Bond Enhances the Electrophilieity of the π-Allyl. *Organometallics* **28,** 1988–1991 (2009).

129. van der Veen, L. Origin of the bite angle effect on rhodium diphosphine catalyzed hydroformylation. *Organometallics* **19,** 872–883 (2000).

130. Van Leeuwen, P. W. N. M. Decomposition pathways of homogeneous catalysts. *Appl. Catal. A Gen.* **212,** 61–81 (2001).

131. Drent, E. & Budzelaar, P. H. M. The oxo-synthesis catalyzed by cationic palladium complexes, selectivity control by neutral ligand and anion. *J. Organomet. Chem.* **593–594,** 211–225 (2000).

132. Banihashemi, A. & Rahmatpour, A. Efficient Condensation of *p*-Substituted Phenols , with Malonaldehyde Tetramethyl Acetal in Trifluoroacetic Acid. *Tetrahedron* **55,** 7271–7278 (1999).

133. Wilkinson., A. D. M. and A. *IUPAC. Compendium of Chemical Terminology*. (Blachwell Scientifc Publications, Oxford, 1997).

134. Bader, A., Stereochemistry and Stability of Free and Coordinated Secondary Phosphines. Crystal and Molecular Structure of [[S-[(R*,R*),(R*)]]-$(+)_{589}$-[PtCl{1,2-$C_6H_4(PMePh)_2$}(PHMePh)]PF_6*CH_2Cl_2. *Inorg. Chem.* **34,** 384–389 (1995).

135. Chan, V. S., Bergman, R. G. & Toste, F. D. Pd-catalyzed dynamic kinetic enantioselective arylation of silylphosphines. *J. Am. Chem. Soc.* **129,** 15122–3 (2007).

136. Gelman, D., Jiang, L. & Buchwald, S. L. Copper-catalyzed C-P bond construction via direct coupling of secondary phosphines and phosphites with aryl and vinyl halides. *Org. Lett.* **5,** 2315–8 (2003).

137. Kalek, M. & Stawinski, J. Palladium-catalyzed C-P bond formation: Mechanistic studies on the ligand substitution and the reductive elimination. An intramolecular catalysis by the acetate group in Pd(II) complexes. *Organometallics* **27,** 5876–5888 (2008).

138. Kraatz, H.-B. & Pletsch, A. P–C bond formation: synthesis of phosphino amino acids by palladium-catalysed cross-coupling. *Tetrahedron: Asymmetry* **11,** 1617–1621 (2000).

139. Wang, T. Experimental and theoretical study on palladium-catalyzed C-P bond formation via direct coupling of triarylbismuths with P(O)-H compounds. *J. Org. Chem.* **79,** 608–17 (2014).

140. Wauters, I., Debrouwer, W. & Stevens, C. V. Preparation of phosphines through C-P bond formation. *Beilstein J. Org. Chem.* **10,** 1064–96 (2014).

141. Xu, J., Copper-Catalyzed P‑Arylation via Direct Coupling of Diaryliodonium Salts with Phosphorus Nucleophiles at Room Temperature. *J. Org. Chem.* **78,** 8176−8183 (2013).

142. Zhao, Y.-L., Wu, G.-J., Li, Y., Gao, L.-X. & Han, F.-S. [$NiCl_2$(dppp)]-catalyzed cross-coupling of aryl halides with dialkyl phosphite, diphenylphosphine oxide, and diphenylphosphine. *Chemistry* **18,** 9622–7 (2012).

143. Ohashi, A., Kikuchi, S., Yasutake, M. & Imamoto, T. Unsymmetrical P-Chirogenic Bis(phosphane) Ligands : Their Preparation and Use in Rhodium-Catalyzed Asymmetric Hydrogenation. *Eur. J. Org. Chem.* 2535–2546 (2002).

144. Gao, Y. & Sharpless, K. B. Vicinal Diol Cyclic Sulfates : Like Epoxides Only More Reactive. *J. Am. Chem. Soc.* **110,** 7538–7539 (1988).

145. T. Nonaka, S. Kihara, T. Fuchigami, M. M. B. Electrochemical Reduction of Cyclic And Acyclic Sulfates. *Bull.Chem.Soc.Jpm.* **57,** 3160–3166 (1984).

146. Megia-Fernandez, A., Morales-Sanfrutos, J., Hernandez-Mateo, F. & Santoyo-Gonzalez, F. Synthetic Applications of Cyclic Sulfites, Sulfates and Sulfamidates in Carbohydrate Chemistry. *Curr. Org. Chem.* **15,** 401–432 (2011).

147. Brevard, C. & P. Granger. *Handbook of high resolution multinuclear NMR*. (Wiley, 1981).

148. Quin, L. D. & Williams, A. J. *P-31 Nmr Spectra and Computer Assisted Structure Verification*. (Advanced Chemistry Development, Inc. Toronto, Canada, 2004).

149. Denehy, E., White, J. M. & Williams, S. J. Electronic structure of the sulfonyl and phosphonyl groups: A computational and crystallographic study. *Inorg. Chem.* **46,** 8871–8886 (2007).

150. Yamada, K. & Koga, N. Variationally determined electronic states for the theoretical analysis of intramolecular interaction. II. Qualitative nature of the P-O bond in phosphine oxides. *J. Comput. Chem.* **34,** 149–161 (2013).

151. Wu, H. C., Yu, J. Q. & Spencer, J. B. Stereospecific deoxygenation of phosphine oxides with retention of configuration using triphenylphosphine or triethyl phosphite as an oxygen acceptor. *Org. Lett.* **6,** 4675–4678 (2004).

152. Kenny, N. P., Rajendran, K. V., Jennings, E. V. & Gilheany, D. G. Cleavage of P=O in the presence of P-N: Aminophosphine oxide reduction with in situ boronation of the P(III) product. *Chem. - A Eur. J.* **19,** 14210–14214 (2013).

153. Dobado, J. a., Martínez-García, H. & Sundberg, M. R. Chemical Bonding in Hypervalent Molecules Revised. Application of the Atoms in Molecules Theory to Y_3X and Y_3XZ (Y = H or CH_3 ; X = N, P or As; Z = O or S) Compounds. *J. Am. Chem. Soc.* **120,** 8461–8471 (1998).

154. Busacca, C. A., Reduction of Tertiary Phosphine Oxides with DIBAL-H. *J. Org. Chem.* **58,** 1524–1531 (2008).

155. Herault, D., Nguyen, D. H., Nuel, D. & Buono, G. Reduction of secondary and tertiary phosphine oxides to phosphines. *Chem. Soc. Rev.* **44,** 2508–2528 (2015).

156. Naumann, K., Zon, G. & Mislow, K. Use of hexachlorodisilane as a reducing agent. Stereospecific deoxygenation of acyclic phosphine oxides. *J. Am. Chem. Soc.* **91,** 7012–7023 (1969).

157. Pietrusiewicz, K. M. & Zablocka, M. Preparation of Scalemic P-Chiral Phosphines and Their Derivatives. *Chem. Rev.* **94,** 1375–1411 (1994).

158. Imamoto, T., Kikuchi, S., Miura, T. & Wada, Y. Stereospecific reduction of phosphine oxides to phosphines by the use of a methylation reagent and lithium aluminum hydride. *Org. Lett.* **3,** 87–90 (2001).

159. J.M. López-Valbuena, E.C. Escuerdo-Adan, J.Benet-Buchholz, Z. Freixa, P. W. N. M. van L. Bridging the gap in catalysis via multidisciplinary approaches. *Dalt. Trans.* 8560–8574 (2010).

160. Condensation, T. H. E. & Glyoxal, O. F. The condensation of glyoxal with *p*-cresol. *Can. J. Chem.* **38,** 6–7 (1960).

161. Ripin, D. H. & Evans, D. A. *pKa's of Nitrogen Acids*. (2005).

162. Butterfield, A. M., Gilomen, B. & Siegel, J. S. Kilogram-scale production of corannulene. *Org. Process Res. Dev.* **16,** 664–676 (2012).

163. Hillebrand, S., Bruckmann, J., Kriiger, C. & Haenel, M. W. Bidentate Phosphines

of Heteroarenes: 9,9-Dimethyl-4,5-bis(diphenylphosphino)xanthenel). *Science* **36,** 75–78 (1995).

164. Reagenti, C. E. Safety data sheet: Bromine. **2006,** 2–9 (2013).

165. Andersh, B., Murphy, D. L. & Olson, R. J. Hydrochloric Acid Catalysis of N-Bromosuccinimide (NBS) Mediated Nuclear Aromatic Brominations in Acetone. *Synth. Commun.* **30,** 2091–2098 (2000).

166. Dickinson, B. Safety Data Sheet: Bromoacetone. 2–7 (2010).

167. Imamoto, T., Oshiki, T., Onozawa, T., Kusumoto, T. & Sato, K. Synthesis and reactions of phosphine-boranes. Synthesis of new bidentate ligands with homochiral phosphine centers via optically pure phosphine-boranes. *J. Am. Chem. Soc.* **112,** 5244–5252 (1990).

168. Miura, T., Yamada, H., Kikuchi, S., Imamoto, T. & Chem, T. P. A. Synthesis and Reactions of Optically Active Secondary Dialkylphosphine-Boranes. *J. Org. Chem.* 3371–3374 (2000).

169. Imamoto, T., Saitoh, Y., Koide, A., Ogura, T. & Yoshida, K. Synthesis and enantioselectivity of p-chiral phosphine ligands with alkynyl groups. *Angew. Chem. Int. Ed. Engl.* **46,** 8636–9 (2007).

170. Imamoto, T., Improved synthetic routes to methylene-bridged P-chiral diphosphine ligands via secondary phosphine-boranes. *Tetrahedron Asymmetry* **21,** 1522–1528 (2010).

171. Imamoto, T. & Crepy, K. V. L. P-Chirogenic Phosphine Ligands and and Their Use in Catalytic Asymmetric Reactions. *Top Curr Chem* **229,** 1–40 (2003).

172. Voskuil, W. & Arens, J. F. Note on the preparation of chloro-di- alkylphosphines. *Recueil* **82,** 1962–1964 (1963).

173. Micovic, V. & Mihailovic, M. The Reduction of Acid Amides with Lithium Aluminum Hydride. *J. Org. Chem.* **18,** 1190–1200 (1953).

174. Zwick, B. D., Synthesis, structure, dynamic behavior, and reactivity of chiral rhenium primary phosphine and phosphido complexes of the formula $[(\eta^5\text{-}C_5H_5)Re(NO)(PPh_3)(PRH_2)]^+X^-$ and $(\eta^5\text{-}C_5H_5)Re(NO)(PPh_3)[P(-)RH]$. *Organometallics* **11,** 2673–2685 (1992).

175. Szafraniec, L. J., Reiff, L. P. & Aaron, H. S. Stereoselective Synthesis and Stereochemistry of Optically Active Isopropyl Methylphosphinothioate. *J. Am. Chem. Soc.* **92,** 6391–6392 (1970).

176. Imamoto, T., Nonomura, T., Kishikawa, K. & Yanagawa, M. Synthesis and Reactions of Optically Pure Cyclohexyl(o-methoxyphenyl)phosphine-borane and t-Bu-(o-methoxyphenyl)phosphine-borane. *Heteroat. Chem.* **4,** 475 (1993).

177. Bader, A., Pabel, M., Willis, A. C. & Wild, S. B. First Resolution of a Free Secondary Phosphine Chiral at Phosphorus and Stereospecific Formation and Structural Characterization of a Homochiral Secondary Phosphine−Borane Complex. *Inorg. Chem.* **35,** 3874–3877 (1996).

178. Coldham, I., Dufour, S., Haxell, T. F. N., Patel, J. J. & Sanchez-Jimenez, G. Dynamic thermodynamic and dynamic kinetic resolution of 2-lithiopyrrolidines. *J. Am. Chem. Soc.* **128,** 10943–10951 (2006).

179. Montchamp, J. L. Phosphinate chemistry in the 21st century: A viable alternative

to the use of phosphorus trichloride in organophosphorus synthesis. *Acc. Chem. Res.* **47,** 77–87 (2014).

180. Petneházy, I., Jászay, Z. M., Szabó, A. & Everaert, K. Convenient One Pot Synthesis of Phosphonites and H-Phosphinates. *Synth. Commun.* **33,** 1665–1674 (2003).

181. Montchamp, J. Phosphinate Chemistry in the 21st Century : A Viable Alternative to the Use of Phosphorus Trichloride in Organophosphorus Synthesis. *Acc. Chem. Res.* **47,** 77–87 (2014).

182. Guyon, C., Métay, E., Popowycz, F. & Lemaire, M. Synthetic applications of hypophosphite derivatives in reduction. *Org. Biomol. Chem.* **13,** 7879–7906 (2015).

183. Hirao, T., Masunaga, T., Yamada, N., Ohshiro, Y. & Agawa, T. Palladium-catalyzed new carbon-phosphorus bond formation. *Chemical Society of Japan* **55,** 909–913 (1982).

184. Bravo-Altamirano, K., Huang, Z. & Montchamp, J. L. Palladium-catalyzed phosphorus-carbon bond formation: Cross-coupling reactions of alkyl phosphinates with aryl, heteroaryl, alkenyl, benzylic, and allylic halides and triflates. *Tetrahedron* **61,** 6315–6329 (2005).

185. Deal, E. L., Petit, C. & Montchamp, J. L. Palladium-catalyzed cross-coupling of H-phosphinate esters with chloroarenes. *Org. Lett.* **13,** 3270–3273 (2011).

186. Berger, O., Petit, C., Deal, E. L. & Montchamp, J.-L. Phosphorus-Carbon Bond Formation: Palladium-Catalyzed Cross-Coupling of H -Phosphinates and Other P(O)H-Containing Compounds. *Adv. Synth. Catal.* **355,** 1361–1373 (2013).

187. Petit, C., Fécourt, F. & Montchamp, J. L. Synthesis of disubstituted phosphinates via palladium-catalyzed hydrophosphinylation of H-phosphinic acids. *Adv. Synth. Catal.* **353,** 1883–1888 (2011).

188. Ribière, P., Bravo-Altamirano, K., Antczak, M. I., Hawkins, J. D. & Montchamp, J. L. $NiCl_2$-catalyzed hydrophosphinylation. *J. Org. Chem.* **70,** 4064–4072 (2005).

189. Zhang, X. Ni(II)/Zn catalyzed reductive coupling of aryl halides with diphenylphosphine oxide in water. *Org. Lett.* **13,** 3478–81 (2011).

190. Anderson, N. G. Generation and Fate of Regioisomeric Side-Chain Impurities in the Preparation of Fosinopril Sodium. *Org. Process Res. Dev.* **1,** 315–319 (1997).

191. Yoo, W.-J. & Kobayashi, S. Hydrophosphinylation of unactivated alkenes with secondary phosphine oxides under visible-light photocatalysis. *Green Chem.* **15,** 1844 (2013).

192. Li, C.-X., Tu, D.-S., Yao, R., Yan, H. & Lu, C.-S. Visible-Light-Induced Cascade Reaction of Isocyanides and *N* -Arylacrylamides with Diphenylphosphine Oxide via Radical C–P and C–C Bond Formation. *Org. Lett.* (2016).

193. Sonia Gouault-Bironneau, Sylvine Deperle, Amber Sutor, and J.-L. M. Radical reaction of sodium hypophosphite with terminal alkynes: Synthesis of 1,1-bis-H-phosphinates. *Org. Lett.* **7,** 5909–5912 (2005).

194. Antczak, M. I. & Montchamp, J.-L. AIBN-Initiated Radical Reactions of Ethyl Phosphinate. *Synthesis (Stuttg).* **2006,** 3080–3084 (2006).

195. Han, L.-B. & Zhao, C.-Q. Stereospecific addition of H-P bond to alkenes: a simple

method for the preparation of (R(P))-phenylphosphinates. *J. Org. Chem.* **70,** 10121–3 (2005).

196. Gouault-Bironneau, S., Deprèle, S., Sutor, A. & Montchamp, J. L. Radical reaction of sodium hypophosphite with terminal alkynes: Synthesis of 1,1-bis-H-phosphinates. *Org. Lett.* **7,** 5909–5912 (2005).

197. Anderson, N. G. Generation and Fate of Regioisomeric Side-Chain Impurities in the Preparation of Fosinopril Sodium. *Org. Process Res. Dev.* **1,** 315–319 (1997).

198. Abrunhosa-Thomas, I., Sellers, C. E. & Montchamp, J.-L. Alkylation of H-phosphinate esters under basic conditions. *J. Org. Chem.* **72,** 2851–6 (2007).

199. Markoulides, M. S. & Regan, A. C. Synthesis of a phosphinate analogue of the anti-tumour phosphate di-ester perifosine via sequential radical processes. *Org. Bomolecular Chem.* **11,** 119–29 (2013).

200. Gavara, L., Petit, C. & Montchamp, J. L. DBU-promoted alkylation of alkyl phosphinates and H-phosphonates. *Tetrahedron Lett.* **53,** 5000–5003 (2012).

201. Belabassi, Y., Antczak, M. I., Tellez, J. & Montchamp, J. L. Borane complexes of the H_3PO_2 P(III) tautomer: useful phosphinate equivalents. *Tetrahedron* **64,** 9181–9190 (2008).

202. Abrunhosa-Thomas, I., Sellers, C. E., Montchamp, J. L., Alkylation of H - Phosphinate Esters under Basic Conditions. *J. Org. Chem.* **72,** 2851–2856 (2007).

203. Uozumi, Y., Tanahashi, A., Lee, S. Y. & Hayashi, T. Synthesis of optically active 2-(diarylphosphino)-1,1'-binaphthyls, efficient chiral monodentate phosphine ligands. *J. Org. Chem.* **58,** 1945–1948 (1993).

204. Kurz, L., Lee, G., Morgans, D., Waldyke, M. J. & Ward, T. Stereospecific functionalization of (R)-(-)-1,1'-bi-2-naphthol triflate. *Tetrahedron Lett.* **31,** 6321–6324 (1990).

205. Korff, C. & Helmchen, G. Preparation of chiral triarylphosphines by Pd-catalysed asymmetric P-C cross-coupling. *Chem. Commun. (Camb).* 530–531 (2004). doi:10.1039/b315009g

206. Hilliard, C. R., Bhuvanesh, N., Gladysz, J. A., Blümel, J. & Blumel, J. Synthesis, purification, and characterization of phosphine oxides and their hydrogen peroxide adducts. *Dalt. Trans.* **41,** 1742 (2012).

207. Alayrac, C., Lakhdar, S., Abdellah, I. & Gaumont, A. C. Recent advances in synthesis of P-BH_3 compounds. *Topics in Current Chemistry* **361,** (Springer Berlin Heidelberg, 2015).

208. Izod, K., Wills, C., Anderson, E., Harrington, R. W. & Probert, M. R. Insights into the Stability and Structures of Phosphine-Boranes and Their α-Metalated Derivatives. *Organometallics* 5283–5294 (2014).

209. Lloyd-Jones, G. C. & Taylor, N. P. Mechanism of Phosphine Borane Deprotection with Amines: The Effects of Phosphine, Solvent and Amine on Rate and Efficiency. *Chem. - A Eur. J.* **21,** 5423–5428 (2015).

210. Uhlig, F., Zur Reaktion Von Phosphorverbindungen Mit Schwesinger Basen-/P-C-Bindungknüpfung an P-H-Funktionellen Phosphorverbindungen. *Phosphorus. Sulfur. Silicon Relat. Elem.* **81,** 155–163 (1993).

211. Fries, G., A new route to achiral and chiral 1,2-bis(phosphino)ethanes, 1-arsino-2-

phosphinoethanes, and 1,3-bis(phosphino)propanes and the molecular structure and catalytic activity of some rhodium(I) complexes derived thereof. *Dalt. Trans.* 1873–1881 (2004).

212. Czauderna, C. F., Synthesis and Reactivity of Chiral, Wide-Bite-Angle, Hybrid Diphosphorus Ligands. *Eur. J. Inorg. Chem.* (2014).

213. Butts, C. P., Structure-based rationale for selectivity in the asymmetric allylic alkylation of cycloalkenyl esters employing the Trost 'Standard Ligand' (TSL): Isolation, analysis and alkylation of the monomeric form of the cationic η^3-cyclohexenyl complex [(η^3-c-C_6H_9)Pd(TSL)]. *J. Am. Chem. Soc.* **131,** 9945–9957 (2009).

214. McKinstry, L. & Livinghouse, T. An Efficient Procedure for the Synthesis of C-Chiral. *Tetrahedron* **51,** 7655–7666 (1995).

215. White, R. E., Miller, J. P., Favreau, L. V & Bhattacharyya, A. Stereochemical dynamics of aliphatic hydroxylation by cytochrome P-450. *J. Am. Chem. Soc.* **108,** 6024–6031 (1986).

216. Issleib, K. & Thomas, G. Zur Synthese der Carbäthoxyalkyl-phosphine. *Chem. Ber.* **94,** 2244–2251 (1961).

217. Issleib, K. Darstellung von Carboxyphosphinen R_2P-$[CH_2]_n$-CO_2H. **597,** 803–808 (1960).

218. Vastra, J. & Saint-jalmes, L. Full Papers Catalytic Mesylation of Alcohols : A Highly Productive Process for Trifluoroethyl Mesylate Abstract : *Org. Process Res. Dev.* (2006).

219. Wolfsberger, W., Wolfgang, B. & Werner, H. Darstellung und Charakterisierung substituierter Phosphinoether und -thioether. *Zeitschrift für Naturforsch.* 3–9 (2015).

220. Wolfsberger, W., Die Darstellung sterisch anspruchsvoller Phosphinoester und ihre Verwendung zur Synthese von Rhodium (I) - und Rhodium (III) -Komplexen [1]. (2015).

221. Guo, S. H., Oxa-Michael addition promoted by the aqueous sodium carbonate. *Tetrahedron Lett.* **55,** 6718–6720 (2014).

222. Schmidle, C. J. & C., R. Carboalkoxyethylation Reactions in Presence of Certain Anion-Exchange Resins, Patent: US 2658070.

223. Wolfsberger, W., Burkart, W. & Werner, H. O-Silylierte Phosphinoketenacetale RR'PCH_2CH=$C(OSiMe_3)$OR". Darstellung und Hydrolyse zu Phosphinoestern. *Zeitschrift für Naturforsch.* 987 (1995).

224. Ragulin, V. V. ω-haloalkylphosphoryl compounds: Synthesis and properties. *Russ. J. Gen. Chem.* **82,** 1928–1937 (2013).

225. Wang, X., Cao, K., Liu, Y., Tsang, B. & Liew, S. Migration Insertion Polymerization(MIP) of Cyclcopentadienyldicarbonyldiphenylphosphino-propyliron(FpP): A New Concept for Main Chain Metal-Containing Polymers(MCPs). *J. Am. Chem. Soc.* **135,** 3399–3402 (2013).

226. Aladzheva, I. M., Intramolecular P=S And P=N Alkylation. General Method for Synthesizing 1,2-Heterophosphacyclanes. *J. Organomet. Chem.* **38,** 95–105 (2002).

227. Guijarro, D., Guillena, G., Mancheño, B. & Yus, M. Direct transformation of dialkyl sulfates into alkyllithium reagents by a naphthalene-catalysed lithiation. *Tetrahedron* **50,** 3427 (1994).

228. Byun, H.-S., He, L. & Bittman, R. Cyclic Sulfites and Cyclic Sulfates in Organic Synthesis. *Tetrahedron* **56,** 7051–7091 (2000).

229. Kaiser, E. T. & Westheiner, F. H. The Hydrolysis of Some Cyclic Esters of Sulfuric Acid's. *J. Am. Chem. Soc.* **85,** 602–607 (1962).

230. Heutz, F. J. L., Samuels, M. C. & Kamer, P. C. J. Solid-phase synthesis of recyclable diphosphine ligands. *Catal. Sci. Technol.* **5,** 3296–3301 (2015).

231. Heutz, F. J. L. & Kamer, P. C. J. Modular solid-phase synthesis, catalytic application and efficient recycling of supported phosphine-phosphite ligand libraries. *Dalt. Trans.* **45,** 2116–2123 (2016).

232. Imamoto, T., Kusumoto, T., Susuki, N. & Sato, K. Phosphine oxides and lithium aluminum hydride-sodium borohydride-cerium(III) chloride: synthesis and reactions of phosphine-boranes. *J. Am. Chem. Soc.* **107,** 5301–5303 (1985).

233. Brisset, H., Gourdel, Y., Pellon, P. & Corm, M. Le. Phosphine-Borane Complexes ; Direct Use in Asymmetric Catalysis. **34,** 4523–4526 (1993).

234. Masudab, H. & Yamaguchic, K. A New P-Chiral Bisphosphine, (S,S)-1,2-Bis[(o-ethylphenyl)phenyl- phosphinolethane, as an Effective Ligand in Catalytic Asymmetric Hydrogenation of α-(Acylamino)acrylic Acids. *Tetrahedron Lett.* **36,** 8271–8274 (1995).

235. Bourumeau, K., Gaumont, A. & Denis, J. P-H bond activation of primary phosphine-boranes: access to α-hydroxy and α,α'-dihydroxyphosphine-borane adducts by uncatalyzed hydrophosphination of carbonyl derivatives. *J. Organomet. Chem.* 205–213 (1997).

236. Michel, J., Faure, B. & Ma, M. Phosphane – boranes : synthesis , characterization and synthetic applications. **180,** 665–698 (1998).

237. McKinstry, L. Acid mediated phosphine-borane decomplexation: A model for characterizing short-lived intermediates with experimental and ab initio NMR data. *J. Org. Chem.* **65,** 2261–2263 (2000).

238. Allen, D. W. Phosphines and related P-C-bonded compounds. *Organophosphorus Chem.* **43,** 1–51 (2014).

239. Honaker, M. T. & Salvatore, R. N. A mild and efficient CsOH-promoted synthesis of ditertiary phosphines. *Phosphorus. Sulfur. Silicon Relat. Elem.* **179,** 277–283 (2004).

240. Li, Y., Das, S., Zhou, S., Junge, K. & Beller, M. General and selective copper-catalyzed reduction of tertiary and secondary phosphine oxides: convenient synthesis of phosphines. *J. Am. Chem. Soc.* **134,** 9727–32 (2012).

241. E.N. Tsetkov, N.A. Bondarenko, I.G. Malakhova, M. I. K. A Simple Synthesis and Some Synthetic Applications of Substituted Phosphide and Phosphinite Anions. *Synthesis (Stuttg).* 198 (1986).

242. Chou, T. S., Tsao, C. H. & Chun Hung, S. Cleavage of phosphorus-carbon bonds with sodium/naphthalene. Facile preparation of unsymmetrical diphosphines. *J. Organomet. Chem.* **312,** 53–58 (1986).

243. Vandoorn, J. A., Frijns, J. H. G. & Meijboom, N. Reductive Cleavage of the Carbon Phosphorus Bond with Alkali-Metals .2. Cleavage of Mixed Functionalized Triarylphosphines - Birch Reduction of Arylphosphines. *Recl. Des Trav. Chim. Des Pays-Bas-Journal R. Netherlands Chem. Soc.* **110,** 441–449 (1991).

244. van Doorn, J. A. & Meijboom, N. Reductive cleavage of the carbon-phosphorus bond with alkali metals. III. Reactions of arylalkylphosphines. *Recl. des Trav. Chim. des Pays-Bas* **111,** 170–177 (1992).

245. Gallagher, J. & Rae, A. D. The Cleavage of P-C bonds in diphosphines by lithium: The crystal structure of $[Li_4\{PhPCH_2CH_2PPh\}_2(OC_4H_8)_8]$. *J. Organomet. Chem.* **323,** 9–12 (1987).

246. Mimeau, D., Delacroixb, O. & Gaumont, A.-C. Regioselective uncatalysed hydrophosphination of alkenes: a facile route to P-alkylated phosphine derivatives. *Chem. Commun.* 2928–2929 (2003).

247. Nell, B. P. & Tyler, D. R. Synthesis, reactivity, and coordination chemistry of secondary phosphines. *Coord. Chem. Rev.* **279,** 23–42 (2014).

248. Moulin, D., Bauduin, C., Darcel, C. & Jugé, S. Asymmetric synthesis of P-stereogenic *o*-hydroxyaryl- phosphine (borane) and phosphine-phosphinite ligands. *Tetrahedron: Asymmetry* **11,** 3939–3956 (2000).

249. KAESZ, H. D. & STONE, F. G. A. Preparation and Characterization of Vinyldichlorophosphine, Vinyldimethyl- phosphine, and Ethyldimethyl-phosphine. **1866,** 1957–1959 (1959).

250. Petit, C., Favre-Réguillon, A., Mignani, G. & Lemaire, M. A straightforward synthesis of unsymmetrical secondary phosphine boranes. *Green Chem.* **12,** 326 (2010).

251. Staendeke, B. H. Methylchlorophosphanes and Their Reaction Products. *Angew. Chem. internat. Ed.* **12,** 877–881 (1973).

252. Method for preparing halogenated organophosphines. (2009).

253. Wolfsberger, W. Darstellung von Alkylphenylphosphanen nach der Methode von Weferling. *Chemiker-Zeitung* **2,** 86–87 (1989).

254. N.Weferling. Neue Methoden zur Chlorierung von Organophosphoverbindungen mit P-H Funktionen. *Z. anorg. allg. Chem.* **548,** 55–62 (1987).

255. N.Weferling. Production of Organophosphorus compounds from hydrogen Phosphide. *Phosphorus and Sulfur* **30,** 641–644 (1987).

256. Toffano, M., Dobrota, C. & Fiaud, J. Synthesis of Enantiopure 1-r-Aryl-2-c,5-t-diphenylphospholane Oxides and Boranes by Pd-Catalyzed C–P Bond Formation. *Eur. J. Org. Chem.* 650–656 (2006).

257. Dhokale, R. A. & Mhaske, S. B. P - Arylation : Arynes to Aryl-Phosphonates, -Phosphinates, and -Phosphine Oxidesand -Phosphine Oxides. *Org. Lett.* **15,** 22218–2221 (2013).

258. Stadler, A. & Kappe, C. O. Rapid Formation of Triarylphosphines by Microwave-Assisted Transition Metal-Catalyzed C−P Cross-Coupling Reactions. *Org. Lett.* **4,** 3541–3543 (2002).

259. Bergbreiter, D. E., Liu, Y., Furyk, S. & Case, B. L. Pd-Catalyzed Synthesis of a

Tethered Soluble Polymeric Phosphine Ligand. *Tetrahedron Lett.* **39,** 8799–8802 (1998).

260. Jiadi Zhang, Ana Bellomo, Nisalak Trongsiriwat, Tiezheng Jia, Patrick Carroll, Spencer D. Dreher, Matthew Thomas Tudge, Patrick J Walsh, Haolin Yin, Jerome Ronald Robinson, and E. J. S. NiXantphos: A Deprotonatable Ligand for Room Temperature Palladium-Catalyzed Cross-Couplings of Aryl Chlorides. *J. Am. Chem. Soc* 1–15 (2014).

261. Kalek, M. & Stawinski, J. Efficient synthesis of mono- and diarylphosphinic acids: a microwave-assisted palladium-catalyzed cross-coupling of aryl halides with phosphinate. *Tetrahedron* **65,** 10406–10412 (2009).

262. Cheng, W. H., Chen, C. H., Wang, S. C., Tu, Y. K. & Hsieh, K. C. Defects in Optoelectronic Materials Due to Phosphorus-Containing Underlayer. *J. Electron. Mater.* **27,** 47–50 (1998).

263. Hissler, M., Lescop, C. & Réau, R. Organophosphorus π-conjugated materials: The rise of a new field. *J. Organomet. Chem.* **690,** 2482–2487 (2005).

264. Hissler, M., Lescop, C. & Réau, R. π-Conjugated derivatives containing phosphole rings: Synthesis, properties and coordination chemistry. *Comptes Rendus Chim.* **8,** 1186–1193 (2005).

265. Xia, F., Wang, H. & Jia, Y. Rediscovering black phosphorus as an anisotropic layered material for optoelectronics and electronics. *Nat. Commun.* **5,** 4458 (2014).

266. Andrey, O., Alexakis, A., Tomassini, A. & Bernardinelli, G. The Use of N-Alkyl-2,2′-bipyrrolidine Derivatives as Organocatalysts for the Asymmetric Michael Addition of Ketones and Aldehydes to Nitroolefins. *Adv. Synth. Catal.* **346,** 1147–1168 (2004).

267. Otsuka, S. Chemistry of platinum and palladium compounds of bulky phosphines. *J. Organomet. Chem.* **200,** 191–205 (1980).

268. Ronconi, L. & Sadler, P. J. Applications of heteronuclear NMR spectroscopy in biological and medicinal inorganic chemistry. *Coord. Chem. Rev.* **252,** 2239–2277 (2008).

269. Marinetti, A. & Voituriez, A. Enantioselective phosphine organocatalysis. *Synlett* 174–194 (2010).

270. Mazzacurati, M. Advanced Studies on the Synthesis of Organophosphorus Compounds Index : (UNIVERSITÀ DI BOLOGNA).

271. Kühl, O. *Phosphoros-31 NMR Spectroscopy*. *Journal of Chemical Information and Modeling* **53,** (2008).

272. Borsari, M. Cadmium: Inorganic & Coordination Chemistry. *Encycl. Inorg. Bioinorg. Chem.* 1–9 (2011).

273. Kroto, H. W., Nixon, J. F., Taylor, M. J., Frew, A. A. & Muir, K. W. Synthesis and 31P NMR spectra of some platinum(II) complexes of the phospha-alkene, (mesityl)P=CPh_2. *Polyhedron* **1,** 89–95 (1982).

274. P.S.Pregosin, R. W. K. *^{31}P and ^{13}C NMR of Transition Metal Phosphine complexes*. (Springer-Verlag, 1976).

275. Pregosin, P. S. *NMR in Organometallic Chemistry*. (Wiley-VCH Verlag GmbH & Co. KGaA, 2012).

276. Pregosin, P. S. & Kunz, R. W. *^{31}P and ^{13}C NMR of Transition Metal Phosphine Complexes*. (1979).

277. Allen, F. H. & Pidcock., A. Nuclear magnetic resonance spectra of some phosphine complexes of platinum alkyls and aryls. *J. Chem. SOC.* 2700–2704 (1968).

278. Arena, G., Scolaro, L. M., Pasternack, R. F. & Romeo, R. Synthesis, Characterization, and Interaction with DNA of the Novel Metallointercalator Cationic Complex (2,2':6',2''-terpyridine)methylplatinum(II). *Inorg. Chem.* **34,** 2994–3002 (1995).

279. Wen, F. & Bönnemann, H. A facile one-pot synthesis of [(COD)Pt(CH_3)$_2$]. *Appl. Organomet. Chem.* **19,** 94–97 (2005).

280. Jain, V. K. & Jain, L. The chemistry of binuclear palladium(II) and platinum(II) complexes. *Coord. Chem. Rev.* **249,** 3075–3197 (2005).

281. Waddell, P. G., Slawin, A. M. Z. & Woollins, J. D. Correlating Pt-P bond lengths and Pt-P coupling constants. *Dalton Trans.* **39,** 8620–3625 (2010).

282. Grossel, M. C., Batson, J. R., Moulding, R. P. & Seddon, K. R. Bis-μ-[Bis(Diphenylphosphino)Methane]Dihalodiplatinum-(Pt-Pt) and its hydrido 'A'-frame derivatives revisited. *J. Organomet. Chem.* **304,** 391–423 (1986).

283. Waddell, P. G., Slawin, A. M. Z. & Woollins, J. D. Correlating Pt-P bond lengths and Pt-P coupling constants. *Dalton Trans.* **39,** 8620–5 (2010).

284. Kaneko, T. in *Ullmann's Encyclopedia of Industrial Chemistry* (Wiley-VCH Verlag GmbH & Co. KGaA, 2000).

285. Mooibroek, T. J., Schoon, L., Bouwman, E. & Drent, E. Carbonylation of nitrobenzene in methanol with palladium bidentate phosphane complexes: an unexpectedly complex network of catalytic reactions, centred around a Pd-imido intermediate. *Chem. Eur. J* **17,** 13318–33 (2011).

286. Thomas, C. M. New diphosphine ligands containing ethyleneglycol and amino alcohol spacers for the rhodium-catalyzed carbonylation of methanol. *Chem. - A Eur. J.* **8,** 3343–3352 (2002).

287. Mooibroek, T. J., Bouwman, E. & Drent, E. Mechanistic Study of the Oxidative Carbonylation of Methanol Catalyzed by Palladium Diphosphane Complexes with Nitrobenzene as Oxidant. *Eur. J. Inorg. Chem.* **2012,** 1403–1412 (2012).

288. Franke, R., Selent, D. & Börner, A. Applied hydroformylation. *Chemi. Rev.* **112,** 5675–732 (2012).

289. Jennerjahn, R., Lyzed isomerization and hydroformylation of olefins. *Chem. - A Eur. J.* **15,** 6383–6388 (2009).

290. Crozet, D., Interception of a Rh(I)–Rh(III) dinuclear trihydride complex revealing the dihydrogen activation by [Rh(CO)$_2${(R,R)-Ph–BPE}]. *Dalt. Trans.* **41,** 3369 (2012).

291. Fang, X., Zhang, M., Jackstell, R. & Beller, M. Selective palladium-catalyzed hydroformylation of alkynes to α,β-Unsaturated Aldehydes. *Angew. Chemie - Int. Ed.* **52,** 4645–4649 (2013).

292. Raynal, M., Ballester, P., Vidal-Ferran, A. & van Leeuwen, P. Supramolecular catalysis. Part 2: artificial enzyme mimics. *Chem. Soc. Rev.* **43,** 1734–1787 (2014).

293. Meppelder, A. New mixed bidentate phosphine ligands and their application in

enantioselective transformations. *New Mix. bidentate phosphine ligands their Appl. enantioselective Transform.*

294. Grushin, V. V. Hydrido Complexes of Palladium. *Chem. Rev.* **96,** 2011–2034 (1996).

295. Dufaud, V. Bimetallic Activation in Homogeneous Catalysis. 3. Mechanistic Study of the Methoxycarbonylation of Tricarbonyl(ch1orobenzene)chromium: Isolation and Reactivity of Possible Reaction Intermediates. *Organometallics* **10,** 4005–4015 (1991).

296. Grushin, V. V. Mixed phosphine-phosphine oxide ligands. *Chem. Rev.* **104,** 1629–1662 (2004).

297. Ohst, H. H. & Kochi, J. K. Electron-transfer catalysis of ligand substitution in triiron clusters. The role of the bridging ligand in anion radical intermediates. *J. Am. Chem. Soc.* **108,** 2897–2908 (1986).

298. Paul J. Dyson, J. S. M. *Transition Metal Carbonyl Cluster Chemistry*. (CRC Press, Taylor & Francis Group, 2000).

299. P. M. Lorz, F. K. Towae, W. Enke, R. Jäckh, N. Bhargava, W. H. *Ullmann's Encyclopedia of Industrial Chemistry*. (John Wiley and Sons, Inc).

300. Roelen, O. No Title. *Chem. Abstr.* **38,** 3631 (1944).

301. O. Roelen. US 2327066. (1943).

302. O. Roelen. DE 849548.

303. Evans, D., Osborn, J. A., Jardine, F. H. & Wllkinson, G. Homogeneous Hydrogenation and Hydroformylation using Ruthenium Complexes. *Nature* **208,** 1203–1204 (1965).

304. Chaudhari, R. V. & Desphpande, B. M. D. S. S. D. B. ; R. M. Process for the Catalytic Hydroformylation of Alkenes. 2–6 (1996).

305. Konya, D. & Len, K. Q. A. Highly Selective Halide Anion-Promoted Palladium-Catalyzed Hydroformylation of Internal Alkenes to Linear Alcohols. *Organometallics* 3166–3174 (2006).

306. Aldehydes, L. Highly Selective Catalyst Systems for the Hydroformylation of Internal Olefins to. *Communications* 3408–3411 (2001).

307. Bronger, R. P. J., Kamer, P. C. J. & Leeuwen, P. W. N. M. Van. Influence of the Bite Angle on the Hydroformylation of Internal Olefins to Linear Aldehydes. *Organometallics* **22,** 5358–5369 (2003).

308. Hartings, M. Reactions coupled to palladium. *Nat. Chem.* **4,** 764–764 (2012).

309. Jiro Tsuji. Expanding Industrial Applications of Palladium Catalysts. *Synthesis (Stuttg).* **9,** 739–749 (1990).

310. Christine Melber, Keller, D. & Mangelsdorf, I. in *Environmental Health Criteria 226* 201 (World Health Organization, 2002). d

311. Drent, E., Van Broekhoven, J. A. M. & Doyle, M. J. Efficient palladium catalysts for the copolymerization of carbon monoxide with olefins to produce perfectly alternating polyketones. *J. Organomet. Chem.* **417,** 235–251 (1991).

312. Education, G. & April, R. I =. **8,** 187–189 (1992).

313. Baya, M., Pd(I) phosphine carbonyl and hydride complexes implicated in the

palladium-catalyzed oxo process. *J. Am. Chem. Soc.* **130,** 10612–24 (2008).

314. Broekhoven, V. E. D. P. H. M. B. Trends in Chemistry. *Recl. Trav. Chim. Pays-Bas* **270,** 263–270 (1996).

315. Drent, E. Palladium-Catalyzed Alternating Copolymerization of Alkenes and Carbon Monoxide. *Chem. rev.* 663–681 (1996).

316. Brennführer, A., Neumann, H. & Beller, M. Palladium-catalyzed carbonylation reactions of alkenes and alkynes. *ChemCatChem* **1,** 28–41 (2009).

317. Cavinato, G. & Toniolo, L. Carbonylation of ethene catalysed by Pd(II)-Phosphine complexes. *Molecules* **19,** 15116–15161 (2014).

318. Delferro, M. & Marks, T. J. Multinuclear Olefin Polymerization Catalysts. *Chem. Rev. (Washington, DC, United States)* **111,** 2450–2485 (2011).

319. Jennerjahn, R. Palladium-catalyzed isomerization and hydroformylation of olefins. *Chem. Eur. J.* **15,** 6383–6388 (2009).

320. Pugh, R. I. & Drent, E. Methoxycarbonylation versus Hydroacylation of Ethene; Dramatic Influence of the Ligand in Cationic Palladium Catalysis. *Adv. Synth. Catal.* **344,** 837–840 (2002).

321. Fang, X., Zhang, M., Jackstell, R. & Beller, M. Selective palladium-catalyzed hydroformylation of alkynes to α,β-unsaturated aldehydes. *Angew. Chem. Int. Ed. Engl.* **52,** 4645–9 (2013).

322. Vasseur, A., Bruffaerts, J. & Marek, I. Remote functionalization through alkene isomerization. *Nat. Chem.* **8,** 209–219 (2016).

323. Beller, M., Zimmermann, B. & Geissler, H. Dual catalytic systems for consecutive isomerization-hydroformylation reactions. *Chem. - A Eur. J.* **5,** 1301–1305 (1999).

324. Veen, L. A. Van Der, Kamer, P. C. J. & Leeuwen, P. W. N. M. Van. Neuartige Rhodiumkatalysatoren für die Hydroformylierung interner Olefine zu. *Angew. Chemie* **111,** 349–351 (1999).

325. Fulmer, G. R. NMR Chemical Shifts of Trace Impurities: Common Laboratory Solvents, Organics, and Gases in Deuterated Solvents Relevant to the Organometallic Chemist. *Organomet.* **29,** 2176–2179 (2010).

326. Julie Bigeault, L. G. and G. B. First [2+1] Cycloaddition of Terminal Alkynes to Norbornene Derivatives Catalyzed by New Palladium-Phosphinous Acid Complexes. *Angew. Chemie* (2005).

327. Yarkevich, a. N., Petrova, L. N. & Bachurin, S. O. Synthesis and biological activity of dialkylamino-substituted phosphine oxides. *Russ. J. Gen. Chem.* **82,** 1659–1664 (2012).

328. Rulke, R. E. New Neutral and Cationic Methylpalladium(II) Complexes Containing Tridentate Nitrogen Ligands. Synthesis, Reactivity and X-ray Crystal Structure of {α-N-2-(N-isopropylcarbaldimino)-6-(N-isopropyl- carbaldimino)-α-N'-pyridyl~chloro)methylpalladium- (II) an. *Inorg. Chim. Acta* **169,** 5–8 (1990).

329. Corey, R. B. & Pauling, L. Models of Amino Acids, Peptides, and Proteins. *Rev. Sci. instruments* **205,** 621–627 (1953).

330. Koltun, W. L. Space filling atomic units and connectors for molecular models. *United States Patent Office* (1965).

331. Couzijn, E. P. A., Slootweg, J. C., Ehlers, A. W. & Lammertsma, K. Stereomutation of pentavalent compounds: Validating the berry pseudorotation, redressing Ugi's turnstile rotation, and revealing the two- and three-arm turnstiles. *J. Am. Chem. Soc.* **132,** 18127–18140 (2010).

332. Kyba, E. P. Nucleophilic Substitution at Phosphorus in Tertiary Phosphines . Evidence against Pseudorotation in a Potential Intermediate. *J. Am. Chem. Soc.* **4,** 4805–4809 (1969).

333. Mamane, V. The diastereoselective ortho-lithiation of Kagans ferrocenyl acetal. *Tetrahedron Asymmetry* **21,** 1019–1029 (2010).

334. Zhang, W. Unexpected reactions of ferrocene acetal derived from tartaric acid with alkyllithium: competition between proton abstraction and nucleophilic attack. *Tetrahedron* **62,** 9038–9042 (2006).

335. Gali, H., Karra, S. R., Reddy, V. S. & Katti, K. V. Design and Development of the First Peptide-Chelating Bisphosphane Bioconjugate from a Novel Functionalized Phosphorus(III) Hydride Synthon. *Angew. Chemie Int. Ed.* **38,** 2020–2023 (1999).

336. King, S. a., Pipik, B., Conlon, D. a. & Bhupathy, M. Preparation of Cyclic Sulfites by Transesterification of Diols and Diisopropyl Sulfite. *Synth. Commun.* **27,** 701–707 (1997).

337. Li, J.-N., Liu, L., Fu, Y. & Guo, Q.-X. What are the pKa values of organophosphorus compounds? *Tetrahedron* **62,** 4453–4462 (2006).

Titre : Synthèse, purification et caractérisation de ligands tétraphosphines

Mots clés : La catalyse bimétallique, phosphines multidentate, chimie de coordination

Résumé : L'évolution récente de la science écologique et durable nécessite des catalyseurs puissants, sophistiquées et dotés de propriétés spécifiques et modulables.
Les catalyseurs bimétalliques qui contiennent deux ou plusieurs sites pour l'activation coopérative de substrats réagissent sur des centres métalliques voisins selon certaines conditions. Un certain nombre de squelettes, spécialement conçus pour générer des complexes exclusivement bimétalliques, ont été développés autour d'échafaudages de méthano-dibenzodioxocine et de benzofurobenzofurane, y compris un certain nombre de ligands qui agissent comme donneurs de monophosphine dans deux centres métalliques différents. Ces ligands génèrent des espèces dinucléaires de manière fiable, mais les modes de coordination résultants sont imprévisibles.
Ce travail de thèse présente la synthèse de ligands de tétraphosphine, dans lesquels des bras chélatants sont disponibles pour coordonner chacun des deux centres métalliques.
La synthèse implique la préparation de 4,8-bis (sec-phosphines) de rac-6,12-méthano-12H-dibenzo [1,3] dioxocines et leur conversion en phosphines doublement chélatantes par l'élaboration de chaque fonctionnalité *sec*-phosphine en dérivés di (R) phosphinopropyle correspondants (R = Ph, Cy). Une étude de chimie de coordination préliminaire indique que l'environnement de coordination est fourni par ces ligands tétraphosphine binucléaires rigides. C'est ainsi que la préparation des complexes bimétalliques de Pd^{II}, Pt^{II} a été réalisé. Chacune des deux molécules de bras chélatants serait coordonnée à un métal. Enfin, des études préliminaires sur l'utilisation des ligands tétraphosphine comme supports pour la chimie de l'hydroformylation ont été réalisées. Les résultats actuels ne permettent pas encore d'établir définitivement un comportement coopératif entre les deux centres métalliques.

Title : Synthesis, Purification, and Characterization of Tetraphosphine Ligands

Keywords : : bimetallic catalysis, multidentate phosphines, coordination chemistry

Abstract : Recent developments in green and sustainable science require more powerful, sophisticated and tunable catalysts. Bimetallic catalysts contain two or more sites for the activation of substrates and, under optimal circumstances, can allow cooperative activation of reacting substrates on neighboring metal centers. A number of backbones, designed specifically to generate exclusively bi-metallic complexes have previously been developed around methanodibenzodioxocin and benzofuro-benzofuran scaffolds, including a number of ligands that act as monophosphine donors to two different metal centers. These ligands generate dinuclear species reliably, but the resulting coordination modes are unpredictable. This work presents the synthesis of tetraphosphine ligands, wherein chelating arms are available to coordinate each of the two metal centers.
synthesis involves preparation of 4,8-bis(sec-phosphines) of *rac*- 6,12-methano-12H-dibenzo[l,3] dioxocins and their conversion into doubly chelating phosphines through the elaboration of each sec-phosphine functionality into the corresponding di(R)phosphinopropyl derivatives (R= Ph, Cy). A preliminary coordination chemistry study indicates that the tightly defined coordination environment provided by these rigid binucleating tetraphosphine ligands under study allowed bimetallic complexes of Pd^{II}, Pt^{II} to be prepared, in which each of the two chelating arms molecule coordinates to one metal. Finally outline studies on the use of the tetra-phosphine ligands as supports for hydroformylation chemistry were performed. The current results do not yet allow cooperative behavior between the two metal centers to be definitively established.

Université Paris-Saclay
Espace Technologique / Immeuble Discovery
Route de l'Orme aux Merisiers RD 128 / 91190 Saint-Aubin, France